

AFFIDAVIT

I declare that I have authored this thesis independently, that I have not used other than the declared sources/resources, and that I have explicitly indicated all material which has been quoted either literally or by content from the sources used. The text document uploaded to TUGRAZonline is identical to the present doctoral thesis.

Date

Signature

Acknowledgements

Undertaking this PhD has been a truly life changing experience for me and it would not have been possible to do without the support and guidance that I received from many people.

First of all I would like to thank DK Molecular Enzymology for an opportunity to do my PhD research at Graz Technical University. My honest gratitude goes to my advisor Prof. Helmut Schwab for his kind supervision, fruitful discussions and assistance in getting financial support from different sources, including ÖAD scholarship. My special thanks goes to my advisor Dr. Petra Heidinger for her permanent assistance through all these years. She encouraged me and gave me a helping hand whenever I needed it.

My research stay abroad would have not been possible without KUWI scholarship and therefore, I appreciate financial assistance from TU Graz. This great experience would have also not be possible without my advisor at the University of Massachusetts in Dartmouth, Christopher Brigham. Many thanks to him and the members of his laboratory for any kind of assistance I got there.

Furthermore, I'm thankful to Prof. Rolf Breinbauer, Prof. Wolfgang Kroutil and the members of their groups for supplying me with the chemicals and the needed knowledge about organic chemistry. Especially, I would like to thank my friend Jakov Ivkovic for his constant help in performing HPLC experiments and the coffee breaks during stressful days. I greatly appreciate support I received from Dr. Margit Winkler and Dr. Kerstin Steiner as well. Dr. Kamila Napora, Elisa Lanfranchi, Bastian Daniel, Dr. Romana Wiedner and Karin Reicher are kindly acknowledge for their assistance during my experimental part of work. Christoph Sensen and Andreea Grecu are kindly acknowledged for the help in computational analysis and correcting the manuscript.

Furthermore, I would like to thank all the people from the first floor of IMBT for their permanent help, friendly talks and discussions. These include Christina Zach, my Erasmus-trainees Joanna Ciesielska and Dorota K. Pomorska, Daniel Schwendenwein, Steffen Gruber, Melanie Hirz, Katharina Maedje, Eva Thaler, Simone Scharl, Clemens Farnleitner, Mudassar Ahmad, Amneris Schlager-Weidinger and others.

From all my heart I would like to thank my family and my friends, especially, Maria Anastasina, Sonja Weissenecker, Heribert Strasser, and my sister Aza for always being on my side and believing in me. This work would have never been possible without their support.

Abstract

The genome of *R. eutropha* H16 contains a remarkable diversity of oxidoreductases. 11 alcohol dehydrogenases as well as 12 short chain dehydrogenases, 10 reductases, aldehyde dehydrogenase and alanine dehydrogenase of *R. eutropha* H16 were cloned and expressed in native and his-tagged versions in *Escherichia coli*. Their activity was analysed by NAD(P)⁺/NAD(P)H dependent enzyme activity assays with different substrates (alcohols, aldehydes and ketones). Out of 19 analysed enzymes originating from *R. eutropha*, which were expressed in *E. coli* BL21, thirteen showed activity. These enzymes were characterized in more details concerning cofactor and substrate specificity. Additionally, homologous expression of two selected alcohol- and short chain dehydrogenases, named A5 and B3, was performed in *R. eutropha* H16 under heterotrophic growth conditions. SDRs A5 and B3 were found to be NAD(P)(H)-dependent and highly (S)-enantioselective. These enzymes showed clear preference towards long-chain and aromatic secondary alcohols, aldehydes and ketones, with diaryl diketone benzil as one of the best substrates. The highest oxidation activity for SDR B3 and SDR A5 was detected at pH 11.0, whereas the optimal pH for reduction activity was pH 6.5 for SDR A5 and between pH 6.0 and pH 7.5 for SDR B3. Preliminary data on whole cell bioconversion for *R. eutropha* H16 expressing SDR B3 showed that the reduction potential of *R. eutrophas* H16 cells in lithoautotrophic environment is high enough to provide sufficient cofactor for NADPH-dependent reactions.

Kurzfassung

Im Genom von *R. eutropha* H16 ist eine bemerkenswerte Vielfalt an Oxidoreduktasen kodiert. Daher wurden insgesamt 11 Alkoholdehydrogenasen, 12 Short-chain Dehydrogenasen, 10 Reduktasen, eine Aldehyddehydrogenase und eine Alanindehydrogenase aus *R. eutropha* H16 kloniert und in ihrer nativen als auch in einer His-tag Variante in *E. coli* exprimiert. Die Aktivität dieser Enzyme wurde anhand eines NAD(P)⁺/NAD(P)H abhängigen Enzyme-Aktivität-Assays mit unterschiedlichen Substraten bestimmt (Alkohole, Aldehyde und Ketone). Von diesen 19 untersuchten aus *R. eutropha* H16 stammenden Enzymen, welche in *E. coli* BL21 exprimiert wurden, wiesen insgesamt 13 Enzymen Aktivität auf. Diese Enzyme wurden in Bezug auf ihre Cofaktor und Substrat Spezifität genauer charakterisiert. Des Weiteren wurden eine Alkohol- und eine Short-chain Dehydrogenasen, A5 und B3, in *R. eutropha* H16 unter heterotrophen Wachstumsbedingungen exprimiert. Die beiden SDRs A5 und B3 zeigten NADPH abhängige Aktivität und wiesen eine starke (S)-Enantioselektivität auf. Zudem zeigten die Enzyme eine Spezifität für langkettige und aromatische sekundäre Alkohole, Aldehyde und Ketone, wobei Diaryl-Diketon-Benzil das Substrat mit der höchsten Aktivität war. Die stärkste Aktivität in Richtung Oxidation für SDR B3 und A5 wurde bei pH 11.0 bestimmt, wobei der optimale pH der Reduktionsreaktion von SDR A5 bei pH 6.5 und von SDR B3 zwischen pH 6.0 und 7.5 lag. Erste Ergebnisse welche sich auf eine Ganzzellumsetzung von SDR B3 exprimierenden rekombinanten *R. eutropha* H16 Zellen beziehen, legen nahe dass das Reduktionspotenzial von *R. eutropha* unter lithotrophen Wachstumsbedingungen ausreicht um den Cofaktor NADPH in ausreichenden Mengen für NAPH abhängige Reaktionen bereitzustellen.

Table of content

Acknowledgements	1
Abstract	2
Kurzfassung	3
Table of content	4
Abbreviations	8
1. Introduction.....	12
1.1. <i>Ralstonia eutropha</i> H16.....	12
1.1.1 General information and taxonomy.....	12
1.1.2 Genome	13
1.1.3 Metabolism.....	15
1.1.4 Co-factor regeneration	20
1.1.5 Use of <i>R. eutropha</i> H16 in biotechnology	24
1.1.6 Expression systems for <i>R. eutropha</i>	27
1.2. Oxidoreductases.....	29
1.2.1. Classification of the enzymes	29
1.2.2. Short-chain dehydrogenases/reductases.....	30
1.2.2.1. Alcohol dehydrogenases. General information and mechanism of action	33
1.2.3. Aldo-keto reductases.....	35
1.2.3.1. General information	35
2. Aim of the study	38
3. Results	39
3.1. Homologous and heterologous expression of oxidoreductases of <i>Ralstonia eutropha</i> H16.....	40
3.1.1. Introduction.....	41
3.1.2. Materials and methods	42
3.1.2.1. Bacterial strains and cultivation conditions	42
3.1.2.2. Plasmids and primers used in this study	43
3.1.2.3. Sequence analysis.....	49
3.1.2.4. DNA preparation	49
3.1.2.5. Agarose gel electrophoresis and DNA preparation.....	49
3.1.2.6. Preparation of electrocompetent <i>E. coli</i> and <i>R. eutropha</i> H16 cells.....	49
3.1.2.7. Plasmid construction for expression in <i>E. coli</i> BL21	50
Construction of the pK470 expression vectors for <i>E. coli</i> BL21.....	50

Construction of the pK470-His ₆ expression vector	50
3.1.2.8. Plasmid construction for expression in <i>R. eutropha</i> H16.....	51
3.1.2.9. Transformation of DNA into electrocompetent <i>E. coli</i> and <i>R. eutropha</i> H16 cells	54
3.1.2.10. Mating procedure for <i>R. eutropha</i> H16.....	54
3.1.2.11. Expression of recombinant enzymes in <i>E. coli</i> BL21 and <i>R. eutropha</i> H16	55
3.1.2.12. Colony assay based on NAD(P)H fluorescence.....	55
3.1.2.13. Purification of His ₆ -tagged recombinant enzymes.....	56
3.1.2.14. Photometric assay based on NAD(P) ⁺ / NAD(P)H fluorescence	56
General conditions	56
Spectrophotometric assay with cell free lysates.....	57
Spectrophotometric assay for the purified enzymes	57
Spectrophotometric enzyme activity assay with SDR B3 purified out of <i>E. coli</i> BL21 and <i>R. eutropha</i> H16.....	58
3.1.2.15. Biochemical characterization and bioinformatics analysis of ADH A5 and SDR B3 ...	59
3.1.2.16. Whole-cell bioconversion.....	59
3.1.3. Results and discussion.....	60
3.1.3.1. Cloning of enzymes of interest into pK470expression vector.....	60
3.1.3.2. Expression of the enzymes in <i>E. coli</i> BL21	61
3.1.3.3. A colony-based activity assay based on NAD(P)H fluorescence	63
3.1.3.4. Photometric assay for the cell free lysates of <i>E. coli</i> BL21 carrying corresponding recombinant dehydrogenases and reductases	66
3.1.3.5. Cloning of His ₆ -tagged enzymes into pK470 expression vector	70
3.1.3.6. Heterologous expression, purification and enzyme activity analysis of His ₆ -tagged enzymes.....	71
3.1.3.7. Cloning of the enzymes into expression vectors for <i>R. eutropha</i> H16.....	76
3.1.3.8. Comparing of the activities of His ₆ -SDR B3 purified out of <i>E. coli</i> BL21 and <i>R. eutropha</i> H16	93
3.1.3.9. Characterization of two novel short-chain alcohol dehydrogenases/reductases from <i>Ralstonia eutropha</i> H16 capable of stereoselective conversion of bulky substrates	95
3.1.3.10. Preliminary data on whole cell bioconversion of benzil performed by lithoautotrophically grown cells of <i>R. eutropha</i> H16 expressing SDR B3.....	130
3.2. Cloning, expression, purification and functional analysis of aldehyde dehydrogenase originating from <i>Ralstonia eutropha</i> H16.....	132
3.2.1. Introduction.....	133
3.2.2. Materials and methods	134
3.2.2.1. General	134
3.2.2.2. His ₆ -tag cloning.....	134

3.2.2.3. Protein expression.....	135
3.2.2.4. Protein purification	136
3.2.2.5. Enzyme activity assay	136
3.2.3. Results and discussion.....	137
3.3. Cloning and expression of bacterial transaminase, alanine dehydrogenases and imine reductases in <i>Ralstonia eutropha</i> H16	141
3.3.1. Introduction.....	142
3.3.2. Material and methods.....	144
3.3.2.1. Bacterial strains and cultivation conditions	144
3.3.2.2. Cultivation conditions.....	145
3.3.2.3. DNA preparation	145
3.3.2.4. Plasmid construction	145
3.3.2.5. Protein expression.....	147
3.3.3. Results and discussion.....	149
4. Contribution to the manuscript on the design of inducible expression systems for protein expression in <i>Ralstonia eutropha</i> H16	153
5. Conclusions.....	181
6. Appendix.....	184
6.1. Cloning, heterologous expression and functional characterisation of esterase-like protein originating from <i>Ralstonia eutropha</i> H16.....	184
6.1.1. Introduction.....	185
6.1.2. Materials and methods	187
6.1.2.1. Bacterial strains, plasmids and cultivation condition.....	187
6.1.2.2. Cloning of esterase/lipase into pK470.....	188
6.1.2.3. Expression of esterase-like protein in <i>E. coli</i> BL21	189
6.1.2.4. Esterase activity assay	189
6.1.2.5. Hydroxynitrile lyase activity	189
6.1.3. Results and discussion.....	190
6.1.3.1. Cloning and heterologous expression of esterase/lipase	190
6.1.3.2. Enzyme activity assays.....	190
6.1.4. Conclusions.....	192
6.2. Report about research stay	193
6.2.1. Introduction.....	194
6.2.2. Materials and methods	195
6.2.3. Results and discussion.....	201
6.2.4. Conclusions.....	204

7. Supplementary information	205
8. References.....	209

Abbreviations

ADH	alcohol dehydrogenase
ADP	adenosine diphosphate
AKR	aldo-keto reductase
ALDH	aldehyde dehydrogenase
Ap	ampicillin
Arg	arginine
ATP	adenosine triphosphate
bp	base pair(s)
CBB	Calvin-Benson-Bassham cycle
CDS	coding sequence
CDS	conserved domain search
CoA	coenzyme A
ddH ₂ O	double-distilled water
DMSO	dimethyl sulfoxide
DNA	deoxyribonucleic acid
dNTP	deoxynucleoside triphosphate
<i>E. coli</i>	<i>Escherichia coli</i>
EC	enzyme class
ED	Entner-Doudoroff pathway
EDTA	ethylenediaminetetraacetic acid
FAD	flavin adenine dinucleotide
FDH	formate dehydrogenase
GDH	glucose dehydrogenase
CFU	colony forming unit
Gly	glycine
Gm	gentamicin

HCl	hydrogen chloride
His	histidine
HPLC	high-pressure liquid chromatography
IMBT	Institute of Molecular Biotechnology, Graz Technical University
IPTG	isopropyl- β -D-thiogalactopyranosid
IRED	imine reductase
IUBMB	International Union of Biochemistry and Molecular Biology
KDPG	2-keto-3-deoxy-6-phosphogluconate pathway
Km	kanamycin
kDa	kilodalton
<i>lacI</i>	gene encoding <i>lac</i> repressor
LB	lysogeny broth
Leu	leucine
Lys	lysine
MBH	membrane-bound hydrogenase
MDR	medium chain dehydrogenase
M-FDH	membrane bound formate dehydrogenase
<i>mob</i>	mobilization region of pBBR1-MCS5 plasmid
<i>mob</i> RP4	mobilization region of RP4 plasmid
MQ	menaquinone
MS	mass spectrometer
MSM	minimal salt medium
NaCl	sodium chloride
NAD(H)	nicotineamid adenine dinucleotide (reduced form)
NADP(H)	nicotineamid adenine dinucleotide phosphate (reduced form)
NaOH	sodium hydroxide
NAR	nitrate reductase
NCBI	National Center for Biotechnology Information, http://www.ncbi.nlm.nih.gov/

NC-IUBMB	Nomenclature Committee of the International Union of Biochemistry and Molecular Biology
NIR	nitrite reductase
NOR	nitric oxide reductase
NOS	nitrous oxide reductase
OD ₆₀₀	optical density at 600 nm
ONC	overnight culture
PCR	polymerase chain reaction
PDB	Protein Data Base
PEG	polyethyleneglycol
PHA	polyhydroxyalkanoate
PHB	polyhydroxybuturate
PHBV	poly(3-hydroxybutyrate-co-3-hydroxyvalerate)
Phe	phenylalanine
rpm	revolutions per minute
RuBisCo	ribulose-1,5-biphosphate carboxylase/oxygenase
RasAIDH	aldehyde dehydrogenase from <i>R. eutropha</i> H16
RED	reductase
<i>R. eutropha</i>	<i>Ralstonia eutropha</i>
RH	regulatory hydrogenase
RNA	ribonucleic acid
RNR	ribonucleotide reductase
rRNA	ribosomal ribonucleic acid
SDR	short-chain dehydrogenase/reductase
SDS	sodium dodecyl sulphate
SDS-PAGE	sodium dodecyl sulphate polyacrylamide gel electrophoresis
Ser	serine
S-FDH	soluble formate dehydrogenase

SH	soluble hydrogenase
TAE	Tris acetate-EDTA
ω -TAm	ω -Transaminase
TCA	tricarboxylic acid cycle
TIM	triose-phosphateisomerase
Tris	2-amino-2-hydroxymethyl-propane-1,3-diol
TA	transaminase
TSB	tryptic soy broth
Tyr	tyrosine
U	enzyme activity unit
UQ	ubiquinone
UniProtKB	Universal Protein Resource Knowledgebase, http://www.uniprot.org/
UV	ultraviolet light

1. Introduction

There is always a high demand for new enzymes that are highly active on a specific substrate. The NAD(P)⁺-dependent oxidoreductases which catalyse redox reactions are very interesting for applications in biocatalytic processes. By means of these enzymes the production of building blocks for fine chemicals and important pharmaceuticals, as well as synthesis of chiral molecules is possible (Scheper et al., 2010). There are two methods to obtain a new catalyst: the first approach includes site-directed mutagenesis of known enzymes, the second one is based on a screening of the enzymes in naturally available sources. Environmental diversity selects for the rare metabolic properties where those enzymes perform unique reactions. Therefore, living organisms with diverse metabolic behaviour are the perfect source for the mining novel enzymes important for industrial applications (Shimizu *et al.*, 1997). One of such organisms is the Gram-negative β -Proteobacterium *Ralstonia eutropha* H16.

1.1. *Ralstonia eutropha* H16

1.1.1 General information and taxonomy

Ralstonia eutropha H16 is a Gram-negative bacterium which is widely distributed in soil and fresh water biotopes (Aragno and Schlegel, 1992). It is also known as a representative of *Knallgas*-bacteria because of the ability to oxidize molecular hydrogen. According to the last taxonomic data it has following scientific classification:

Kingdom: Bacteria

Phylum: Proteobacteria

Class: β -proteobacteria

Order: Burkholderiales

Family: Ralstoniaceae

Genus: *Ralstonia*

Bacterial cultures containing *R. eutropha* H16 were isolated in 1957 by Bovell and later by Wilde and studied for their ability to metabolize hydrogen (Repaske, 1962; Wilde, 1962). *R. eutropha* H16 can oxidize hydrogen and use it as a source of energy. This bacterium is able to grow under autotrophic, heterotrophic and mixotrophic conditions, depending on the available types of carbon sources.

In the first half of last century a group of microorganisms capable of hydrogen oxidation was described and named *Hydrogenomonas* (Repaske, 1962). One of the representatives was named *Hydrogenomonas eutrophus* (in Ancient Greek “eutrophus” means “well nourished”). Later, after

General information on the genome of *R. eutropha* H16 is provided in Table 1.

Chromosome 1.

Chromosome 1 has a size of 4,052,032 bp and contains mostly housekeeping genes responsible for DNA replication, transcription, translation, including the ribosomal proteins synthesis, degradation of acids and heterotrophic carbon metabolism (Pohlmann et al., 2006). Chromosome 2 is smaller in size and comprises 2,912,490 bp. Genes for central steps of the 2-keto-3-deoxy-6-phosphogluconate (KDPG) pathway, also named Entner-Doudoroff pathway, where sugars and sugar acids are metabolized, are located on this replicon (Pohlmann et al., 2006).

Chromosome 2.

Chromosome 2 also harbours genes for autotrophic carbon dioxide fixation via Calvin-Benson-Bassham (CBB) cycle encoded in the *cbb_c* operon and the *cbbR* gene for transcription activator. *R. eutropha* H16, as all other *Ralstonia* strains, can degrade aromatic compounds, and genes responsible for that feature are present on chromosome 2. Among other genes located on this replicon are those, responsible for denitrification, utilization of alternative carbon and nitrogen sources, terminal oxidases and reductases for alternative electron acceptors. Chromosome 2 also carries genes responsible for aromatic compounds degradation, motility, biosynthesis of flagella, chemotaxis and the gene for a putative aerotaxis sensor. Nonspecific adherence to surfaces is encoded on two clusters on chromosome 1 and one cluster on chromosome 2 (Pohlmann et al., 2006; Schwartz et al., 2009).

Table 1. General features of the genome of *R. eutropha* H16.

Feature	Chromosome 1	Chromosome 2	Megaplasmid pHG1
Size (bp)	4,052,032	2,912,490	452,156
G+C ratio (mol%)	66,4	66,7	62,3
Percentage coding	88,1	88,6	79,7
tRNA	51	7	1
rRNA operons	3	2	1
Total number of CDS	3,651	2,555	420

Table modified from Pohlmann et al., 2006

Megaplasmid.

The self-transmissible megaplasmid pHG1 has a size of 452,156 bp and carries 420 protein coding sequences (Friedrich et al., 1981). This includes genes which are involved in facultative H₂-/CO₂-based lithoautotrophy, which form the largest cluster on this replicon. This is, for example, the

hox operon, encoding the genes for hydrogen oxidation. Another example is the operon for carbon dioxide fixation, known as *cbb_p* (Schwartz and Friedrich, 2001; Schwartz et al., 2003).

The megaplasmid is also responsible for the facultative anaerobic lifestyle of *R. eutropha*. This ability is important for a soil organism that has to deal with anoxic environmental conditions. The bacterium can grow on nitrate or nitrite, respiring them to N₂, and, thus, is able to survive in anoxic conditions. The genes responsible for the denitrification including the genes for the cytochrome b biosynthesis, represent the second large cluster on the megaplasmid after the one involved in lithoautotrophic lifestyle (Schwartz et al., 2003).

Interestingly, *R. eutropha* H16 can reorganize its respiratory chain as a response to available energy source and terminal electron acceptors by attracting extensive inventory of genes for respiratory chain components. Moreover, the genome of this bacterium includes a large set of genes for potential regulatory and signalling proteins. Therefore, this bacterium can successfully respond to changing environmental conditions (Schwartz et al., 2009).

The megaplasmid, as the chromosome 2, also carries genes responsible for the degradation of aromatic compounds (Johnson and Stanier, 1971; Schwartz et al., 2003). pHG1 also possesses some other metabolically important properties, such as genes for conjugative plasmid transfer, pilus biosynthesis and polyhydroxyalkanoates (PHAs) metabolism (Schwartz et al., 2003).

1.1.3 Metabolism

Heterotrophic growth.

R. eutropha H16 is a heterotrophic organism, able to grow chemolithoautotrophically under certain conditions (Fig. 2). In case of heterotrophic growth, organic carbon and energy sources including sugar acids, fatty acids, amino acids, alcohols, aromatic compounds and sugars are used (Schwartz et al., 2009). Due to its ability to decompose aromatic compounds, *R. eutropha* H16 can even grow on benzoates or tetrahydrofurfuryl alcohol (Zarnt et al., 1997). Despite of the wide range of acceptable organic compounds, *R. eutropha* H16 is known to metabolize only two sugars: fructose and N-acetylglucosamine (Johnson and Stanier, 1971). Fructose is catabolized via the oxidative decarboxylation known as Entner-Doudoroff pathway (Gottschalk and Eberhardt, 1964). The activities of other sugar degradation pathways like Embden-Meyerhoff-Parnas and oxidative phosphate way were not detected (Cramm, 2008). Interestingly, genes for anabolically operating Embden-Meyerhoff-Parnas pathway, also known as gluconeogenesis, are present on the chromosome 1 (Pohlmann et al., 2006). D-glucose, which is used as an energy source in most of living organisms, from bacteria to humans, is not metabolized by *R. eutropha* H16 because there is no

active transport system. However, mutants able to grow on D-glucose as a source of sugar were known for a long time and recently characterized (Franz et al., 2012; Sichert et al., 2011).

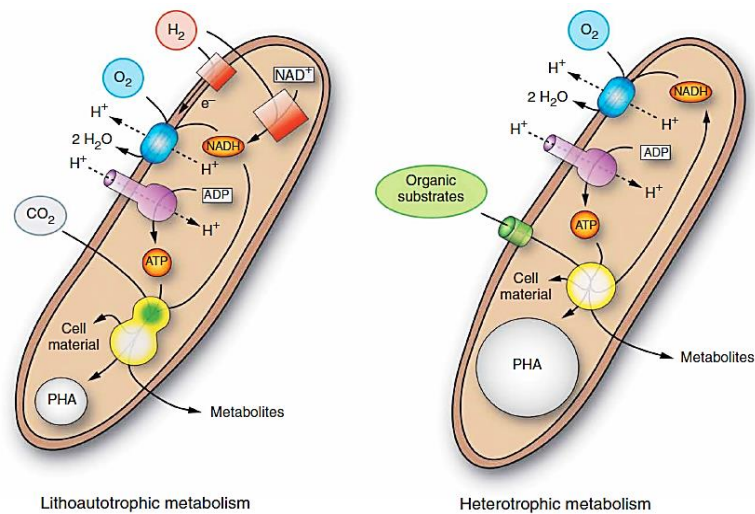


Figure 2. Schematic overview demonstrating the key aspects of heterotrophic and lithoautotrophic growth of *R. eutropha* H16. The lithoautotrophic metabolism is characterized by two energy-conserving hydrogenases (represented by two red squares) and CO₂ fixation (symbolized by the yellow/green circle). Heterotrophic growth is determined by uptake and usage of organic substrates as energy and carbon source. The central metabolism is illustrated through a yellow circle. Picture taken from Pohlmann et al., 2006

Lithoautotrophic growth.

In absence of organic compounds the metabolism of this bacterium is switched to chemolithoautotrophic mode (Kusian and Bowien, 1997). Chemolithoautotrophy is a type of metabolism where energy is obtained through the oxidation of inorganic compounds and inorganic compounds like CO₂ are used as carbon source. The most common metabolic pathway for carbon dioxide fixation is the Calvin-Benson-Bassham reductive pentose phosphate cycle (CBB) with ribulose-1,5-biphosphate carboxylase/oxygenase (RuBisCO) as a key enzyme (Bowien and Kusian, 2002).

Up to now, *R. eutropha* H16 is one of the best studied organisms for lithoautotrophic growth, based on the use of molecular hydrogen and carbon dioxide as sole sources for energy and carbon, respectively (Friedrich and Schwartz, 1993). *R. eutropha* H16 fixes CO₂ via the CBB cycle. Interestingly, recent data show that the CBB cycle is also active during aerobic heterotrophic growth conditions and participates in reutilization of CO₂ emitted through sugar degradation (Shimizu et al., 2015). *R. eutropha* H16 possess the largest known *cbb* operon cluster. The *cbb_c* operon located on the chromosome 2 includes 13 genes, the *cbb_p* operon located on the megaplasmid pHG1 contains 12 genes and 2 additional genes are encoded on the chromosome 1 (Schwartz and Friedrich, 2001). Both of the operons are regulated by LysR-type transcriptional regulator CbbR, which is connected to

the carbon state of the cell (Bowien and Kusian, 2002). The corresponding gene is located on the chromosome 2 next to the *cbb_c* operon (Kusian and Bowien, 1995). An inactive copy of this gene (*cbbR0*) can also be found upstream of the *cbb_p* operon (Schwartz et al., 2003).

RuBisCo, the key enzyme of the CBB cycle, is not directly able to utilise CO₂, but bicarbonate. Merlin and co-workers showed that transport of CO₂ from gas phase into the liquid phase and subsequent conversion to bicarbonate inside the cell are not sufficient for the needs of bacterial cells (Merlin et al., 2003). Four different carbonic anhydrases of *R. eutropha* H16 are responsible for providing the cell with HCO₃⁻ when only low CO₂ concentration is available in the environment (Kusian et al., 2002). The genes *can*, *can2*, *caa* and *cag*, coding these enzymes are located either on chromosome 1 or on chromosome 2 (Pohlmann et al., 2006). Recently, Gai and co-authors reported the characterization of these carbonic anhydrases and showed that all of them have the same function in the cells, but play unique roles within the machinery for CO₂ metabolism (Gai et al., 2014).

Energy metabolism.

There are two possible sources to supply energy for autotrophic CO₂ fixation: molecular hydrogen or formate in case of organotrophic growth. Two metal-dependent hydrogenases encoded on the megaplasmid oxidize H₂. Alternatively, at least three different formate dehydrogenases utilize formate (Pohlmann et al., 2006; Cramm, 2008).

Molecular hydrogen as a source of energy.

A lot of studies have been devoted to *Ralstonias* NiFe hydrogenases (Friedrich and Schwartz, 1993; Lenz et al., 2002). Molecular hydrogen is split into electrons and protons by a NAD(P)-reducing membrane-bound hydrogenase (MBH) and a cytoplasmic hydrogenase (SH) which is linked to the respiratory chain. MBH acts at the first step of the electron transport chain during respiration, whereas SH is responsible for the production of NADH in the cytoplasm of the cell. These arising reducing equivalents are used for the CO₂ fixation and also in the respiratory chain. There is also a third, non-energy-conserving regulatory hydrogenase (RH). It serves as a hydrogen sensor and interacts with the regulatory system, causing hydrogen-dependent activation of MBH and SH gene expression (Lenz et al., 2002). In more detail, RH causes activation of a histidine kinase, which binds to the transcription factor HoxA and initiates the transcription of MHB and SH genes start (Schwartz et al., 1998). Additional NiFe hydrogenase is encoded on pHG1 but the physiological role of this enzyme is not clear since it doesn't restore ability of the organism to grow on hydrogen when MBH and SH enzymes are not active (Cramm, 2008).

Formate as a source of energy.

Formate can serve as an alternative carbon source for autotrophic growth of *R. eutropha* H16. Oxidation of HCOO^- supplies cells with CO_2 which is afterwards utilized via the CBB cycle (Bowien and Kusian, 2002). The soluble Mo-dependent formate dehydrogenase (S-FDH) plays one of the key roles under organoautotrophic conditions. It couples the reaction of formate oxidation with direct reduction of NAD^+ and thereby provides reducing equivalents for the CO_2 fixation. Operon of five genes encodes S-FDH on the chromosome 1. Second active formate dehydrogenase is membrane bound enzyme (M-FDH). In contrast to S-FDH, which is only induced when formate is present in the environment, M-FDH is active under different growth conditions (Burgdorf et al., 2006). Two separate gene clusters encode the M-FDH on the chromosomes 1 and 2. Because of this and the fact that molybdenum-dependent activity of M-FDH was found only under organoautotrophic conditions while tungsten-dependent activity was detected when cells were grown under lithoautotrophic and energy-limiting conditions (Bömmmer et al., 1996; Burgdorf et al., 2001), there are suggestions that two different types of enzyme could be formed: a W-containing and a Mo-containing M-FDH. Additionally few proteins with putative FDH-related activity are also found in the genome of *R. eutropha* H16 (Pohlmann et al., 2006).

Aerobic growth

R. eutropha H16 can grow under aerobic or anaerobic conditions. In the first case the respiratory chain involves a NADH dehydrogenase, a succinate dehydrogenase, a bc_1 complex and the terminal oxidases (Fig. 3). The NADH dehydrogenase is a big membrane bound protein which couples the oxidation of NADH with a proton translocation. Genes for all subunits of this enzyme are located on chromosome 1. The succinate dehydrogenase is part of the citric acid cycle. It oxidizes succinate to fumarate and consigns two electrons to quinol (Lancaster, 2002). This enzyme is encoded by 4 genes (*sdhC*, *sdhD*, *sdhA*, *sdhB*) which are located on the chromosome 2. The next players, ubiquinone Q_8 and menaquinone (vitamine K_2), are electron carriers (Fig. 3). Under aerobic respiration conditions ubiquinone is more active than menaquinone, which starts playing a more significant role during denitrification (Bongers, 1967). Following electron carrier, quinol-cytochrome *c* oxidoreductase (bc_1 complex), transfer electrons to the terminal step. The last reaction in the electron transfer chain is the reduction of dioxygen to water. This reaction is catalysed by terminal oxidases (Fig. 3). In the genome of *R. eutropha* H16 five genes for quinol oxidases and three genes coding for cytochrome oxidases can be found. This indicates that the aerobic respiration chain adapts to varying concentrations of molecular oxygen (Cramm, 2008).

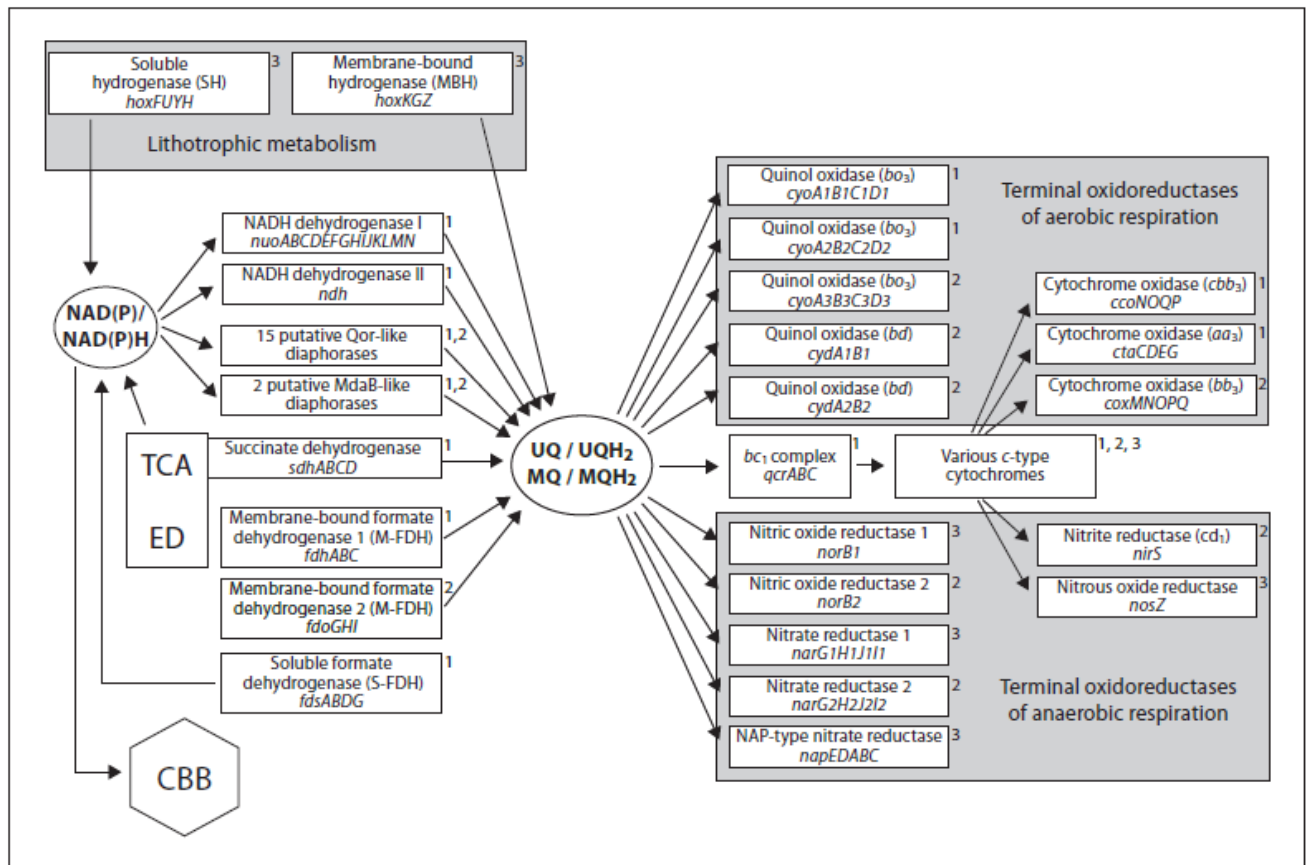


Figure 3. Schematic representation of energy metabolism in *R. eutropha* H16. Replicons are indicated by numbers: 1 = chromosome 1; 2 = chromosome 2; 3 = megaplasmid pHG1. CBB = Calvin-Benson-Bassham pathway; TCA = tricarboxylic acid cycle; ED = Entner-Doudoroff pathway; UQ = ubiquinone; MQ = menaquinone. Picture taken from Cramm, 2008

Anaerobic metabolism

R. eutropha H16 is capable of alternative respiration by denitrification process. This ability of *R. eutropha* H16 was first described more than 40 years ago (Pfitzner and Schlegel, 1973). The bacterium can use nitrate, nitrite, nitric oxide or nitrous oxide as alternative electron acceptors (Romermann and Friedrich, 1985). Terminal reductases in this case are nitrate reductase (NAR), nitrite reductase (NIR), nitric oxide reductase (NOR) and nitrous oxide reductase (NOS), respectively (Fig. 3). All essential genes for this process are located on the megaplasmid. Interestingly, chromosome 2 also encodes genes for all key enzymes but lacks two genes for anaerobic class III ribonucleotide reductase (RNR) (Siedow et al., 1999). RNRs provide deoxyribonucleotides by reduction of ribonucleotides and thus are essential for DNA synthesis. An exact role of these enzymes in the denitrification is not clear; however, their activity seems to be crucial for the whole process since megaplasmid-free mutants of *R. eutropha* H16 are not able to respire by denitrification (Cramm, 2008).

Schlegel et al. demonstrated that under conditions of restricted oxygen supply, *R. eutropha* H16 produces a variety of NAD(P)(H)-dependent dehydrogenases such as alcohol dehydrogenase, butanediol dehydrogenase and lactate dehydrogenase (Schlegel and Steinbüchel, 1981; Vollbrecht et al., 1979). The postulated role of the upregulated dehydrogenases is to serve as a safety valve for the release of excess reducing power in the absence of terminal electron acceptors (Steinbüchel and Schlegel, 1983; Alexander Steinbüchel and Schlegel, 1983; Steinbüchel and Schlegel, 1984).

1.1.4 Co-factor regeneration

Soluble NAD(H) and NADP(H) are the major redox cofactors of living cells. NADP⁺ structurally differs from NAD⁺ only by the presence of an additional phosphate group (Fig. 4a). The secondary structures of the enzyme-binding domains of both NAD⁺ and NADP⁺ are very similar.

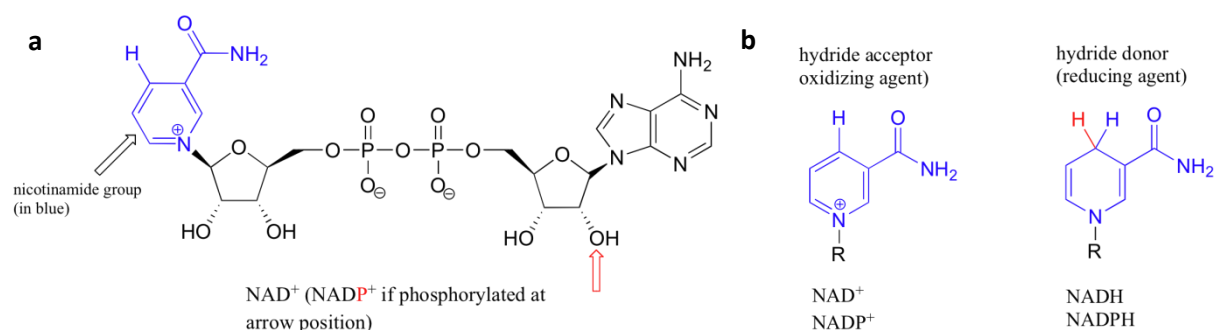


Figure 4. Chemical structure of NAD(P)(H). a – detailed chemical structure for NAD(P)⁺. b - oxidized and reduced forms of the cofactors. Picture taken from Soderberg, 2010

NADP(H) participates in anabolic redox reactions, acting in dehydrogenase-catalysed reactions that transport electrons to intermediates of biosynthesis processes. NAD(H) is used in dehydrogenase-catalysed reactions involved in respiration and therefore, is used for oxidation reactions. This is possible because in the cells the phosphorylated cofactor is generally maintained in a reduced NADPH state and non-phosphorylated cofactor is present in its oxidized NAD⁺ form (Fig. 4b) (Chenault, H. Keith Simon, Ethan S. Whitesides, 1988).

NAD(P)(H) are essential cofactors for the activity of NAD(P)(H)-dependent oxidoreductases. These enzymes are widely used in industry, for example to produce ketones, which are often difficult to be chemically synthesized, or to resolve racemic mixtures of chiral alcohols and amines (May and Padgette, 1983). Therefore, NAD(P)(H) regeneration is one of the most relevant issues in enzymatic catalysis, while cofactors needed for these reaction are of high costs, especially, in its phosphorylated form (Hummel, 1999). This is a reason why reusability of coenzymes has for a long time been a target for process optimization.

Regeneration of nicotinamide cofactors can be done in different ways: enzymatic, chemical, photochemical or electrochemical. Simple chemical, electrochemical or photochemical reductants,

such as dithionite, free electrons and light, have some considerable benefits such as low costs and the utilization of a regenerating agent (Shumilin et al., 1992; Van Der Donk and Zhao, 2003). However, the lack of specificity for the enzymatically active 1,4-NAD(P)H isomer, and incompatibility with most enzymes, make these methods not as effective as an enzymatic approach. So far, only few organometallic complexes are the only non-enzymatic catalysts that have been used for NAD(P)H regeneration in chemical, electrochemical or photochemical approaches (Hollmann et al., 2006; Scheper et al., 2010).

The best studied methods for regeneration of nicotinamide cofactors are enzymatic approaches, as they show high selectivity for the formation of the active form of the cofactor, have high compatibility with other reagents and can be monitored in an easy way (Hummel and Kula, 1989). There are two main approaches of the enzymatic method: the enzyme-coupled and the substrate-coupled method (Fig. 5). The enzyme-coupled approach requires a second enzyme as well as a second substrate for regeneration (Fig. 5a). In some cases, a product of the initial reaction can serve as a substrate for the cofactor recycling reaction and, as a result, the final desired product is produced in the second, cofactor-regenerating step (Fig. 5b). Both of these variations belong to the enzyme-coupled approach.

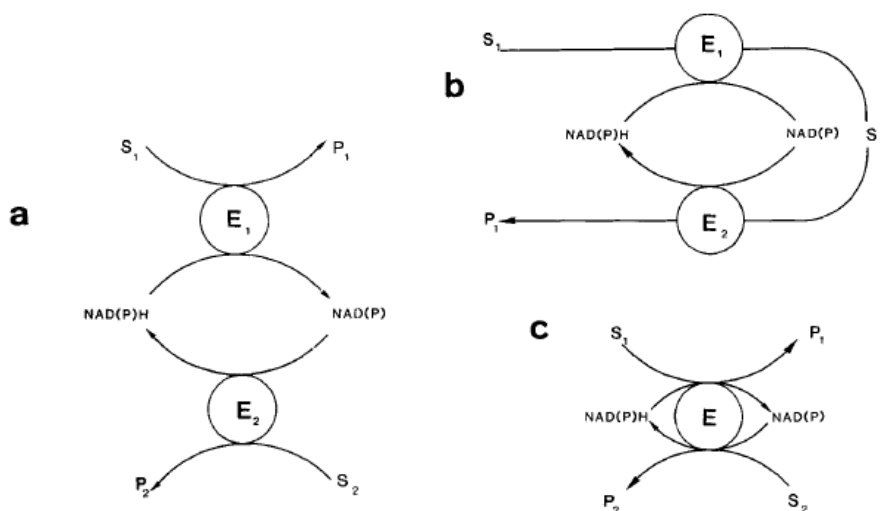


Figure 5. Enzymatic NAD(P)H regeneration. a – enzyme-coupled regeneration, applying a second enzyme (E₂) and a second substrate S₂. b - enzyme-coupled regeneration of the coenzyme.: the substrate (S₂) of the desired product (P₁) is formed *in situ* from the precursor S₁; both reactions (enzyme E₁ and enzyme E₂) depend on the same coenzyme; c – substrate coupled approach, utilizing the same (E) for the reduction of the substrate S₁ to the desired product P₁ as well as for the coenzyme NAD(P)H regeneration by oxidation of S₂ to P₂. Picture taken from Hummel and Kula, 1989

In the substrate-coupled approach of the enzymatic method, one single enzyme is responsible for the formation of the desired product as well as for the cofactor regeneration (Fig. 5c) (Drepper et al., 2006). The benefit of this approach is the possibility to use it in oxidation and

reduction way. However, it should be considered that the co-substrate should be supplied in large excess to maintain the equilibrium towards the desired direction (Kroutil et al., 2004). This method was used, for example, for the production of chiral alcohols from bulky substrates by an overexpressed short-chain alcohol dehydrogenase from *Ralstonia. sp.* DSM 6425 in *E. coli* (Ivan Lavandera et al., 2008).

For the enzyme-coupled method oxidation and reduction ways require separate cofactor-recycling systems. Formate dehydrogenase (FDH), which oxidizes formate to carbon dioxide, or glucose dehydrogenase (GDH), which oxidizes glucose to gluconolactone, are commonly used enzymes to recycle NAD^+ or NADP^+ (Goldberg et al., 2007; Hummel and Kula, 1989). FDH is the most widely used enzyme as formate is a cheap and non-hazardous reductant, which produces CO_2 as a co-product, and the regeneration reaction becomes irreversible because of the volatility of CO_2 (Hollmann et al., 2006). In 1980, Shaked and co-authors were first to demonstrate the regeneration of a coenzyme in a preparative synthesis by coupling FDH from *Candida boidinii* (Shaked and Whitesides, 1980). This was a simple NADH-consuming reaction – the production of D-lactate from pyruvate. A whole-cell biotransformation system using an ADH from *Lactobacillus brevis* to produce chiral compounds in combination with a FDH from *Mycobacterium vaccae* N10 for cofactor regeneration has been described in *E. coli*. Weckbecker et al. showed that GDH from *B. subtilis* can be used for cofactor regeneration while acetophenone was stereoselectively converted by NADP^+ -dependent (*R*)-specific alcohol dehydrogenase from *Lactobacillus kefir* (Weckbecker and Hummel, 2005). Production of chiral alcohols with GDH as a cofactor recycling system was also performed in *E. coli* by overexpressed short-chain alcohol dehydrogenase from *Ralstonia. sp.* DSM 6425 (Ivan Lavandera et al., 2008). Interestingly, GDH being naturally NADP^+ -dependent, can also successfully convert NAD^+ (Scheper et al., 2010). This is in contrast to ADHs, which are sometimes also used as enzymatic cofactor recycling systems and are in major strictly NAD^+ - or NADP^+ - dependent (Lauterbach et al., 2013).

Methods of *in situ* NAD(P)^+ regeneration have a number of limitations. There are several requirements that have to be met: inexpensive method of recycling, stability over a long period of time, easy product separation, absence of cross reactions between reaction products and the compounds needed for cofactor regeneration, thermodynamic and kinetic preference of product formation, regioselectivity of NAD(P)^+ in order to avoid production of partly inactive form of the recycled cofactor, and stability of the enzymes (Scheper et al., 2010). These obstacles could be partially overcome by whole cell biotransformations. When producing and regenerating enzymes are available in one single strain, no addition of expensive cofactor is necessary: the intracellular cofactor pool can be used. Therefore, whole cell biotransformations are very promising for technical

applications (Hollmann et al., 2006). As an example, Li and co-authors applied an electric field for the production of formic acid from CO₂ and H₂O. Subsequently, formic acid was converted to CO₂ and NADH by the cells of *R. eutropha* H16 and, as a result, higher alcohols were produced in this reaction (Li et al., 2012).

R. eutropha H16 can synthesize *de novo* all essential cofactors, such as biotin, thiamine, riboflavin and NAD⁺ (Pohlmann et al., 2006). Two pathways for the biosynthesis of NAD⁺ in *R. eutropha* H16 can be performed, starting from aspartate or tryptophan, respectively. The synthesis of NAD(P)H could be performed by four transhydrogenases identified in the genome of this organism (Pohlmann et al., 2006). Additionally, continuous supply of regenerated NADH cofactor comes from the ability of *R. eutropha* H16 to utilize H₂. In nature, this molecular hydrogen arises, for example, from the metabolic activity of N₂-fixing microbes. This process is performed by two oxygen-tolerant NiFe hydrogenases, which oxidize H₂, providing the organism with energy and reductant (Lauterbach et al., 2013; Pohlmann et al., 2006). The principle of cofactor recycling based on oxidation of hydrogen by hydrogenase of *R. eutropha* H16 was used to catalyze electrochemical reduction of NAD⁺ (Cantet et al., 1996). Recently, the use of these enzymes has been shown for *in vivo* cofactor regeneration in an enzyme-coupled approach, where (*R*)-1,2-propanediol was successfully produced in cells of *R. eutropha* H16 by an alcohol dehydrogenase originating from *Kluyveromyces lactis* (Oda et al., 2013). Cofactor regeneration by use of molecular hydrogen is attractive because this reducing agent is cheap and doesn't give considerable by-products (Fig. 6).

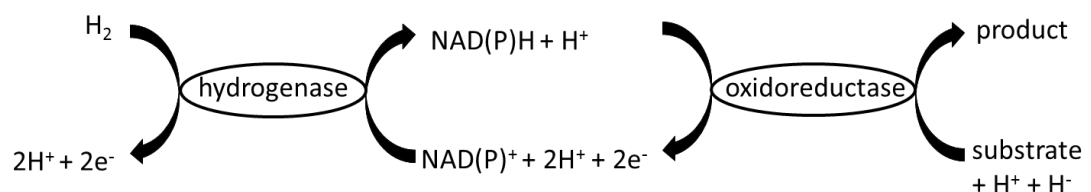


Figure 6. H₂-driven cofactor regeneration involving an NAD⁺-reducing hydrogenase coupled with an NADH-dependent oxidoreductase. All hydrogen atoms and electrons are included for the coupled enzymatic reaction; thereby, the hydride for substrate conversion comes from NADH. Picture taken from Lauterbach et al., 2013

Whole cells of *R. eutropha* that have been permeabilized with detergent have been used in combination with isolated horse liver ADH for reduction of cyclohexanone in a two-phase heptane/water system (Andersson et al., 1998). Another example is a combined two-species reaction system with permeabilized *R. eutropha* and *Gluconobacter oxydans* cells used for reduction of 2-octanone to (*S*)-2-octanol (Rundbäck et al., 2012).

Under lithoautotrophic growth conditions cells of *R. eutropha* H16 acquires a strong reduction potential as a result of hydrogenase activity (Buhrke et al., 2005; Lauterbach et al., 2013; Löwenstein et al., 2015). Interestingly, soluble hydrogenase of this bacterium could possibly also perform oxidation of NADH when there is an excess of NADH cofactors (Kuhn et al., 1984). These free cofactors can be applied for the NAD(P)H-dependent oxidoreductase reactions interesting from a biotechnological point of view. This approach for the generation of valuable products has not only the advantage of a natural cofactor recycling system but also significantly lowers the costs of the bioprocess, since the cells only need to be supplied with a mixture of hydrogen, oxygen and carbon dioxide.

1.1.5 Use of *R. eutropha* H16 in biotechnology

R. eutropha H16 first attracted biotechnological interest nearly 50 years ago with the realization that this organism can store carbon within its cytoplasm in the form of specialized polyhydroxyalkanoate (PHA) storage granules (Fig. 7). PHA granules usually consist of short chains of poly(3-hydroxybutyrate) (PHB) and poly(3-hydroxybutyrate-co-3-hydroxyvalerate) (PHBV) (Schlegel et al., 1961). PHB and other polyesters could be used for biodegradable plastics production. These granules are dynamic organelles and serve as a stockpile of organic carbon which can be used by the cells whenever carbon is needed (Pötter et al., 2004).

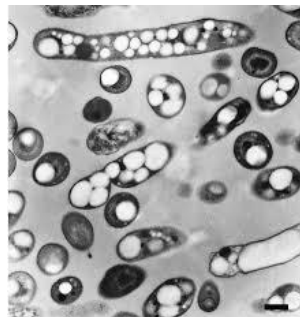


Figure 7. PHA granules in the cells of *R. eutropha* H16. Bar, 0.5 μm . Picture taken from Tian et al., 2005

This PHA storage in the cells represents an adaptation to changes in the O_2 levels (Reinecke and Steinbüchel, 2009). It was shown that granules are formed whenever an abundance of carbon is available, but other factors such as molecular oxygen, bound nitrogen or phosphate are growth-limiting (Pohlmann et al., 2006). Nowadays, the commercial production of the biodegradable thermoplastic Biopol from *R. eutropha* H16 is available (<http://www.metabolix.com>). These kinds of bio-plastics are highly desirable since they represent an example of “green technology”. Being a source of carbon sink and biodegradable, they also share desired properties of the traditionally produced plastics (Jajesniak et al., 2014). Many studies have been done by genetic engineering to obtain different types of PHA copolymers that exhibit better mechanical properties than PHB using diverse carbon sources such as plant oils, fructose or glycerol (Brigham et al., 2012c; Budde et al.,

2011; Fukui et al., 2014, 2002; Riedel et al., 2012). Up to 40% cellular dry weight of cyanophycin, a useful protein-like polymer, was obtained in *R. eutropha* strain H16 (Voss and Steinbüchel, 2006). Recently it was shown that a novel class of bioplastics, polythioesters, can be produced by this organism when fed with 3-mercaptopropionate or other organic thio chemicals (Lütke-Eversloh et al., 2002). Diverse and improved polymer production in this bacterium is an on-going topic which attracts new biotechnological approaches. System-level analysis of metabolic, regulatory and signalling networks, termed systems biotechnology, gives new targets and strategies for metabolic engineering for optimal production of bioproducts (Fig. 8) (Lee, 2006a).

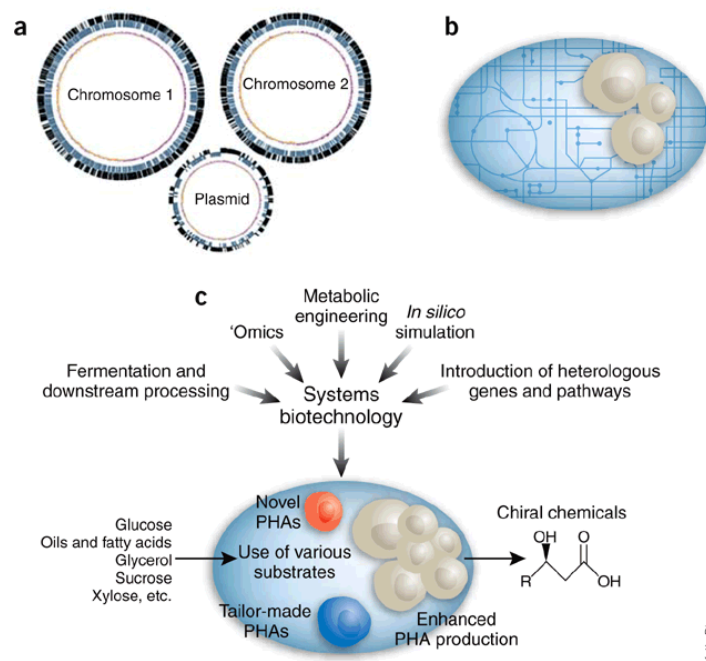


Figure 8. Systems biotechnology of PHA production in *R. eutropha* H16. Availability of the complete genome sequence (a) and a metabolic blueprint (b) of this microorganism provide the necessary tools for engineering improved strains (c). Improvements include increased production of PHAs, biosynthesis of new PHAs and the production of chiral chemicals for other applications. Picture taken from Lee, 2006b

As with all Proteobacteria, *R. eutropha* is known for its metabolic diversity (Sezenna, 2011). This nutritional versatility requires efficient overall control of the metabolism in order to perform fast flexible switches between different pathways (Bowien and Kusian, 2002). The different aspects of the versatile metabolism of *R. eutropha* H16 have been intensively studied in order to understand the regulatory networks that coordinate metabolic activity in response to ambient conditions (Cramm, 2008; Raberg et al., 2011; Riedel et al., 2014). As a result, this bacterium is a potential treasure of enzymes with undiscovered, highly interesting functions for industrial applications. *R. eutropha* H16 is an important model organism for the analysis of H_2 -/ CO_2 -based lithoautotrophy (Schwartz et al., 2009). It uses O_2 as a terminal electron acceptor, and this means, that all three of these hydrogenases are oxygen-tolerant in contrast to most other hydrogenases (Buhrke et al., 2005;

Burgdorf et al., 2006; Fritsch et al., 2013). Functionality at the presence of oxygen makes these enzymes perfect for biotechnological application, for example for the regeneration of NADH cofactors in an enzyme-coupled bioprocess (Lauterbach et al., 2013; Rundbäck et al., 2012). Recently, it was shown that membrane-bound hydrogenase of *R. eutropha* H16 can be used for establishing of biological fuel cells (Armstrong et al., 2006) and for light-driven production of H₂ from water by a hybrid protein complex (Ihara et al., 2006). Additionally, the use of *R. eutropha* H16 hydrogenase for the construction of an H₂-sensing device was shown (Lutz et al., 2005).

Apart from all mentioned applications, *R. eutropha* is also desired for its diverse carbon utilization pathways and its bio-compatibility for the production of medical compounds, for example, isotope-labelled compounds for use in medical diagnostics (Brigham et al., 2010; Lütte et al., 2012). Production of biomolecules labelled with stable isotopes has also been performed under lithoautotrophic growth conditions (Heumann, 2000). One of the most desired outcomes from *R. eutropha* is its ability to capture CO₂ and utilize it to produce chemicals of commercial value. These compounds, that can be produced in significant quantities from genetically modified *R. eutropha* H16, include ferulic acid, which is a precursor to vanillin biotransformation (Overhage et al., 2002) and 2-methylcitric acid, which is used in such pharmaceutical products like creams and antiperspirants and could also be a potential inhibitor for fast growing cancer cells (Ewering et al., 2006). Production of such biofuel molecules like isobutanol and 3-methyl-1-butanol from CO₂ using an integrated electromicrobial process with final yield of 1.4 g/L was performed in 2012 (Li et al., 2012). Later Müller and his colleagues engineered *R. eutropha* for the production of methyl ketones, the promising candidates for the diesel fuel blending agents. They achieved a productivity of 50–180 mg/L under chemolithoautotrophic growth conditions (Müller et al., 2013). *R. eutropha* H16 has several following characteristics which make this organism suitable for an industrial production of bio-based products: easy genetic manipulation, wide range of acceptable carbon sources, robust carbon storage pathway, ability to grow autotrophically, non-pathogenicity and resistance to some toxic compounds (Brigham et al., 2012c). The main carbon metabolism pathways of *R. eutropha* H16 regarding their use in industrial application are shown in Table 2.

Table 2. Some of the *R. eutropha* H16 carbon flux pathways and their relevance in biotechnological production of materials and chemicals. Table taken from Brigham et al., 2012b

Pathway	Relevance in biomaterials and bioproducts synthesis	References
Tricarboxylic acid (TCA) cycle	PHA biosynthesis; utilization of most carbon sources	(Yu and Si, 2004)
Calvin-Benson-Bassham	Production of biomaterials	(Bowien and Kusian, 2002)

cycle	and chemicals from CO ₂	
Entner-Doudoroff pathway	Utilization of sugars for growth and product formation	(Lee et al., 2003)
Fatty acid β-oxidation	Production of biomaterials and chemicals from triacylglycerols and fatty acids	(Brigham et al., 2010)
Glyoxylate cycle	Utilization of acetate/acetyl-CoA (incl. β-oxidation by-products)	(Wang et al., 2003) (Yu and Si, 2004)
Branched chain amino acid biosynthesis	Production of branched carbon chain products (e.g. isobutanol)	(Li et al., 2012) (Lu et al., 2012)
		(Brigham et al., 2012a)

Additionally, it should be mentioned, that *R. eutropha* H16, as a typical aerobic H₂ oxidizer, is easy to handle compared to obligate anaerobe. Grown heterotrophically it can reach very high cell density of more than 200 g/L (Reinecke and Steinbüchel, 2009). It's also important, that *R. eutropha* H16 has never been recognized as a human, animal or plant pathogen, and therefore has good potential for use in production processes (Pohlmann et al., 2006).

1.1.6 Expression systems for *R. eutropha*

Despite the biotechnological significance of *R. eutropha* and great potential in production of desired compounds directly from CO₂, there has been for a long time an absence of diverse genetic toolbox for this organism. A number of different plasmid systems have been characterized for expression in *R. eutropha* H16, both for autonomous replication and for integration into the genome (Srinivasan et al., 2002; Voss and Steinbüchel, 2006). The commonly used inducible expression system for *R. eutropha* is a pBBR1-derived vector with a *P_{BAD}* promoter (Delamarre and Batt, 2006). Two years ago, Bi et al. reported a set of plasmids bearing a variety of origins of replication (pCM62 (IncP), pBBR1, pKT (IncQ)), promoters (*P_{BAD}*, *P_{T7}*, *P_{XylS/PM}*, *P_{IacUV5}*) and ribosomal binding sites (Bi et al., 2013). All these genetic elements were analysed and characterized in details. Additionally, Bi and co-authors managed to use isopropyl-β-D-thiogalactopyranosid (IPTG)-inducible expression system for *R. eutropha* H16 strain, which normally lacks the galactose permease gene *lacY* responsible for ability to transport lactose or its analogue IPTG through the cell membrane (Fritsch et al., 2011). Other reported inducible expression systems are based on induction of *BAD* promoter by L-arabinose, the *phaP* promoter, induced by phosphate depletion during PHB synthesis and the *cbbL* promoter that is induced under chemolithoautotrophic conditions (Barnard et al., 2004; Fukui et al., 2002; Lütte et al., 2012).

Recent studies performed by Gruber and co-workers, made available additional versatile expression plasmids (Gruber et al., 2015, 2014, unpublished data). These stably maintained plasmid expression vectors are based on replication systems exhibiting different copy numbers and a choice of suitable promoters that facilitate well-tuned homologous and heterologous protein expression at desired levels. The partitioning region of the plasmid RP4 was included into constructs to stabilize these expression vectors. The bacteriophage T5 derived promoters, especially P_{j5} , were found to be the strongest among those ever applied with *R. eutropha* H16 under constitutive expression conditions (Gruber et al., 2014). Expression of the recombinant protein eGFP under the control of P_{j5} was four times stronger when compared to the expression under the control of P_{Tac} . In the following, fine-tuneable inducible expression system based on cumate operator/repressor or *lacO/lacI* was developed to regulate expression in precise manner and thereby to increase the final product yield (Gruber et al., manuscript in preparation).

On the base of previously performed studies it can be seen, that proper choice of expression system can significantly increase the yield of the desirable products in *R. eutropha* H16 and can help to reveal the whole biotechnological potential of this unique bacterium (Gruber et al., 2014; Jajesniak et al., 2014).

1.2. Oxidoreductases

1.2.1. Classification of the enzymes

Enzymes are biological catalysts which accelerate chemical reactions. Most of the enzymes are protein macromolecules, though RNA catalytic molecules, named ribozymes, have also been identified (Kruger et al., 1982). According to the International Union of Biochemistry and Molecular Biology (IUBMB), all enzymes are classified on the basis of the reaction type they perform. Altogether, six groups of enzymes are known (Fig. 9):

EC 1 – Oxidoreductases. They transfer hydrogen and oxygen atoms or electrons from one substrate to another.

EC 2 – Transferases. These enzymes transfer a specific group from one substrate to another.

EC 3 – Hydrolases. This group of enzymes catalyses the hydrolysis of a chemical bond.

EC 4 – Isomerases. This group of enzymes change a molecular form of the substrate.

EC 5 – Lyases (or Synthases). Lyases non-hydrolytically remove a group or add it to a substrate.

EC 6 – Ligases (or Synthetases). They join two molecules by the formation of new bonds.

Class	Reaction type	Important subclasses
1 Oxidoreductases	<p>○ = Reduction equivalent</p>	Dehydrogenases Oxidases, peroxidases Reductases Monoxygenases Dioxygenases
2 Transferases		C-Transferases Glycosyltransferases Aminotransferases Phosphotransferases
3 Hydrolases		Esterases Glycosidases Peptidases Amidases
4 Lyases ("synthases")		C-C-Lyases C-O-Lyases C-N-Lyases C-S-Lyases
5 Isomerases		Epimerases <i>cis trans</i> Isomerases Intramolecular transferases
6 Ligases ("synthetases")		C-C-Ligases C-O-Ligases C-N-Ligases C-S-Ligases

Figure 9. Classification of the enzymes according IUBMB. Picture was downloaded from <http://www.namrata.co/classification-of-enzymes/> on 01.01.2015

Oxidoreductases are widely distributed in all forms of life. For example, in *R. eutropha* H16 genes encoding oxidoreductases represent the largest part of all enzymes present in the genome of this bacterium (Fig. 10).

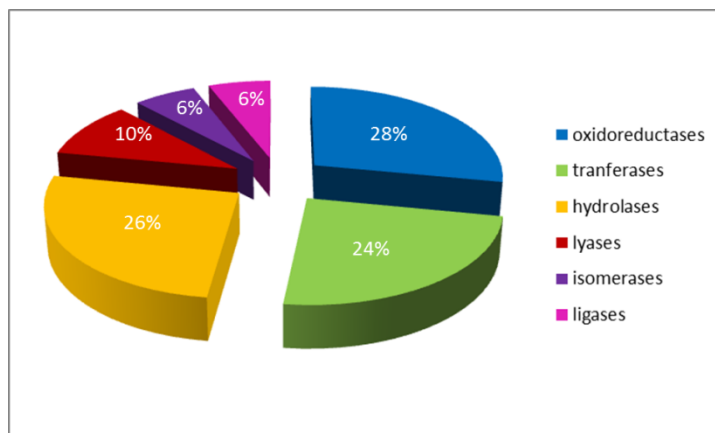


Figure 10. Distribution of the different types of IUBMB enzyme classes of *R. eutropha* H16 according to UniProtKB

Oxidoreductases catalyse transfer of electrons or redox equivalents from one molecule, the reductant, also called the electron donor, to another, the oxidant, also called the electron acceptor (NC-IUBMB, 2015). A scheme for oxidoreductase reaction is shown below:



In the given example, A is the reductant (electron donor) and B is the oxidant (electron acceptor).

The recommended name for these enzymes is “*dehydrogenase*” whenever possible but “*reductase*” can also be used. Term “*oxidase*” is used when molecular oxygen acts as acceptor for reduction (Aehle, 2006). Oxidoreductases themselves are divided in 22 subclasses. Additionally, there is the subclass ([EC 1.97](#)) which is reserved for oxidoreductases not included in the previous categories. In some cases the classification is difficult as specificity towards the acceptor is missing. One of the main representatives of oxidoreductases are NAD(P)(H)-dependent oxidoreductases. A significant part of this enzyme class is represented by the short-chain dehydrogenases/reductases superfamily (SDR) (Jörnvall et al., 1999). This group of enzymes is classified according to their structure, mechanism of action and, in most cases, the size of the protein monomer. However, it should be noticed that the division is not straightforward since lyases and isomerases may also contain the motif similar to oxidoreductases of SDR superfamily (Kavanagh et al., 2008).

1.2.2. Short-chain dehydrogenases/reductases

Short-chain dehydrogenases/reductases represent a part of a large, functionally diverse class of NAD(P)(H)-dependent oxidoreductases, distinct from the medium-chain dehydrogenase (MDR) and aldo-keto reductase (AKR) superfamilies. They represent one of the largest protein families

known so far. SDRs were established as a separate group of oxidoreductases in the 1970/80s and got their name in 1991 (Persson et al., 2009). SDR has the simplest build-up and widest spread in nature, suggesting a very early origin from $\alpha\beta$ elements to a Rossmann-fold domain in the universal cellular ancestor for subsequent Darwinian evolution in the cells of different kingdoms of life (Jörnvall et al., 2010). They metabolize a wide range of substrates, such as alcohols, aldehydes, ketones, steroids, polycyclic aromatic hydrocarbons and retinoids (Jörnvall et al., 1999; Kallberg et al., 2002; Kavanagh et al., 2008). The number of identified SDRs is permanently growing and up to now there are over 140.000 SDRs members listed in the sequence databases (Jörnvall et al., 2015). These enzymes typically have a size between 250 and 300 amino acid residues. Their sequence identities between each other are low and represent about 15-30%. Nevertheless, 3D structures show highly similar α/β -folding patterns with a central β -sheet, which is typical for the Rossmann-fold (Fig. 11) (Oppermann et al., 2003).

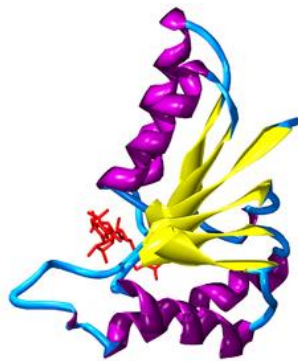


Figure 11. Rossmann fold in part of the lactate dehydrogenase of *Cryptosporidium parvum*, showing NAD⁺ in red, beta sheets in yellow, and alpha helices in purple. Picture taken from Senkovich et al., 2005

All members of this superfamily possess this common structural motif for the nucleotide binding, which includes the TGxxxGxG co-factor binding sequence (Kavanagh et al., 2008). A further common feature is the YXXXK active site motif, which can be slightly altered within different SDRs subfamilies. Altogether five of these subfamilies have been characterized, based on the sequence composition of the cofactor binding domain and of the active catalytic site: classical, extended, intermediate, divergent and complex SDRs (Kallberg et al., 2002) (Table 3). Recently two more subfamilies were denoted: “atypical” and “unknown” (Persson et al., 2009).

Table 3. Cofactor and active site sequence motifs for the five SDR subfamilies. Table taken from Kavanagh et al., 2008

Subfamily	Cofactor binding	Active site
‘classical’	TGxxx[AG]xG	YxxxK
‘extended’	[ST]GxxGxxG	YxxxK

'intermediate'	[GA]xxGxx[GA]	YxxxK
'divergent'	GxxxxxSxA	YxxMxxxK
'complex'	GGxGxxG	YxxxN

'x' is any amino acid residue. Brackets mark alternatives that can be present or absent

Classical and extended SDRs are the major types of SDR subfamilies and can be further divided into groups (Table 4). First of all, there are NAD(H)- and NADP(H)-binding classical and extended SDRs. NAD(H)-binding classical SDR proteins are split in 4 groups depending on the position of the acidic residue after second β -sheet: cD1d, cD1e, cD2 and cD3. NADP(H)-binding SDRs are assigned in cP1, cP2 and cP3 groups. Sequences with a basic residue in the Gly-motif belong to the group cP1, while those with a basic residue adjacent to the second β -strand are part of the group cP2. Sequences with basic residues at both of these key positions are sorted into group cP3. For the extended SDRs, altogether three different groups were defined: two NAD(H)-binding and one NADP(H)-binding. NAD(H)-binding eD1 group members have an acidic residue at the end of second β -sheet. Another NAD(H)-binding group eD2 representatives have an acidic residue two amino acid positions downchain. The third group eP1 consists of NADP(H)-bound sequences which have a basic residue adjacent to the second β -sheet (Persson, 2002; Persson et al., 2003).

Table 4. Key positions for assignments of coenzyme specificity for classical and extended SDRs.
Table modified from Persson *et al.*, 2003

Subfamily	Coenzyme	Group	Key AAs location	
			Gly-motif	Second β -sheet
Classical	NAD(H)	cD1d		D
		cD1e		E
		cD2		D/E
		cD3		D/E
	NADP(H)	cP1	K/R	
		cP2		K/R
		cP3	K/R	K/R
Extended	NAD(H)	eD1		D/E
		eD2		D/E
	NADP(H)	eP1		K/R

Regarding biotechnological applications, SDR enzymes are of considerable interest and are useful as potential catalysts for the production of optically pure compounds, as well as in the bioremediation of halogenated aliphatics that are found in polluted soil and water (Persson et al.,

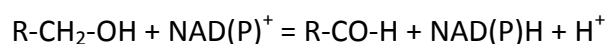
2009). SDRs constitute an enzyme class, which is highly attractive for pharmaceutical industry (Kavanagh et al., 2008; May and Padgette, 1983).

1.2.2.1. Alcohol dehydrogenases. General information and mechanism of action

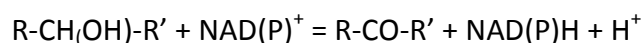
Short-chain alcohol dehydrogenases (ADHs) are representatives of the SDR superfamily. However, it should be considered that there is also a group of medium-chain alcohol dehydrogenases. In fact, knowledge of SDR and MDR as separate superfamilies with different mechanism of action and size started with the observation of alcohol dehydrogenases. It was shown that an ADH originating from fruit fly clearly differs from ADHs from human liver or yeast (Jörnvall et al., 1981). Further studies revealed two distinct groups of enzymes which are now known as SDRs and MDRs (Jörnvall and Persson, 1995; Jörnvall et al., 1999).

Alcohol dehydrogenases belong to EC 1.1.1 - oxidoreductases acting on the hydroxyl group of donors with NAD(P)⁺ as acceptor (NC-IUBMB, 2015). In detail, ADHs perform interconversion between alcohols and aldehydes or ketones with the reduction of NAD(P)⁺ to NAD(P)H:

a) primary alcohol is oxidized into an aldehyde



b) secondary alcohol is oxidized into a ketone



The reactions of many NAD(P)⁺-linked dehydrogenases start with binding of the respective coenzyme to the free enzyme. Short-chain ADHs, like all other SDRs, are usually homotetramers and each subunit contains one active site, therefore, four coenzymes act on one enzyme unit (Verstraete et al., 2013). After cofactor binding, alcohols, aldehydes or ketones bind the corresponding binary enzyme–NAD(P)⁺ or enzyme–NAD(P)H complexes (Persson, 2002; Tanaka et al., 2001). The Rossmann-fold domain and particularly the Gly-rich motif play a crucial role in connection with FAD, NAD or NADP cofactors (Fig. 12). The Rossmann fold belongs to one of the most common and widely distributed super-secondary structures. This domain normally consists of seven parallel beta strands and a variable number of alpha helices. The initial beta-alpha-beta (β α β) fold is the most conserved segment and is called an "adenosine diphosphate (ADP)-binding β α β fold" (Hanukoglu, 2015).

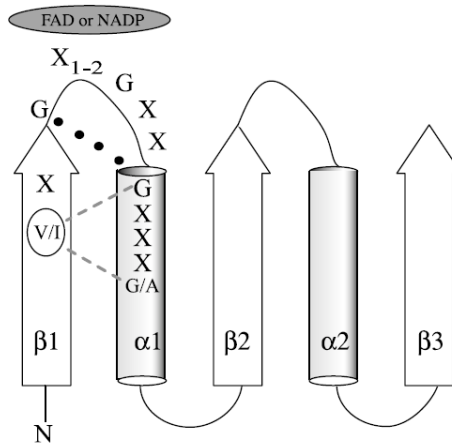


Figure 12. Secondary structure and sequence motifs of the FAD or NAD(P)-binding Rossmann fold. Black-dotted line shows a C^α-H · · · O hydrogen bond; gray- broken lines form van der Waals interactions with a residue located on β-strand 1 (this residue is either valine or isoleucine). Picture taken from Kleiger and Eisenberg, 2002

After the binding of the coenzyme, the pyrophosphate moiety of NAD(P)H is fixed on the GxxxGxG motif. Several hydrogen bonds connect the pyrophosphate to the protein. This connection causes the sharp turn of the polypeptide (Tanaka et al., 2001).

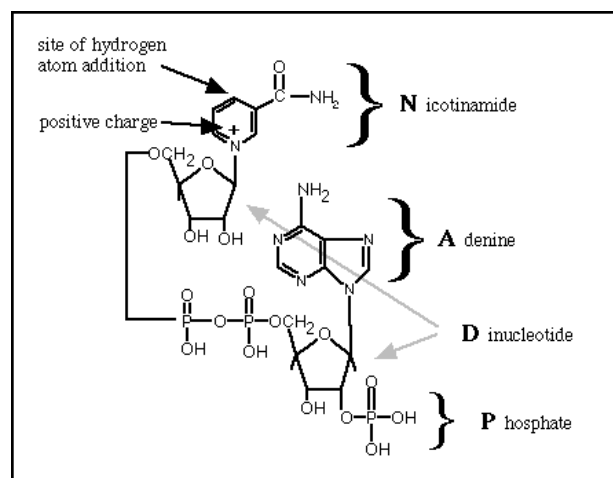


Figure 13. Chemical formula of NADP⁺. The NAD(P)⁺ molecule consists of adenine dinucleotide with an attached nicotinamide; additional phosphate group is present in case of NADP⁺. Picture was downloaded from <http://bio.davidson.edu/courses/Bio111/NADPH.html> on 01.10.2015

The nicotinamide part of NAD(P)⁺ (Fig. 13) is buried in the active site cavity. This active site is highly conserved among all members of the SDR superfamily and is called ‘Ser-Tyr-Lys triad’. Catalytic Ser and Tyr directly interact with the susceptible group of the substrate: the hydroxyl group of an alcohol molecule creates hydrogen bonds to the hydroxyl groups of Ser and Tyr (Fig. 14). The side chain of Lys is hydrogen bonded to the two hydroxyl groups of the nicotinamide ribose. The C-terminal sequence of the protein specifies substrate preferences of the enzyme (Kavanagh et al., 2008). The proposed mechanism of hydrogen binding is shown in Figure 14. The deprotonated Tyr

residue extracts hydrogen from the OH- group of the substrate. This initial Tyr deprotonation must occur at the optimum pH (~8-9) of the dehydrogenase reactions of the SDR enzymes and, therefore, depends on the environmental conditions. It's likely, that the positively charged side chain of the conserved Lys residue and possibly NAD(P)⁺ also influence the process of the Tyr deprotonation. At the same time when Tyr extracts the hydrogen from the OH- group of the substrate, NAD(P)⁺ accepts a second hydrogen of the substrate on the nicotinamide ring. As a result, the product (C=O) and NAD(P)H are produced (Kavanagh et al., 2008; Tanaka et al., 2001).

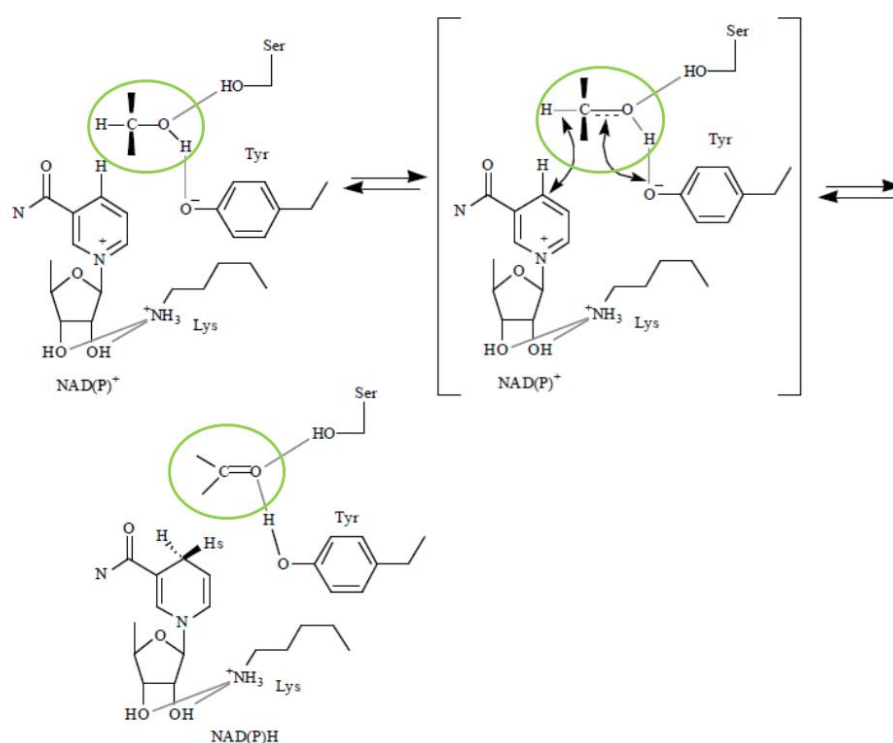


Figure 14. Proposed catalytic mechanism for the SDR enzymes with 2-propanol as a substrate. The susceptible part of the substrate, the 'Ser-Tyr-Lys triad', and the nicotinamide nucleoside moiety of NAD(P)⁺ (or NAD(P)H) are shown. The substrate and the resulting product are shown in green circles. Picture taken from Tanaka et al., 2001

1.2.3. Aldo-keto reductases

1.2.3.1. General information

The reduction of aldehydes and ketones to primary and secondary alcohols are often catalysed not only by short-chain dehydrogenases/reductases (SDRs) but also by aldo-keto reductases (AKRs). The aldo-keto reductase superfamily is a group of enzymes that includes a number of related NAD(P)H-dependent oxidoreductases. They are present in almost all forms of life. Most of them are soluble and monomeric (Mindnich and Penning, 2009). The enzymes have a broad substrate specificity and transform sugar and lipid aldehydes, keto-steroids, keto-prostaglandin and chemical carcinogens, e.g., nicotine derived nitrosamines as well as carcinogen metabolites (Penning, 2014). Members of

this superfamily show a triose-phosphate isomerase (TIM) barrel, also known as a $(\alpha\beta)_8$ -barrel and originally observed in triose-phosphate isomerase, with several additional helices in their structure (Fig. 15). The active site is formed by a conserved catalytic tetrad of Tyr, Lys, His, Asp. 16 groups of AKRs are identified based on the protein function and sequence identity, as for example, AKR9 group includes aryl alcohol dehydrogenases. Within any of these groups members share more than 40% homology with each other. In contrast, compared to the members of other groups, given enzymes have less than 40% homology (Hyndman et al., 2003).

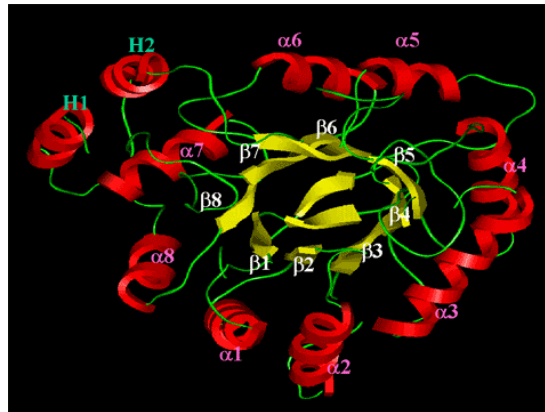


Figure 15. The $(\alpha\beta)_8$ -barrel motif of aldoketo reductases (AKRs). H1 and H2 represent additional helices typical for members of this superfamily. Picture was downloaded from https://www.med.upenn.edu/akr/akr_graphic.html on 01.10.2015

1.2.3.2. Mechanism of action

Initial step of the chemical reaction catalysed by AKRs includes binding of a cofactor to an enzyme at the first step. Afterwards substrate joins the complex and stay there until the end of its transformation into the product. At the last step, when the product leaves, the cofactor-enzyme complex dissociates (Barski et al., 2008).

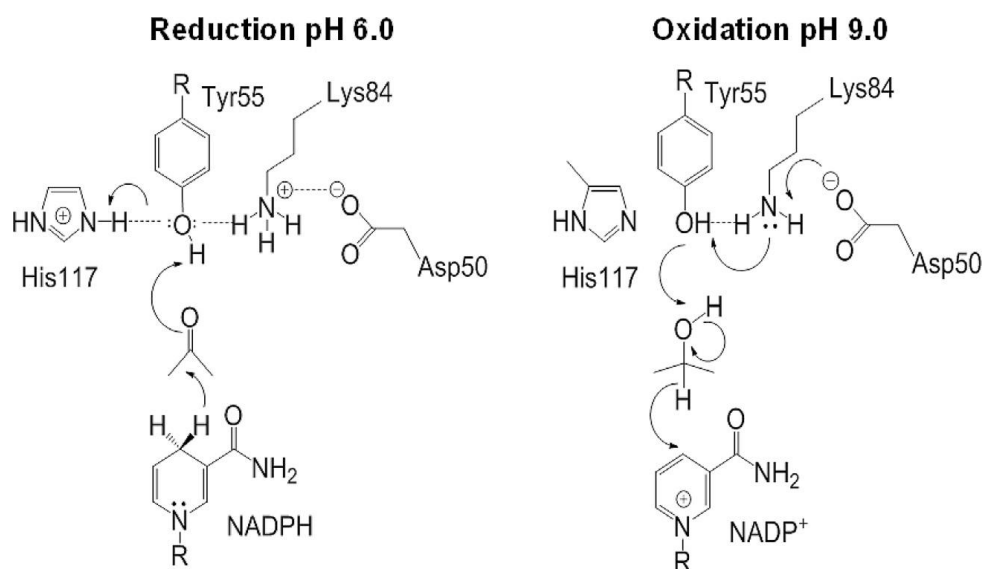


Figure 16. “Push–Pull” mechanism for acid–base catalysis in AKRs. Left: reduction of a carbonyl requires Tyr55 to act as a general acid facilitated by His117; right: oxidation of an alcohol requires Tyr 55 to act as a general base facilitated by Lys 84 and Asp 50. Amino acid numbering according to rat 3- α hydroxysteroid dehydrogenase AKR1C9. Picture taken from Penning, 2014

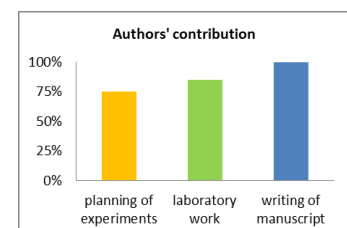
In the reduction direction, the 4-pro-R hydride from NAD(P)H is taken by the substrate carbonyl group, at the same time, the carbonyl oxygen is protonated by a conserved tyrosine acting as a general acid (Fig. 16). In the oxidation direction the catalytic Tyr is deprotonated by Lys and as a consequence, tyrosine gets the proton back from an alcohol. At the same time the second hydride from the substrate is trapped by NAD(P)⁺. As it can be seen, the microenvironment is important for the direction of the reaction since it makes catalytic Tyr exhibiting more or less of acidic properties (Penning, 2014). However, it should be mentioned that despite the fact that AKRs are capable of performing both ways of oxidoreductase reaction, it was shown that *in vivo* they likely act solely as reductase since in metabolically active cells, NADP(H) is given mostly in the reduced form. Additionally, AKRs prefer NADPH over NADH as coenzyme (Barski et al., 2008).

2. Aim of the study

The focus of this project was, on the one hand, to explore the great diversity of oxidoreductases of *R. eutropha* H16 in terms of novel biotechnologically interesting enzymes. The available genome of *R. eutropha* H16 provides a good basis to identify the enzymes capable of performing reactions which might lead to new industrial processes. These reactions include oxidation of secondary alcohols, converting substrates with sterically demanding residues, reduction of long chain and aromatic ketones, as well as aldehydes. A set of enzymes will be chosen for the detailed characterization towards their substrate specificity and enantioselectivity. On the other hand, the reduction reactions by homologously overexpressed enzymes are of interest to be performed under lithoautotrophic growth conditions by using H₂ and CO₂ as the sources of energy and carbon. The particular concern was establishing *R. eutropha* H16 as a cell factory for performance of the oxidoreductase reactions by overexpression of homologous and/or heterologous enzymes with efficient cofactor regeneration by hydrogen.

3. Results

3.1. Homologous and heterologous expression of oxidoreductases of *Ralstonia eutropha* H16



Editing and additional suggestions for writing of manuscript were provided by Dr. P. Heidinger and Prof. H. Schwab

3.1.1. Introduction

Ralstonia eutropha H16 is a promising organism for biotechnology. It can use H₂ and CO₂ as sole sources of energy and carbon in the absence of organic substrates. Furthermore this bacterium has already been applied for the production of biodegradable polyhydroxyalkanoates on an industrial scale (Brigham et al., 2011; Steinbüchel, 2001). *R. eutropha* also serves as a model organism for the mechanisms involved in the control of autotrophic carbon dioxide fixation, hydrogen oxidation and denitrification.

One of the main types of oxidoreductase reactions is performed by dehydrogenases, which have a wide range of possible biotechnological applications. Biotransformations involving the interconversion of alcohols, aldehydes and ketones have great potential for the commercial production of pure optically active compounds and also for other processes such as the treatment of industrial effluents. Moreover recently it was shown that reduction of certain aldehydes in modified strain of *R. eutropha* H16 can be used for the production of alternative biofuel (Lu et al., 2012).

3.1.2. Materials and methods

3.1.2.1. Bacterial strains and cultivation conditions

Bacterial strains used in this study are listed in Table 5. *E. coli* strains created in this study were handed over to IMBT strain collection under the indicated numbers (Supplementary Table 1).

Table 5. Bacterial strains used in this study.

Strain	Genotype	Reference
<i>Ralstonia eutropha</i>		
H16	Wild-type <i>R. eutropha</i> , gentamicin resistant (Gm ^r)	DSMZ 428 ¹
<i>Escherichia coli</i>		
TOP10	F' mcrA Δ(mr(R)-hsdRM(S)-mcrBC) φ80lacZΔM15 ΔlacX74 nupG recA1 araD139 Δ(ara-leu)7697 galE15 galK16 rpsL(Str ^R) endA1 λ ⁻	Invitrogen
BL21	F' Δcm ompT hsdS(r _B ⁻ m _B ⁻) gal [malB ⁺] _{K-12} (λ ^S)	Invitrogen
S17-1	TpR SmR recA, thi, pro, hsdR-M+RP4: 2-Tc:Mu: Km Tn7	#679 IMBT strain collection
HB101	Helper strain; F- λ- hsdS20(r _B ⁻ m _B ⁻) recA13 leuB6(Am) araC14 Δ(gpt-proA)62 lacY1 galK2(Oc) xyl-5 mtl-1 thiE1 rpsL20(SmR) glnX44(AS)	(Boyer <i>et al.</i> , 1969)

¹Deutsche Sammlung von Mikroorganismen und Zellkulturen

All chemicals, reagents and basic media components were obtained from Becton, Dickinson and Company (Franklin Lakes, NJ, USA), Sigma-Aldrich (St. Luis, MO, USA) and Carl Roth (Arlenheim, Germany), respectively, unless mentioned otherwise.

E. coli Top10 and *E. coli* S17-1 cells were used for cloning experiments and amplification of expression vectors. *E. coli* BL21 cells were used for protein expression experiments. *E. coli* HB101 was used for mating experiments with *R. eutropha* H16.

E. coli strains were propagated at 37°C at 120 rpm in lysogeny broth (LB). *R. eutropha* H16 strains were grown at 28°C at 100 rpm in tryptic soy broth (TSB) supplemented with 20 µg/ml gentamicin under heterotrophic growth conditions and in MSM (minimal salt medium) supplemented with 20 µg/ml gentamicin under lithoautotrophic growth conditions. Gas atmosphere for lithoautotrophic growth included 10% CO₂, 10% O₂ and 80% H₂. Pre-cultures for the lithoautotrophic growth were inoculated by the harvested cells of 5 mL ONCs heterotrophically

grown in MSM medium supplemented with 0.6 % fructose. For antibiotic selection kanamycin was added when necessary in a concentration of 40 µg/ml for *E. coli* strains and 200 µg/ml for *R. eutropha* H16 strains. For protein expression experiments 1 % glucose was added into the LB media for *E. coli* strains and 0.6 % fructose into TSB or MSM media for *R. eutropha* H16 strains (Table 6). Medium was solidified with 20g/l agar-agar (Carl Roth, Arlesheim, Germany) when needed.

Table 6. Media composition

Media	Composition
LB	Yeast extract (5 g/L), Trypton (10 g/L), Sodium chloride (0,5–10 g/L)
TSB	Bacto Trypton (17.0 g/L), Bacto Soyton (3.0 g/L), Dextrose (2.5 g/L), Sodium chloride (5.0 g/L), Dipotassium hydrogen phosphate (2.5 g/L)
MSM	<p><u>Solution A (30x)</u>: Na₂HPO₄ x12 H₂O (270 g/L), KH₂PO₄ (45 g/L)</p> <p><u>Solution B (30x)</u>: MgSO₄ x 7H₂O (6 g/L), NH₄Cl (60g /L), Fe(III)NH₄-Citrat (125 mg/L), SL7 (30 mL)</p> <p><u>Solution C (100x)</u>: CaCl₂ x 2H₂O (250 mg), ad 250 mL</p> <p><u>Trace elements solution (SL7)</u>: 25 % (w/v) HCl (1.3 mL/L), H₃BO₃ (62 mg/L), CoCl₂ x 6H₂O (190 mg/L), CuCl₂ x 2H₂O (17 mg/L), MnCl₂ x 4H₂O (100 mg/L), Na₂MoO₄ x 2H₂O (36 mg/L), NiCl₂ x 6H₂O (24 mg/L), Zn Cl₂ (70 mg/L); pH 6,5</p> <p>Mix solution A and B with ddH₂O (1:1:28), pH7.0; after autoclaving add 0.01 volume of an sterile filtered solution C</p>

All standard chemicals are from Carl Roth GmbH CO. KG. Exceptions are mentioned in the text.

3.1.2.2. Plasmids and primers used in this study

Table 7. Plasmids used in this study

Plasmid	Number in internal list of plasmids	Description	Reference
pRK2013	195	Km ^r , <i>colE1</i>	(Figurski and Helinski, 1979)
pK470Δ	94	Km ^r , <i>P_{tac}</i> , <i>lacI</i>	this study
pK470-ADH A1	36	Km ^r , <i>P_{tac}</i> , <i>lacI</i> , <i>H16_A0757</i>	this study
pK470-ADH A3	100	Km ^r , <i>P_{tac}</i> , <i>lacI</i> , <i>H16_A0861</i>	this study
pK470-ADH A4	58	Km ^r , <i>P_{tac}</i> , <i>lacI</i> , <i>H16_A0602</i>	this study
pK470-ADH A5	45	Km ^r , <i>P_{tac}</i> , <i>lacI</i> , <i>H16_A1168</i>	this study
pK470-ADH B1	101	Km ^r , <i>P_{tac}</i> , <i>lacI</i> , <i>H16_B0663</i>	this study
pK470-ADH B2	84	Km ^r , <i>P_{tac}</i> , <i>lacI</i> , <i>H16_B1834</i>	this study
pK470-ADH B5	57	Km ^r , <i>P_{tac}</i> , <i>lacI</i> , <i>H16_B0517</i>	this study

pK470-ADH B6	37	$Km^r, P_{tac}, lacI, H16_B1699$	this study
pK470-ADH B8	38	$Km^r, P_{tac}, lacI, H16_B2470$	this study
pK470-ADH P1	102	$Km^r, P_{tac}, lacI, H16_PHG229$	this study
pK470-ADH P2	42	$Km^r, P_{tac}, lacI, H16_PHG230$	this study
pK470-SDR A1	61	$Km^r, P_{tac}, lacI, H16_A3164$	this study
pK470-SDR A2	60	$Km^r, P_{tac}, lacI, H16_A1888$	this study
pK470-SDR A3	82	$Km^r, P_{tac}, lacI, H16_A1490$	this study
pK470-SDR A4	55	$Km^r, P_{tac}, lacI, H16_A0874$	this study
pK470-SDR B1	56	$Km^r, P_{tac}, lacI, H16_B1732$	this study
pK470-SDR B2	103	$Km^r, P_{tac}, lacI, H16_B1767$	this study
pK470-SDR B3	59	$Km^r, P_{tac}, lacI, H16_B1297$	this study
pK470-SDR B4	44	$Km^r, P_{tac}, lacI, H16_B2339$	this study
pK470-SDR B6	29	$Km^r, P_{tac}, lacI, H16_B0101$	this study
pK470-SDR B7	83	$Km^r, P_{tac}, lacI, H16_B0634$	this study
pK470-SDR B9	30	$Km^r, P_{tac}, lacI, H16_B0630$	this study
pK470-SDR B11	48	$Km^r, P_{tac}, lacI, H16_B1240$	this study
pK470-RED A1	43	$Km^r, P_{tac}, lacI, H16_A2592$	this study
pK470-RED A2	34	$Km^r, P_{tac}, lacI, H16_A3136$	this study
pK470-RED A4	105	$Km^r, P_{tac}, lacI, H16_A3600$	this study
pK470-RED A5	33	$Km^r, P_{tac}, lacI, H16_A3186$	this study
pK470-RED A6	106	$Km^r, P_{tac}, lacI, H16_A2132$	this study
pK470-RED A9	107	$Km^r, P_{tac}, lacI, H16_A1400$	this study
pK470-RED A10	81	$Km^r, P_{tac}, lacI, H16_A1814$	this study
pK470-RED A11	41	$Km^r, P_{tac}, lacI, H16_A1960$	this study
pK470-RED B1	108	$Km^r, P_{tac}, lacI, H16_B1974$	this study
pK470-RED B4	39	$Km^r, P_{tac}, lacI, H16_B2508$	this study
pK470-His ₆ -ADH A5	104	$Km^r, P_{tac}, lacI,$ N-terminally 6xHis-tagged <i>H16_A1168</i>	this study
pK470-His ₆ -SDR A1	77	$Km^r, P_{tac}, lacI, H16_A3164,$	(Zach, 2013)

		N-terminal His tag coding sequence	
pK470-His ₆ SDR B3	78	Km ^r , P _{tac} , <i>lacI</i> , H16_B1297,	(Zach, 2013)
		N-terminal His tag coding sequence	
pK470-His ₆ -SDR B6	135	Km ^r , P _{tac} , <i>lacI</i> , H16_B0101,	this study
		N-terminal His tag coding sequence	

Expression vectors for *R. eutropha* H16

Expression vectors for *R. eutropha* H16 with encoded *LacI* repressor

pKR-P _{tac} -delEstC	3	Km ^r , P _{tac} , <i>oriV</i> REP, <i>lacI</i>	by S. Gruber
		cloning vector for <i>E. coli</i> and <i>R. eutropha</i> H16	
pKR-P _{tac} -ADH A4	*	Km ^r , P _{tac} , <i>oriV</i> REP, <i>lacI</i> , H16_A0602	this study
		cloning vector for <i>E. coli</i> and <i>R. eutropha</i> H16	
pKR-P _{tac} -ADH A5	*	Km ^r , P _{tac} , <i>oriV</i> REP, <i>lacI</i> , <i>par</i> 29.1, H16_A1168	this study
		cloning vector for <i>E. coli</i> and <i>R. eutropha</i> H16	

Expression vectors for *R. eutropha* H16 with encoded *LacI* repressor and *Par*29.1 region

pKR-P _{tac} - <i>par</i> 29.1-ADH A3	*	Km ^r , P _{tac} , <i>oriV</i> REP, <i>par</i> 29.1, <i>lacI</i> , H16_A0861	this study
		cloning vector for <i>E. coli</i> and <i>R. eutropha</i> H16	
pKR-P _{tac} - <i>par</i> 29.1-ADH A4	*	Km ^r , P _{tac} , <i>oriV</i> REP, <i>par</i> 29.1, <i>lacI</i> , H16_A0861	this study
		cloning vector for <i>E. coli</i> and <i>R. eutropha</i> H16	

Expression vectors for *R. eutropha* H16 with deleted *LacI* repressor and complete *Par* region

pKR-P _{tac} - Δ <i>lacI</i> - <i>par</i> -ADH A4	339	Km ^r , P _{tac} , <i>oriV</i> REP, H16_A0602, <i>par</i> , Δ <i>lacI</i>	cloning and expression vector for <i>E. coli</i> and <i>R. eutropha</i> H16	this study
pKR-P _{tac} - Δ <i>lacI</i> - <i>par</i> -ADH A5	340	Km ^r , P _{tac} , <i>oriV</i> REP, H16_A1168, <i>par</i> , Δ <i>lacI</i>	cloning and expression vector for <i>E. coli</i> and <i>R. eutropha</i> H16	this study
pKR-P _{tac} - Δ <i>lacI</i> - <i>par</i> -His ₆ -SDR B3	117	Km ^r , P _{tac} , <i>oriV</i> REP, H16_B1297,	N-terminal His tag coding sequence,	this study
		<i>par</i> , Δ <i>lacI</i>	cloning and expression vector for <i>E. coli</i> and <i>R. eutropha</i> H16	
pKR-P _{lac} - Δ <i>lacI</i> - <i>par</i> -His ₆ -SDR B3	118	Km ^r , P _{lac} , <i>oriV</i> REP, H16_B1297,	N-terminal His tag coding sequence,	this study
		<i>par</i> , Δ <i>lacI</i> ,	cloning and expression vector for <i>E. coli</i> and <i>R. eutropha</i> H16	

Plasmids created to use IPTG-inducible T7 expression system for *R. eutropha* H16

pKR-P _{tac} - <i>par</i> -T7MCS- <i>lacI</i> -His ₆ -SDR B3	128	cloning and expression vector for <i>E. coli</i> and <i>R. eutropha</i> H16, encoding the T7MCS consisting of T7 promoter, T7 terminator; <i>lacI</i> , <i>par</i> , <i>oriV</i> REP, Km ^r	this study
pKR-P _{tac} - <i>par</i> -T7Pol/T7MCS-His ₆ -SDR B3- <i>lacI</i>	132	cloning and expression vector for <i>E. coli</i> and <i>R. eutropha</i> H16, encoding the T7MCS consisting of T7 promoter, and T7 terminator; <i>lacI</i> , <i>par</i> , <i>oriV</i> REP, Km ^r	this study

T7 Polymerase

pKR-P _{tac} -par-T7Pol/T7MCS-His ₆ -SDR B3-lacI-mob	134	cloning and expression vector for <i>E. coli</i> and <i>R. eutropha</i> H16, encoding the T7MCS consisting of T7 promoter and T7 terminator, pBBR1 mobilization region <i>mob</i> , <i>lacI</i> , <i>par</i> , <i>oriV</i> REP, Km ^r T7 Polymerase	this study
---	-----	---	------------

Expression vectors for R. eutropha H16 with pBBR1 mobilization region and origin of replication

pKR-P _{tac} -par-mob-His ₆ -SDR A1	145	Km ^r , P _{tac} , <i>mob</i> , <i>oriV</i> REP, <i>par</i> , H16_A316 N-terminal His tag coding sequence	this study
pKR-P _{tac} -par-mob-His ₆ -SDR B3	146	Km ^r , P _{tac} , <i>mob</i> , <i>oriV</i> REP, <i>par</i> , H16_1297 N-terminal His tag coding sequence	this study
pKR-P _{tac} -par-mob-SDR B6	148	Km ^r , P _{tac} , <i>mob</i> , <i>oriV</i> REP, <i>par</i> , H16_B0101	this study
pKR-P _{tac} -par-mob-His ₆ -ADH A5	149	Km ^r , P _{tac} , <i>mob</i> , <i>oriV</i> REP, <i>par</i> , H16_A1168 N-terminal His tag coding sequence	this study
pKR-P _{tac} -par-mob-His ₆ -SDR B6	150	Km ^r , P _{tac} , <i>mob</i> , <i>oriV</i> REP, <i>par</i> , H16_B0101 N-terminal His tag coding sequence	this study
pKR-P _{tac} -par-mob-SDR A1	156	Km ^r , P _{tac} , <i>mob</i> , <i>oriV</i> REP, <i>par</i> , H16_A3164	this study
pKR-P _{tac} -par-mob-SDR B3	155	Km ^r , P _{tac} , <i>mob</i> , <i>oriV</i> REP, <i>par</i> , H16_1297	this study

Expression vectors for R. eutropha H16 with pBBR1 origin of replication and mobilization region from RP4 plasmid

pKREP-P _{T5} -ADH A5	186	Km ^r , P _{T5} , <i>oriV</i> REP, RP4 <i>mob</i> , <i>par</i> , H16_A1168	this study
pKREP-P _{T5} -SDR B6	187	Km ^r , P _{T5} , <i>oriV</i> REP, RP4 <i>mob</i> , <i>par</i> , H16_B0101	this study
pKREP-P _{T5} -His ₆ -SDR B3	189	Km ^r , P _{T5} , <i>oriV</i> REP, RP4 <i>mob</i> , <i>par</i> , H16_B1297 N-terminal His tag coding sequence	this study
pKREP-P _{T5} -His ₆ -ADH A5	190	Km ^r , P _{T5} , <i>oriV</i> REP, RP4 <i>mob</i> , <i>par</i> , H16_A1168 N-terminal His tag coding sequence	this study
pKREP-P _{T5} -SDR B3	191	Km ^r , P _{T5} , <i>oriV</i> REP, RP4 <i>mob</i> , <i>par</i> , H16_B1297	this study
pKREP-P _{T5} -SDR A1	192	Km ^r , P _{T5} , <i>oriV</i> REP, RP4 <i>mob</i> , <i>par</i> , H16_A3164	this study
pKREP-P _{T5} -Δinsert	193	Km ^r , P _{T5} , <i>oriV</i> REP, RP4 <i>mob</i> , <i>par</i>	this study

Expression vectors for R. eutropha H16 with RSF1010 mobilization region and origin of replication and T5 promoter

pKRSF1010-P _{T5} -ADH A5	231	Km ^r , <i>oriV</i> and <i>mob</i> RSF1010, P _{T5} , <i>par</i> , H16_A1168	this study
pKRSF1010-P _{T5} -SDR B3	243	Km ^r , <i>oriV</i> and <i>mob</i> RSF1010, P _{T5} , <i>par</i> , H16_B1297	this study
pKRSF1010-P _{T5} -SDR A1	232	Km ^r , <i>oriV</i> and <i>mob</i> RSF1010, P _{T5} , <i>par</i> , H16_A3164	this study
pKRSF1010-P _{T5} -SDR B6	233	Km ^r , <i>oriV</i> and <i>mob</i> RSF1010, P _{T5} , <i>par</i> , H16_B0101	this study
pKRSF1010-P _{T5} -His ₆ -ADH A5	239	Km ^r , <i>oriV</i> and <i>mob</i> RSF1010, P _{T5} , <i>par</i> , H16_A116 N-terminal His tag coding sequence	this study
pKRSF1010-P _{T5} -His ₆ -SDR B3	241	Km ^r , <i>oriV</i> and <i>mob</i> RSF1010, P _{T5} , <i>par</i> , H16_B1297 N-terminal His tag coding sequence	this study
pKRSF1010-P _{tac} -Δinsert	179	Km ^r , <i>oriV</i> and <i>mob</i> RSF1010, P _{Tac} , <i>par</i> ,	this study

Cumate inducible expression systems for R. eutropha H16

pKRSF1010-P _{J5} -SDR B3-cymR	245	Km ^r , <i>oriV</i> and <i>mob</i> RSF1010, P _{J5} , <i>par</i> , <i>cymR</i> , H16_B1297, one cumate operator upstream the promoter region, one cumate operator downstream the promoter region	this study
pKRSF1010-P _{J5} -cyOO-His ₆ -ADH A5-cymR	331	Km ^r , <i>oriV</i> and <i>mob</i> RSF1010, P _{J5} , <i>par</i> ,	this study

pKRSF1010-P _{J5} -cyOO-His ₆ -SDR B3-cymR	332	<i>cymR</i> , H16_A1168, N-terminal His tag coding sequence, both cumate operators downstream the promoter region Km ^r , <i>oriV</i> and <i>mob</i> RSF1010, P _{J5} , <i>par</i> , <i>cymR</i> , H16_B129, N-terminal His tag coding sequence, both cumate operators downstream the promoter region	this study
---	-----	---	------------

*Plasmids were not preserved due to their instability

colE1 – origin of replication; *lacI* – gene encoding the LacI repressor protein; *cymR* – gene encoding the CymR repressor protein; *mob* – mobilization sequence; *oriV* – origin of replication; *par* – partition region; cyOO in the name of the plasmid indicates that both cumate operators are located downstream the promoter region

Table 8. Primers used in this study

Name	Number	Sequence	Restriction site
in internal list of primers			
<i>Alcohol dehydrogenases:</i>			
A-1-fwd	1	5' - ttatgcatgctcagtcggtgatgg - 3'	<i>SphI</i>
A-1-rev	2	5' - tcgcatatgaccgcaatgatgaaagcc - 3'	<i>NdeI</i>
A-2-fwd	54	5' - ccgatttaaattcagccgagattcac - 3'	<i>SmaI</i>
A-2-rev	4	5' - ctccatatgacctccaggcattgc - 3'	<i>NdeI</i>
A-3-fwd	5	5' - actaagcttttacatcgctgcagcg - 3'	<i>HindIII</i>
A-3-rev	6	5' - atacatatgagcgagaccg - 3'	<i>NdeI</i>
A-4-fwd	7	5' - cgaaagctttacttgggctgcatcc - 3'	<i>HindIII</i>
A-4-rev	8	5' - gcccatatgcaaatccaaggcaacg - 3'	<i>NdeI</i>
A-5-fwd	9	5' - ccgaagcttttagtagttgaggatcg - 3'	<i>HindIII</i>
A-5-rev	10	5' - cgccatatgagcgaagccaatcacc - 3'	<i>NdeI</i>
B-1-fwd	11	5' - gatcatatgggaatctgcgacgc - 3'	<i>NdeI</i>
B-1-rev	12	5' - aattgcatgctcagctgccgtagacc - 3'	<i>SphI</i>
B-2-fwd	13	5' - tatgcatgctcagatggcccgg - 3'	<i>SphI</i>
B-2-rev	14	5' - ccacatatgctggagctatcagaccag - 3'	<i>NdeI</i>
B-5-fwd	19	5' - aatcatatggcgctggcagggaatcag - 3'	<i>NdeI</i>
B-5-rev	20	5' - cttaagctttcagcgagccgcac - 3'	<i>HindIII</i>
B-6-fwd	21	5' - atccgatgctcagaaccctccagcacc - 3'	<i>SphI</i>
B-6-rev	22	5' - ccgcatatgaaagccatcgctgacc - 3'	<i>NdeI</i>
B-8-fwd	25	5' - tacggcatgcttaatcgaacaggatcacc - 3'	<i>SphI</i>
B-8-rev	26	5' - tgccatatgaaggccgctgtcctg - 3'	<i>NdeI</i>
P-1-fwd	27	5' - atacatatggcccagaccatgagc - 3'	<i>NdeI</i>
P-1-rev	28	5' - actaagctttcatgggatctgccc - 3'	<i>HindIII</i>
P-2-fwd	29	5' - actcatatggcttctcctgagcgc - 3'	<i>NdeI</i>
P-2-rev	30	5' - atcaagcttttagtgacggattctcaggac - 3'	<i>HindIII</i>
<i>Short-chain dehydrogenases/reductases:</i>			
SCDH A1-Nde fwd	78	5' - catatgaaactgcaggtcggg - 3'	<i>NdeI</i>
SCDH A1-Nde rev	79	5' - aagctttcagagcgacatgccgc - 3'	<i>HindIII</i>
SCDH A2-Nde fwd	213	5' - aacatagaaactgaccaatagtccg - 3'	<i>NdeI</i>
SCDH A2-Hind-rev	214	5' - tcaagctttcagcggtgcc - 3'	<i>HindIII</i>
SCDH A3-Nde-fwd	215	5' - atccatagacgaccaacaccc - 3'	<i>NdeI</i>
SCDH A3-Hind-rev	216	5' - atcaagctttcagcgctgcaag - 3'	<i>HindIII</i>
SCDH A4-Nde fwd	217	5' - cgccatagcaagtcaatctcgatt - 3'	<i>NdeI</i>
SCDH A4-Hind-rev	218	5' - ctaaagctttcagccggcttt - 3'	<i>HindIII</i>

SCDH B1-Nde fwd	74	5' - <u>catatgag</u> taattcccttgaaggaaaa - 3'	<i>NdeI</i>
SCDH B1-HindIII rev	75	5' - <u>aagcttt</u> caaactgtctcaatccgc - 3'	<i>HindIII</i>
SCDH B2-Nde fwd	76	5' - <u>catatga</u> atcgcttcgaaggc - 3'	<i>NdeI</i>
SCDH B2-HindIII rev	77	5' - <u>aagcttt</u> tacagttggctcatgccg - 3'	<i>HindIII</i>
SCDH B3-Nde fwd	80	5' - <u>catatgaa</u> actgcagggctcggg - 3'	<i>NdeI</i>
SCDH B3-HindIII rev	81	5' - <u>aagcttt</u> cagagcgacatgccgc - 3'	<i>HindIII</i>
SCDH B4-Nde fwd	82	5' - <u>catatggg</u> acgcttctgctgaaa - 3'	<i>NdeI</i>
SCDH B4-HindIII rev	83	5' - <u>aagcttt</u> caggtgcgctgatc - 3'	<i>HindIII</i>
SCDH B6-Nde fwd	221	5' - caac <u>atgat</u> acctccacccag - 3'	<i>NdeI</i>
SCDH B6-Hind-rev	222	5' - taca <u>agcttt</u> caggcaaagcccc - 3'	<i>HindIII</i>
SCDH B7-Nde fwd	223	5' - ctacat <u>atg</u> accatggcggcaaac - 3'	<i>NdeI</i>
SCDH B7-Hind-rev	224	5' - att <u>aagcttt</u> cagagcgcgaacgcc - 3'	<i>HindIII</i>
SCDH B9-Nde fwd	227	5' - cagcat <u>atg</u> ctgttgaaagacaag - 3'	<i>NdeI</i>
SCDH B9-Hind-rev	228	5' - ctca <u>agcttt</u> cagggcatgaaat - 3'	<i>HindIII</i>
SCDH B11-Nde fwd	231	5' - gcgcat <u>atg</u> ctattgttgatctg - 3'	<i>NdeI</i>
SCDH B11-Hind-rev	232	5' - ct <u>aagcttt</u> cagatggtcacgc - 3'	<i>HindIII</i>

Reductases:

redA1-fwd	158	5' - atccat <u>atg</u> gacttgagcattcc - 3'	<i>NdeI</i>
redA1-rev	159	5' - ct <u>aagcttt</u> cagtcgaacaccg - 3'	<i>HindIII</i>
redA2-fwd	160	5' - tccat <u>atg</u> aacgagctcgac - 3'	<i>NdeI</i>
redA2-rev	161	5' - ata <u>agcttt</u> caggtgcggatc - 3'	<i>HindIII</i>
redA4-fwd	164	5' - taacat <u>atg</u> gcaaaccaacg - 3'	<i>NdeI</i>
redA4-rev	165	5' - tct <u>aagcttt</u> tacttgcgatc - 3'	<i>HindIII</i>
redA5-fwd	166	5' - atgcat <u>atg</u> aagcaagtcacc - 3'	<i>NdeI</i>
redA5- rev	167	5' - cca <u>agcttt</u> caaagcatttc - 3'	<i>HindIII</i>
redA6-fwd	168	5' - ctacat <u>atg</u> agcctgcaatttc - 3'	<i>NdeI</i>
redA6-rev	169	5' - tt <u>aagcttt</u> catggcagagc - 3'	<i>HindIII</i>
redA9-fwd	170	5' - tcacat <u>atg</u> gaaaccatccgac - 3'	<i>NdeI</i>
redA9- rev	175	5' - att <u>aagcttt</u> tattgcgctggg - 3'	<i>HindIII</i>
redA10-fwd	176	5' - tgcat <u>atg</u> cttgaaggaaaatc - 3'	<i>NdeI</i>
redA10- rev	177	5' - att <u>aagcttt</u> cagtgctgggtc - 3'	<i>HindIII</i>
redA11-fwd	178	5' - ttcat <u>atg</u> agcaaggagcacgac - 3'	<i>NdeI</i>
redA11- rev	179	5' - att <u>aagcttt</u> cagccctgatccc - 3'	<i>HindIII</i>
redB1-fwd	180	5' - gccat <u>atg</u> gaagtacgcaacaag - 3'	<i>NdeI</i>
redB1-rev	181	5' - ata <u>agcttt</u> ctataccgcatgcc - 3'	<i>HindIII</i>
redB4-fwd	184	5' - aacat <u>atg</u> cccgccaccacc - 3'	<i>NdeI</i>
redB4-rev	187	5' - att <u>aagcttt</u> caggctgcctgctg - 3'	<i>HindIII</i>

Sequencing primers:

pM(S)-prom-fwd	39	5' - gcataattcggtcgctcaagg - 3'	
Tac-pM(S)-Stop-neu-rev	40	5' - gcaaattctgtttatcagacc - 3'	
Tac Seq 5712	149	5' - gtgagcggataacaatttcac - 3'	
MOB Fwd	353	5' - cactgcagtcatcccaggtggcacttttc - 3'	
MOB Rev	354	5' - cactgcagatggcggcatacgcgat - 3'	
3'PAR_fwd	473	5' - acctcatgacgcgacttgcc - 3'	
Rep Seq 2830 fw	90	5' - cttgacgcgcctggaacgac - 3'	
REP-PstI-rev	69	5' - ggaactgcagatagtctggaacagcgcactt - 3'	
KanR Seq 969 rev	104	5' - taccagaccgcttctgcgttct - 3'	
Fwd-PT5	501	5' - actctagaaaatcataaaaaattttattt - 5'	
Par2_fwd	138	5' - acgcccacacatgtgctaag - 3'	
Tac Seq 5712	147	5' - gtgagcggataacaatttcac - 3'	
Pj5-CymO-fwd-1	516	5' - gaacaaacagacaatctggtctgtttgtattataaattcgagctcggtaccgc - 3'	

The underlined sequences (*Hind*III; *Nde*I; *Sma*I; *Sph*I) represent the additional restriction sites at the 5' ends of forward and reverse primers.

3.1.2.3. Sequence analysis

The UniprotKB [<http://www.uniprot.org/>] and NCBI [<http://www.ncbi.nlm.nih.gov/>] databases were used to screen for probable alcohol dehydrogenases, short chain dehydrogenases and reductases of *R. eutropha* H16. The BLAST program [<http://www.uniprot.org/blast/>] was used within the all proteins of database to search for the enzymes that shared homologies. The conserved domain search (CDS) tool from the NCBI database [<http://www.ncbi.nlm.nih.gov/Structure/cdd/wrpsb.cgi>] was used to search for conserved domains within a protein sequence.

3.1.2.4. DNA preparation

Standard procedures were used for PCR, DNA preparation and manipulation as well as genomic DNA isolation (Green and Sambrook, 2012). Restriction enzymes, Fast DNA End Repair Kit, DreamTaq Green DNA Polymerase, Phusion Polymerase and GeneJET Plasmid Miniprep Kits by Thermo Scientific (Waltham, MA, USA), Q5® High-Fidelity DNA Polymerase from NEB (New England Biolabs, Ipswich, MA), T4 DNA Ligation reaction and Wizard SV Gel and PCR Clean-Up System by Promega™ (Madison, WI, USA) and Easy-DNA Kit by Invitrogen (Carlsbad, California, USA) were used according to the supplier's protocols. LGC Genomics GmbH (Berlin, Germany) performed the DNA sequencing.

3.1.2.5. Agarose gel electrophoresis and DNA preparation

DNA was analysed using electrophoretic separation on a 1 % agarose gel depending on the size of the DNA of interest. The appropriate amount of agarose (Biozym Scientific GmbH; Hessisch Oldendorf, Germany) was dissolved in 1 x TAE buffer (40 mM Tris acetate, 1 mM EDTA, pH 8.2 - 8.4 at 25°C) by heating for 5 min using a microwave. To visualize DNA on the gel, ethidium bromide (3µl) was added. To determine the size and the concentration of the DNA bands 0,5 µg of either the GeneRuler™ DNA Ladder Mix or the GeneRuler™ Low Range DNA Ladder Mix (Thermo Science Inc, Waltham; USA) were loaded onto the gel. Control gels were run for 30 min at 120 V, whereas preparative gels were run for 90 min at 90 V.

3.1.2.6. Preparation of electrocompetent *E. coli* and *R. eutropha* H16 cells

15 mL of LB Medium in a 100 mL flask was inoculated with a single colony of *E. coli* TOP10 or *E. coli* BL21 respectively and incubated over night at 37 °C 110 rpm. 500 mL of LB Medium in a 2 L flask were inoculated to an OD₆₀₀ (optical density at 600nm) of 0,1 and grown at 37 °C 110 rpm to an OD₆₀₀ between 0,7 and 0,8. The main culture was pre-chilled on ice for 30 min before harvesting the cells by centrifuging for 15 min at 2500 rpm 4 °C (Avanti™ J-20 XP centrifuge, JA-10 rotor, Beckman

Coulter Inc.; Vienna, Austria). The supernatant was removed and the pellets were dissolved in 5 mL of ice-cold water. Then 250 mL of ddH₂O was added and the suspension was centrifuged for 15 min at 4500 rpm 4 °C. This step was repeated three times. Afterwards the pellets were resuspended in 5 mL of ice-cold 10% glycerol. Then 20 mL of 10% ice cold glycerol was added and the suspension was centrifuged for 15 min at 4500 rpm 4 °C. After removing the supernatant the pellet is dissolved in 2-3 mL of ice-cold 10% glycerol. The competent cells were aliquoted to 90 µl portions, frozen in liquid nitrogen and stored at -80 °C.

For the preparation of electrocompetent *R. eutropha* H16 cells the preculture (30 mL TSB media with 20 µg/mL gentamycin, 50 mL flask with a triangular magnetic stirrer) was inoculated with a glycerol stock from *R. eutropha* H16 and incubated at 28°C at 500 rpm overnight. The main culture (100 mL TSB media, 300 mL flask with a triangular magnetic stirrer) was inoculated to an OD₆₀₀ of 0.1 and incubated at 28°C at 500 rpm till an OD₆₀₀ of 0.8-1.0. After reaching the right OD₆₀₀ the cells were cooled on ice for 30 min and then centrifuged in a 50 mL flacon at 4°C for 15 min at 4000 rpm (centrifuge 5810 R, Eppendorf; Hamburg, Germany). The supernatant was removed and the pellet was resuspended in 5 mL of 0.3 M ice-cold sucrose. After centrifuging again at 4°C for 10 min at 4000 rpm the pellet was washed in 2.5 mL of 0.3 M sucrose. After the last centrifugation for 5 min at 4°C at 4000 rpm the cells were diluted with ~1 mL of 0.3 M sucrose to reach an OD₆₀₀ about 30. The OD₆₀₀ as measured with the Eppendorf BioPhotometer (Eppendorf, Hamburg, Germany). Portions of 100 µl were filled into 1.5 mL Eppendorf tubes, frozen in liquid nitrogen and stored at -80°C.

3.1.2.7. Plasmid construction for expression in *E. coli* BL21

Construction of the pK470 expression vectors for *E. coli* BL21.

11 putative alcohol dehydrogenases, 12 putative short chain dehydrogenases/reductases and 10 putative reductases were amplified out of the genomic DNA of *R. eutropha* H16 via PCR and cloned into pK470 vector for expression in *E. coli* TOP10 via *Nde*I and *Hind*III, *Sph*I or *Sma*I restriction sites. Primers used for PCR are listed in Table 8. pK470Δ, which does not contain any insert, was used as a control empty vector.

Construction of the pK470-His₆ expression vector

Alcohol dehydrogenase ADH A5 as well as three short chain dehydrogenases/reductases SDR A1, SDR B3 and SDR B6 were cloned in pK470-His₆ and used for protein purification via N-terminally attached 6 x histidine tag and hence better functional analyses. SDR A1 and SDR B3 were cloned in pK470-His₆ by Christina Zach during her Master thesis research (Zach, 2013). The same protocol was used for the construction of expression vector for His-tagged protein described in chapter 3.2 and is given in detail in the section “His₆-tag cloning” in chapter 3.2.2. The genes for ADH A5 and SDR B6

were inserted into the pK470-His₆-SCDHB3 vector by exchanging the SCDH B3 insert for the corresponding sequences using *Nde*I and *Hind*III restriction sites. Success of the cloning experiments was proved by restriction analysis and DNA sequencing (LGC Genomics GmbH; Berlin, Germany). Oligonucleotides used for sequencing are given in Table 8.

3.1.2.8. Plasmid construction for expression in *R. eutropha* H16

To express the various proteins of interest in *R. eutropha* H16, several expression systems were constructed as listed in Table 9. Success of the cloning experiments was proven by restriction analysis and DNA sequencing (LGC Genomics GmbH; Berlin, Germany). Constructed expression vectors were transferred into *R. eutropha* H16 via conjugation or electroporation and expression of the cloned enzymes was verified by SDS-PAGE. Detailed description of each construct is given in Table 7.

Table 9. Overview of the constructs created for the expression in *R. eutropha* H16 in chronological order.

Name	Number in internal list of plasmids	Sequencing primers	Cloning strategy
<i>Expression vectors for R. eutropha</i> H16 with encoded <i>LacI</i> repressor			
pKR-P_{tac}			
pKR-P _{tac} -ADH A4	*	104, 147	<i>adh</i> A4 and <i>adh</i> A5 were cut out of the corresponding pK470 constructs with <i>Nde</i> I and <i>Hind</i> III endonucleases and cloned into pKR-Tac (#2) also cut with <i>Nde</i> I and <i>Hind</i> III
pKR-P _{tac} -ADH A5	*	104, 147	
pKR-P_{tac}-par			
pKR-P _{tac} -par-ADH A3	*	104, 147	<i>adh</i> A3 and <i>adh</i> A5 were cut out of the corresponding pK470 constructs with <i>Nde</i> I and <i>Hind</i> III endonucleases and cloned into pKR-Tac-Par (#3) also cut with <i>Nde</i> I and <i>Hind</i> III
pKR-P _{tac} -par-ADH A5	*	104, 147	
<i>Expression vectors for R. eutropha</i> H16 with deleted <i>LacI</i> repressor			
pKR-P_{tac}-Δ<i>lacI</i>-par			
pKR-P _{tac} -Δ <i>lacI</i> -par-ADH A4	*	104, 147	<i>adh</i> A4, <i>adh</i> A5 and <i>his</i> ₆ - <i>sdr</i> B3 were cut out of the corresponding pK470 constructs with endonucleases <i>Nde</i> I and <i>Hind</i> III for <i>adh</i> A4 and <i>adh</i> A5 and <i>Xba</i> I and <i>Hind</i> III for <i>his</i> ₆ - <i>sdr</i> B3 and cloned into pKR-Tac-Par-Δ <i>lacI</i> (#6) also cut with the corresponding endonucleases
pKR-P _{tac} -Δ <i>lacI</i> -par-ADH A5	*	104, 147	
pKR-P _{tac} -Δ <i>lacI</i> -par-His ₆ -SDR B3	117	104, 147	
pKR-P _{lac} -Δ <i>lacI</i> -par-His ₆ -SDR B3	118	104, 147	<i>his</i> ₆ - <i>sdr</i> B3 was cut out of the corresponding pK470 construct with endonucleases <i>Xba</i> I and <i>Hind</i> III and cloned into pKR-Tac-Par-Δ <i>lacI</i> (#7) also cut with <i>Xba</i> I and <i>Hind</i> III

Plasmids created to establish IPTG-inducible expression system for R. eutropha H16

pKR-P_{tac}-par-T7MCS-lacI

pKR-P _{tac} -par-T7MCS-lacI-His ₆ -SDR B3	128	-	<i>his₆-sdr B3</i> was cut out of the corresponding pK470 construct with endonucleases <i>XbaI</i> and <i>HindIII</i> and cloned into pKR-P _{tac} -par-T7MCS-Δinsert-lacI (#120) also cut with <i>XbaI</i> and <i>HindIII</i>
---	-----	---	---

pKR-P_{tac}-par-T7Pol/T7MCS-lacI

pKR-P _{tac} -par-T7Pol/T7MCS-lacI-His ₆ -SDR B3	132	-	<i>his₆-sdr B3</i> was cut out of the corresponding pKR-Tac-Par-T7MCS-lacI construct (#128) with <i>XbaI</i> and <i>NotI</i> endonucleases and ligated with pKR-P _{tac} -par-T7Pol/T7MCS-lacI (#95) also cut with <i>XbaI</i> and <i>NotI</i>
---	-----	---	---

pKR-P_{tac}-par-T7Pol/T7MCS-lacI-mob

pKR-P _{tac} -par-T7Pol/T7MCS-lacI-mob-His ₆ -SDR B3	134	-	<i>mob</i> region was cut out from construct #131 with <i>PstI</i> endonuclease and ligated with pKR-Tac-Par-T7Pol/T7MCS-His ₆ -SDRB3-lacI (#132) also cut with <i>PstI</i>
---	-----	---	--

Expression vectors for R. eutropha H16 with pBBR1 mobilization region and origin of replication

pKR-P_{tac}-par-mob

pKR-P _{tac} -par-mob-SDR A1	156	147	<i>sdr A1, sdr B3, sdr B6, his₆-adh A5, his₆-sdr A1</i>
pKR-P _{tac} -par-mob-SDR B3	155	147	<i>his₆-sdr B3</i> and <i>his₆-sdr B6</i> were cut out of the corresponding pK470 constructs with
pKR-P _{tac} -par-mob-SDR B6	148	147	endonucleases <i>NdeI</i> and <i>HindIII</i> for
pKR-P _{tac} -par-mob-His ₆ -ADH A5	149	147	<i>sdr A1, sdr B3</i> and <i>sdr B6</i> and <i>XbaI</i> and <i>HindIII</i> for
pKR-P _{tac} -par-mob-His ₆ -SDR A1	145	147	<i>his₆-adh A5, his₆-sdr A1, his₆-sdr B3</i> and
pKR-P _{tac} -par-mob-His ₆ -SDR B3	146	147	<i>his₆-sdr B6</i> and ligated with
pKR-P _{tac} -par-mob-His ₆ -SDR B6	150	147	pKR-P _{tac} -par-mob-egfp (#250) also cut with the corresponding endonucleases

Expression vectors for R. eutropha H16 with pBBR1 origin of replication and mobilization region from RP4 plasmid

pKREP-P_{T5}

pKREP-P _{T5} -ADH A5	186	473, 104	<i>adh A5, sdr A1, sdr B3, sdr B6, his₆-adh A5</i>
pKREP-P _{T5} -SDR A1	192	473, 104	and <i>his₆-sdr B3</i> were cut out of the corresponding pK470 constructs with
pKREP-P _{T5} -SDR B3	191	473, 104	endonucleases <i>NdeI</i> and <i>HindIII</i> for
pKREP-P _{T5} -SDR B6	187	473, 104	<i>adh A5, sdr A1, sdr B3</i> and <i>sdr B6</i> and
pKREP-P _{T5} -His ₆ -ADH A5	190	473, 104	<i>XbaI</i> and <i>HindIII</i> for <i>his₆-adh A5</i> and <i>his₆-sdr B3</i>
pKREP-P _{T5} -His ₆ -SDR B3	189	473, 104	and ligated with pKREP-P _{T5}
pKREP-P _{T5} -Δinsert	193	-	(#334) also cut with the corresponding endonucleases. For pKREP-P _{T5} -Δinsert

construction pKREP-P_{T5} was cut with *Nde*I, *Hind*III, sticky ends were treated by Fast DNA End Repair Kit and the construct was religated

Expression vectors for R. eutropha H16 with RSF1010 mobilization region and origin of replication and T5 promoter

pKRSF1010-P_{T5}

pKRSF1010-P _{T5} -ADH A5	231	501, 138	<i>adh A5, sdr A1, sdr B3, sdr B6, his₆-adh A5</i>
pKRSF1010-P _{T5} -SDR A1	232	501, 138	and <i>his₆-sdr B3</i> were cut out of the
pKRSF1010-P _{T5} -SDR B3	243	501, 138	corresponding pKREP-P _{T5} constructs with
pKRSF1010-P _{T5} -SDR B6	233	501, 138	endonucleases <i>Not</i> I and <i>Spe</i> I and
pKRSF1010-P _{T5} -His ₆ -ADH A5	239	501, 138	ligated with pCRSF1010-P _{tac} -egfp-reversed
pKRSF1010-P _{T5} -His ₆ -SDR B3	241	501, 138	(#335) also cut with the endonucleases
			<i>Not</i> I and <i>Spe</i> I
pKRSF1010-Tac-Δinsert	179	-	For pKRSF1010-P _{tac} -Δinsert construction
			pKRSF1010-P _{tac} (by S. Gruber) cut with <i>Nde</i> I,
			<i>Hind</i> III, sticky ends were treated by
			Fast DNA End Repair Kit and the construct was
			religated

Cumate inducible expression systems for R. eutropha H16

pKRSF1010-P_{J5}-cymR

pKRSF1010-P _{J5} -SDR B3-cymR	245	648 80, 81	PCR with the forward primer to <i>sdr b3</i> (#80) and rev primer #649 (Table 10) was performed from pKRSF1010-P _{T5} -SDR B3 construct (#243), PCR product was digested with <i>Stu</i> I and <i>Nde</i> I endonucleases and ligated into pCRSF1010-P _{J5} -cymR (#336) also cut with <i>Stu</i> I and <i>Nde</i> I endonucleases
--	-----	---------------	--

pKRSF1010-P_{J5}-cyOO-cymR

pKRSF1010-P _{J5} -cyOO-His ₆ -SDR A5-cymR	331	647 9, 10	PCRs with the forward primer #519 and rev primer #649 (Table 10) were performed from
pKRSF1010-P _{J5} -cyOO-His ₆ -SDR B3-cymR	332	648 80, 81	corresponding pKRSF1010-P _{T5} constructs for <i>his₆-sdr b3</i> and <i>his₆-adh a5</i> , PCR products were digested with <i>Stu</i> I and <i>Nde</i> I endonucleases and ligated into pCRSF1010-P _{J5} -cyOO-cymR (#337) also cut with <i>Stu</i> I and <i>Nde</i> I endonucleases

*Plasmids were not preserved due to their instability

Table 10. Primers used for sequencing and PCRs for construction of the plasmids listed in Table 9.

Name	Number in internal list of plasmids	Sequence 5'-3'	Restriction site
KanR Seq 969 rev	104	TATCAGACCGCTTCTGCGTTCT	
Tac Seq 5712	147	GTGAGCGGATAACAATTTAC	
PAR2_fwd	138	ACGCCCACACATGTGCTAATG	
Fwd-PT5	501	ACTCTAGAAAATCATAAAAAATTTATTT	<i>Xba</i> I
3'PAR_fwd	473	ACCTCATGACGCGACTTGCC	

ter_KanR_rev_Stul/AvrII/SpeI	649	ACTAGTCCTAGGAGGCTGTCTGACGCTCAGTGGAAACG	Stul/AvrII/SpeI
Pj5-lacO- fwd-1	519	GTGAGCGGATAACAATTCAATTGAGCTCGGTACCCG	
adhA5-mid-rev	647	GGATGTCGAGCGTATCGAG	
SCDHB3-mid-rev	648	GTGCCGGCGTTGTTGAAGG	

*Forward primers to the corresponding genes of interest are listed in the Table 8

3.1.2.9. Transformation of DNA into electrocompetent *E. coli* and *R. eutropha* H16 cells

Either 40 µl of competent *E. coli* TOP10 or BL21 cells were mixed with approximately 100 ng of DNA and transferred into pre-chilled electroporation cuvettes. After incubation on ice for 5 min the transformation was performed using the MicroPulser™ (Bio-Rad Hercules; California, USA) program EC 2 (5-6 sec 2,5 kV). The cells were regenerated in 900 µl of LB Medium for one hour at 37 °C and 650 rpm in a thermomixer. After centrifuging for 15 sec, the cells were resuspended in 100 µl of LB Medium and plated on LB^{Kan} agar plates containing 40 µg/ml kanamycin or 100 µg/ml ampicillin and incubated on 37 °C overnight.

For the transformation in *R. eutropha* H16 cells an aliquot of 100 µl competent cells was mixed with 100-300 ng DNA and incubated on ice for 30 min. Transformation was performed with the EC 2 program of MicroPulser™. After the electroporation the cells were regenerated in 1 ml of TSB media and incubated for 2 h at 28°C and 900 rpm. Afterwards the cells were centrifuged for 5 min at 4000 rpm and resuspended in 100 µl TSB media and plated out on TSB plates containing 200 µg/ml kanamycin and 20 µg/ml gentamycin.

3.1.2.10. Mating procedure for *R. eutropha* H16

Plasmid transfer into *R. eutropha* H16 was performed via modified triparental conjugative mating procedure (Goldberg and Ohman, 1984) from the donor strain *E. coli* TOP10 carrying desirable construct to the recipient strain *R. eutropha* H16 with the help of the *E. coli* HB101 [pRK2013] strain.

Alternatively, the conjugation in *R. eutropha* H16 was done using the *E. coli* S17-1 as donor strain. For the cultivation of the donor strain *E. coli* S17-1 with the corresponding plasmid 5 ml of LB_{Kan} medium were inoculated with a single colony and incubated over night at 30°C and 110 rpm. The recipient strain *R. eutropha* H16 was cultivated in 5 ml of TSB_{Gm} medium over night at 30°C and 110 rpm. After the cultivation the donor and recipient cells were harvested via centrifugation in 15 ml grainer tubes for 15 min at 4000 rpm at 4°C. Afterwards the cell pellets were resuspended in 500 µl of 0.9 % NaCl solution. For the conjugative plasmid transfer 0.2 ml of the donor suspension as well as 0.2 ml of the recipient suspension were spotted on the middle of an TSB agar plate. The plates were incubated over night at 30°C. Additional control plates with either 0.2 ml donor suspension or 0.2 ml recipient suspension were also incubated. For the selection of the positive transconjugates the grown cells from the conjugation plate were transferred to TSB_{Gm+Kan} agar plates. The donor cells are not able to grow on gentamycin, whereas empty recipient cells would not survive the high level of

kanamycin. The cells grown on the conjugation plate were resuspended in 3 ml of 0.9 % NaCl solution and then diluted stepwise to 10^{-5} . From each dilution step 0.1 ml were plated out on the TSB_{Gm+Kan} plates. From these plates single colonies were picked and used for a single streak out.

3.1.2.11. Expression of recombinant enzymes in *E. coli* BL21 and *R. eutropha* H16

The completed constructs were transformed into *E. coli* BL21 expression strain via standard electroporation procedure (Green and Sambrook, 2012). ONC of the corresponding strain was used to inoculate the main culture with a starting OD₆₀₀ 0.1. The cultivation of main culture was performed in 300 ml LB medium supplemented with 1 % glucose and 40 µg/ml kanamycin. For the additional experiment with the Zn-dependent alcohol dehydrogenases, an expression of *E. coli* BL21 strains carrying corresponding expression vectors was performed in usual manner but LB medium was also supplemented with Zn²⁺ in the various concentrations of 50, 100 and 200 µM. The recombinant enzyme expression was initiated by adding 0.1 mM IPTG at an OD₆₀₀ 0.6-0.8 and carried out over night at 28°C at 120 rpm.

Expression in *R. eutropha* H16 was performed in 300 ml TSB medium supplemented with 0.6 % fructose, 20 µg/ml gentamicin and 200 µg/ml kanamycin. The main culture was inoculated with ONC of the corresponding strain to a starting OD₆₀₀ 0.2. The induction of the enzyme expression in plasmid harbouring strains was started at an OD₆₀₀ 1.0 by adding 60 µg/ml cumate and cultures were grown over night at 28°C at 100 rpm.

Following expression, the cells were harvested by centrifugation at 4000 rpm at 4°C. Cell disruption was performed via sonification in 50 mM sodium phosphate buffer pH 7.4, unless protein purification experiments when appropriate binding buffer was used (see below). Power was supplied with a Branson Sonifier 250 (Duty Cycle % 80; Output Control 8) and the cell free extract was obtained by centrifugation for 60 min at 20 000 rpm and 4 °C (Avanti TM J-20 XP centrifuge, JA-25,50 rotor, Beckman Coulter Inc.; Vienna, Austria). Clear lysates were then used for the enzyme activity assays or for the purification.

3.1.2.12. Colony assay based on NAD(P)H fluorescence

A colony assay, based on the production of nicotinamide adenine dinucleotide NADH, or nicotinamide adenine dinucleotide phosphate NADPH fluorescence, was performed in order to screen for functional active enzymes (Reisinger et al., 2006). All expression vectors were transformed into competent *E. coli* BL21 cells. Serial dilutions of *E. coli* BL21 overnight cultures harbouring the appropriate plasmid were plated out on LB_{Kan} agar plates and incubated overnight at 37 °C. The plates were replica stamped onto LB_{Kan} agar plates containing additional 1 % glucose, as well as 0.1 mM isopropyl β-D- thiogalactopyranoside (IPTG) and incubated at 28 °C overnight. Subsequently, the colonies were lifted onto Ø 8.5 cm filter paper disks (Whatman International Ltd; Maidstone, United

Kingdom) and air dried for 5 min. Dried filters were soaked in 0.1 M HEPES buffer pH 8.0 containing 10 mM substrate and 5 mM NAD(P)⁺. The tested substrates were (S)-(+)-2-octanol, (R)-(-)-2-octanol, rac-butan-2,3-diol, 2-methyl-propanol, butanol, 3-methyl-butanol and rac-4-methyl-2-pentanol. The increased fluorescence of NAD(P)H was measured using a G:BOX (Syngene; Cambridge, United Kingdom).

3.1.2.13. Purification of His₆-tagged recombinant enzymes

Protein purification was performed on the basis of PD10 desalting columns (GE Healthcare, UK Limited, Little Chalfont, Buckinghamshire, UK), prepacked with Ni Sepharose™ Fast Flow (GE Healthcare Bio-Sciences AB, Uppsala, Sweden), according to the manufacturer's protocols. 20mM sodium phosphate buffer pH 7.4 with 0.5 M NaCl and imidazole was used for purification of His-tagged ADH A5, SDR A1, SDR B3, SDR B6. Concentration of imidazole was 20 mM for the binding buffer, 30 mM for the washing buffer and 100 mM for the elution buffer. After purification the buffer of the protein samples was replaced with 20 mM TrisCl and 0.2 M NaCl storage buffer pH 7.4 via the PD10 desalting columns. Different composition of purification buffers was additionally tested for two SDRs. 100 mM HEPES buffer pH 7.4 supplemented with 0.2 M NaCl and 20 mM, 30 mM and 100 mM imidazole in binding, washing and elution buffers, respectively, was used for SDR B3 and SDR B6. After the purification steps buffer of the protein samples was replaced with 100mM HEPES pH 7.4 supplemented with 0.2 M NaCl.

If the amount of purified protein was too low, the protein was concentrated using a 20 mL Vivaspin column (Satorius AG; Göttingen, Germany). Therefore up to 20 mL were centrifuged at 4000 rpm 4°C for 10-20 min until the appropriate concentration was reached.

The amount of total protein in the lysate and the concentration of purified enzymes were determined according to the Bradford procedure using Protein Assay Dye Reagent (Bio-Rad Laboratories Inc.; Hercules USA) and bovine serum albumin served as a standard.

SDS PAGE analysis was performed using 12 % Tris-glycine SDS-polyacrylamide gels. For the proteins' molecular weight estimation PageRuler™ Prestained Protein Ladder (10-170 kDa) (Thermo Science Inc., Waltham; USA) was applied. After electrophoresis the gels were stained with Coomassie Brilliant Blue solution.

3.1.2.14. Photometric assay based on NAD(P)⁺/ NAD(P)H fluorescence

General conditions

The specific enzyme activity was determined by a NAD(P)⁺/NAD(P)H dependent spectrophotometric assay. The light absorbance at 340 nm was monitored over 20 min at 28°C, using the Synergy Mx Monochromator-Based Multi-Mode Microplate Reader (BioTek Instruments GmbH;

Bad Friedrichshall, Germany). Based on the absorbance data, the enzyme activity units were defined as the amount of enzyme producing 1 μmol of NAD(P)H per min according to the following formula (1). Specific activity was defined as units per mg of protein.

The specific enzyme activity [Units /mg] of the respective dehydrogenases was calculated using the following formula (1):

$$\text{specific enzyme activity} = \frac{V_{\text{tot}} \times \frac{\Delta \varepsilon}{\Delta t} \times D}{[\text{mg}] \text{ of protein} \times \varepsilon_{\text{NAD(P)H}} \times d} \quad (1)$$

V_{tot}	total reaction volume (0,2 mL)
$\frac{\Delta \varepsilon}{\Delta t}$	slope* of absorbance at 340 nm
D	dilution factor
$\varepsilon_{\text{NAD(P)H}}$	Extinction coefficient of NADH (6,22 mL / μmol x cm) or NADPH (6,2 mL / μmol x cm)
d	height of the 200 μl mixture in the wells (0,45 cm)

*The absorbance of control with highest background reaction was subtracted from the sample absorbance before calculating the slope.

Spectrophotometric assay with cell free lysates

For the spectrophotometric assay with the lysates the reaction mixture for reduction reaction included 1 mM substrate 10 mM TrisCl buffer pH 5.9, 0.5 mg of the total protein lysate and 0.5 mM of NAD(P)H. For oxidation reaction 1 mM substrate 10 mM TrisCl buffer pH 7.4, 0.3 mg of protein and 0.5 mM NAD(P)⁺ was used. For the control sample cell free extract of the *E. coli* BL21 [pK470 Δ] strain carrying empty vector control was used.

For the oxidation reaction (*R*)- and (*S*)-2-octanol, *rac*-4-methyl-2-pentanol, isoamylalcohol, 2,3-butanediol, 2-methyl-1-propanol, *rac*-2-propanol, propanol, butanol and ethanol were tested as a substrate. For the reduction reaction isobutyraldehyde, propiophenone, valerophenone, butyrophenone, 2-hydroxyacetophenone, 4-phenyl-2-butanone, 2-octanone, 2-heptanone, isovaleraldehyde and benzophenone were used as a substrate.

For the final specific activity units calculations, the value calculated for the control sample was subtracted from the value calculated for the sample of interest.

Spectrophotometric assay for the purified enzymes

For the spectrophotometric assay with the purified enzymes the reaction mixture for reduction reaction included 1 mM substrate, 50 mM sodium phosphate buffer pH 7.5, 0.03 mg of the purified protein and 0.5 mM NAD(P)H. For oxidation reaction 1 mM substrate, 50 mM sodium

phosphate buffer pH 6.0, 0.03 mg of the purified protein and 0.5 mM NAD(P)⁺ was used. In the control sample reaction mixture, substrate was replaced by corresponding volume of the reaction buffer.

For the oxidation reaction (*R*)- and (*S*)-2-octanol, *rac*-4-methyl-2-pentanol, isoamylalcohol, 2,3-butanediol, 2-methyl-1-propanol, *rac*-2-propanol and propanol were tested as substrate. For the reduction reaction isobutyraldehyde, propiophenone, valerophenone, butyrophenone, 2-hydroxyacetophenone, 4-phenyl-2-butanone, 2-octanone, 2-heptanone, isovaleraldehyde and benzophenone were used as substrate. All substrates were dissolved in DMSO. The substrates were kindly provided by the Institute of Organic Chemistry, TU Graz, group of Prof. R. Breinbauer, and Institute of Chemistry - Organic & Bioorganic Chemistry department, UniGraz, group of Prof. W. Kroutil.

Spectrophotometric enzyme activity assay with SDR B3 purified out of *E. coli* BL21 and *R. eutropha* H16

Comparison of the activity of the heterologously and homologously expressed SDR B3 was performed in NADP⁺/NADPH dependent spectrophotometric assay. The light absorbance at 340 nm was monitored over 20 min at the temperatures 30°C, 32°C, 34°C, 36°C, 38°C, 40°C, 42°C, 44°C, 46°C, 48°C, using the Synergy Mx Monochromator-Based Multi-Mode Microplate Reader (BioTek Instruments GmbH; Bad Friedrichshall, Germany). The reaction mixture for oxidation reaction contained 1 mM (*S*)-2-octanol, 50 mM bicarbonate buffer pH 9.5, 0.01 mg of purified SDR B3 protein and 0.5 mM NADP⁺.

For pH range studies the light absorbance at 340 nm was monitored over 20 min, using the Synergy Mx Monochromator-Based Multi-Mode Microplate Reader (BioTek Instruments GmbH; Bad Friedrichshall, Germany). The reaction mixture for reduction reaction included 1 mM substrate 50 mM buffer, 0.02 mg of purified protein and 0.5 mM NADPH. For oxidation reaction 1 mM substrate 50 mM buffer, 0.01 mg of protein and 0.5 mM NADP⁺ was used. Following 50 mM buffers were used: citrate buffer pH 4.0, 4.5, 5.0, 5.5; sodium phosphate buffer pH 6.0, 6.5, 7.0, 7.5, 8.0; Tris-HCl buffer pH 8.0, 8.5, 9.0; bicarbonate buffer pH 9.5, 10.5, 11.0. Measurements in oxidation and reduction way of reaction were performed at 32°C; (*S*)-(+)-2-octanol and hexane-3,4-dione were used as a substrate, respectively.

Three different types of controls were used for all studies. Therefore, the protein, substrate or cofactor part in the mixture was replaced by reaction buffer. All measurements were biologically and technically performed in triplicates. Based on the absorbance data, the enzyme activity units were defined as the amount of enzyme producing 1 μmol of NAD(P)H per min. Specific activity was

expressed as units per mg of protein. While calculating relative activities in %, the highest specific activity was defined as 100%.

3.1.2.15. Biochemical characterization and bioinformatics analysis of ADH A5 and SDR B3

Description of materials and methods used for the detail characterisation of ADH A5 and SDR B3 is provided in manuscript in chapter 1.3.9.

3.1.2.16. Whole-cell bioconversion

R. eutropha H16 [pKRSF1010-P_{J5}-His₆-SDR B3-cymR] and *R. eutropha* H16 [pKRSF1010-P_{T5}] strains were grown in 30 ml MSM media supplemented with 20 µg/ml gentamicin and 200 µg/ml kanamycin under lithoautotrophic growth condition with the following gases mixture: 10% CO₂, 10% O₂, 80% H₂ at 28°C at 120 rpm. 5 mL of ONCs were grown heterotrophically in MSM medium supplemented with 0.6 % fructose. Harvested cells of the ONCs were used to inoculate pre-cultures for the lithoautotrophic growth. In their turn, pre-cultures were used to inoculate the main cultures for the lithoautotrophic growth to a starting OD₆₀₀ 0.2. The enzyme expression was initiated by adding 30 µg/ml cumate at OD₆₀₀ 1.0-1.2. When OD₆₀₀ reached 5.0, benzil (or phenylacetaldehyde in case of experiment described in chapter 6.2), which was dissolved in DMSO, was added to the final concentration of 5mM. The cultures were left under mixture of air and H₂ in the ratio 75%:25% respectively at 28°C at 120 rpm. After 3 hours 1 ml of supernatant of each culture was proceeded for extraction with n-heptane and isopropanol. Therefore, 1 ml of n-heptane and isopropanol mixture (in ratio 90 to 10, respectively) was added to the sample, vortexed for 1 min and filtered through the cottonwool covered with Mg₂SO₄ in a glass tip. In case when 1 ml of a whole cell culture was used for an analysis, the time of the vortexing was increased in 10 times. The upper phase of the mixture was analyzed with a high-pressure liquid chromatography (HPLC) apparatus Agilent Technologies 1100 Series System (Agilent Technologies, Waldbronn, Germany) using a Chiralpack AD-H Analytical column (partical size 5 µm, 250 mm x 4,6 mm; Daicel Chemical Industry, Japan) with isocratic eluent n-heptane/isopropanol (90/10). Data were analyzed with Agilent ChemStation software (Agilent Technologies, Waldbronn, Germany). HPLC experiments were performed with the help of Jakov Ivkovic from the group of Prof. R. Breinbauer, Institute of Organic Chemistry, TU Graz.

3.1.3. Results and discussion

3.1.3.1. Cloning of enzymes of interest into pK470 expression vector

The online databases NCBI and UniprotKB were used to screen for alcohol dehydrogenases, short chain dehydrogenases/reductases and reductases of *R. eutropha* H16. Based on the complexity of the protein molecule, corresponding gene localization, co-factors, required for the reaction, protein blast and conserved domains search results, 33 enzymes, including 11 putative alcohol dehydrogenases, 12 putative short chain dehydrogenases/reductases and 10 putative reductases, were chosen for further analysis. Preference was given to the putative non-complex homomeric proteins that were annotated as oxidoreductases requiring NAD(P)⁺/NAD(P)H cofactors to perform the reaction. Special attention received the proteins which shared homologies to the alcohol dehydrogenase from *Ralstonia* sp. DSMZ 6428 previously described by members of Prof. W. Kroutil group and shown to be highly stereoselective towards the bulky-bulky ketones (Iván Lavandera et al., 2008a).

The genes coding for the enzymes of interest were amplified from the genomic DNA of *R. eutropha* H16 via PCR. The genes coding for two of the proteins, ADH P1 and ADH P2, which are located on the megaplasmid, failed to be amplified in a first approach. Genomic DNA, used for these PCRs was isolated from *R. eutropha* H16, which was restored from the glycerol stock of IMBT strain collection under the numbers ##7597-7630 and ##7636-7666 (Table S.1). As it was figured out by a more detailed PCR analysis, this strain had lost its megaplasmid pHG1 and, therefore, none of the megaplasmid genes could be amplified from this strain. Therefore, a new *R. eutropha* H16 wild type strain was ordered (#1 in IMBT strain collection) and from the genomic DNA of this strain PCR products were obtained for ADHs P1 and P2 (Fig. 17). Since the megaplasmid of *R. eutropha* H16 does not encode essential housekeeping genes, the loss of this replicon does not influence the viability of the cells under heterotrophic growth conditions (Schwartz et al., 2003).

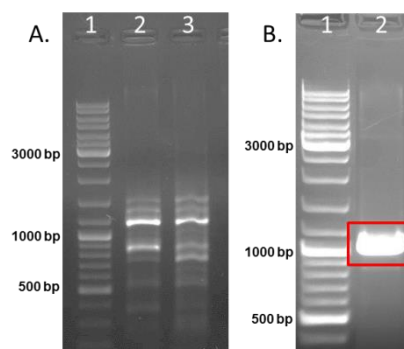


Figure 17. Agarose gel for PCR products of ADH P1 gene from the genomic DNA of *R. eutropha* H16. Expected size for *adhP1* is about 1030 bp. Amplified *adhP1* is indicated in red box. A – genomic DNA of *R. eutropha* H16 without pHG1 was used as a template for PCR. 1– GeneRuler DNA Ladder Mix (0.5 µg); 2, 3– unspecific PCR products for *adhP1* amplification. B – genomic DNA of *R. eutropha*

H16 carrying pHG1 was used as a template for PCR. 1– GeneRuler DNA Ladder Mix (0.5 µg); 2– PCR product for *adhP1* amplification.

As a result of the cloning experiments, 33 genes were amplified, digested by corresponding restriction sites, *HindIII* at the 3' end of the gene and *NdeI*, *SphI* or *SmaI* at the 5' end of the gene, and cloned into pK470 vector which was also cut by the corresponding endonucleases. An example of the constructed expression vector is shown in Fig. 18. All constructs are listed in Table 7.

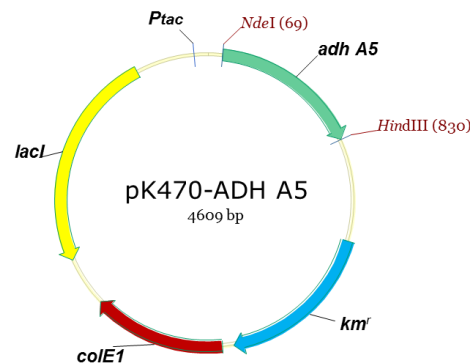


Figure 18. Illustration of the pK470-ADH A5 expression plasmid for *E. coli*. The plasmid backbone encodes gene for *lacI* repressor, *colE1* origin of replication, *kmr* gene encoding kanamycin resistance, promoter *tac* and gene encoding ADH A5

The success of the plasmid construction was proven by the restriction analysis and DNA sequencing (LGC Genomics GmbH; Berlin, Germany) with the primers #39 and #40 (Table 8). Constructed expression vectors were transformed into *E. coli* BL21 strain and overexpression of the proteins was performed.

3.1.3.2. Expression of the enzymes in *E. coli* BL21

Expression of the enzymes was done in 30 mL cultures after induction with 0.1 mM IPTG induction at OD₆₀₀ 0.6-0.8. The cultures were grown at 28 °C overnight at 120 rpm. The whole cell lysates were analysed on a 12 % SDS polyacrylamide gel. For 6 alcohol dehydrogenases (ADH A1, ADH A3, ADH B5, ADH B8, ADH P1 and ADH P2), 3 short-chain dehydrogenases/reductases (SDR A3, SDR B2 and SDR B11) and 5 reductases (RED A2, RED A9, RED A11, RED B1 and RED B4) no visible expression at the protein level could be detected under the tested experimental conditions (SDS PAGE). Presence of the original plasmid constructs in the corresponding fermented strains was verified by plasmid isolation and following restriction analysis. Growth conditions used during fermentation can influence the translation process in the cells. In order to determine if different temperature conditions can improve the expression, induced cultures were incubated at different temperatures (20°C, 25°C and 28°C) and the whole cell lysates were analysed via SDS-PAGE. Nevertheless, no expression could be observed under all tested conditions. ADH A1, ADH A3 and ADH B8 are annotated as putative Zn-dependent alcohol dehydrogenases, therefore a Zn²⁺ ion in the

active site of the enzyme is needed for the proper folding of the active enzyme (Baker et al., 2009). In order to determine if low zinc concentration in the used media was a limiting factor for the expression of examined ADHs, expression of *E. coli* BL21 strains carrying corresponding expression vectors was performed in 30 ml LB medium supplemented with Zn^{2+} at various concentrations of 50, 100 and 200 μM at 28°C. After induction with 0.1 mM IPTG at OD_{600} 0.6-0.8 the cultures were grown overnight at 25°C and 120 rpm. The visualization of the protein expression pattern of the fermented strains by SDS-PAGE did not show any changes in the expression (data not shown).

It should also be considered that the genome of *R. eutropha* H16 has a high GC content which is almost 70%. This is significantly higher than the average 50 % of the GC content for *E. coli* (http://www.genscript.com/cgi-bin/tools/rare_codon_analysis). Therefore, the absence of expression for the tested dehydrogenases and reductases may be explained by the difference in the codon usage of *E. coli* and *R. eutropha* H16, since the genes of our interest were not codon-optimized prior to heterologous expression in *E. coli* BL21. Consequently, a protein could be expressed in the cells but the level of the expression might be too low to be detected on the SDS gel (Rosano and Ceccarelli, 2014). Another explanation may be that the heterologous protein exhibits a harmful effect on the cell (Dumon-Seignovert et al., 2004). On the other hand, no difference in growth was determined for the cultures with the heterologous protein. It could also not be excluded that the protein might not exist in nature, since the proteins of our interest were only predicted to exist by bioinformatics tools based on the coding sequences given in the databases.

For one enzyme, ADH B2, with the expected size of 26 kDa, a clear band was visible on the SDS gel, with a size of about 33 kDa. This discrepancy between the theoretical MW and the MW observed during SDS-PAGE may be a result of an incomplete protein unfolding during SDS-PAGE sample preparation. However, this is unlikely in our case, since the denaturation of the cells mixed with SDS sample buffer (10mM NaOH, 1 % SDS and 0.6 % 2-mercaptoethanol) was performed at 99°C for 10 min. This temperature is higher than the standard 95°C used for the denaturation of the proteins for SDS-PAGE and normally under these conditions the denaturation of a protein should be completed. Additionally, the ADH B2 protein was visible at the same size in all performed SDS gels, which indicates that this is the size of the completely denatured monomer. The observed molecular weight of the protein may differ from the theoretical value when the protein binds more or less SDS than it should on average bind and this might happen due to the amino acid composition of a protein. As a result, the protein appears to be larger or smaller than expected (Sallantin et al., 1990).

18 enzymes, including 4 ADHs (ADH A4, ADH A5, ADH B1 and ADH B6), 9 SDRs (SDR A1, SDR A2, SDR A4, SDR B1, SDR B3, SDR B4, SDR B6, SDR B7, SDR B9) and 5 REDs (RED A1, Red A4, RED A5,

RED A6 and RED A10) were properly expressed in *E. coli* BL21 cultures after 0.1 mM IPTG induction at OD₆₀₀ 0.6-0.8. The cultures were grown at 28 °C overnight at 120 rpm. An example is shown in Fig. 19.

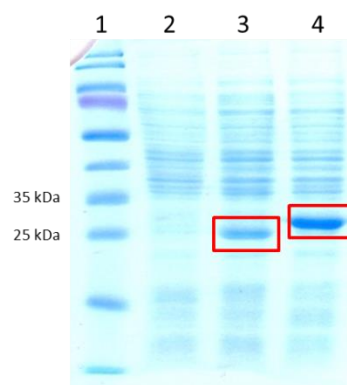


Figure 19. SDS-PAGE of the whole cell lysates from *E. coli* BL21 fermentation expressing the respective short-chain dehydrogenases/reductases. Expressed enzymes are shown in red boxes. Lane 1 – PageRuler™ Prestained protein ladder; lane 2 – negative control *E. coli* BL21 [pK470Δ]; lane 3 – *E. coli* BL21 [pK470-SDR B6], expected size 26 kDa; lane 4 – *E. coli* BL21 [pK470-SDR B9], expected size 29 kDa

To prove the functionality of heterologously expressed enzymes, *E. coli* BL21 strains carrying plasmids with the corresponding dehydrogenases, were tested for their oxidation activity in a colony-based activity assay.

3.1.3.3. A colony-based activity assay based on NAD(P)H fluorescence

A colony-based activity assay (Reisinger et al., 2006) is a convenient method to screen for the enzymes with NAD(P)/NAD(P)H-dependent oxidation activity. If the dehydrogenases are active, the respective substrates are oxidized and the cofactor NAD(P)⁺ is reduced to NAD(P)H as shown in Fig. 20.

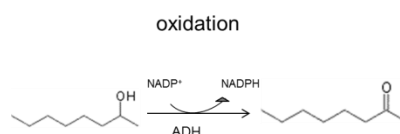


Figure 20. Schematic overview of 2-octanol oxidation performed by dehydrogenase.

The reduced form of the cofactor NAD(P)(H) should give fluoresce under UV. Subsequently, fluorescence of the cells expressing an active enzyme can be observed. An example of a colony-based activity assay performed in this study is shown in Fig. 21.

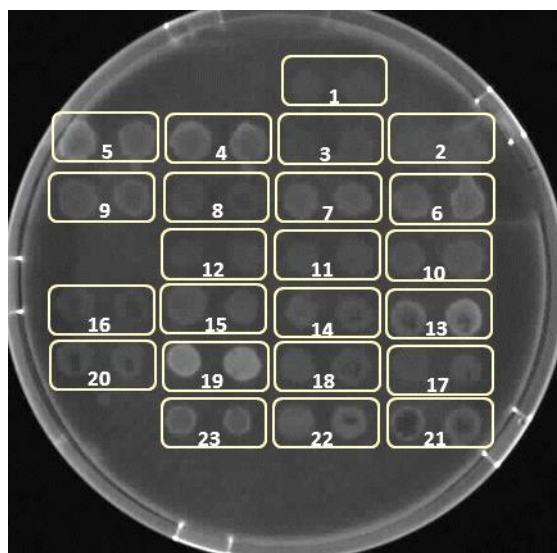


Figure 21. Example of enzyme activity screening – a colony-based activity assay with *E. coli* BL21 strains. Alcohol oxidation reaction is performed by overexpressed dehydrogenase with the help of NAD(P)^+ . Subsequently, the reduced form of the cofactor NAD(P)H is produced by active cells expressing an active enzyme and thus resulting in fluorescence.

A filter-paper disk with cells of different *E. coli* BL21 strains carrying the indicated plasmids was soaked in reaction mixture containing 10 mM *rac*-2-octanol, 5 mM NADP^+ and 0.1 M HEPES buffer pH 8.0; time of exposure 3 min. The positions contain: 1. negative control strain *E. coli* BL21 [pK470 Δ]; 2. *E. coli* BL21 [pK470-ADH A1]; 3. *E. coli* BL21 [pK470-ADH A3]; 4. *E. coli* BL21 [pK470-ADH A4]; 5. *E. coli* BL21 [pK470-ADH A5]; 6. *E. coli* BL21 [pK470-ADH B1]; 7. *E. coli* BL21 [pK470-ADH B2]; 8. *E. coli* BL21 [pK470-ADH B5]; 9. *E. coli* BL21 [pK470-ADH B6]; 10. *E. coli* BL21 [pK470-ADH B8]; 11. *E. coli* BL21 [pK470-ADH P1]; 12. *E. coli* BL21 [pK470-ADH P2]; 13. *E. coli* BL21 [pK470-SDR A1]; 14. *E. coli* BL21 [pK470-SDR A2]; 15. *E. coli* BL21 [pK470-SDR A3]; 16. *E. coli* BL21 [pK470-SDR A4]; 17. *E. coli* BL21 [pK470-SDR B1]; 18. *E. coli* BL21 [pK470-SDR B2]; 19. *E. coli* BL21 [pK470-SDR B3]; 20. *E. coli* BL21 [pK470-SDR B4]; 21. *E. coli* BL21 [pK470-SDR B6]; 22. *E. coli* BL21 [pK470-SDR B7]; 23. *E. coli* BL21 [pK470-SDR B9]

The tested substrates and the results of the colony-based activity assay are summarised in Table 11. ADH A4, ADH A5, SDR A1 showed strong activity towards all of the tested substrates regardless of the form of the used cofactor. ADH B1 and ADH B9 were active with all substrates but showed preference for NADP^+ as cofactor. In contrast, ADH B6 was active with all tested substrates only with NAD^+ as cofactor. SDR B7 did not show a clear preference for the cofactor. Additionally, relatively low fluorescence was observed with all tested substrates for the corresponding strain. This enzyme did not show a reaction with (*R*)-2-octanol, and therefore, might be a (*S*) - stereoselective dehydrogenase. Butanol was also not oxidized by SDR B7, in contrast to butan-2,3-diol and 3-methylbutanol, suggesting that this enzyme has a preference for branch-chained alcohols as a substrate. SDR A2, SDR A4, SDR B1 and SDR B4 did not show any activity with the tested substrates. Interestingly, ADH B2, which was expressed but showed a bigger size than expected, was also active in a colony-based activity assay. This data support the assumption that ADH B2 is expressed in *E. coli* BL21 in proper condition and only acquires wrong position on the SDS-gel because too less SDS molecules binds the protein and, therefore, protein was less charged. Strains with overexpressed ADH A1, ADH B3, ADH B5, ADH B8, ADH P1, ADH P2, SDR A3 and SDR B2 were also tested in a colony-

based activity assay, though no expression was detected on SDS gel for the corresponding enzymes. As expected, for all of the strains, except, *E. coli* BL21 [pK470-ADH B8], no cell fluorescence was observed. A possible explanation for the conversion of 3-methyl-propanol and racemic 4-methyl-2-pentanol by the cells of *E. coli* BL21 [pK470-ADH B8] may be that the protein itself is expressed in active form but the level of expression is too low to be detected on a SDS-PAGE. As it was mentioned, low level of heterologous expression might depend on the differences in the codon usage of *E. coli* and *R. eutropha* H16.

Table 11. Summary of the results obtained from the colony-based activity assay with different *E. coli* BL21 strains carrying the indicated plasmids. The intensity of the observed fluorescence is marked with '+': +++ – relative strong fluorescence; ++ – relative moderate fluorescence; + – relative weak fluorescence; - – no fluorescence

	(S)-(+)-2-octanol	(R)-(-)-2-octanol	rac-butan-2,3-diol	2-methyl-propanol	rac-4-methyl-2-pentanol	butanol	3-methyl-butanol	
<i>E. coli</i> BL21 [pK470-ADH A4]	+++	+++	++	++	++	++	+++	NAD ⁺
	++	++	++	++	+++	++	++	NADP ⁺
<i>E. coli</i> BL21 [pK470-ADH A5]	+++	++	++	++	++	++	++	NAD ⁺
	++	++	++	++	+++	++	++	NADP ⁺
<i>E. coli</i> BL21 [pK470-ADH B1]	++	+	+	+	+	-	++	NAD ⁺
	++	++	++	++	+	+	+	NADP ⁺
<i>E. coli</i> BL21 [pK470-ADH B2]	+	+	+	+	+	+	++	NAD ⁺
	+	+	+	+	+	-	+	NADP ⁺
<i>E. coli</i> BL21 [pK470-ADH B6]	+	+	+	+	+	+	+	NAD ⁺
	+	+	+	-	+	+	-	NADP ⁺
<i>E. coli</i> BL21 [pK470-ADH B8]	-	-	-	-	-	-	-	NAD ⁺
	+	-	-	+	+	-	-	NADP ⁺
<i>E. coli</i> BL21 [pK470-SDR A1]	+	+	++	++	++	++	+++	NAD ⁺
	++	++	++	++	+++	++	++	NADP ⁺
<i>E. coli</i> BL21 [pK470-SDR B3]	+++	+++	+++	+++	+++	+++	+++	NAD ⁺
	+++	+++	+++	+++	+++	+++	+++	NADP ⁺
<i>E. coli</i> BL21 [pK470-SDR B6]	+	+	+	+	+	+	+	NAD ⁺
	+	+	+	+	+	+	+	NADP ⁺
<i>E. coli</i> BL21 [pK470-SDR B7]	+	-	+	-	+	-	+	NAD ⁺
	+	-	+	+	+	-	+	NADP ⁺
<i>E. coli</i> BL21 [pK470-SDR B9]	+	+	+	+	+	+	+	NAD ⁺
	++	+	+	++	++	+	+	NADP ⁺

There were no activities detected for the strains *E. coli* BL21 [pK470-ADH A1], *E. coli* BL21 [pK470-SDR A2], *E. coli* BL21 [pK470-ADH A3], *E. coli* BL21 [pK470-ADH B5], *E. coli* BL21 [pK470-ADH P1], *E. coli* BL21 [pK470-ADH P2], *E. coli* BL21 [pK470-SDR A3], *E. coli* BL21 [pK470-SDR A4], *E. coli* BL21 [pK470-SDR B1], *E. coli* BL21 [pK470-SDR B2], *E. coli* BL21 [pK470-SDR B4], *E. coli* BL21 [pK470-RED A1], *E. coli* BL21 [pK470-RED A4], *E. coli* BL21 [pK470-RED A5], *E. coli* BL21 [pK470-RED A6], *E. coli* BL21 [pK470-RED A10]

Putative reductases RED A1, RED A4, RED A5, RED A6, RED A10 have also been tested in the colony-based activity assay; however they did not show any clear oxidation activity. Aldo-keto

reductases are capable of performing both ways of oxidoreductase reaction, nevertheless, it was shown that *in vivo* they likely act solely as reductase (Barski et al., 2008).

All strains with the dehydrogenases ADH A4, ADH A5, ADH B1, ADH B2, ADH B6, ADH B8, SDR A1, SDR B3, SDR B6, SDR B7, SDR B9, which clearly were active in the colony-based activity assay, and with the properly expressed reductases were fermented overnight in 300 ml cultures volume at 28°C (IPTG induction at OD₆₀₀ about 0.6-0.8). Cell free lysates of the sonicated cells were used for the photometric assay based on NAD(P)⁺/NAD(P)H absorption.

3.1.3.4. Photometric assay for the cell free lysates of *E. coli* BL21 carrying corresponding recombinant dehydrogenases and reductases

Cell lysates used for the photometric assay were before analysed for proper enzyme expression via SDS-PAGE (Fig. 22). As it can be seen, the major quantity of the enzymes c present in the soluble fraction, though in some cases a certain amount of the respective protein can also be found in the pellet. An example is shown in Fig. 22.

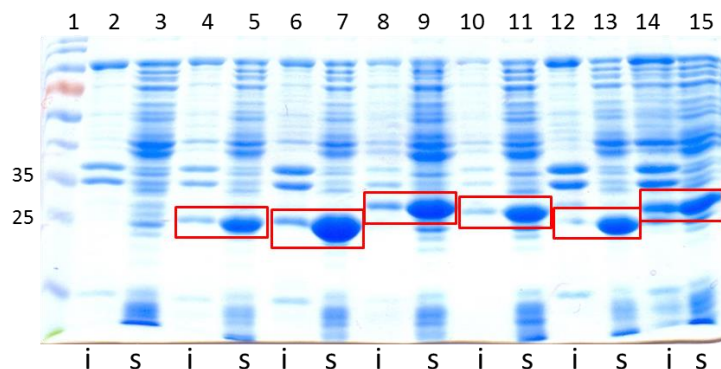


Figure 22. SDS-PAGE of the soluble (s) and insoluble (i) fractions after the sonication of the cell lysates from *E. coli* BL21 fermentations of the respective dehydrogenases. Expressed proteins are indicated in red boxes. Lane 1 - PageRuler™ Prestained protein ladder; lane 2 – *E. coli* BL21 [pK470], insoluble fraction; lane 3 – *E. coli* BL21 [pK470], soluble fraction; lane 4 – *E. coli* BL21 [pK470-SDR A1], insoluble fraction, expected size 26 kDa; lane 5 – *E. coli* BL21 [pK470-SDR A1], soluble fraction, expected size 26 kDa; lane 6 – *E. coli* BL21 [pK470-SDR A2], expected size 27 kDa, insoluble fraction; lane 7 – *E. coli* BL21 [pK470-SDR A2], expected size 27 kDa, soluble fraction; lane 8 – *E. coli* BL21 [pK470-SDR A4], expected size 29 kDa, insoluble fraction; lane 9 – *E. coli* BL21 [pK470-SDR A4], expected size 29 kDa, soluble fraction; lane 10 – *E. coli* BL21 [pK470-SDR B1], expected size 26 kDa, insoluble fraction; lane 11 – *E. coli* BL21 [pK470-SDR B1], expected size 26 kDa, soluble fraction; lane 12 – *E. coli* BL21 [pK470-SDR B3], expected size 26 kDa, insoluble fraction; lane 13 – *E. coli* BL21 [pK470-SDR B3], expected size 26 kDa, soluble fraction; lane 14 – *E. coli* BL21 [pK470-SDR B4], expected size 30 kDa, insoluble fraction; lane 15 – *E. coli* BL21 [pK470-SDR B4], expected size 30 kDa, soluble fraction

When the recombinant protein is overexpressed, especially in a foreign host, the hydrophobic residues of the polypeptide chain tend to interact with each other and form protein aggregates (Hartley and Kane, 1988). Slower rates of the protein production will give time for the

proper formation of the recombinant protein. The most common way to lower protein synthesis rate is to reduce the incubation temperature. Additionally, it decreases the formation of inclusion bodies due to the temperature-dependent character of the hydrophobic aggregation (Rosano and Ceccarelli, 2014). Therefore, to increase the amount of desirable protein in the soluble fraction, cultivation temperature conditions were optimized. The fermentation of the cultures was performed at 25°C. Additionally, the sonification settings were also optimized. As a result, time of the ultrasound treatment was 5 min.

The NAD(P)⁺/NAD(P)H-dependent spectrophotometric assay is based on the change in the absorbance of the reaction mixture while the oxidoreductase activity takes place. The reduced form of the cofactor absorbs light at 340 nm wavelength. Subsequently, consumption or production of the NAD(P)H during the oxidation/reduction reaction can be monitored with the spectrophotometer (Fig. 23). Lysate from *E. coli* BL21 [pK470] was used as a negative control. Two ways of reaction were measured for the various enzymes of interest. Oxidation of a set of the alcohols was tested with the alcohol dehydrogenases and short-chain dehydrogenases/reductases (Table 12).

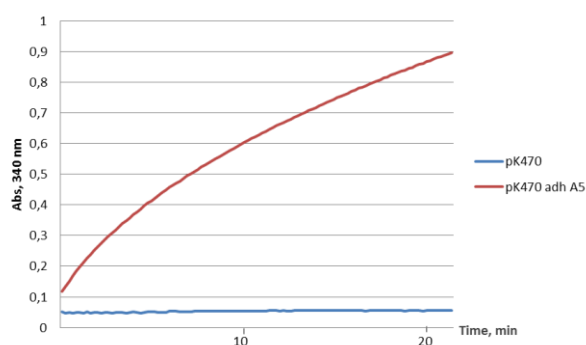


Figure 23. Oxidation of 2-octanol by the whole cell lysate of *E. coli* BL21 with overexpressed ADH A5. Whereas the substrate is oxidized, the cofactor NAD⁺ is reduced. The increasing amount of NADPH due to enzyme activity was monitored over 20 min. *E. coli* BL21 [pK470] was used as a control.

The results of the colony-based activity assay, performed *in vivo*, did not reveal strong differences in the preference of NAD⁺/NADP⁺ cofactors. In contrast, the results obtained with the spectrophotometric assay performed with the lysates showed a clear preference to one form of the cofactor almost for each active enzyme (Table 12). ADH A4, ADH B1, SDR A1 and SDR B7 accepted only NAD⁺, whereas ADH A5 and SDR B3 were more active with NADP⁺ as cofactor. Not only more substrates were converted in the presence of the preferable cofactor type but also the activity was higher comparing to the activity in case of undesirable form of cofactor. ADH B2 and SDR B6 showed equal preferences towards NAD⁺ or NADP⁺.

Table 12. Overview of the enzyme oxidation activity of the cell free lysates of *E. coli* BL21 with the corresponding overexpressed dehydrogenases. Specific enzyme activity is given in mU/mg

	(R)-2-octanol	(S)-2-octanol	rac-4-methyl-2-pentanol	Isoamylalcohol	2,3-butanediol	2-methyl-1-propanol	rac-2-propanol	propanol	butanol	ethanol	
Adh A4	4	2,3	4	1	-	-	-	-	-	-	NAD+
	-	-	-	-	-	-	-	-	-	-	NADP+
Adh A5	-	1,5	-	-	-	0,7	-	-	-	-	NAD+
	1	8	3	-	1,4	0,6	3,5	0,3	-	-	NADP+
Adh B1	2,5	2,3	1,7	-	-	-	-	-	-	-	NAD+
	-	-	-	-	-	-	-	-	-	-	NADP+
Adh B2	0,8	0,8	-	-	-	-	-	-	-	0,4	NAD+
	0,9	0,9	-	-	-	-	-	-	-	-	NADP+
SDR A1	1	-	1	-	-	-	-	-	-	-	NAD+
	-	-	-	-	-	-	-	-	-	-	NADP+
SDR B3	-	-	-	-	-	-	-	-	-	-	NAD+
	4,6	11,4	6	2,2	5	1,4	2	0,3	0,7	-	NADP+
SDR B6	0,4	0,6	-	0,1	-	-	0,2	0,5	0,7	-	NAD+
	0,3	2,4	-	1,2	0,2	0,6	-	-	-	1	NADP+
SDR B7	0,4	1,4	-	-	-	-	-	-	-	-	NAD+
	-	-	-	-	-	-	-	-	-	-	NADP+

E. coli BL21 [pK470-ADH B6], *E. coli* BL21 [pK470-ADH B8] and *E. coli* BL21 [pK470-SDR B9] were also tested but did not show any activity under the tested conditions

The long-chain secondary alcohol 2-octanol was accepted as the best substrate by each tested enzyme. In order to determine stereoselectivity of the dehydrogenases, (*R*)- and (*S*)-2-octanol enantiomers were used as substrate in the oxidation reaction. Regarding (*S*)-2-octanol SDR B3 showed a specific activity of 11.4 mU/mg, which represents the best oxidation activity determined via photometric assay with the cell free lysates. Specificity of SDR B3 towards (*R*)-2-octanol was more than 2 times lower. Other enzymes, which also showed (*S*)-stereoselective behaviour, were ADH A5, SDR B6 and SDR B7. In contrast, ADH A4 and SDR A1 were determined as (*R*)-stereoselective. ADH B1 and ADH B2 equally accepted both enantiomers. Another secondary alcohol such as 4-methyl-2-pentanol was converted with relatively high specific activity, especially by ADH A4, ADH A5 and SDR B3. The simplest secondary alcohol 2-propanol was only accepted by ADH A5, SDR B3 and SDR B6.

When compared to the other substrates, short-chain alcohols like propanol, butanol and ethanol are converted with relatively low specific activity and, therefore, they probably do not belong to the natural substrates of the tested dehydrogenases. In contrast, branch-chained alcohols such as 4-methyl-2-pentanol, isoamylalcohol and 2-methyl-propanol were accepted in a better way. For example, SDR B3 had specific activity of 6 mU/mg with 4-methyl-2-pentanol, 2.2 mU/mg with isoamylalcohol, 1.4 mU/mg with 2-methyl-1-propanol and only 0.3 mU/mg with propabool, 0.7 mU/mg with butanol and no activity with ethanol as a substrate. Alcohol with 2 hydroxy groups such as 2,3-butanediol was only converted by ADH A5, SDR B3 and SDR B6. Three enzymes, ADH B6, ADH B8 and SDR 9, did not react as oxidases with any of tested substrates.

As a next step dehydrogenases were tested for their oxidation activity via photometric assay in the reduction direction of the reaction. Additionally, reductases were also included in this experiment. The results are summarized in Table 13.

Table 13. Overview of the enzyme reduction activity of the cell lysates of *E. coli* BL21 with the corresponding overexpressed dehydrogenases. Specific enzyme activity is given in mU/mg

	Isobutyraldehyde	Propiophenone	Valerophenone	Butyrophenone	2-hydroxyacetophenone	4-phenyl-2-butanone	2-octanone	2-heptanone	Isovaleraldehyde	Benzo phenone	
Adh A5	-	-	-	-	-	2,6	-	-	-	-	NADH
	-	-	-	-	-	6,4	1,9	4,5	4,8	8,3	NADPH
Adh B1	-	-	-	-	-	-	3,2	6,7	-	-	NADH
	-	-	-	-	-	-	-	-	-	-	NADPH
Adh B2	5,3	2	-	-	-	-	1,1	-	2	-	NADH
	3,2	7,9	2,1	2,7	5,6	4,7	2,9	3,6	3,5	4	NADPH
Adh B6	6,4	11,5	9,9	-	8,3	6,1	-	-	1	1,5	NADH
	-	1,9	-	-	2,3	-	-	-	-	6,6	NADPH
SDR A1	-	2	2,5	-	3,4	7,5	-	5	7	-	NADH
	-	4,3	-	-	3	-	-	-	-	-	NADPH
SDR A2	-	-	-	-	-	7	-	3,7	4	-	NADH
	-	3,5	-	-	1,3	-	-	-	-	-	NADPH
SDR A4	-	-	-	-	-	6	1,6	-	2	-	NADH
	-	-	-	-	-	-	-	-	-	-	NADPH
SDR B3	-	16	12,5	11	22	-	-	-	-	-	NADH
	3	17	-	4,4	2	4,8	-	9	2,7	6	NADPH
SDR B6	-	-	-	-	6,8	-	-	-	-	-	NADH
	-	1	-	-	7	-	-	-	-	-	NADPH
SDR B7	-	19,3	-	-	-	1,4	-	-	-	-	NADH
	-	1,2	-	-	-	-	-	-	-	-	NADPH
SDR B9	-	-	0,6	-	-	2,1	1,2	-	3,9	-	NADH
	-	-	-	-	-	-	-	-	-	-	NADPH
Red A4	-	-	0,7	-	7	5,7	-	-	5,2	-	NADH
	-	-	-	-	-	-	-	-	-	-	NADPH
Red A5	-	2,7	7,9	1	3	5,1	2,2	2,4	6,2	3,2	NADH
	-	-	-	-	-	-	-	-	-	-	NADPH
Red A10	-	-	-	-	3,9	2,3	-	3,1	3,9	1,1	NADH
	-	-	-	-	-	-	-	-	-	-	NADPH

E. coli BL21 [pK470-ADH A4], *E. coli* BL21 [pK470-ADH B8], *E. coli* BL21 [pK470-RED A1] and *E. coli* BL21 [pK470-RED A6] were also tested but did not show any activity under given conditions

As expected, the cofactor preference remains the same in the reduction way of reaction for almost all of the tested enzymes. The only exception is ADH B2, which accepted in reduction reaction in most cases NADPH. However, it should be considered that only two substrates were oxidized by ADH B2 with a relatively low specific activity, one substrate with both cofactors and another one only with NAD⁺. These data are not sufficient to define the cofactor preference in the oxidation way of reaction.

As in case of the oxidation experiments, the highest reduction activity within all tested enzymes was determined for SDR B3. This enzyme seems to be especially active with aromatic ketones like propiophenone, valerophenone, butyrophenone and 2-hydroxyacetophenone. A ketone

with two aromatic rings, benzophenone, was also converted by SDR B3 with a relatively average specific activity of 6 mU/mg. In general, this enzyme seems to have a wide range of acceptable substrates since an activity was also detected in the reaction with alkyl ketones such as 2-heptanone. Propiophenone, valerophenone, 2-hydroxyacetophenone, 4-phenyl-2-butanone and isovaleraldehyde were converted by most of the enzymes. As it was noticed, under the tested conditions in general reductases were less active than dehydrogenases.

The NAD(P)⁺/NAD(P)H-dependent photometric assay may be non-favoured in case of reactions performed with cell free lysates, especially in the reduction direction. The cell free lysate implies difficulties by giving background reactions due to the other proteins present in the soluble fraction. Therefore, enzyme activity analysis with the purified proteins is more desirable. Based on the results of the performed enzyme activity analysis four dehydrogenases, ADH A5, SDR A1, SDR B3 and SDR B6, were chosen for further examination. Subsequently, His-tag cloning was performed for the enzymes of interest.

3.1.3.5. Cloning of His₆-tagged enzymes into pK470 expression vector

Two dehydrogenases, SDR A1 and SDR B3 were N-terminally His-tagged by Christina Zach during the Master work (Zach, 2013). For cloning the His-tagged versions of ADH A5 and SDR B6, genes coding corresponding enzymes were cut out of pK470-ADH A5 and pK470-SDR B6 constructs by *Nde*I and *Hind*III endonucleases and ligated with pK470-His₆-SDR B3 where *sdr B3* insert was removed by endonucleases *Nde*I and *Hind*III. According to the protein models generated by SwissProt online tool (Biasini et al., 2014), N-termini of the ADH A5 and SDR B6 are exposed and therefore, are optimal for the His-tag attachment (Fig. 24).

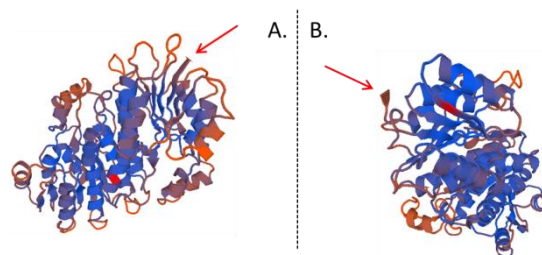


Figure 24. Swiss-Prot protein models of alcohol dehydrogenase ADH A5 (A) and short-chain dehydrogenase/reductase SDR B6 (B) dimers

An example of created construction is shown in Fig. 25.

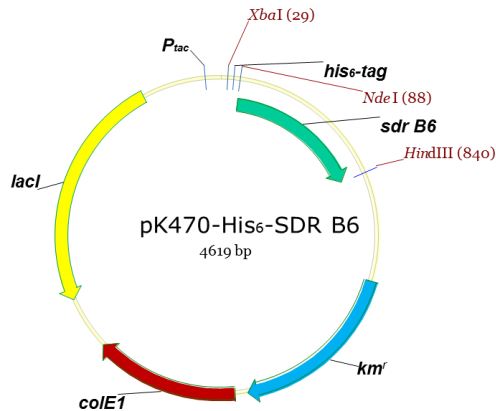


Figure 25. Illustration of the expression vector pK470-His₆-SDR B6. The plasmid backbone encodes promoter *tac*, replication origin *colE1*, gene encoding kanamycin resistance *km^r* and *lacI* gene for repressor protein, N-terminal his₆-tag coding sequence and *sdr B6*

The success of the plasmid construction was proven by the restriction analysis and DNA sequencing (LGC Genomics GmbH; Berlin, Germany) with the primers #39 and #40 (Table 8). The cloned vectors pK470-His₆-ADH A5, pK470-His₆-SDR B3, pK470-His₆-SDR A1 and pK470-His₆-SDR B6 were transformed into *E. coli* BL21 and the grown colonies were analysed and used for expression experiments. Strains generated in this study were handed over to the IMBT strain collection under the numbers ##7631 – 7632 (Supplementary Table 1).

3.1.3.6. Heterologous expression, purification and enzyme activity analysis of His₆-tagged enzymes

The strains were fermented for the further enzyme purifications as described in Materials and methods in chapter 3.1.2. Protein purification was performed on the basis of PD10 desalting columns (GE Healthcare, UK Limited, Little Chalfont, Buckinghamshire, UK), prepacked with Ni Sepharose™ Fast Flow (GE Healthcare Bio-Sciences AB, Uppsala, Sweden).

His₆-ADH A5 was purified with the 20mM sodium phosphate buffer, pH 7.4, supplemented with 0.5 M NaCl. Additionally binding, washing and elution buffers included 20 mM, 30 mM and 100 mM imidazole, respectively. Samples from different purification steps were analysed via SDS-PAGE (Fig. 26).

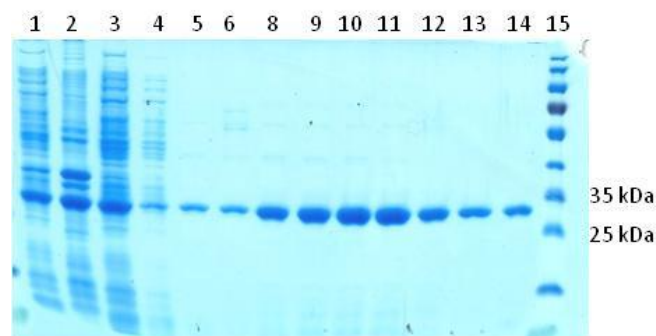


Figure 26. SDS-PAGE of *E. coli* BL21 [pK470-His₆-ADH A5] fermentation samples and His₆-ADH A5 purification fractions. Expected size for His₆-tagged alcohol dehydrogenase A5 is 28 kDa. Lane 1: *E. coli* BL21 [pK470-His₆-ADH A5], soluble fraction; lane 2: *E. coli* BL21 [pK470-His₆-ADH A5], pellet; lane 3: flow through fraction of the protein purification; lanes 4-5: washing fractions of the protein purification; lanes 6-14: elution fractions of the protein purification; lane 15: PageRuler™ Prestained protein ladder

As can be seen from the Fig. 26, significant amount of the protein is present in insoluble fraction. Therefore, in the next fermentation process, lower temperature of cultivation was used to increase the amount of soluble protein. Additionally, part of the His₆-ADH A5 did not bind the column. This problem was solved by increasing the volume of Ni Sepharose™ Fast Flow suspension on the column and decreasing the concentration of imidazole in the binding buffer from 20 to 15 mM. After purification the buffer of His₆-ADH A5 sample was replaced with 20 mM TrisCl and 0.2 M NaCl storage buffer pH 7.4.

His₆-SDR A1 was also purified with the 20mM sodium phosphate buffer, pH 7.4, supplemented with 0.5 M NaCl. Additionally binding, washing and elution buffers included 20 mM, 30 mM and 100 mM imidazole, respectively. Samples from different purification steps were analysed via SDS-PAGE (Fig. 27).

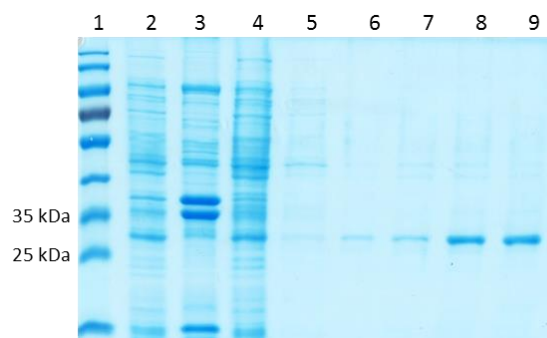


Figure 27. SDS-PAGE of *E. coli* BL21 [pK470-His₆-SDR A1] fermentation samples and His₆-SDR A1 purification fractions. Expected size for His₆-tagged SDR A1 is 27 kDa. Lane 1: PageRuler™ Prestained protein ladder; lane 2: *E. coli* BL21 [pK470-His₆-SDR A1], soluble fraction; lane 3: *E. coli* BL21 [pK470-His₆-SDR A1], pellet; lane 4: flow through fraction of the protein purification; lanes 5-6: washing fractions of the protein purification; lanes 7-9: elution fractions of the protein purification

As it can be seen in Fig. 27, His₆-SDR A1 protein yield after expression was low. Probably this happened because expression induction was started at OD₆₀₀ 0.9 instead of recommended 0.6-0.8, therefore the cell status was not optimal for the production of sufficient amount of His₆-SDR A1. Additionally, it can be noticed from Fig. 27, that half of the protein did not bind the column. For a better yield of purified protein the concentration of imidazole in the binding buffer was decreased from 20 to 15 mM. After purification the buffer of His₆-SDR A1 sample was replaced by storage buffer (20 mM TrisCl and 0.2 M NaCl storage buffer pH 7.4).

His₆-SDR B3 was purified with the 20mM sodium phosphate buffer, pH 7.4, supplemented with 0.5 M NaCl. Additionally binding, washing and elution buffers included 20 mM, 30 mM and 100 mM imidazole, respectively. Samples from different purification steps were analysed via SDS-PAGE (Fig. 28). After purification the buffer of His₆-SDR B3 sample was replaced with 20 mM TrisCl and 0.2 M NaCl storage buffer pH 7.4.

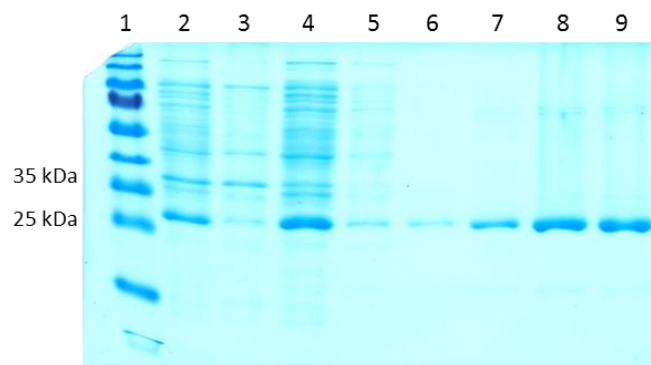


Figure 28. SDS-PAGE of *E. coli* BL21 [pK470-His₆-SDR B3] fermentation samples and His₆-SDR B3 purification fractions. Expected size for His₆-tagged SDR B3 is 27 kDa. Lane 1: PageRuler™ Prestained protein ladder; lane 2: *E. coli* BL21 [pK470-His₆-SDR B3], soluble fraction; lane 3: *E. coli* BL21 [pK470-His₆-SDR B3], pellet; lane 4: flow through fraction of the protein purification; lanes 5-6: washing fractions of the protein purification; lanes 7-9: elution fractions of the protein purification

As it can be noticed from Fig. 28, a big amount of the protein did not bind the column. This problem was solved by increasing the volume of Ni Sepharose™ Fast Flow suspension on the column and decreasing the concentration of imidazole in the binding buffer from 20 to 15 mM.

According to the results obtained by C. Zach during her Master thesis research HEPES buffer was most suitable for His₆-SDR B3 purification (Zach, 2013). Therefore 100 mM HEPES buffer pH 7.4 supplemented with 0.2 M NaCl and 20 mM, 30 mM and 100 mM imidazole in binding, washing and elution buffers, respectively, was used in next purification experiment. However, the final concentration of His₆-SDR B3 did not significantly differ from the concentration of His₆-SDR B3 purified in sodium phosphate buffer and comprised about 0.8 mg/ml.

His₆-SDR B6 was purified with the 20mM sodium phosphate buffer, pH 7.4, supplemented with 0.5 M NaCl. Additionally binding, washing and elution buffers included 20 mM, 30 mM and 100 mM imidazole, respectively. Samples from different purification steps were analysed via SDS-PAGE. After purification the buffer of His₆-SDR B6 sample was replaced with 20 mM TrisCl and 0.2 M NaCl storage buffer pH 7.4. However, final concentration of the purified SDR B6 was too low for further analysis. Therefore alternative HEPES buffer system has also been tested. 100 mM HEPES buffer pH 7.4 supplemented with 0.2 M NaCl and 20 mM, 30 mM and 100 mM imidazole in binding, washing and elution buffers, respectively, was used in next purification experiment. Samples from different purification steps were analysed via SDS-PAGE (Fig. 29). After purification the buffer of His₆-SDR B6 sample was replaced with 20 mM TrisCl and 0.2 M NaCl storage buffer pH 7.4.

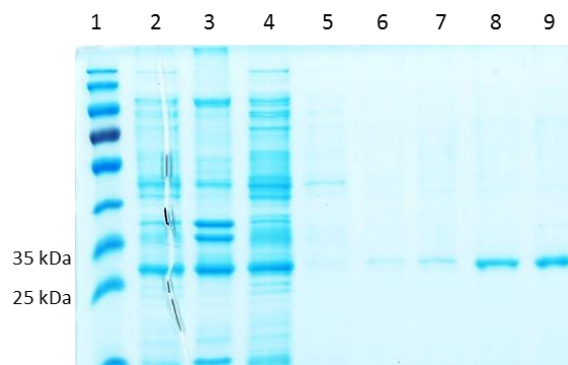


Figure 29. SDS-PAGE of *E. coli* BL21 [pK470-His₆-SDR B6] fermentation samples and His₆-SDR B6 purification fractions. Expected size for His₆-tagged SDR B6 is 26 kDa. Lane 1: PageRuler™ Prestained protein ladder; lane 2: *E. coli* BL21 [pK470-His₆-SDR B6], soluble fraction; lane 3: *E. coli* BL21 [pK470-His₆-SDR B6], pellet; lane 4: flow through fraction of the protein purification; lanes 5-6: washing fractions of the protein purification; lanes 7-9: elution fractions of the protein purification

HEPES buffer was found to be the better choice in case of His₆-SDR B6. However, significant amount of the protein did not bind the column. This problem was solved by decreasing the concentration of imidazole in the binding buffer from 20 to 15 mM. A major part of the recombinant protein was also found in the pellet. Unfortunately, change of growth conditions for cultivation of *E. coli* BL21 [pK470- His₆-SDR B6] by lowering temperature to 25°C and 22°C did not significantly improve the situation. Probably, presence of the His-tag destabilizes folding of the expressed recombinant protein. As a result, the final concentration of His₆-SDR B6 was not higher than 0.3 mg/ml. The protein was concentrated using a 20 mL Vivaspin column (Satorius AG; Göttingen, Germany) for further analysis.

Purified proteins were analysed via NAD(P)⁺/NAD(P)H-dependent photometric assay. The results obtained for the activity of His₆-SDR A1 and His₆-SDR B3 were combined with the results previously reported in the Master thesis of C. Zach (Zach, 2013) and are summarized in Table 14.

Table 14. Overview of the enzyme activities of the purified His₆-tagged enzymes. Data obtained by C. Zach and Z. Magomedova

Enzyme	Substrate	Cofactor	Specific enzyme activity
His ₆ -ADH A5	(S)-2-octanol	NADP ⁺	40 mU/mg
	4-methyl-2-pentanol	NADP ⁺	3 mU/mg
His ₆ -SDR A1	(R)-2-octanol	NAD ⁺	8 mU/mg
	(S)-2-octanol	NAD ⁺	1 mU/mg
	4-methyl-2-pentanol	NAD ⁺	8 mU/mg
	2,3-butanediol	NADP ⁺	1 mU/mg
His ₆ -SDR B3	(R)-2-octanol	NADP ⁺	12 mU/mg
	(S)-2-octanol	NADP ⁺	60 mU/mg
	4-methyl-2-pentanol	NADP ⁺	22 mU/mg
	2,3-butanediol	NADP ⁺	15 mU/mg
	2-methyl-1-propanol	NADP ⁺	8 mU/mg
	2-propanol	NADP ⁺	24 mU/mg
	Butanol	NADP ⁺	1 mU/mg
	Propiophenone	NADPH	58 mU/mg
	Valerophenone	NADPH	34 mU/mg
	Butyrophenone	NADPH	24 mU/mg
His ₆ -SDR B6	4-methyl-2-pentanol	NADP ⁺	23 mU/mg

As expected, the best substrate for His₆-ADH A5, His₆-SDR A1 and His₆-SDR B3 in oxidation way of the reaction was 2-octanol with specific activity of 40, 8 and 60 mU/mg, respectively. Stereoselectivity and cofactor preference of the enzymes was also shown to be in agreement with the results obtained in the photometric assay with the cell free lysates. However, reduction activity could be shown only for His₆-SDR B3 with propiophenone as the best substrate. His₆-SDR B6 was only active with the secondary alcohol 4-methyl-2-pentanol though no activity was reported in the assay with the cell free lysate of the corresponding enzyme.

In accordance with the results of the NAD(P)/NAD(P)H-dependent photometric assay His₆-SDR B3 and His₆-ADH A5 showed the best activities, and therefore they were characterized in more

detail. This work is summarized in the draft manuscript given in the section 3.1.3.9. The examination of the purified His₆-ADH A5 and His₆-SDR B3 was performed after homologous expression on the basis of the novel expression system for *R. eutropha* H16 designed by Steffen Gruber within his PhD project. Expression constructs for His₆-tagged ADH A5 and SDR B3 were obtained as a result of experiments devoted to the establishing of homologous expression of dehydrogenases in *R. eutropha* H16. Different type of the expression vectors created by the members of the group of Dr. P. Heidinger and Prof. H. Schwab were subsequently used for cloning and tested in expression experiments.

3.1.3.7. Cloning of the enzymes into expression vectors for *R. eutropha* H16

In parallel to the characterization of the enzymes in *E. coli*, the characterization of the dehydrogenases expression in *R. eutropha* H16 was performed. Members of the group of Dr. Petra Heidinger and Prof. Helmut Schwab used several strategies to establish novel expression systems for the use in *R. eutropha* H16. These studies were performed by Steffen Gruber, Elisabeth Dornisch, Jeremias Hagen and Daniel Schwendewein.

Despite the significant expansion in the number of potential biochemicals produced by *R. eutropha*, in most reported cases *R. eutropha* was cultivated under conditions of utilizing organic compounds as a carbon source instead of CO₂. Overexpression of recombinant proteins under the growth conditions based on inorganic source of carbon provides additional stress to the cells. This may cause problems with the stability of the recombinant DNA constructs. One of the reasons for that is the lack of suitable genetic tools for this bacterium. However, during the last years more work has been done in this direction (Bi et al., 2013; Gruber et al., 2014). In these studies a set of plasmids with a variety of origins of replication, promoters, mobilization and partition regions were tested. New expression systems developed in our group were used for the homologous protein expression of the selected dehydrogenases.

The first tested systems were pKR-P_{tac} and pKR-P_{tac}-par29.1 expression vectors which contain the REP origin of replication from the pBBR1 plasmid, the kanamycin resistance gene and the *tac* promoter (created by S. Gruber). pKR-P_{tac}-par29.1 additionally carries the partitioning system derived from the broad-host plasmid RK4, named *par* region. This system is used for the distribution of newly replicated plasmids into the daughter cells, which is especially important in case of low-copy-number plasmids. According to the literature, this *par* system efficiently works in several Gram-negative bacteria (Saurugger et al., 1986). Therefore, the *par* region was used to increase the plasmid stability.

Genes coding for ADH A4 and ADH A5 were cloned into pKR-P_{tac} via *Nde*I and *Hind*III restriction sites. Genes coding for ADH A3 and ADH A4 were cloned into pKR-P_{tac}-Par via *Nde*I and *Hind*III restriction sites. Examples of vector maps for the created plasmids are shown in Fig. 30.

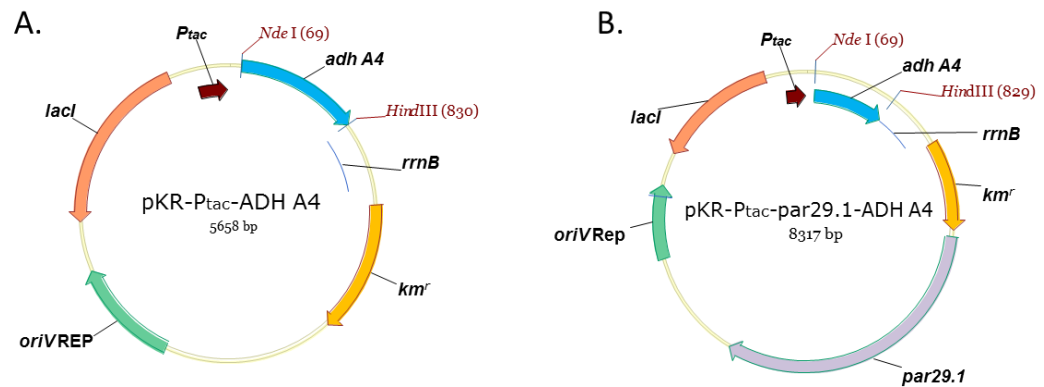


Figure 30. Vector maps of pKR-P_{tac}-ADH A4 and pKR-P_{tac}-par29.1-ADH A4. A. pKR-P_{tac}-ADH A4 contains the pBBR1 REP origin of replication, kanamycin resistance gene *kmr*^r, *lacI* gene, *tac* promoter and gene of alcohol dehydrogenase A4. B. pKR-P_{tac}-par29.1-ADH A4 contains REP origin of replication, kanamycin resistance gene *kmr*^r, *lacI* gene encoding repressor protein, *tac* promoter, alcohol dehydrogenase A4 and *par29.1* region.

The success of the plasmid construction was proven by the restriction analysis and DNA sequencing (LGC Genomics GmbH; Berlin, Germany) with the primers #39 and #40 (Table 8). An example of the restriction analysis is shown in Fig. 31.

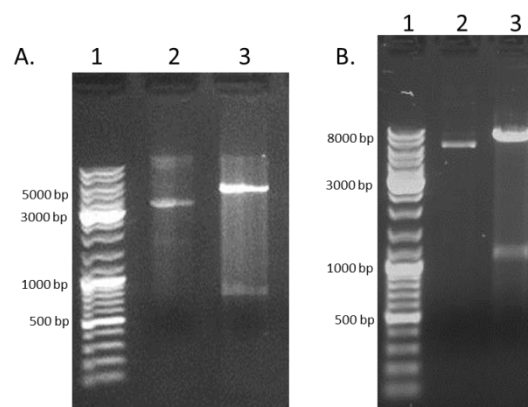


Figure 31. Agarose gel for restriction analysis of pKR-P_{tac}-ADH A4 and pKR-P_{tac}-par29.1-ADH A3. A. Restriction analysis of pKR-P_{tac}-ADH A4 with *Nde*I and *Hind*III endonucleases. Expected size of vector backbone is 4895 bp, expected size of insert *adh* A4 is 761 bp. Lane 1 - GeneRuler DNA Ladder Mix (0.5 µg); lane 2 - pKR-P_{tac}-ADH A4, uncut; lane 3 - pKR-P_{tac}-ADH A4, cut with *Nde*I and *Hind*III. B. Restriction analysis of pKR-P_{tac}-par29.1-ADH A3 with *Nde*I and *Hind*III endonucleases. Expected size of vector backbone is 7557 bp, expected size of insert *adh* A3 is 1103 bp. Lane 1 - GeneRuler DNA Ladder Mix (0.5 µg); lane 2 - pKR-P_{tac}-ADH A4, uncut; lane 3 - pKR-P_{tac}-ADH A4, cut with *Nde*I and *Hind*III.

Constructed expression vectors pKR-P_{tac}-ADH A3, pKR-P_{tac}-ADH A4, pKR-P_{tac}-par29.1-ADH A4 and pKR-P_{tac}-par29.1-ADH A5 were transferred into *R. eutropha* H16 via electroporation as described in chapter 3.1.2. The presence of the expression vector in *R. eutropha* H16 was verified via colony PCR with the primer #39 and the reverse primer to the corresponding gene of dehydrogenase. Colonies, which were proven to carry an expression vector, were analysed for the corresponding dehydrogenase activity by the colony-based activity assay as described in chapter 3.1.2.12 and octanol was used as a substrate. However, no activity was detected for any of the tested enzymes. An intense literature search revealed that *R. eutropha* H16 is lacking necessary transporter systems for the uptake of sugars like lactose or the synthetic inducer IPTG. Thus an IPTG inducible expression system based on the *lac* operator/repressor could not be operable (Sichwart et al., 2011; Wilde, 1962).

In order to overcome this problem, the expression vector system was improved by the deletion of the *lacI* gene (performed by S. Gruber), and thereby enabled constitutive expression. Additionally, enlarged, complete version of partition region *par* was used instead of previously cloned *par29.1*. Several constructs were generated: pKR-P_{tac}-par- Δ *lacI*-ADH A4, pKR-P_{tac}-par- Δ *lacI*-ADH A5, pKR-P_{tac}-par- Δ *lacI*-His₆-SDR B3. The *tac* and the *lac* promoters were previously described as the strongest promoters within those applied for the expression of the genes in *R. eutropha* H16 (Fukui et al., 2011; Kovach et al., 1995; Sichwart et al., 2011). Additionally, the pKR-P_{lac}-par- Δ *lacI*-His₆-SDR B3 expression vector was generated by cloning *his₆-sdr B3* into pKR-P_{lac}-par- Δ *lacI* via *Xba*I and *Hind*III restriction sites. pKR-P_{lac}-par- Δ *lacI* was created by S. Gruber by replacing the *tac* promoter by P_{lac} in pKR-P_{tac}- Δ *lacI*-par expression vector (Fig. 32).

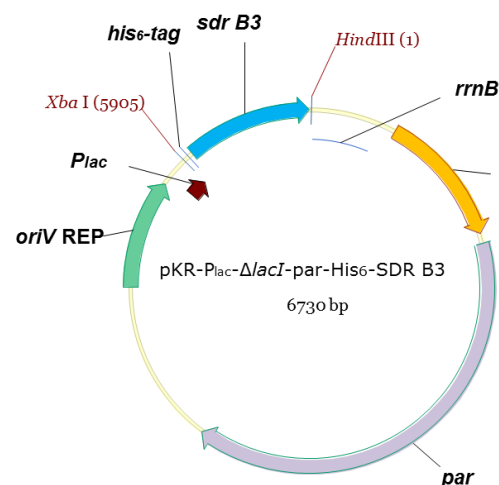


Figure 32. Vector maps of pKR-P_{lac}-par- Δ *lacI*-His₆-SDR B3. pKR-P_{lac}-par- Δ *lacI* contains the pBBR1 origin of replication, a kanamycin resistance gene *km^r*, the *lac* promoter, the *par* region, a coding sequence for N-terminal His-tag and the gene for SDR B3

The success of the plasmid constructions was verified by restriction analysis and DNA sequencing (LGC Genomics GmbH; Berlin, Germany) with the primers #39 and #40 (Table 8). An example of the restriction analysis is shown in Fig. 33.

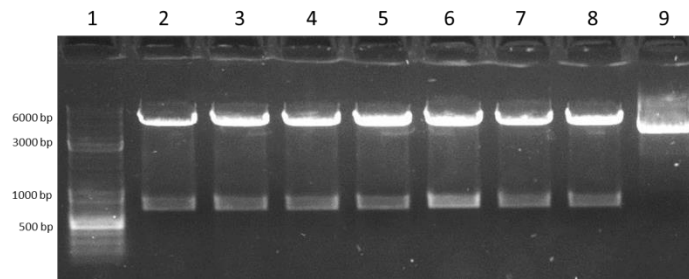


Figure 33. Agarose gel for restriction analysis of pKR-P_{tac}-par- Δ lacI-ADH A4. Restriction analysis of pKR-P_{tac}-par- Δ lacI-ADH A4 with *Nde*I and *Hind*III endonucleases. Expected size of vector backbone is 5963 bp, expected size of insert *adh A4* is 761 bp. Lane 1 - GeneRuler DNA Ladder Mix (0.5 μ g); lanes 2-8 – pKR-P_{tac}-par- Δ lacI-ADH A4, clones 1-7; lane 9 – uncut pKR-P_{tac}-par- Δ lacI-ADH A4

The constructed expression vectors pKR-P_{tac}- Δ lacI-par-ADH A4, pKR-P_{tac}- Δ lacI-par-ADH A5, pKR-P_{tac}- Δ lacI-par-His₆-SDR B3 and pKR-P_{lac}- Δ lacI-par-His₆-SDR B3 were transferred into *R. eutropha* H16 via electroporation. The presence of the expression vector in *R. eutropha* H16 was verified via colony PCR with the primer #39 and the reverse primer annealing to the corresponding dehydrogenase gene. *R. eutropha* H16 colonies, which carried corresponding vector with the gene of dehydrogenase were selected, the proteins were expressed and crude cell lysates of the expression cultures were analysed by SDS-PAGE. As a result, no expression of the desired proteins was detectable.

To overcome the problem of inability of *R. eutropha* H16 to uptake the lactose/IPTG uptake, a strategy for establishment of an IPTG-inducible expression system was developed. The incapability to uptake lactose (and IPTG) could be overcome by the introduction of the *E. coli lacY* gene, which encodes lactose permease into the genome of *R. eutropha* H16. The *lacY* gene was planned to be under the control of promoter *H16_B1772* (derived from *R. eutropha* H16) (Gruber et al., 2014). At the same time the gene encoding His₆-tagged SDR B3 was cloned into pKR-P_{tac}-par-T7Pol/T7MCS-lacI-mob in 3 steps as described in Materials and methods in chapter 3.1.2.8. Upstream to the cloning site of a *T7* promoter, a *T7* terminator and the gene for *T7* polymerase for the protein translation. Since pKR-P_{tac} is a low copy number plasmid, the strong *T7* promoter was introduced into expression vector. Additionally, the mobilization sequence derived from pBBR1MCS-5 was introduced to enable direct transfer of expression vector from *E. coli* S17-1 to *R. eutropha* H16 via conjugation process (Gruber et al., 2014). Unfortunately, integration of *lacY* into the genome of *R. eutropha* H16 was not successful at that time and, therefore, we were not able to test the newly constructed expression system.

To search for further options for expression of the desirable proteins, the mobilization region derived from the pBBR1MCS-5 and origin of replication from the same pBBR1 plasmid were combined in pKR-P_{tac}-par-mob construct. Genes coding for SDR A1, SDR B3, SDR B6 and their His-tagged versions together with His₆-ADH A5 were cloned in this expression vector as described in chapter 3.1.2. An example of the created construct can be seen in Fig. 34.

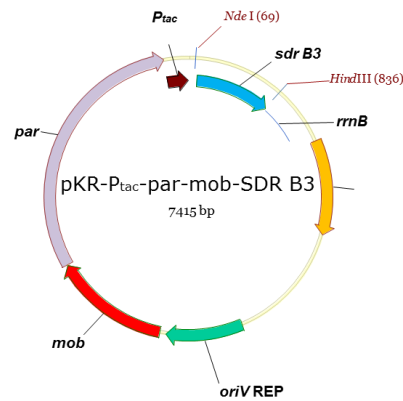


Figure 34. Vector maps of pKR-P_{tac}-par-mob-SDR B3. pKR-P_{tac}-par-mob-SDR B3 contains pBBR1 REP origin of replication, kanamycin resistance gene *km^r*, promoter *tac*, pBBR1 mobilization region *mob* and the gene for SDR B3

The success of plasmid construction was verified by restriction analysis and DNA sequencing (LGC Genomics GmbH; Berlin, Germany) with the primers #39 and #40 (Table 8). An example of the restriction analysis is shown in Fig. 35.

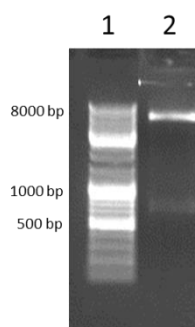


Figure 35. Agarose gel for restriction analysis of pKR-P_{tac}-par-mob-SDR B3. Restriction analysis of pKR-P_{tac}-par-mob-SDR B3 with *NdeI* and *HindIII* endonucleases. Expected size of vector backbone is 6648 bp, expected size of insert *sdrb3* is 767 bp. Lane 1 - GeneRuler DNA Ladder Mix (0.5 µg); lane 2 – pKR-P_{tac}-par-mob-SDR B3

Constructed expression vectors pKR-P_{tac}-par-mob-SDR A1, pKREP-P_{tac}-par-mob-SDR B3 and pKREP-P_{tac}-par-mob-SDR B6, pKREP-P_{tac}-par-mob-His₆-ADH A5, pKREP-P_{tac}-par-mob-His₆-SDR A1, pKREP-P_{tac}-par-mob-His₆-SDR B3 and pKREP-P_{tac}-par-mob-His₆-SDR B6 were transferred into *R. eutropha* H16 via conjugation process and after expression analysed by SDS-PAGE (Fig. 36).

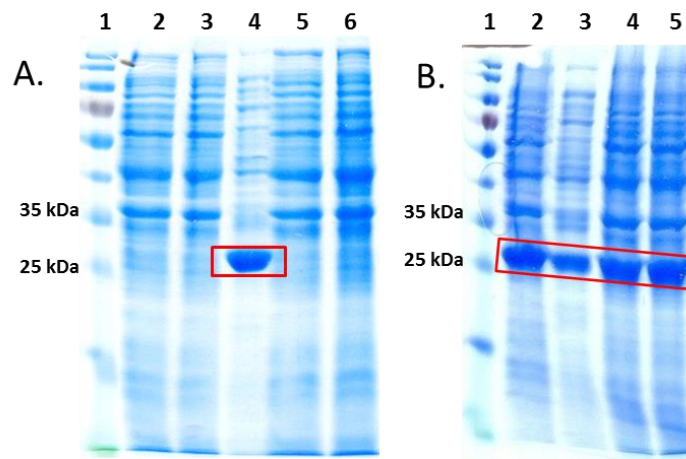


Figure 36. An example of SDS-PAGE of the whole cell lysates from *E. coli* S17 and *R. eutropha* H16 with overexpressed corresponding dehydrogenases. Expressed enzymes are shown in red boxes. A. SDS-PAGE for *R. eutropha* H16 [pKR-P_{tac}-par-mob-His₆-SDR B3]. Expected size for His₆-SDR B3 is 27 kDa. Lane 1 – PageRuler™ Prestained protein ladder; lanes 2, 3 – *R. eutropha* H16 as a negative control; lane 4 – *E. coli* S17-1 [pKREP-P_{tac}-par-mob-His₆-SDR B3] as a positive control; lanes 5-6 – *R. eutropha* H16 [pKREP-P_{tac}-His₆-par-mob-SDR B3], clones 1-2. A. SDS-PAGE for *R. eutropha* H16 [pKREP-P_{tac}-par-mob-His₆-SDR A1]. Expected size for His₆-SDR A1 is 27 kDa. Lane 1 – PageRuler™ Prestained protein ladder; lanes 2, 4, 5 – *R. eutropha* H16 [pKREP-P_{tac}-par-mob-His₆-SDR A1], clones 1-3; lane 4 – *E. coli* S17-1 [pKREP-P_{tac}-par-mob-His₆-SDR A1] as a positive control.

A visualization of the homologous expression of the dehydrogenases in *R. eutropha* H16 via SDS-PAGE revealed only expression for SDR A1. The cell material of *R. eutropha* H16 strains, where no expression of the corresponding dehydrogenases could be detected, was used for various colony PCRs in order to determine if the corresponding expression system is still present in the cells. For each clone 3 types of the colony PCRs were performed. A set of primers, #353 and #354, annealing to the mobilization region was used to verify the presence of pKR-P_{tac}-par-mob vector backbone (Table 8). A second colony PCR was performed to clarify the presence of the gene for the corresponding dehydrogenase on pKR-P_{tac}-par-mob vector. For this PCR two primers were used: forward primer #147, which binds upstream the gene of interest, and reverse primer, which binds on 3' end of the gene of interest (Table 8). The third colony PCR served as control to verify that the expression host is a *R. eutropha* H16 strain. Thereby, the gene for ADH P2, which is located on the pHG1 megaplasmid, was amplified with forward and reversed primers, #29 and #30, annealing to *adh P2*. An example of the performed colony PCRs is shown in Fig. 37.

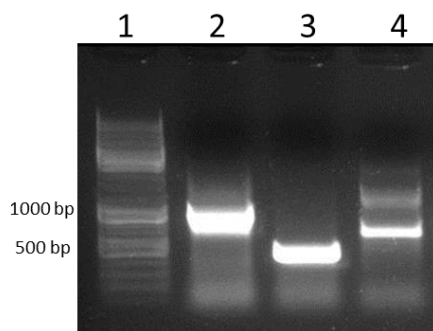


Figure 37. Agarose gel for colony PCR of *R. eutropha* H16 [pKR-P_{tac}-par-mob-SDR B3]. Three types of the colony PCR was performed with the same cell material of a fermentation culture, which had previously been analysed by SDS-PAGE: one colony PCR to verify presence of vector backbone, second colony PCR to confirm *R. eutropha* H16 as a host organism used for cultivation and the third colony PCR to verify presence of a proper dehydrogenase gene on an expression vector. Lane 1 - GeneRuler DNA Ladder Mix (0.5 µg); lane 2 – *R. eutropha* H16 [pKR-P_{tac}-par-mob-SDR B3], PCR to *mob* region, expected size 1000 bp; lane 3 – *R. eutropha* H16 [pKREP-P_{tac}-par-mob-SDR B3], PCR to *adh P2*, expected size 450 bp; lane 4 – *R. eutropha* H16 [pKREP-P_{tac}-par-mob-SDR B3], PCR to *sdr B3*, expected size 800 bp.

Performed colony PCR analysis verified the presence of the proper corresponding expression construct in the cells. Therefore, it may be speculated that due to the stress provided by overexpression, mutations were introduced in the plasmid DNA sequence, thereby preventing the transcription process.

A modified version of pKR-P_{tac}-par-mob expression vector, named pKREP-P_{T5} (created by S. Gruber), was also used for cloning of the genes of interest. In this construct the mobilization region from the pBBR1 plasmid was replaced by the mobilization region derived from the RP4 plasmid. As it was previously shown, such replacement of *mob* region yielded in increase of mobilization efficiency approximately in 50,000 times in comparison with the values obtained for pBBR1 *mob* sequence (Gruber et al., 2014). The mobilization efficiency is determined by the number of colony forming units CFU/ml *R. eutropha* H16 transconjugants related to the number of CFU/ml of *E. coli* S17-1 transformants before mobilization (Meyer, 2000). Additionally, a *T5* promoter was used instead of the *tac* promoter. This promoter is derived from bacteriophage T5 and exhibits strong expression in *E. coli* as well as in *R. eutropha* H16 cells. The genes for the enzymes ADH A5, SDR A1, SDR B3, SDR B6, His₆-ADH A5 and His₆-SDR B35 were cloned into pKREP-P_{T5}. An example can be seen in Fig. 38.

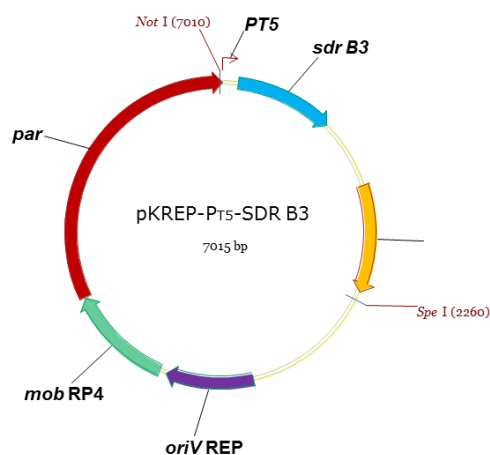


Figure 38. Vector map of pKREP-PT5-SDR B3. pKREP-PT5 contains the pBBR1 REP origin of replication and *par* region, a kanamycin resistance gene *km^r*, the promoter *T5*, a mobilization region *mob* RP4 and the gene for SDR B3

The success of the plasmids construction was proven by the restriction analysis and DNA sequencing (LGC Genomics GmbH; Berlin, Germany) with the primers #473 and #40 (Table 8). An example of the restriction analysis is shown in Fig. 39.

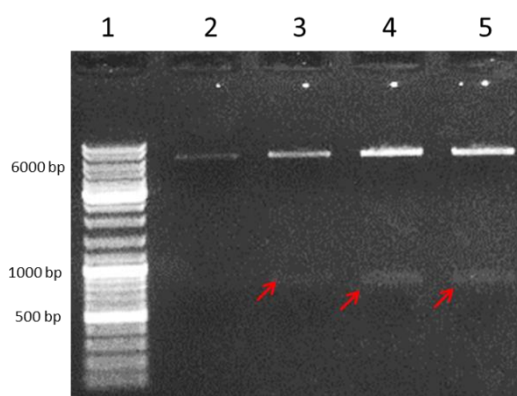


Figure 39. Agarose gel for restriction analysis of pKREP-PT5-ADH A5 and pKREP-PT5-SDR B3. Restriction analysis of pKREP-PT5-ADH A5 and pKREP-PT5-SDR B6 with *Nde*I and *Hind*III endonucleases. Expected size of the vector backbone is 6273 bp, expected size of the inserts *sdr a5* and *sdr b6* are 761 bp and 752 bp, respectively. Bands of the inserts are indicated with red arrows. Lane 1 - GeneRuler DNA Ladder Mix (0.5 µg); lanes 2-3 – pKREP-PT5-ADH A5, clones 1-2; lanes 4-5 – pKREP-PT5-SDR B6, clones 1-2

The constructed expression vectors pKREP-PT5-ADH A5, pKREP-PT5-SDR A1, pKREP-PT5-SDR B3, pKREP-PT5-SDR B6, pKREP-PT5-His₆-ADH A5 and pKREP-PT5-His₆-SDR B3 were transferred into *R. eutropha* H16 via conjugation. The presence of the expression constructs in *R. eutropha* H16 was verified by colony PCR with the primers #104 and #473 (Table 8). An example can be seen in Fig. 40.

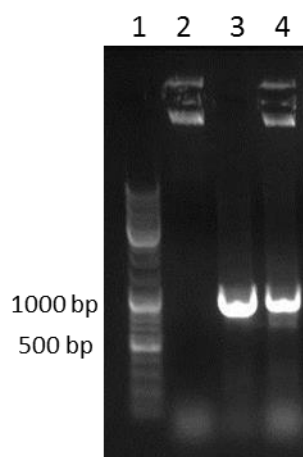


Figure 40. Agarose gel for colony PCR of *R. eutropha* H16 [pKREP-P_{T5}-ADH A5]. A colony PCR to verify presence of a proper expression vector in *R. eutropha* H16 was performed with the primers #104 and #473. Lane 1 - GeneRuler DNA Ladder Mix (0.5 µg); lane 2 – *R. eutropha* H16 as a negative control; lane 3 – pKREP-P_{T5}-ADH A5 plasmid as a positive control; lane 4 - *R. eutropha* H16 [pKREP-P_{T5}-ADH A5], expected size of the PCR product is 1050 bp.

After colony PCR a fermentation of the *R. eutropha* H16 strains with the expression constructs was performed and analysed via SDS-PAGE. An example is shown in Fig. 41.

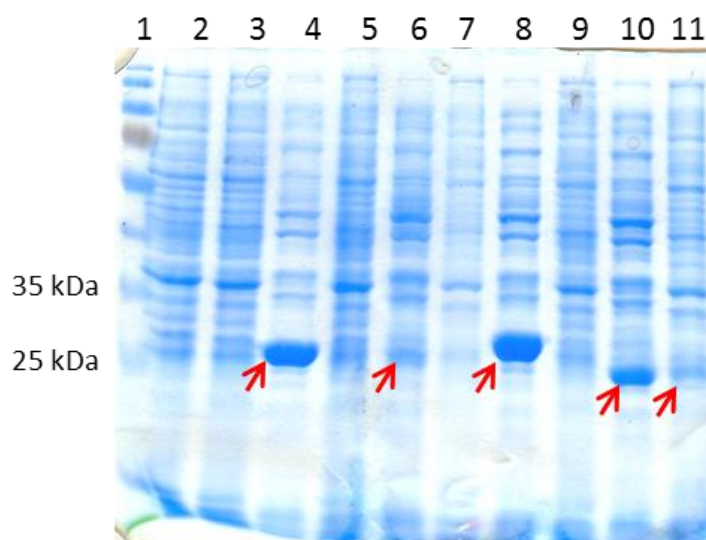


Figure 41. SDS-PAGE of the whole cell lysates from *E. coli* S17 and *R. eutropha* H16 with overexpressed corresponding dehydrogenases. Expressed enzymes are shown with red arrows. Lane 1 – PageRuler™ Prestained protein ladder; lane 2 – *R. eutropha* H16; lane 3 – *R. eutropha* H16 [pKREP-P_{T5}-Δinsert] used as a negative control; lane 4 – *E. coli* S17 [pKREP-P_{T5}-ADH A5], expected size 27 kDa; lane 5 – *R. eutropha* H16 [pKREP- P_{T5}-ADH A5], expected size 27 kDa; lane 6 – *E. coli* S17 [pKREP- P_{T5}-SDR A1], expected size 26 kDa; lane 7 – *R. eutropha* H16 [pKREP-P_{T5}-SDR A1], expected size 26 kDa; lane 8 – *E. coli* S17 [pKREP-P_{T5}-SDR B3], expected size 26 kDa; lane 9 – *R. eutropha* H16 [pKREP-P_{T5}-SDR B3], expected size 26 kDa; lane 10 – *E. coli* S17 [pKREP-P_{T5}-SDR B6], expected size 25 kDa; lane 11 – *R. eutropha* H16 [pKREP- P_{T5}-SDR B6], expected size 25 kDa

A visualization of the homologous expression of the dehydrogenases in *R. eutropha* H16 via SDS-PAGE revealed only expression for SDR B3 (data not shown) and SDR B6. Unfortunately,

expression of SDR B3 and SDR B6 was not observed via SDS-PAGE for each fermented clone. The cultures, *R. eutropha* H16 [pKREP-P_{T5}-SDR B3] and *R. eutropha* H16 [pKREP-P_{T5}-SDR B6], which were shown to have proper expression of a corresponding dehydrogenase, were plated out on TSB_{Gm+Km+fructose} plates in order to obtain single colonies. Few of the grown single colonies were used for the next fermentation and analysed via SDS-PAGE together with new fermentation cultures for *R. eutropha* H16 [pKREP-P_{T5}-His₆-SDR B3] (Fig. 42).

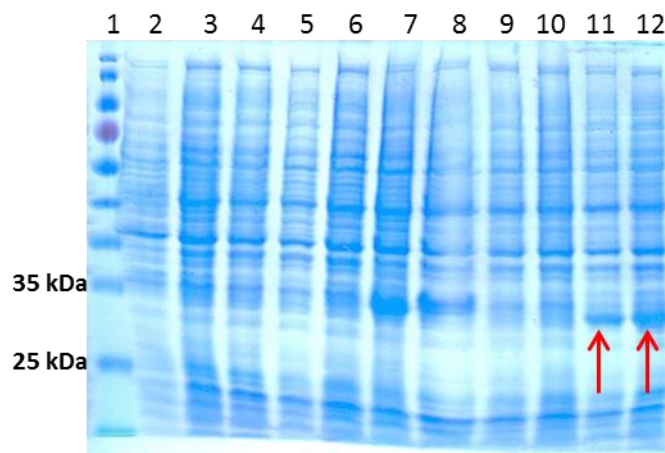


Figure 42. SDS-PAGE of the whole cell lysates from *R. eutropha* H16 with overexpressed corresponding dehydrogenases. Expressed enzymes are shown with red arrows. Lane 1 – PageRuler™ Prestained protein ladder; lane 2 – *R. eutropha* H16 [pKREP-P_{T5}-Δinsert] used as a negative control; lanes 3-6 – *R. eutropha* H16 [pKREP-P_{T5}-SDR B3], clones 1-4, expected size 26 kDa; lanes 7-8 – *R. eutropha* H16 [pKREP-P_{T5}-His₆-SDR B3], clones 1-2, expected size 27 kDa; lanes 9-12 – *R. eutropha* H16 [pKREP-P_{T5}-SDR B6], clones 1-4, expected size 25 kDa

As it can be seen in Fig. 42, no expression was detected on SDS gel for *R. eutropha* H16 [pKREP-P_{T5}-SDR B3] and *R. eutropha* H16 [pKREP-P_{T5}-His₆-SDR B3]. For two clones out of four, which were derived from the culture with expressed SDR B6, no expression was detected under tested conditions. In order to determine the problem, expression constructs from the corresponding strains of *R. eutropha* H16, where no expression of a dehydrogenases of interest was detected after cultivation, were transferred into *E. coli* TOP10 via electroporation, amplified, isolated from the cells and sent for DNA sequencing (LGC Genomics GmbH; Berlin, Germany) with the primers #90 and #69. The results of the DNA sequencing revealed presence of a single mutation of a same type in all expression constructs. This mutation always appears Rep protein of pBBR1 replication region and leads to amino acid exchange (Fig.43). Probably, this happened as a respond to a stress provided to the cells by the overexpression of the dehydrogenases.

```

5' nnn cgc tgg atc tcc gtc gtg aag ctc aac ggc ccc ggc nnn 3'
   Arg Trp Ile Ser Val Val Lys Leu Asn Gly Pro Gly
                                     ↓
5' nnn cgc tgg atc tcc gtc gtg aag ttc aac ggc ccc ggc nnn 3'
   Arg Trp Ile Ser Val Val Lys Phe Asn Gly Pro Gly

```

Fig. 43. Mutation in the gene sequence of Rep protein in pBBR1 origin of replication. Point mutation leads to an amino acid exchange. Picture taken from Lab seminar presentation of S. Gruber.

To overcome this problem, the genes of interest were cloned into the low copy number RSF1010 plasmid. Genes encoding ADH A5, SDR A1, SDR B3, SDR B6 and His-tagged ADH A5 and B3 were cloned into pKRSF1010- P_{T5} expression vector (Fig. 44).

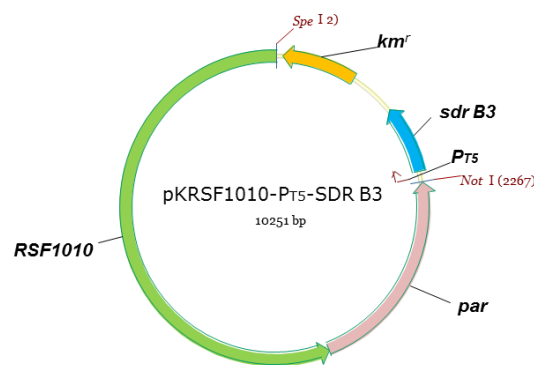


Figure 44. Vector map of pKRSF1010- P_{T5} -SDR B3. pKRSF1010- P_{T5} -SDR B3 contains the RSF1010 origin of replication and mobilization region, a kanamycin resistance gene km^r , a promoter $T5$, and the gene for SDR B3

Success of the cloning of expression vectors pKRSF1010- P_{T5} -ADH A5, pKRSF1010- P_{T5} -SDR A1, pKRSF1010- P_{T5} -SDR B3, pKRSF1010- P_{T5} -SDR B6, pKRSF1010- P_{T5} -His₆-ADH A5 and pKRSF1010- P_{T5} -His₆-SDR B3 was verified by restriction analysis and DNA sequencing (LGC Genomics GmbH; Berlin, Germany) with the primers #501 and #40 (Table 8).

pKRSF1010- P_{T5} -ADH A5, pKRSF1010- P_{T5} -SDR A1, pKRSF1010- P_{T5} -SDR B3, pKRSF1010- P_{T5} -SDR B6, pKRSF1010- P_{T5} -His₆-ADH A5 and pKRSF1010- P_{T5} -His₆-SDR B3 were transferred into *R. eutropha* H16 via conjugation. The presence of the expression constructs in *R. eutropha* H16 was verified by colony PCR with the primers #138 and #40 (Table 8). An example can be seen in Fig. 45.

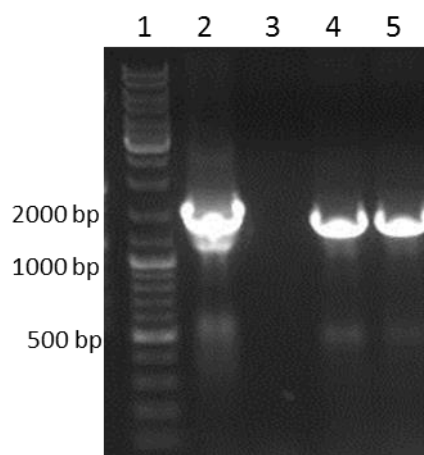


Figure 45. Agarose gel for colony PCR of *R. eutropha* H16 [pKRSF1010-P_{T5}-SDR B3]. A colony PCR to verify presence of a proper expression vector in *R. eutropha* H16 was performed with the primers #138 and #40. Lane 1 - GeneRuler DNA Ladder Mix (0.5 µg); lane 2 – pKRSF1010-P_{T5}-SDR B3 plasmid as a positive control; lane 3 – *R. eutropha* H16 as a negative control; lanes 4-5 - *R. eutropha* H16 [pKRSF1010-P_{T5}-SDR B3], expected size of the PCR product is about 1700 bp.

After colony PCR a fermentation of the *R. eutropha* H16 strains with the expression constructs was performed and proteins were analysed by SDS-PAGE. An example is shown in Fig. 46.

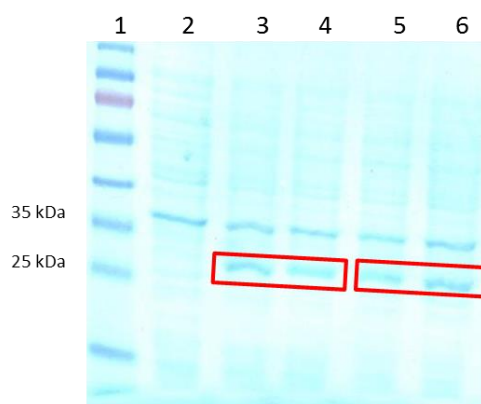


Figure 46. SDS-PAGE of the whole cell lysates from *R. eutropha* H16 with overexpressed corresponding dehydrogenases. Expressed enzymes are shown in red boxes. Lane 1 – PageRuler™ Prestained protein ladder; lane 2 – *R. eutropha* H16; lanes 3-4 – *R. eutropha* H16 [pKRSF1010-P_{T5}-SDR A1], clones 1-2, expected size for SDR A1 is 26 kDa; lanes 5-6 – *R. eutropha* H16 [pKRSF1010- P_{T5}-SDR B6], clones 1-2, expected size for SDR B6 is 25 kDa

A visualization of the homologous expression of the dehydrogenases in *R. eutropha* H16 via SDS-PAGE revealed expression for all dehydrogenases of interest. A colony-based activity assay was performed for *R. eutropha* H16 strains with corresponding expression vectors. An example can be seen in Fig. 47.

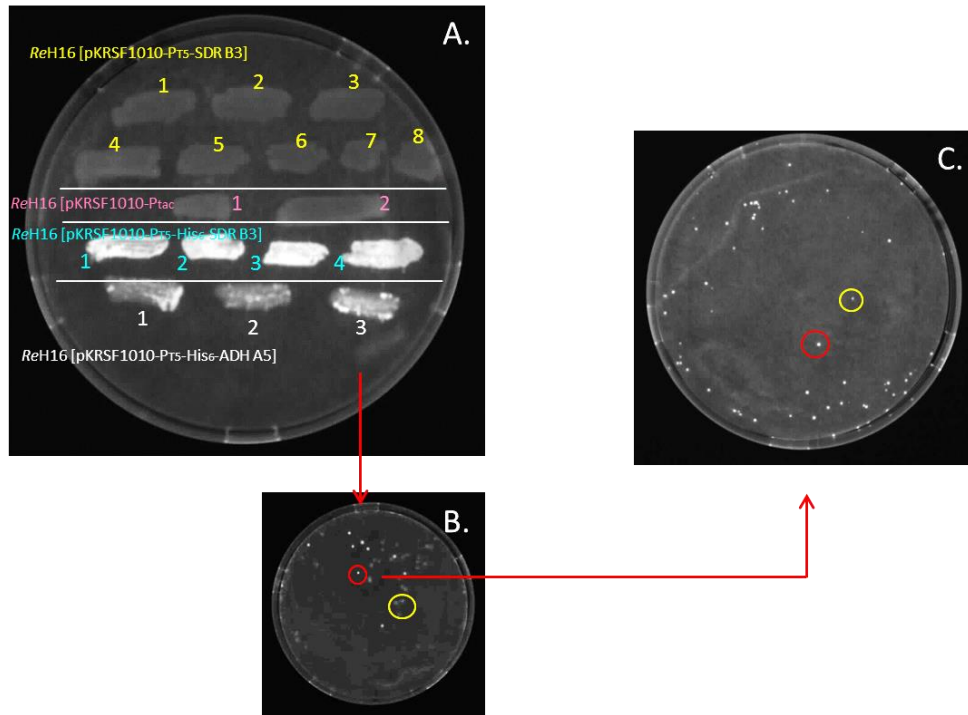


Figure 47. A colony-based activity assay with *R. eutropha* H16 carrying corresponding expression system. A, B, C – results from three subsequently performed colony-based activity assays (see detailed description in the text). Alcohol oxidation reaction is performed by overexpressed dehydrogenase with the help of NAD(P)^+ . Subsequently, reduced form of cofactor, NAD(P)H , is produced by active cells resulting in fluorescence. A filter-paper disk with the cells was soaked in reaction mixture containing 10 mM *rac*-2-octanol, 5 mM NADP^+ and 0.1 M HEPES buffer pH 8.0; exposure time 3 min. Numbers indicate different clones of the strains. *R. eutropha* H16 [pKRSF1010- P_{T5} -SDR B3], *R. eutropha* H16 [pKRSF1010- P_{T5} -His₆-SDR B3] and *R. eutropha* H16 [pKRSF1010- P_{T5} -ADH A5] strains were tested for the enzyme activity. *R. eutropha* H16 [pKRSF1010] was used as a negative control. Active colonies are indicated with red circles; inactive colonies are indicated with yellow circles.

A results for colony-based activity assay revealed that some of the colonies did not express the corresponding dehydrogenases or expressed them in inactive form. *R. eutropha* H16 [pKRSF1010- P_{T5} -ADH A5] cells showed non-uniform fluorescence (Fig. 47A). In order to determine the reason for that, the cells from this plate were grown overnight in the selective media and on the next day serial dilutions of the ONC were plated out on the next day. A plate showing single colonies was used again for the analysis via colony-based activity assay. The results can be seen in Fig. 47B. Colonies of two types were detected: one type included the colonies with active dehydrogenases, another type of the cells represented non-fluorescing cells. Other ONCs were done for the active clones from this plate. The ONCs were plated out on the next day and the plates showing single colonies were used again for the analysis via colony-based activity assay (Fig. 47C). As a result the same two types of the colonies as in previous colony-based activity assay were observed. In order to clarify if the cells without fluorescence do not express the corresponding dehydrogenase or express inactive recombinant enzyme, the cells from the filter paper used in colony-based activity assay were analysed via SDS-PAGE. An example is shown in Fig. 48.

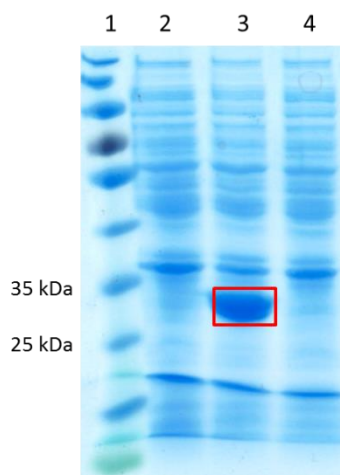


Figure 48. SDS-PAGE of the whole cell lysates from *R. eutropha* H16 [pKRSF1010-P_{T5}-ADH A5]. Expressed enzyme is shown in red boxes. Lane 1 – PageRuler™ Prestained protein ladder; lane 2 – *R. eutropha* H16; lanes 3 – *R. eutropha* H16 [pKRSF1010-P_{T5}-ADH A5], clone, which showed the fluorescence in a colony-based activity assay, expected size for SDR A5 is 26 kDa; lane 4 – *R. eutropha* H16 [pKRSF1010-P_{T5}-ADH A5], clone, which did not show the fluorescence in a colony-based activity assay, expected size for SDR A5 is 26 kDa

As can be seen in Fig. 48, no expression of the overexpressed dehydrogenase was detected for the colony, which did not show fluorescence. In order to determine the problem, expression constructs from the corresponding strains of *R. eutropha* H16, where no expression of a dehydrogenases of interest was detected, were transferred into *E. coli* TOP10 via electroporation, amplified, isolated from the cells and sent for DNA sequencing (LGC Genomics GmbH; Berlin, Germany) with the reversed primer to the gene of interest. The results of the DNA sequencing revealed presence of the mutations in promoter regions in all expression constructs. An explanation for this phenomenon may be that the cells are not able to handle the stress originating from the high overexpression of the enzyme. Obviously, an inducible system is needed to facilitate protein expression in *R. eutropha* H16.

A cumate-inducible expression system created by S. Gruber, was used on the next steps of the cloning experiments (Gruber et al., paper in print). Gene for SDR B3 was cloned into pKRSF1010-P_{J5}-cymR expression vector creating pKRSF1010-P_{J5}-SDR B3-cymR (Fig. 49). It includes RSF1010 replication and mobilization regions, partition region from pBBR1 plasmid, gene encoding cumate repressor, cumate operator upstream the promoter region and cumate operator downstream the promoter region. The used *j5* promoter, which was derived from the bacteriophage T5 and was previously shown to be the strongest promoter ever applied in *R. eutropha* H16 (Gruber et al., 2014), was used in this construct.

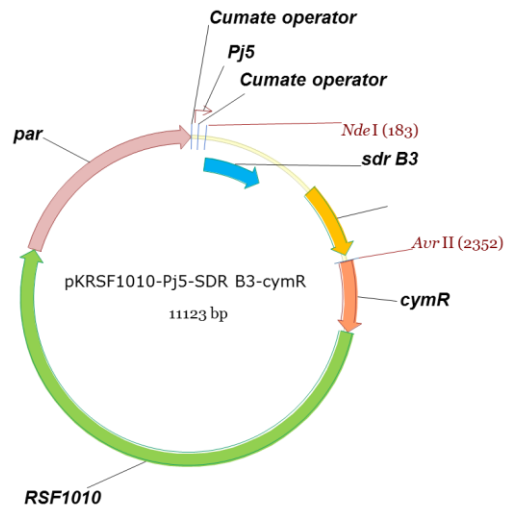


Figure 49. Vector maps of pKRSF1010-P_{j5}-SDR B3-cymR. pKRSF1010-P_{j5}-SDR B3-cymR contains RSF1010 origin of replication and the mobilization region, the *par* region from pBBR1, a kanamycin resistance gene *km^r*, promoter *j5*, a cumate operator upstream the promoter region and a cumate operator downstream the promoter region, a cumate repressor gene *cymR* and the gene for SDR B3

Success of the cloning of expression vectors pKRSF1010-P_{j5}-SDR B3-cymR was verified by restriction analysis and DNA sequencing (LGC Genomics GmbH; Berlin, Germany) with the primers #40 and #80 (Table 8). On the next step pKRSF1010-P_{j5}-SDR B3-cymR was transferred into *R. eutropha* H16 via conjugation. To verify presence of a proper construct transconjugants were analysed via colony PCR with the primers #40 and #516 (Table 8). On the next step positive transconjugants were used for fermentation. The results were visualized by SDS-PAGE as shown in Fig. 50.

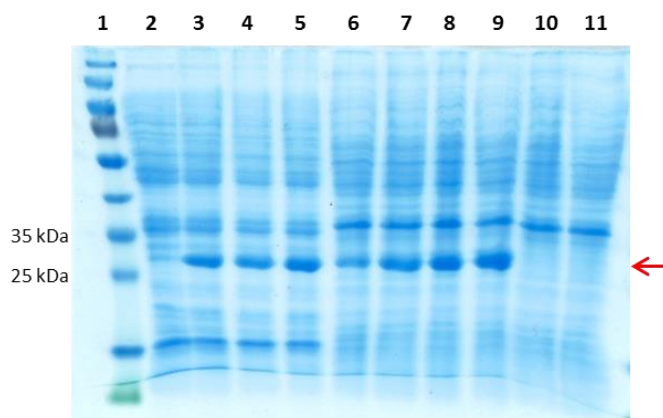


Figure 50. SDS-PAGE of the whole cell lysates from *E. coli* TOP10 [pKRSF1010-P_{j5}-SDR B3-cymR] and *R. eutropha* H16 [pKRSF1010-P_{j5}-SDR B3-cymR]. The position of the expressed SDR B3 is shown with a red arrow. Lane 1 – PageRuler™ Prestained protein ladder; lane 2 – *E. coli* TOP10 [pKRSF1010-P_{j5}-SDR B3-cymR], uninduced; lanes 3-5 – *E. coli* TOP10 [pKRSF1010-P_{j5}-SDR B3-cymR], induced with 5, 10 and 30 µg/ml cumate respectively; lane 6 – *R. eutropha* H16 [pKRSF1010-P_{j5}-SDR B3-cymR], uninduced; lanes 7-9 – *R. eutropha* H16 [pKRSF1010-P_{j5}-SDR B3-cymR], induced with 5, 10 and 30

µg/ml cumate respectively; lane 10 – *R. eutropha* H16, uninduced; lane 11 – *R. eutropha* H16, induced with 30 µg/ml cumate

As can be seen in the position of lane 6 in Fig. 50, a certain level of SDR B3 expression is visible for an uninduced clone of *R. eutropha* H16 [pKRSF1010-P_{j5}-SDR B3-cymR].

In order to refine the inducible system, the same vector with the alternative position of the cumate operators was constructed as well. In this version both of the operators are located right after the promoter, thus enabling tighter regulation of the transcription (created by S. Gruber). Coding sequences for His-tagged SDR B3 and A5 were cloned into this version of the expression system via *Xba*I and *Stu*I restriction sites as described in chapter 3.1.2. Thereby, pKRSF1010-P_{j5}-cyOO-His₆-SDR B3-cymR and pKRSF1010-P_{j5}-cyOO-His₆-ADH A5-cymR constructs were generated. An example of vector map is shown in Fig. 51.

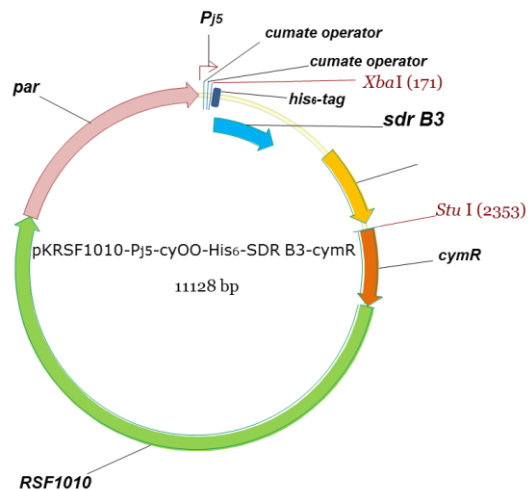


Figure 51. Vector maps of pKRSF1010-P_{j5}-cyOO-His₆-SDR B3-cymR. pKRSF1010-P_{j5}-cyOO-His₆-SDR B3-cymR contains the RSF1010 origin of replication and the mobilization region, the *par* region from pBBR1, a kanamycin resistance gene *km^r*, a *j5* promoter, two cumate operators downstream the promoter region, a cumate repressor gene *cymR* and the gene for SDR B3

Success of the cloning of expression vectors pKRSF1010-P_{j5}-cyOO His₆-SDR B3-cymR and pKRSF1010-P_{j5}-cyOO-His₆-ADH A5-cymR was verified by restriction analysis and DNA sequencing (LGC Genomics GmbH; Berlin, Germany) with the forward primer #40 and reversed primer to the corresponding gene (Table 8). On the next step pKRSF1010-P_{j5}-cyOO-His₆-SDR B3 -cymR and pKRSF1010-P_{j5}-cyOO-His₆-ADH A5 -cymR were transferred into *R. eutropha* H16 via conjugation. To verify presence of a proper construct, transconjugants were analysed via colony PCR with the primers #40 and #516 (Table 8). On the next step positive transconjugants were used for the fermentation. The results were visualized by SDS-PAGE as shown in Fig. 52.

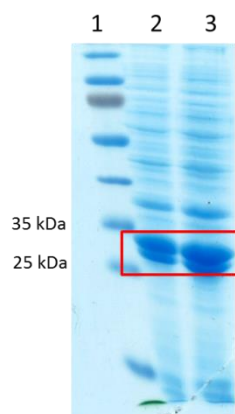


Figure 52. SDS-PAGE of the whole cell lysates from *R. eutropha* H16 [pKRSF1010-P_{j5}-cyOO-His₆-ADH A5 -cymR]. Expressed ADH A5 is shown in a red box. Lane 1 – PageRuler™ Prestained protein ladder; lanes 2-3 – *R. eutropha* H16 [pKRSF1010-P_{j5}-cyOO-His₆-ADH A5-cymR], induced with 30 µg/ml cumate

A strong expression of His₆-ADH A5 can be seen in Fig. 52. Additional small band visible on the SDS gel below the band representing His₆-ADH A5 belongs to non-His-tagged version of the ADH A5. Internal start codon is present upstream the region of *sdr* A5, thereby enabling alternative start of the translation process. This phenomenon has only been observed when recombinant His-tagged proteins were homologously expressed in *R. eutropha* H16. For the uninduced *R. eutropha* H16 [pKRSF1010-P_{j5}-cyOO-His₆-ADH A5-cymR] and *R. eutropha* H16 [pKRSF1010-P_{j5}-cyOO-His₆-SDR B3-cymR] no expression was detected.

As a result, the novel cumate-inducible expression system for *R. eutropha* H16 was successfully applied for the stable fine-tuneable homologous expression of the dehydrogenases. With this vector no instability was observed over time and expression of the desired enzymes was successfully performed. *R. eutropha* H16 strains carrying the corresponding expression plasmids for the enzymes of our interest were fermented for the subsequent protein purification. Additionally, whole cell bioconversion was performed with the lithoautotrophically grown *R. eutropha* H16 [pKRSF1010-P_{j5}-SDR B3-cymR] strain as described in chapter 3.1.3.10.

3.1.3.8. Comparing of the activities of His₆-SDR B3 purified out of *E. coli* BL21 and *R. eutropha* H16

When expressed in *E. coli*, recombinant protein interfaces the microenvironment, which may differ from that of the original organism in terms of pH, osmolarity, redox potential, cofactors and folding mechanisms (Rosano and Ceccarelli, 2014). In order to determine host possesses optimum conditions for the expression, comparison of the activities for SDR B3 purified out of *E. coli* BL21 and *R. eutropha* H16 was performed. The fermentations were done as described in chapter 3.1.2 “Expression of the recombinant enzymes in *E. coli* BL21 and *R. eutropha* H16”. Comparison of purified His₆-SDR B3 activity after expression in the different host organisms was performed via NAD(P)⁺/NAD(P)H-dependent spectrophotometric assay. Three different types of experiments were performed. In the first experiment activity was monitored for the oxidation way of reaction at various temperature conditions as described in section “Spectrophotometric enzyme activity assay with SDR B3 purified out of *E. coli* BL21 and *R. eutropha* H16”, in chapter 3.1.2. The results are shown in Fig. 53.

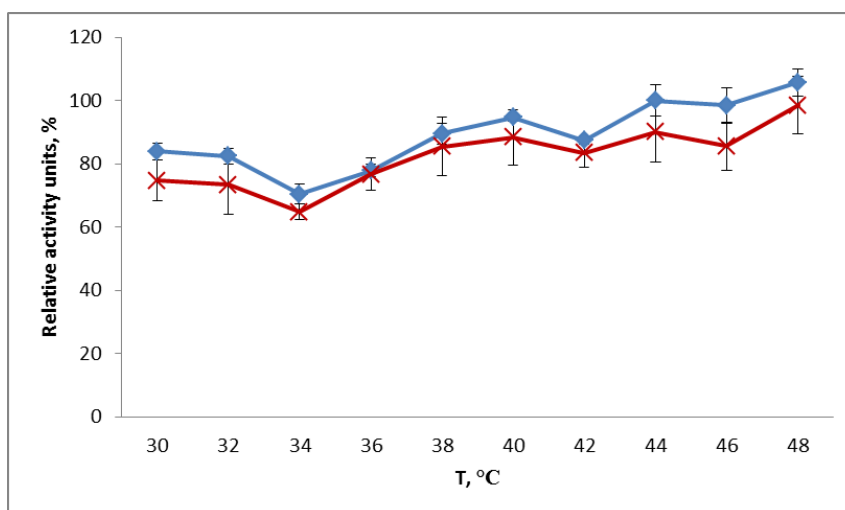


Figure 53. Oxidation of (S)-2-octanol by the purified His₆-SDR B3 out of *E. coli* BL21 and *R. eutropha* H16 under various temperature conditions. Whereas the substrate is oxidized, the cofactor NADP⁺ is reduced. The increasing amount of NADPH due to enzyme activity was monitored over 20 min. Red line indicates the activity for homologously expressed SDR B3, blue line indicates the activity for the enzyme purified out of *E. coli* BL21.

As it can be seen in Fig. 53, no significant difference in the activities of His₆-SDR B3 purified out of *E. coli* BL21 and *R. eutropha* H16 was observed in this experiment.

In the second and third experiments activity was monitored for the oxidation and reduction ways of reaction, respectively, at various pH conditions as described in section “Spectrophotometric enzyme activity assay with SDR B3 purified out of *E. coli* BL21 and *R. eutropha* H16”, in chapter 3.1.2. The results are shown in Fig. 54.

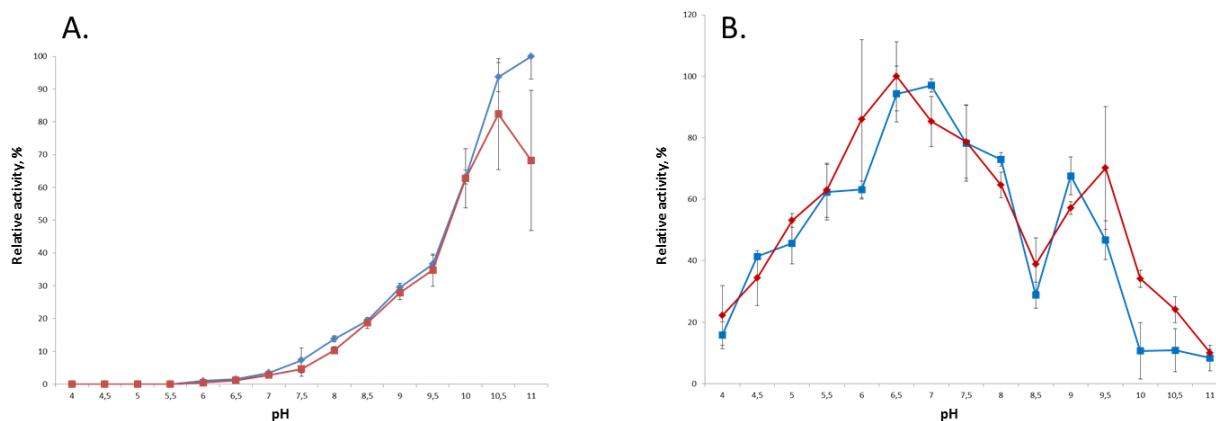


Figure 54. Oxidation of (S)-2-octanol (A) and reduction of 2,3-hexanedione (B) by the purified His₆-SDR B3 out of *E. coli* BL21 and *R. eutropha* H16 under different pH conditions. Red line indicates the activity for homologously expressed SDR B3, blue line indicates the activity for the enzyme purified out of *E. coli* BL21. A. When the substrate is oxidized, the cofactor NADP⁺ is reduced. The increasing amount of NADPH due to enzyme activity was monitored over 20 min. B. When the substrate is reduced, the cofactor NADPH is oxidized. The decreasing amount of NADPH due to enzyme activity was monitored over 20 min.

Too low values for the reduction at pH 8.5 (Fig. 54B) may be explained by use of TrisCl buffer system. Tris-Cl buffer components may have the destabilization effect on the protein structure (Ugwu and Apte, 2004).

As can be seen in Fig. 53 and Fig. 54, no significant difference in the activities of His₆-SDR B3 purified out of *E. coli* BL21 and *R. eutropha* H16 was observed. Short-chain dehydrogenases, including alcohol dehydrogenases, do not require additional certain metal ions in their active site for the proper folding as it is known to be in case of, for example, medium or long chain alcohol dehydrogenases (Kavanagh et al., 2008). Therefore, it seems that the cellular environment might not be crucial for the proper folding of the chosen SDRs originating from *R. eutropha* H16. However, for the characterization of the purified enzymes of interest, recombinant protein production was performed in the native organism *R. eutropha* H16. Additionally, the yield of the recombinant enzyme expressed on the cumate-inducible system, amount of the purified protein and activity of the enzyme were at least as high as for expression in *E. coli* BL21.

According to the results of the colony-based activity assay and the NAD(P)⁺/NAD(P)H-dependent photometric assays, the enzymes SDR B3 and ADH A5 showed the best activities and, thus, were chosen for further detailed characterization. The results of these work is summarized in the following draft paper. Alcohol dehydrogenase A5 belongs to the class of short-chain dehydrogenases and, therefore, can also be named as a SDR. For ease of description in the following paper ADH A5 is named as SDR A5.

3.1.3.9. Characterization of two novel short-chain alcohol dehydrogenases/reductases from *Ralstonia eutropha* H16 capable of stereoselective conversion of bulky substrates

Zalina Magomedova, Andreea Grecu, Christoph W. Sensen, Helmut Schwab, Petra Heidinger

Institute of Molecular Biotechnology, Graz University of Technology, NAWI Graz, Petersgasse 14/1, A-8010 Graz, Austria

Paper draft

Corresponding author:

Petra Heidinger

tel.: +43 316 873 4086

fax: +43 316 873 4071

e-mail address: petra.heidinger@tugraz.at

Abstract

Biocatalysis has significant advantages over organic synthesis in the field of chiral molecule production and several types of stereoselective enzymes are already in use in industrial biotechnology. However, there is still a high demand for new enzymes capable of transforming bulky molecules with sufficient operability. In order to reveal novel high-potential biocatalysts, the complete genome of the β -proteobacterium *Ralstonia eutropha* H16 was screened for potential short-chain dehydrogenases/reductases (SDRs). We were able to identify two (*S*)-enantioselective SDRs named A5 and B3. These showed clear preference towards long-chain and aromatic secondary alcohols, aldehydes and ketones, with diaryl diketone benzil as one of the best substrates. In addition the phylogenetic analysis of all known enzyme types, which are known to facilitate benzil reduction, revealed at least two separate evolutionary clusters. Our results indicate the biotechnological potential of SDRs A5 and B3 for the production of chiral molecules with potential commercial value.

Key words: short-chain dehydrogenase/reductase, alcohol oxidoreductase, *Ralstonia eutropha* H16, benzil, 2-octanol

Introduction

Short-chain dehydrogenases/reductases (SDRs) represent a part of the large functionally diverse class of NAD(P)(H)-dependent oxidoreductases, and one of the largest protein families known up to now. They can be found in all forms of life from viruses up to mammals. SDRs metabolize a wide range of substrates, such as alcohols, aldehydes, ketones, steroids, polycyclic aromatic hydrocarbons and retinoids (Jörnvall *et al.*, 1999; Kallberg *et al.*, 2002; Kavanagh *et al.*, 2008). All members of this family possess a common protein structural motif for nucleotide binding called Rossmann-fold, which includes the TGxxxGxG sequence (Kavanagh *et al.*, 2008). A further common feature is the YXXXK active site motif, which can be slightly altered within different SDRs subfamilies. Altogether five of these subfamilies have been characterized, based on the sequence composition of the cofactor binding domain and of the active catalytic site: classical, extended, intermediate, divergent and complex SDRs (Kallberg *et al.*, 2002). The number of identified SDRs is permanently growing and up to now there are over 140.000 SDRs members listed in the sequence databases (Jörnvall *et al.*, 2015). However, there is always a high demand for new enzymes that are highly active on specific substrates. There are two methods to obtain new catalysts: the first approach includes site-directed mutagenesis of known enzymes, the second one is based on a screening for enzymes in naturally available sources. Environmental diversity selects for rare metabolic properties where those enzymes are capable of performing unique reactions. Therefore, living organisms with diverse metabolic behaviour are the perfect source for mining novel enzymes important for industrial application (Shimizu *et al.*, 1997). One of such organisms is the Gram-negative beta-proteobacterium *Ralstonia eutropha* H16 (now named *Cupriavidus necator*).

R. eutropha H16 is commonly found in soil and fresh water and shows flexible metabolic behavior. It adapts to both, heterotrophic and autotrophic growth conditions, using organic compounds or hydrogen as the energy source. Moreover, in the absence of oxygen *R. eutropha* H16 can perform anaerobic oxidation by denitrification. This bacterium also serves as a model organism for studying the mechanisms involved in the control of autotrophic carbon dioxide fixation, hydrogen oxidation and denitrification (Friedrich and Schwartz, 1993; Kusian *et al.*, 1995; Bowien and Kusian, 2002; Gai *et al.*, 2014; Shimizu *et al.*, 2015). A significant amount of studies are devoted to the production of biodegradable polyhydroxyalkanoates in *R. eutropha* H16, based on different carbon sources (Steinbüchel and Fuchtenbusch, 1998; Atlić *et al.*, 2011; Park *et al.*, 2011; Brigham *et al.*, 2012; Kunasundari *et al.*, 2013; Insomphun *et al.*, 2014; Riedel *et al.*, 2014; Hyeon *et al.*, 2015; Saratale and Oh, 2015). The genome of *R. eutropha* H16 contains a remarkable collection of diverse oxidoreductases. One of the main types of oxidoreductase reactions is performed by dehydrogenases. They catalyse the transfer of hydrides from a substrate to an acceptor or coenzymes, usually NAD⁺ or NADP⁺ or a flavin coenzyme like FAD or FMN in an oxidation-reduction reaction. Dehydrogenases have a wide range of possible biotechnological applications. As an example, it was shown that reduction of certain aldehydes in modified strains of *R. eutropha* H16 can be used for the production of alternative biofuels (Atsumi *et al.*, 2008; Li *et al.*, 2012; Müller *et al.*, 2013; Grousseau *et al.*, 2014; Torella *et al.*, 2015). In addition, the subgroup of short chain dehydrogenases/reductases (SDRs) has great potential for stereoselective reduction of ketones and production of optically pure compounds (*e.g.* Kroutil *et al.*, 2004; Ni and Xu, 2012). Up to now, a set of SDRs from yeasts and bacteria have already been applied on an industrial scale for this purpose (Nakamura *et al.*, 2003; Moore *et al.*, 2007; Matsuda *et al.*, 2009; Huisman *et al.*, 2010). Furthermore, asymmetric reduction of ketones was performed in combined reaction systems where whole cells of *R. eutropha* H16 were used for a cofactor regeneration (Rundbäck *et al.*, 2012; Oda *et al.*, 2013). The

dehydrogenases, which in our opinion are the most interesting are those which are able to convert ketones with bulky substituents, since only few enzymes are capable of accepting stereo-demanding molecules (Ivan *et al.*, 2008; Lavandera *et al.*, 2008a; Kulig *et al.*, 2012).

We have examined the genome of *R. eutropha* H16 (Schwartz *et al.*, 2003; Pohlmann *et al.*, 2006) in order to reveal SDRs capable of performing reactions which might lead to new industrial processes. These reactions include oxidation of secondary alcohols, converting substrates with sterically demanding residues, reduction of long chain and aromatic ketones, as well as aldehydes. We were able to identify two novel short chain dehydrogenases originating from *R. eutropha* H16, which are capable of converting bulky-bulky substrates, such as benzil, with high enantioselectivity.

Materials and methods

Bacterial strains and plasmids

Bacterial strains and plasmids used in this study are listed in Table 1.

Medium and cultivation conditions

All chemicals, reagents and basic media components were obtained from Becton, Dickinson and Company (Franklin Lakes, NJ, USA), Sigma-Aldrich (St. Luis, MO, USA) and Carl Roth (Arlesheim, Germany), respectively, unless mentioned otherwise.

E. coli strains were propagated at 37°C at 120 rpm in lysogeny broth (LB). *R. eutropha* H16 strains were grown at 28°C at 100 rpm in tryptic soy broth (TSB) supplemented with 20 µg/ml gentamicin. For antibiotic selection kanamycin was added when necessary in a concentration of 40 µg/ml for *E. coli* strains and 200 µg/ml for *R. eutropha* H16 strains. Medium was solidified with 20g/l agar-agar (Carl Roth, Arlesheim, Germany) when needed.

Sequence analysis

The UniprotKB [<http://www.uniprot.org/>] and NCBI [<http://www.ncbi.nlm.nih.gov/>] databases were used to screen for probable alcohol dehydrogenases and short chain dehydrogenases/reductases of *R. eutropha* H16. The BLAST program [<http://www.uniprot.org/blast/>] was used to search for the proteins that shared homologies. The CDS tool from the NCBI database [<http://www.ncbi.nlm.nih.gov/Structure/cdd/wrpsb.cgi>] was used to search for conserved domains within a protein sequence or protein-coding nucleotide sequence. Multiple sequence alignments were made using the Espresso mode of the T-coffee tool set (Kemena and Notredame, 2009; Di Tommaso *et al.*, 2011). The resulting alignments were visualized with the graphical viewer Jalview 2.8.2 (Waterhouse *et al.*, 2009).

The bootstrapped phylogenetic analysis was performed with PHYLIP 3.696 (Felsenstein, 2005). *Seqboot* was used to produce 1000 new data sets from the original input data, using the Delete-half-jackknife resampling method (Wu, 1986). Distance analysis with *protdist* was followed by the Neighbor-Joining clustering method (Nei, 1987) provided by the script *neighbor*. For both programs, the default parameters suggested by the two programs were changed to allow for processing of

multiple datasets. Human short chain dehydrogenase/reductase (UniProt [O75911](#)) was used as the outgroup for the phylogenetic analysis. The resulting phylogenetic trees were used as input to the *consense* program. The final tree was visualized and rearranged with the graphical viewer FigTree [<http://tree.bio.ed.ac.uk/software/figtree/>].

DNA preparation

Standard procedures were used for PCR, DNA preparation and manipulation as well as genomic DNA isolation (Green and Sambrook, 2012). Restriction enzymes, Fast DNA End Repair Kit, DreamTaq Green DNA Polymerase, Phusion Polymerase and GeneJET Plasmid Miniprep Kits by Thermo Scientific (Waltham, MA, USA), T4 DNA Ligation reaction and Wizard SV Gel and PCR Clean-Up System by Promega TM (Madison, WI, USA) and Easy-DNA Kit by Invitrogen (Carlsbad, California, USA) were used according to the supplier's protocols. LGC Genomics GmbH (Berlin, Germany) performed the DNA sequencing.

Plasmid construction

A putative alcohol dehydrogenase H16_A1168 (SDR A5, UniProt [Q0KCG2](#)) and a short chain dehydrogenase H16_B1297 (SDR B3, UniProt [Q0K1N7](#)) were amplified from genomic DNA of *R. eutropha* H16 via PCR and cloned into pK470 vector for expression in *E. coli* and pKRSF1010-P_{j5}-cymR vector for expression in *R. eutropha* H16 via *Nde*I and *Hind*III restriction sites. Additional 20 dehydrogenases originating from *R. eutropha* H16 were cloned in the same way in the expression vector pK470 (primers and generated expression plasmids are listed in Tables S1 and S2, respectively). To generate N-terminally His₆-tagged versions of the enzymes, *double-strand* DNA fragment containing 6His-tag was prepared by annealing two synthesized oligonucleotides and cloned into expression vectors via *Xba*I and *Nde*I restriction sites.

Primers used for PCR are listed in Table 2.

Colony assay based on NAD(P)H fluorescence

A colony assay, based on the production of nicotinamide adenine dinucleotide NADH, or nicotinamide adenine dinucleotide phosphate NADPH fluorescence, was performed in order to screen for functional active enzymes (Reisinger *et al.*, 2006). All expression vectors were transformed into competent *E. coli* BL21 cells. Serial dilution of *E. coli* BL21 overnight cultures harboring the appropriate plasmid were plated out on LB^{Kan} agar plates and incubated overnight at 37 °C. The plates were replica stamped onto LB^{Kan} agar plates containing additional 1 % glucose, as well as 0.1 mM isopropyl β-D-thiogalactopyranoside (IPTG) and incubated at 28 °C overnight. Subsequently, the colonies were lifted onto Ø 8.5 cm filter paper disks (Whatman International Ltd; Maidstone, United Kingdom) and air dried for 5 min. Dried filters were soaked in 0.1 M HEPES buffer pH 8.0 containing 10 mM substrate and 5 mM NAD(P)⁺. The tested substrates were (S)-(+)-2-octanol, (R)-(-)-2-octanol, *rac*-butan-2,3-diol, 2-methyl-propanol, butanol, 3-methyl-butanol and *rac*-4-methyl-2-pentanol. The increased fluorescence of NAD(P)H was measured using a G:BOX (Syngene; Cambridge, United Kingdom).

Expression and purification of His₆-tagged recombinant enzymes

The completed constructs were transformed into *E. coli* BL21 expression strain via standard electroporation procedure. The cultivation was performed in LB medium supplemented with 1 % glucose. The recombinant enzyme expression was initiated by adding 0.1 mM IPTG at an OD₆₀₀ 0.6-0.8 and carried out over night at 28°C at 120 rpm.

Plasmid transfer into *R. eutropha* H16 was performed via modified triparental conjugative mating procedure (Goldberg and Ohman, 1984) from the donor strain *E. coli* TOP10 carrying desirable construct to the recipient strain *R. eutropha* H16 with the help of the *E. coli* HB101 [pRK2013] strain. Expression in *R. eutropha* H16 was performed in TSB medium supplemented with 0.6 % fructose. The induction of the enzyme expression in plasmid harboring strains was started at an OD₆₀₀ 1.0 by adding 60 µg/ml cumate and cultures were grown over night at 28°C at 100 rpm.

Following expression, the cells were harvested by centrifugation at 4000 rpm at 4°C. Cell disruption was performed via sonification in 50 mM sodium phosphate buffer pH 7.4. After centrifugation at 20000 rpm at 4°C for 1 h, clear lysates were used for the enzyme activity assays or for purification (therefore, the cells were resuspended in 50 mM sodium phosphate buffer pH 7.4 with 0.5 mM NaCl and 20 mM imidazole).

Protein purification was performed on the basis of PD10 desalting columns (GE Healthcare, UK Limited, Little Chalfont, Buckinghamshire, UK), prepacked with Ni Sepharose™ Fast Flow (GE Healthcare Bio-Sciences AB, Uppsala, Sweden), according to the manufacturer's protocols. For the purification 20 mM sodium phosphate buffer pH 7.4 with 0.5 M NaCl was used with additionally added 20, 30 and 100 mM imidazole in binding, washing and elution steps respectively. After purification protein samples were replaced with 20 mM TrisCl and 0.2 M NaCl storage buffer pH 7.4 via the PD10 desalting columns.

The amount of total protein in the lysate and the concentration of purified enzymes were determined according to the Bradford procedure using Protein Assay Dying Reagent (Bio-Rad Laboratories Inc.; Hercules USA) and bovine serum albumin served as a standard.

SDS PAGE analysis was performed using 10 % Tris-glycine SDS-polyacrylamide gels. For the proteins' molecular weight estimation PageRuler™ Prestained Protein Ladder (10-170 kDa) (Thermo Science Inc., Waltham; USA) was applied. After electrophoresis the gels were stained with Coomassie Brilliant Blue solution.

Enzyme activity assays

The specific enzyme activity was determined by a NAD(P)⁺/NAD(P)H dependent spectrophotometric assay. The light absorbance at 340 nm was monitored over 20 min, using the Synergy Mx Monochromator-Based Multi-Mode Microplate Reader (BioTek Instruments GmbH; Bad Friedrichshall, Germany). The reaction mixture for reduction reaction included 1 mM substrate 50 mM sodium phosphate buffer pH 6.5, 0.02 mg of purified protein and 0.5 mM NAD(P)H. For oxidation reaction 1 mM substrate 50 mM bicarbonate buffer pH 10.5, 0.01 mg of protein and 0.5 mM NAD(P)⁺ was used. Three different types of controls were used. Therefore, the protein, substrate or cofactor part in the mixture was replaced by reaction buffer. All measurements were biologically

and technically performed in triplicates. Based on the absorbance data, the enzyme activity units were defined as the amount of enzyme producing 1 μmol of NAD(P)H per min. Specific activity was expressed as units per mg of protein.

To determine the substrate scope of the SDR A5 and SDR B3 all substrates given in Fig. 1 were tested.

For pH range studies following 50 mM buffers were used: citrate buffer pH 4.0, 4.5, 5.0, 5.5; sodium phosphate buffer pH 6.0, 6.5, 7.0, 7.5, 8.0; Tris-HCl buffer pH 8.0, 8.5, 9.0; bicarbonate buffer pH 9.5, 10.5, 11.0. Measurements in oxidation and reduction way of reaction were performed at 40°C; (S)-(+)-2-octanol and hexane-3,4-dione were used as a substrate, respectively.

To determine the optimum temperature studies were performed in oxidation way of reaction over 20 min using the Cary 100 UV-visible spectrophotometer (Agilent Technologies; Santa Clara, CA, USA) at the temperatures 20°C, 30°C, 40°C, 50°C, 60°C and 70°C. Measurements were performed in 50 mM carbonate-bicarbonate buffer pH 10.5 with (S)-(+)-2-octanol as a substrate.

Stability

Determination of stereoselectivity

The reaction mixture included 0.2 mg of the purified protein SDR A5 or SDR B3, 10 mM benzil (dissolved in dimethylsulfoxide) and 5 mM NADPH (dissolved in ddH₂O) in sodium phosphate reaction buffer (50 mM pH 6.5). In total a volume of 1 mL was reached. In the control reaction, the protein was replaced by the additional volume of reaction buffer. The reaction proceeded at 38°C in a thermomixer at 400 rpm. After 3 hours the products were extracted with n-heptane and isopropanol (in ratio 90 to 10, respectively) and analyzed with a high-pressure liquid chromatography (HPLC) apparatus Agilent Technologies 1100 Series System (Agilent Technologies, Waldbronn, Germany) using a Chiralpack AD-H Analytical column (particle size 5 μm , 250 mm x 4,6 mm; Daicel Chemical Industry, Japan) with isocratic eluent n-heptane/isopropanol (90/10). Data were analyzed with *Agilent ChemStation software* (Agilent Technologies, Waldbronn, Germany).

Results and Discussion

Screening of the dehydrogenases potentially applicable in biotechnology

An examination of the publicly accessible sequence databases revealed around 400 potential dehydrogenases in the *R. eutrophas* genome. Based on the BLAST results, conserved domain searches and complexity of the proteins, 11 alcohol dehydrogenases (ADHs) and 11 short chain dehydrogenases/reductases (SDRs) were selected, cloned and expressed in *E. coli* BL21 (see Fig.1).

The initial screening for functional enzymes was performed by direct visualization of the activity of the enzymes expressed by bacterial colonies. Fluorescence of different intensity was observed for *E. coli* BL21 cells with heterologously expressed dehydrogenases and tested with different substrates. An example of this assay is shown in Fig. 1.

A number of dehydrogenases found to be active towards tested alcohols are listed in Table 3. As can be seen, the most promising enzymes candidates were ADH A4, SDR A1, SDR A5 and SDR B3. Accordingly, they were N-terminally 6His-tagged, overexpressed in *E. coli* BL21, purified and

characterized for their oxidizing and reducing abilities. In accordance with the results of the colony-based activity assay SDR B3 and SDR A5 showed the best activities and were homologously overexpressed in *R. eutropha* H16 in order to provide the optimal functional expression conditions (Fig. S1). Subsequently, they were purified and further characterized in more detail.

The results of the spectrophotometric assay revealed a preference for NADP⁺/NADPH as cofactor, which is especially strong for SDR B3. The cofactor specificity is attributed to certain amino-acid positions in the cofactor-binding site of the enzyme. Altogether, a positively charged environment correlates with phosphorylated cofactor preference (Tanaka *et al.*, 1996). NADP(H) preference is caused by the presence of basic residues, arginine or lysine, in the TGxxxGxG cofactor binding motif and/or at the C-terminal end of the second β -sheet (Tanaka *et al.*, 1996; Persson *et al.*, 2003). Depending on the distribution of these residues in given positions, classical SDRs can be divided in three subfamilies. SDRs of the cP1 subfamily show only one arginine or lysine in the cofactor binding glycine rich domain, members belonging to the cP2 subfamily show an Arg or Lys at the beginning of the second β -sheet, and cP3 SDRs possess positively charged arginine or lysine both in Gly-rich motif and at the beginning of second β -sheet. SDR B3 is a member of cP2 subfamily and SDR A5 belongs to the cP3 subfamily (see Fig. 2).

According to the results of the colony-based activity assay, SDRs B3 and A5 accept both cofactors (NAD⁺ and NADP⁺) in a similar manner. However, purified enzymes showed strong preference to the phosphorylated form of the cofactor. This may be explained due to the activity of the NAD kinase, which is present in *E. coli* BL21 cells. Cellular NADP⁺ in living organisms is produced *de novo* through the phosphorylation of NAD⁺ by NAD kinase, and this enzyme can be found ubiquitously, from bacteria to human cells (Kawai *et al.*, 2001). From the biotechnological point of view, NAD(H) is of a greater interest than NADP(H) because of lower costs. To overcome this problem, NAD kinase can be used to increase the amount of available NADP⁺ from NAD⁺ moiety/pool. For example, Li and co-authors (Li *et al.*, 2009) employed this enzyme to increase the NADP⁺ concentration using intracellular NAD⁺ and thus improved NADP⁺-dependent PHB production in recombinant *E. coli* harbouring the PHB synthesis pathway from *R. eutropha*.

Biochemical properties of SDR B3 and SDR A5

a) pH optimum

Pyridine-nucleotide dependent dehydrogenase reactions are pH dependent: in case of alkaline conditions the oxidation pathway is preferred and, in contrast, an acidic environment catalyzes the reduction reaction. As shown in Fig. 3, the pH optima for the activity of SDR B3 and SDR A5 show a similar pattern. The highest oxidation activity for SDR B3 and SDR A5 was detected at pH 11.0 (Fig. 3B and 3D). However, the enzymes are not stable at extreme alkaline conditions. For instance, after 3 hours of storage at pH 11.0 the activity of SDR A5 was decreased fourfold (data not shown).

For SDR A5, the optimal pH for reduction activity is 6.5 (Fig. 3C). For SDR B3, the favorable pH range for reduction is within the range of 6 to 7.5 and therefore broader (Fig. 3A). In contrast to the alkaline conditions, the reducing activity of the enzymes, which were kept at pH 6.5 for 3 hours did not decrease significantly and showed an activity lowered by only one third, in comparison with the initial activity (data not shown). This may be explained by the fact that pH parameters of the reaction buffer did not differ substantially from the pH of the storage buffer, which are 7.5 for both of enzymes.

Additionally, we have determined that the chemical content of the buffer influences the reducing activity of SDR B3. All measurements in Tris-HCl buffer demonstrated lower activities, when compared to those performed in sodium phosphate or carbonate-bicarbonate buffers at the same pH. The same observations have already been reported by Kulig and co-authors for an alcohol dehydrogenase from *Ralstonia* sp. (Kulig *et al.*, 2013). This may be explained by the destabilization effect of Tris-Cl buffer components on the protein structure (Ugwu and Apte, 2004).

b) Temperature optimum

The influence of temperature on the enzyme activity was tested for the oxidation reaction between 20 and 70°C. The highest activity for SDR B3 was detected at 40°C (Fig. 4A). The enzyme kept more than 60 % of its relative activity within a broad temperature range from approximately 25° to 65°C. SDR A5 showed a more narrow temperature interval to keep 60 % of its relative activity, which is within 30° and 60°C, and had the best activity between 40 and 50°C (Fig 4B). For both of the enzymes the activity at 20°C dropped twice in comparison to the activity at the optimum temperature. In general, SDR A5 and SDR B3 showed the same optimum temperatures as it was described previously for dehydrogenases originating from *Ralstonia* sp. (Zarnt *et al.*, 1997; Kulig *et al.*, 2013).

Substrate range and stereoselectivity for oxidation activity of SDR B3 and SDR A5

55 different substrates (Fig. 5) were tested for oxidation and reduction activity of SDR B3 and A5. In the oxidation pathway of the reaction, both of the enzymes showed preference towards secondary long-chain aliphatic alcohols or secondary alcohols with phenyl as a substituent (Fig. 6), respectively. Both of the enzymes showed high preference for such substrates as (S)-(+)-2-octanol, (S)-(+)-4-phenyl-2-butanol and (S)-(+)-hexanol. Additionally, SDRs A5 and B3 react with (S)-(-)-1-phenylethanol and 1-phenyl-2-propanol. No activity could be detected with *R*- enantiomers. The obtained results demonstrate that both enzymes are specific for *S*- enantiomers.

Enantiomerically pure chemicals are essential building blocks for the production of chiral pharmaceuticals, drugs, flavors and agrochemicals (Hummel, 1999; Goldberg *et al.*, 2007; Huisman *et al.*, 2010). In contrast to chemical catalysis, biocatalysts can perform reactions under mild conditions and, thus, do not cause problems with isomerization, racemization, epimerization, and rearrangement of the molecules (Patel, 2008). Another advantage is the high chemo-, regio-, and stereoselective (Goldberg *et al.*, 2007). There is a variety of approaches for introducing asymmetry with microbial enzymes and cells, such as kinetic resolution, deracemization, desymmetrization reactions and biocatalytic asymmetric synthesis (Wohlgemuth, 2010). Thus, chiral alcohols can be produced by either asymmetric reduction of prochiral ketones or kinetic resolution of racemic alcohols. As a consequence, stereoselective dehydrogenases/reductases are desirable enzymes in biotechnology.

SDR B3 is able to convert a broader range of substrates in comparison to SDR A5 and, additionally, shows higher activities with nearly all of the tested substrates. However, the highest oxidation activity was detected for SDR A5 in the reaction with (S)-(+)-2-octanol, as shown in Fig. 6, where 100% relative activity refers to 1.2 U/mg specific activity units. (S)-(+)-2-octanol was among the best substrates for SDR B3, with a detected specific activity of 640 mU/mg, although the highest activity for this enzyme was detected in the reaction with (S)-(-)-1-phenylethanol and the calculated specific activity units were 870 mU/mg.

According to the literature, several microbial enzymes capable of producing different 1-phenylethanol enantiomers have been described up to now and only three of them were characterized as 1-phenylethanol dehydrogenases (Peters *et al.*, 1993; Hummel, 1999, 1997; Itoh *et al.*, 1997; Kniemeyer and Heider, 2001; Makino *et al.*, 2005; Höffken *et al.*, 2006; Rulli *et al.*, 2013; Dudzik *et al.*, 2015). Secondary alcohol dehydrogenases are of interest in biotechnology for their ability to produce optically active molecules. Enzymes with a preference for long-chain alcohols, or alcohols with bulky aromatic substituents, are especially valuable and a number of them have already been characterized and used for enantioselective bioconversion of secondary alcohols (*e.g.* Ludwig *et al.*, 1995; Kroutil *et al.*, 2004; Musa *et al.*, 2007; Lavandera *et al.*, 2008; Kern *et al.*, 2008; Wu *et al.*, 2013).

The corresponding ketones, which were obtained as products in the oxidation reactions were also used as substrates to test SDRs A5 and B3 for their reduction activity in the reverse reactions. Our results showed weak activity for SDR A5 and almost no activity for SDR B3 with ketones such as 2-octanone, benzylacetone, 2-hexanone and acetophenone (Fig. 7). In general, oxidoreductase reactions are reversible for most of the alcohol dehydrogenases; however, in case of poor substrate affinity only one way of the reaction might be favoured.

Substrate range and stereoselectivity for reduction activity of SDR B3 and SDR A5

SDR A5 and SDR B3 were checked for reduction activity with 28 substrates (Fig. 5B). As expected, the tendency to convert long-chain or bulky substrates remains in the reduction pathway of the reaction. Interestingly, the most stereo-demanding molecule, benzil, was found to be the best substrate for SDR B3 and was converted more than five times better than octanal, which is the second best substrate for SDR B3 (Fig. 7). 100 % of the relative activity shown in Fig. 7 corresponds to 1.8 U/mg of specific activity for SDR B3 with benzil; this is ten times higher than 180 mU/mg of specific activity detected for SDR A5 with the same substrate. Among others good substrates for SDR B3 are octanal, diketones hexane-3,4-dione and butane-2,3-dione, bulky aldehyde 2-phenylacetaldehyde and bulky ketone propiophenone. SDR A5 also accepted all of these molecules, except 2-phenylacetaldehyde, although with a lower efficiency. Additionally, SDR A5 converts bulky ketone 4-(4-hydroxyphenyl)-2-butanone. The best substrate for SDR A5 was shown to be hexane-3,4-dione with specific activity units 180 mU/mg.

Chemical reactions of SDRs A5 and B3 with benzil are highly stereoselective. According to the results of HPLC experiments, purified enzymes transform benzil to (*S*)-benzoin with enantiomeric excess 96 % for SDR B3 and >96 % for SDR A5. This reaction is irreversible, since neither SDR A5, nor SDR B3, were able to oxidize racemic benzoin.

The reduction of dicarbonyl compounds, like benzil, is a current topic in biotechnology. Enantiopure benzoin is a valuable intermediate for pharmaceuticals and useful chiral auxiliary reagents in stereoselective organic synthesis (Pal *et al.*, 2015). Benzil is a diketone, which is widely environmentally distributed. It has been shown in experiments with whole cells that different microorganisms are capable of benzil transformation (Hoyos *et al.*, 2010). In 2001 R. Maruyama and co-authors reported for the first time the isolation and expression of benzil reductase originating from *Bacillus cereus* (Maruyama *et al.*, 2001). Only a few novel benzil reductases have thus far been characterized in more detail (Maruyama *et al.*, 2002; Pennacchio *et al.*, 2013). SDR A5, in contrast to SDR B3, is also capable of reducing the second carbonyl group of benzil. It accepts benzoin as a substrate, although SDR A5 converts it with a lower efficiency than benzil. As for all tested secondary

alcohols, it operates only on the *S*-enantiomer of the benzoin molecule, as no reaction was detected for SDR A5 with *R*-(-)-benzoin.

To summarize, SDR A5 shows the highest activities in the oxidation pathway of the reaction, while it accepts a relative small number of substrates when compared to the reduction pathway of the reaction, where it accepts a larger number of substrates, while showing only lower activities. In the case of SDR B3, the range of oxidized substrates is wider, with relatively low activities, whereas the reducing activity is high with a narrow substrate range.

Stereo-demanding molecules are poorly accepted by most of the enzymes. Novel enzymes able to transform bulky-bulky substrates are always desirable targets (Kroutil *et al.*, 2004). On the basis of the performed experiments it can be concluded that SDR A5 and B3 are stereoselective oxidoreductases, with a preference to sterically demanding alcohols, aldehydes or ketones. Therefore, they are among those very rare enzymes that can be used for the production of bulky chiral compounds.

Computational analysis of SDRs A5 and B3 in relationship with the enzymes with known benzil reduction activity.

Up to now, several enzymes have been reported to show benzil-reduction activity. (*S*)-benzoin-forming benzil reductases from *B. cereus*, *B. subtilis* and *Saccharomyces cerevisiae* (Uniprot [Q8RJB2](#), [O32099](#) and [P40580](#), respectively) were isolated by R. Maruyama and co-authors (Maruyama *et al.*, 2002, 2001). Additionally, a SDR from *Sulfolobus acidocaldarius* (Uniprot [Q4J9F2](#)) was highly active in the anti-Prelog reduction of benzil (Pennacchio *et al.*, 2013). Two mammalian sepiapterin reductases (Uniprot [P18297](#) and [Q8R536](#)) were also shown to exhibit benzil reduction activity (Citron *et al.*, 1990; Maruyama *et al.*, 2002, respectively), as well as an alternatively spliced isoform of human NADP(H)-dependent retinol dehydrogenase/reductase (Uniprot [Q9BTZ2](#)) (Yan *et al.*, 2012). Sequences of all listed enzymes and SDRs A5 and B3 were aligned and, subsequently, phylogenetic trees were built using a Neighbor-Joining Distance Bootstrapping algorithm (Fig. 8). Additionally a few enzymes with high sequence identity to SDR A5, SDR B3 and sepiapterine reductase [P18297](#) were added in order to increase significance of the phylogenetic tree. As a result, two distinct groups can be inferred in the evolution of the observed benzil reductases. Most of the enzymes capable of reducing benzil, including the one with the highest activity ([Q8R536](#)), are grouped together with SDR A5 shown in red (Fig. 8). Interestingly, SDR B3, which in our study was the most active one with benzil, clearly map into a different cluster within the phylogenetic tree (marked in green, Fig. 8). Only two more enzymes showing relatively low or average benzil reduction activity are located in the same group ([Q4J9F2](#) and [Q9BTZ2](#)).

Conclusion

In this study we have characterized two novel short-chain dehydrogenases/reductases originating from the Gram-negative bacterium *R. eutropha* H16. The two enzymes are (*S*)-stereoselective and operate on long chain and bulky aromatic substrates. Additionally, through computational analysis of all enzymes with proven benzil reduction activity, we concluded that SDR A5 and B3 belong to different evolutionary lineages. To summarize, preference for bulky substrates, high stereoselectivity and one-way reaction behavior make SDR A5 and SDR B3 good candidates for the production of

chiral compounds. Therefore these novel characterized enzymes are among those very rare ones that can be applied for the biotechnological production of highly valuable bulky chiral compounds.

Conflict of interests

The authors declare that there is no conflict of interests.

Authors' contributions

The experimental work was planned and performed by ZM. The manuscript was written by ZM and PH. HS suggested additional ideas concerning the outline of the study. Computational analysis was performed by AG, ZM and CWS. All authors read, corrected and approved the final version of this paper.

Acknowledgements

This work was financed by the FWF DK Molecular Enzymology project W901. Special thanks to Prof. Wolfgang Kroutil, Prof. Rolf Breinbauer and Jakov Ivkovic.

References

- Atlić, A., Koller, M., Scherzer, D., Kutschera, C., Grillo-Fernandes, E., Horvat, P., Chiellini, E., Braunegg, G., 2011. Continuous production of poly([R]-3-hydroxybutyrate) by *Cupriavidus necator* in a multistage bioreactor cascade. *Appl. Microbiol. Biotechnol.* 91, 295–304. doi:10.1007/s00253-011-3260-0
- Atsumi, S., Hanai, T., Liao, J.C., 2008. Non-fermentative pathways for synthesis of branched-chain higher alcohols as biofuels. *Nature* 451, 86–89. doi:10.1038/nature06450
- Bowien, B., Kusian, B., 2002. Genetics and control of CO₂ assimilation in the chemoautotroph *Ralstonia eutropha*. *Arch. Microbiol.* 178, 85–93. doi:10.1007/s00203-002-0441-3
- Boyer, H.W., Roulland-Dussoix, D., Francisco, S., Prancisco, B., 1969. A Complementation Analysis of the Restriction and Modification of DNA in *Escherichia coli*. *J. Mol. Biol.* 41, 459–472.
- Brigham, C.J., Speth, D.R., Rha, C., Sinskey, A.J., 2012. Whole-genome microarray and gene deletion studies reveal regulation of the polyhydroxyalkanoate production cycle by the stringent response in *Ralstonia eutropha* H16. *Appl. Environ. Microbiol.* 78, 8033–8044. doi:10.1128/AEM.01693-12
- Citron, B. a, Milstien, S., Gutierrez, J.C., Levine, R. a, Yanak, B.L., Kaufman, S., 1990. Isolation and expression of rat liver sepiapterin reductase cDNA. *Proc. Natl. Acad. Sci. U. S. A.* 87, 6436–6440. doi:10.1073/pnas.87.16.6436
- Di Tommaso, P., Moretti, S., Xenarios, I., Orobittg, M., Montanyola, A., Chang, J.M., Taly, J.F., Notredame, C., 2011. T-Coffee: A web server for the multiple sequence alignment of protein and RNA sequences using structural information and homology extension. *Nucleic Acids Res.* 39, 13–17. doi:10.1093/nar/gkr245
- Dudzik, A., Snoch, W., Borowiecki, P., Opalinska-Piskorz, J., Witko, M., Heider, J., Szalaniec, M., 2015. Asymmetric reduction of ketones and β -keto esters by (S)-1-phenylethanol dehydrogenase from denitrifying bacterium *Aromatoleum aromaticum*. *Appl. Microbiol. Biotechnol.* 99, 5055–5069. doi:10.1007/s00253-014-6309-z
- Felsenstein, J., 2005. PHYLIP (Phylogeny Inference Package) version 3.6.
- Figuerski, D.H., Helinski, D.R., 1979. Replication of an origin-containing derivative of plasmid RK2 dependent on a plasmid function provided in trans. *Proc. Natl. Acad. Sci. U. S. A.* 76, 1648–1652. doi:10.1073/pnas.76.4.1648
- Friedrich, B., Schwartz, E., 1993. Molecular biology of hydrogen utilization in aerobic chemolithotrophs. *Annu. Rev. Microbiol.* 47, 351–83.
- Gai, C.S., Lu, J., Brigham, C.J., Bernardi, A.C., Sinskey, A.J., 2014. Insights into bacterial CO₂ metabolism revealed by the characterization of four carbonic anhydrases in *Ralstonia eutropha* H16. *AMB Express* 4, 2. doi:10.1186/2191-0855-4-2
- Goldberg, J.B., Ohman, D.E., 1984. Cloning and expression in *Pseudomonas aeruginosa* of a gene involved in the production of alginate. *J. Bacteriol.* 158, 1115–1121.

- Goldberg, K., Schroer, K., Lütz, S., Liese, A., 2007. Biocatalytic ketone reduction - A powerful tool for the production of chiral alcohols - Part II: Whole-cell reductions. *Appl. Microbiol. Biotechnol.* 76, 249–255. doi:10.1007/s00253-007-1005-x
- Green, M.R., Sambrook, J., 2012. *Molecular cloning: a laboratory manual*, Cold Spring. ed.
- Grousseau, E., Lu, J., Gorret, N., Guillouet, S.E., Sinskey, A.J., 2014. Isopropanol production with engineered *Cupriavidus necator* as bioproduction platform. *Appl. Microbiol. Biotechnol.* 98, 4277–90. doi:10.1007/s00253-014-5591-0
- Gruber, S., Schwab, H., Koefinger, P., 2015. Versatile plasmid-based expression systems for Gram-negative bacteria—General essentials exemplified with the bacterium *Ralstonia eutropha* H16. *N. Biotechnol.* 00. doi:10.1016/j.nbt.2015.03.015
- Höffken, H.W., Duong, M., Friedrich, T., Breuer, M., Hauer, B., Reinhardt, R., Rabus, R., Heider, J., Ho, H.W., 2006. Crystal Structure and Enzyme Kinetics of the (S)-Specific 1-Phenylethanol Dehydrogenase of the Denitrifying Bacterium Strain EbN1. *Filtration* 45, 82–93. doi:10.1021/bi051596b
- Hoyos, P., Sinisterra, J.-V., Molinari, F., Alcántara, A.R., Domínguez de María, P., 2010. Biocatalytic strategies for the asymmetric synthesis of alpha-hydroxy ketones. *Acc. Chem. Res.* 43, 288–299. doi:10.1021/ar900196n
- Huisman, G.W., Liang, J., Krebber, A., 2010. Practical chiral alcohol manufacture using ketoreductases. *Curr. Opin. Chem. Biol.* 14, 122–129. doi:10.1016/j.cbpa.2009.12.003
- Hummel, W., 1999. Large-scale applications of NAD(P)-dependent oxidoreductases: recent developments. *Trends Biotechnol.* 17, 487–492. doi:10.1016/S0167-7799(98)01207-4
- Hummel, W., 1997. New alcohol dehydrogenases for the synthesis of chiral compounds, *Advances in Biochemical Engineering/Biotechnology*. Springer Berlin Heidelberg, Berlin, Heidelberg. doi:10.1007/BFb0103299
- Hyeon, J.E., Kim, S.W., Park, C., Han, S.O., 2015. Efficient biological conversion of carbon monoxide (CO) to carbon dioxide (CO₂) and for utilization in bioplastic production by *Ralstonia eutropha* through the display of an enzyme complex on the cell surface. *Chem. Commun.* 51, 10202–10205. doi:10.1039/C5CC00832H
- Insomphun, C., Mifune, J., Orita, I., Numata, K., Nakamura, S., Fukui, T., 2014. Modification of β -oxidation pathway in *Ralstonia eutropha* for production of poly(3-hydroxybutyrate-co-3-hydroxyhexanoate) from soybean oil. *J. Biosci. Bioeng.* 117, 184–190. doi:10.1016/j.jbiosc.2013.07.016
- Itoh, N., Morihama, R., Wang, J., Okada, K., Mizuguchi, N., 1997. Purification and characterization of phenylacetaldehyde reductase from a styrene-assimilating *Corynebacterium* strain, ST-10. *Appl. Environ. Microbiol.* 63, 3783–3788.
- Ivan, L., Kern, A., Ferreira-silva, B., Glieder, A., Wildeman, S. De, Kroutil, W., 2008. Stereoselective Bioreduction of Bulky-Bulky Ketones by a Novel ADH from *Ralstonia* sp. *J. Org. Chem.* 73, 6003–6005. doi:10.1021/jo800849d

- Jörnvall, H., Höög, J.O., Persson, B., 1999. SDR and MDR: Completed genome sequences show these protein families to be large, of old origin, and of complex nature. *FEBS Lett.* 445, 261–264. doi:10.1016/S0014-5793(99)00130-1
- Jörnvall, H., Landreh, M., Östberg, L.J., 2015. Alcohol dehydrogenase, SDR and MDR structural stages, present update and altered era. *Chem. Biol. Interact.* 234, 75–79. doi:10.1016/j.cbi.2014.10.017
- Kallberg, Y., Oppermann, U., Jörnvall, H., Persson, B., 2002. Short-chain dehydrogenase/reductase (SDR) relationships: A large family with eight clusters common to human, animal, and plant genomes. *Protein Sci.* 11, 636–641. doi:10.1110/ps.26902.spite
- Kavanagh, K.L., Jörnvall, H., Persson, B., Oppermann, U., 2008. Medium- and short-chain dehydrogenase/reductase gene and protein families: the SDR superfamily: functional and structural diversity within a family of metabolic and regulatory enzymes. *Cell. Mol. Life Sci.* 65, 3895–906. doi:10.1007/s00018-008-8588-y
- Kawai, S., Mori, S., Mukai, T., Hashimoto, W., Murata, K., 2001. Molecular characterization of *Escherichia coli* NAD kinase. *Eur. J. Biochem.* 268(15), 4359–65. doi:10.1046/j.1432-1327.2001.02358.x
- Kemena, C., Notredame, C., 2009. Upcoming challenges for multiple sequence alignment methods in the high-throughput era. *Bioinformatics* 25, 2455–2465. doi:10.1093/bioinformatics/btp452
- Kniemeyer, O., Heider, J., 2001. (S)-1-phenylethanol dehydrogenase of *Azoarcus* sp. strain EbN1, an enzyme of anaerobic ethylbenzene catabolism. *Arch. Microbiol.* 176, 129–135. doi:10.1007/s002030100303
- Kroutil, W., Mang, H., Edegger, K., Faber, K., 2004. Recent advances in the biocatalytic reduction of ketones and oxidation of sec-alcohols. *Curr. Opin. Chem. Biol.* 8, 120–126. doi:10.1016/j.cbpa.2004.02.005
- Kulig, J., Frese, A., Kroutil, W., Pohl, M., Rother, D., 2013. Biochemical characterization of an alcohol dehydrogenase from *Ralstonia* sp. *Biotechnol. Bioeng.* 110, 1838–48. doi:10.1002/bit.24857
- Kulig, J., Simon, R.C., Rose, C.A., Husain, S.M., Häckh, M., Lüdeke, S., Zeitler, K., Kroutil, W., Pohl, M., Rother, D., 2012. Stereoselective synthesis of bulky 1,2-diols with alcohol dehydrogenases. *Catal. Sci. Technol.* 2, 1580. doi:10.1039/c2cy20120h
- Kunasundari, B., Murugaiyah, V., Kaur, G., Maurer, F.H.J., Sudesh, K., 2013. Revisiting the Single Cell Protein Application of *Cupriavidus necator* H16 and Recovering Bioplastic Granules Simultaneously. *PLoS One* 8, 1–15. doi:10.1371/journal.pone.0078528
- Kusian, B., Bednarski, R., Husemann, M., Bowien, B., Kusian, B., Bednarski, R., Husemann, M., 1995. Characterization of the duplicate ribulose-1,5-bisphosphate carboxylase genes and *cbp* promoters of *Alcaligenes eutrophus*. *Am. Soc. Microbiol.* 177, 4442–4450.
- Lavandera, I., Kern, A., Ferreira-Silva, B., Glieder, A., De Wildeman, S., Kroutil, W., 2008a. Stereoselective bioreduction of bulky-bulky ketones by a novel ADH from *Ralstonia* sp. *J. Org. Chem.* 73, 6003–6005. doi:10.1021/jo800849d

- Lavandera, I., Kern, A., Schaffenberger, M., Gross, J., Glieder, A., de Wildeman, S., Kroutil, W., 2008b. An exceptionally DMSO-tolerant alcohol dehydrogenase for the stereoselective reduction of ketones. *ChemSusChem* 1, 431–436. doi:10.1002/cssc.200800032
- Li, H., Opgenorth, P.H., Wernick, D.G., Rogers, S., Wu, T.-Y., Higashide, W., Malati, P., Huo, Y.-X., Cho, K.M., Liao, J.C., 2012. Integrated Electromicrobial Conversion of CO₂ to Higher Alcohols. *Science* 335 (6076), 1596–1596. doi:10.1126/science.1217643
- Li, Z., Cai, L., Wu, Q., Chen, G., 2009. Overexpression of NAD kinase in recombinant *Escherichia coli* harboring the *phbCAB* operon improves poly (3-hydroxybutyrate) production. *Appl. Microbiol. Biotechnol.* 83, 939–947. doi:10.1007/s00253-009-1943-6
- Ludwig, B., Akundi, A., Kendall, K., 1995. A Long-Chain Secondary Alcohol Dehydrogenase from *Rhodococcus erythropolis* ATCC 4277 61, 3729–3733.
- Makino, Y., Inoue, K., Dairi, T., Itoh, N., 2005. Engineering of Phenylacetaldehyde Reductase for Efficient Substrate Conversion in Concentrated 2-Propanol. *Appl. Environ. Microbiol.* 71, 4713–4720. doi:10.1128/AEM.71.8.4713
- Maruyama, R., Nishizawa, M., Itoi, Y., Ito, S., Inoue, M., 2002. The enzymes with benzil reductase activity conserved from bacteria to mammals. *J. Biotechnol.* 94, 157–169. doi:10.1016/S0168-1656(01)00426-6
- Maruyama, R., Nishizawa, M., Itoi, Y., Ito, S., Inoue, M., 2001. Isolation and expression of a *Bacillus cereus* gene encoding benzil reductase. *Biotechnol. Bioeng.* 75, 630–633. doi:10.1002/bit.1191
- Matsuda, T., Yamanaka, R., Nakamura, K., 2009. Recent progress in biocatalysis for asymmetric oxidation and reduction. *Tetrahedron Asymmetry* 20, 513–557. doi:10.1016/j.tetasy.2008.12.035
- Moore, J.C., Pollard, D.J., Kosjek, B., Devine, P.N., 2007. Advances in the Enzymatic Reduction of Ketones Background: Whole Cell Bioreductions. *Acc. Chem. Res.* 40, 1412–1419. doi:10.1021/ar700167a
- Müller, J., MacEachran, D., Burd, H., Sathitsuksanoh, N., Bi, C., Yeh, Y.C., Lee, T.S., Hillson, N.J., Chhabra, S.R., Singer, S.W., Beller, H.R., 2013. Engineering of *Ralstonia eutropha* H16 for autotrophic and heterotrophic production of methyl ketones. *Appl. Environ. Microbiol.* 79, 4433–4439. doi:10.1128/AEM.00973-13
- Musa, M.M., Ziegelmann-Fjeld, K.I., Vieille, C., Zeikus, J.G., Phillips, R.S., 2007. Asymmetric reduction and enantioselective oxidation using W110A secondary alcohol dehydrogenase from *Thermoanaerobacter ethanolicus*. *J. Org. Chem.* 72, 30–34.
- Nakamura, K., Yamanaka, R., Matsuda, T., Harada, T., 2003. Recent developments in asymmetric reduction of ketones with biocatalysts. *Tetrahedron-Asymmetry* 14, 2659–2681. doi:10.1016/s0957-4166(03)00526-3
- Nei, M., 1987. The Neighbor-joining Method: A New Method for Reconstructing Phylogenetic Trees'. *Mol. Biol. Evol.* 4, 406–425.
- Ni, Y., Xu, J.H., 2012. Biocatalytic ketone reduction: A green and efficient access to enantiopure alcohols. *Biotechnol. Adv.* 30, 1279–1288. doi:10.1016/j.biotechadv.2011.10.007

- Oda, T., Oda, K., Yamamoto, H., Matsuyama, A., Ishii, M., Igarashi, Y., 2013. Hydrogen-driven asymmetric reduction of hydroxyacetone to (R)-1,2-propanediol by *Ralstonia eutropha* transformant expressing alcohol dehydrogenase from *Kluyveromyces lactis*. *Microb. Cell Fact.* 12, 1–9.
- Pal, M., Srivastava, G., Sharma, A.N., Kaur, S., Jolly, R.S., 2015. Biocatalyzed asymmetric reduction of benzils to either benzoin or hydrobenzoin: pH dependent switch. *Catal. Sci. Technol.* 5, 4017–4028. doi:10.1039/C5CY00158G
- Park, J.M., Kim, T.Y., Lee, S.Y., 2011. Genome-scale reconstruction and in silico analysis of the *Ralstonia eutropha* H16 for polyhydroxyalkanoate synthesis, lithoautotrophic growth, and 2-methyl citric acid production. *BMC Syst. Biol.* 5, 101. doi:10.1186/1752-0509-5-101
- Patel, R.N., 2008. Synthesis of chiral pharmaceutical intermediates by biocatalysis. *Coord. Chem. Rev.* 252, 659–701. doi:10.1016/j.ccr.2007.10.031
- Pennacchio, A., Sannino, V., Sorrentino, G., Rossi, M., Raia, C. a., Esposito, L., 2013. Biochemical and structural characterization of recombinant short-chain NAD(H)-dependent dehydrogenase/reductase from *Sulfolobus acidocaldarius* highly enantioselective on diaryl diketone benzil. *Appl. Microbiol. Biotechnol.* 97, 3949–3964. doi:10.1007/s00253-012-4273-z
- Persson, B., Oppermann, U., Jo, H., 2003. Coenzyme-based functional assignments of short-chain dehydrogenases/reductases (SDRs). *Chem. Biol. Interact.* 143-144, 271–278.
- Peters, J., Minuth, T., Kula, M.R., 1993. A novel NADH-dependent carbonyl reductase with an extremely broad substrate range from *Candida parapsilosis*: Purification and characterization. *Enzyme Microb. Technol.* 15, 950–958. doi:10.1016/0141-0229(93)90171-W
- Pohlmann, A., Fricke, W.F., Reinecke, F., Kusian, B., Liesegang, H., Cramm, R., Eitinger, T., Ewering, C., Pötter, M., Schwartz, E., Strittmatter, A., Voss, I., Gottschalk, G., Steinbüchel, A., Friedrich, B., Bowien, B., 2006. Genome sequence of the bioplastic-producing “Knallgas” bacterium *Ralstonia eutropha* H16. *Nat. Biotechnol.* 24, 1257–1262. doi:10.1038/nbt1244
- Reisinger, C., van Assema, F., Schürmann, M., Hussain, Z., Remler, P., Schwab, H., 2006. A versatile colony assay based on NADH fluorescence. *J. Mol. Catal. B Enzym.* 39, 149–155. doi:10.1016/j.molcatb.2006.01.014
- Riedel, S.L., Lu, J., Stahl, U., Brigham, C.J., 2014. Lipid and fatty acid metabolism in *Ralstonia eutropha*: Relevance for the biotechnological production of value-added products. *Appl. Microbiol. Biotechnol.* 98, 1469–1483. doi:10.1007/s00253-013-5430-8
- Rulli, G., Heidlindemann, M., Berkessel, A., Hummel, W., Gröger, H., 2013. Towards catalyst compartmentation in combined chemo- and biocatalytic processes: Immobilization of alcohol dehydrogenases for the diastereoselective reduction of a β -hydroxy ketone obtained from an organocatalytic aldol reaction. *J. Biotechnol.* 168, 271–276. doi:10.1016/j.jbiotec.2013.08.031
- Rundbäck, F., Fidanoska, M., Adlercreutz, P., 2012. Coupling of permeabilized cells of *Gluconobacter oxydans* and *Ralstonia eutropha* for asymmetric ketone reduction using H₂ as reductant. *J. Biotechnol.* 157, 154–158. doi:10.1016/j.jbiotec.2011.09.029

- Saratale, G.D., Oh, M.-K., 2015. Characterization of poly-3-hydroxybutyrate (PHB) produced from *Ralstonia eutropha* using an alkali-pretreated biomass feedstock. *Int. J. Biol. Macromol.* 80, 627–635. doi:10.1016/j.ijbiomac.2015.07.034
- Schwartz, E., Henne, A., Cramm, R., Eitinger, T., Friedrich, B., Gottschalk, G., 2003. Complete nucleotide sequence of pHG1: A *Ralstonia eutropha* H16 megaplasmid encoding key enzymes of H₂-based lithoautotrophy and anaerobiosis. *J. Mol. Biol.* 332, 369–383. doi:10.1016/S0022-2836(03)00894-5
- Shimizu, R., Dempo, Y., Nakayama, Y., Nakamura, S., Bamba, T., Fukusaki, E., Fukui, T., 2015. New Insight into the Role of the Calvin Cycle: Reutilization of CO₂ Emitted through Sugar Degradation. *Sci. Rep.* 5, 11617. doi:10.1038/srep11617
- Shimizu, S., Ogawa, J., Kataoka, M., Kobayashi, M., 1997. Screening of novel microbial enzymes for the production of biologically and chemically useful compounds. *Adv. Biochem. Eng. Biotechnol.* 58, 45–87.
- Steinbüchel, A., Fuchtenbusch, B., 1998. Bacterial and other biological systems for polyester production. *Trends Biotechnol.* 16, 419–427.
- Tanaka, N., Nonaka, T., Nakanishi, M., Deyashiki, Y., Hara, A., Mitsui, Y., 1996. Crystal structure of the ternary complex of mouse lung carbonyl reductase at 1.8 Å resolution: the structural origin of coenzyme specificity in the short-chain dehydrogenase/reductase family. *Structure.* doi:10.1016/S0969-2126(96)00007-X
- Torella, J.P., Gagliardi, C.J., Chen, J.S., Bediako, D.K., Colón, B., Way, J.C., Silver, P. a., Nocera, D.G., 2015. Efficient solar-to-fuels production from a hybrid microbial–water-splitting catalyst system. *Proc. Natl. Acad. Sci.* 112, 2337–2342. doi:10.1073/pnas.1424872112
- Ugwu, S.O., Apte, S.P., 2004. The Effect of Buffers on Protein Conformational Stability. *Pharm. Technol.* 28, 86–109. doi:10.1016/j.saa.2011.06.021
- Waterhouse, A.M., Procter, J.B., Martin, D.M. a, Clamp, M., Barton, G.J., 2009. Jalview Version 2-A multiple sequence alignment editor and analysis workbench. *Bioinformatics* 25, 1189–1191. doi:10.1093/bioinformatics/btp033
- Wohlgemuth, R., 2010. Asymmetric biocatalysis with microbial enzymes and cells. *Curr. Opin. Microbiol.* 13, 283–292. doi:10.1016/j.mib.2010.04.001
- Wu, C.F.J., 1986. Jackknife, Bootstrap and other resampling methods in regression analysis. *Ann. Stat.* 14, 1261–1295. doi:10.1214/aos/1176350161
- Wu, X., Zhang, C., Orita, I., Imanaka, T., Fukui, T., Xing, X.H., 2013. Thermostable alcohol dehydrogenase from *Thermococcus kodakarensis* KOD1 for enantioselective bioconversion of aromatic secondary alcohols. *Appl. Environ. Microbiol.* 79, 2209–2217. doi:10.1128/AEM.03873-12
- Yan, Y., Song, X., Liu, G., Su, Z., Du, Y., Sui, X., Chang, X., Huang, D., 2012. Human NRDRB1, an alternatively spliced isoform of NAD(P)(H)-dependent retinol dehydrogenase/reductase enhanced enzymatic activity of Benzil. *Cell. Physiol. Biochem.* 30, 1371–1382. doi:10.1159/000343326

Zarnt, G., Schröder, T., Andreesen, J.R., 1997. Degradation of tetrahydrofurfuryl alcohol by *Ralstonia eutropha* is initiated by an inducible pyrroloquinoline quinone-dependent alcohol dehydrogenase. *Appl. Environ. Microbiol.* 63, 4891–4898.

Figures.

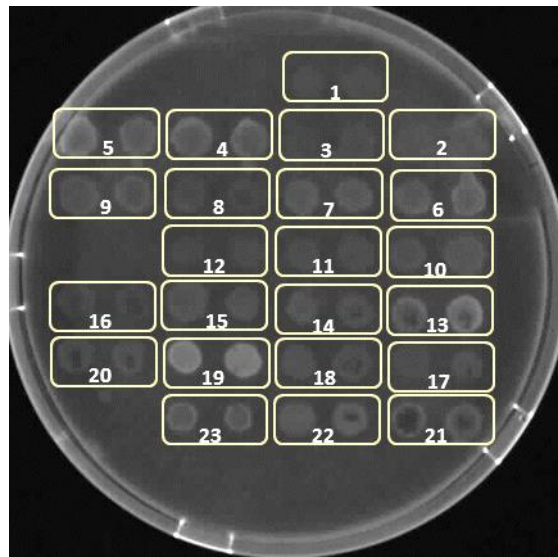


Fig. 1. Example of enzyme activity screening – a colony assay with *E. coli* BL21 strains. Alcohol oxidation reaction is performed by overexpressed dehydrogenase with the help of NAD(P)^+ . Subsequently, reduced form of cofactor, NAD(P)H , is produced by active cells resulting in fluorescence.

A filter-paper disk with the cells of different *E. coli* BL21 strains carrying indicated plasmids was soaked in reaction mixture containing 10 mM *rac*-2-octanol, 5 mM NADP^+ and 0.1 M HEPES buffer pH 8.0; time of exposure 3 min. The positions contain: 1. *E. coli* BL21 with empty vector control; 2. *E. coli* BL21 [pK470-ADH A1]; 3. *E. coli* BL21 [pK470-ADH A3]; 4. *E. coli* BL21 [pK470-ADH A4]; 5. *E. coli* BL21 [pK470-SDR A5]; 6. *E. coli* BL21 [pK470-ADH B1]; 7. *E. coli* BL21 [pK470-ADH B2]; 8. *E. coli* BL21 [pK470-ADH B5]; 9. *E. coli* BL21 [pK470-ADH B6]; 10. *E. coli* BL21 [pK470-ADH B8]; 11. *E. coli* BL21 [pK470-ADH P1]; 12. *E. coli* BL21 [pK470-ADH P2]; 13. *E. coli* BL21 [pK470-SDR A1]; 14. *E. coli* BL21 [pK470-SDR A2]; 15. *E. coli* BL21 [pK470-SDR A3]; 16. *E. coli* BL21 [pK470-SDR A4]; 17. *E. coli* BL21 [pK470-SDR B1]; 18. *E. coli* BL21 [pK470-SDR B2]; 19. *E. coli* BL21 [pK470-SDR B3]; 20. *E. coli* BL21 [pK470-SDR B4]; 21. *E. coli* BL21 [pK470-SDR B6]; 22. *E. coli* BL21 [pK470-SDR B7]; 23. *E. coli* BL21 [pK470-SDR B9]

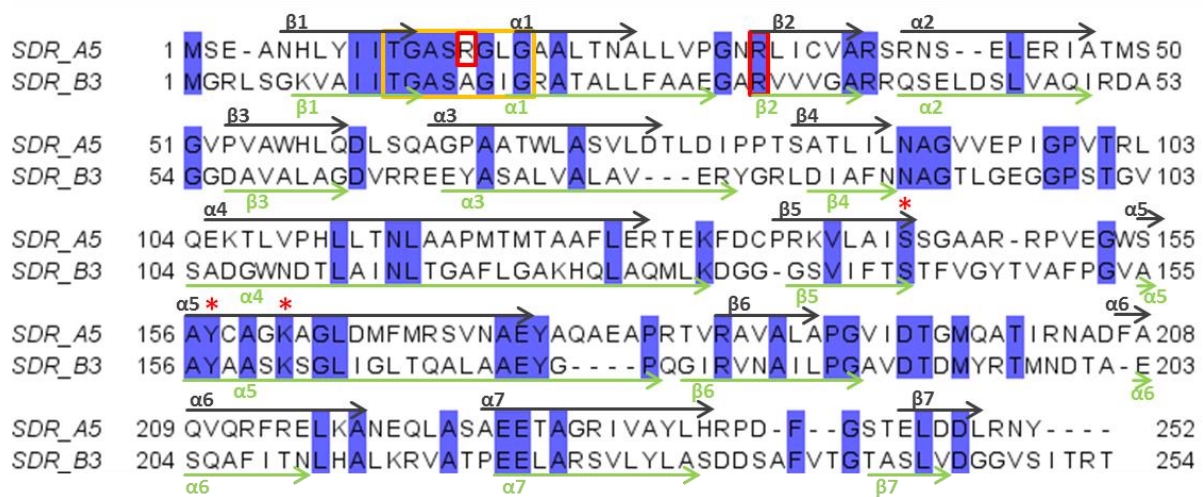


Fig. 2. Sequence alignment of SDR A5 and SDR B3. The amino acid sequences of the classical short-chain dehydrogenases SDR A5 and SDR B3 were aligned using the T-coffee tool set. The result was visualized with the graphical viewer Jalview 2.8.2. Identical residues are highlighted in blue. The conserved Gly-rich motif for the cofactor binding is marked with the orange box. Residues critical for NADP(H) preference are shown in red boxes. Red stars show conserved residues of the catalytic triad. Black arrows represent β -sheets and α -helix regions for SDR A5. Green arrows indicate β -sheets and α -helix regions for SDR B3.

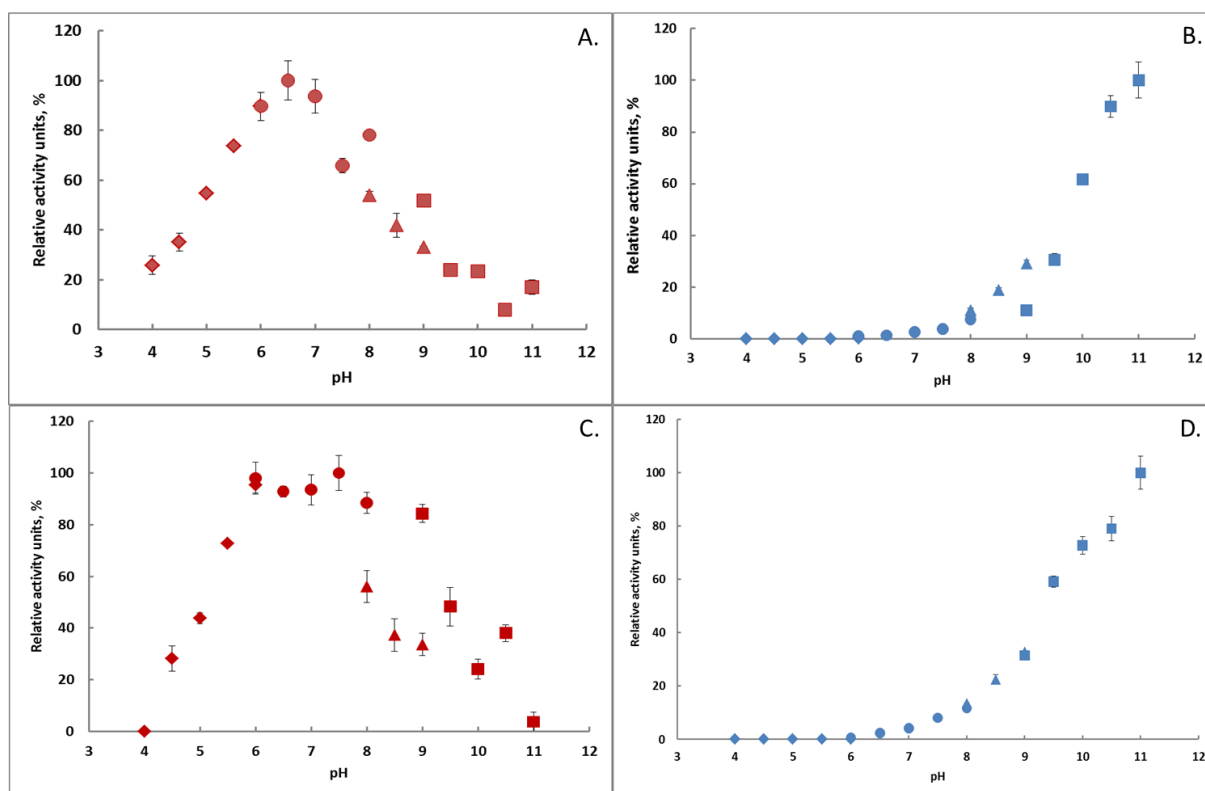


Fig. 3. pH optimum for the activity of SDR A5 and SDR B3. Reaction conditions for reduction: T= 40°C, 50 mM buffer, 1mM hexane-3,4-dione, 0.5 mM NADPH. Reaction conditions for oxidation: T= 40°C, 50 mM buffer, 1 mM (S)-(+)-2-octanol, 0.5 mM NADP⁺. **A** - Influence of pH on SDR B3 reduction activity; **B** - Influence of pH on SDR B3 oxidation activity; **C** - Influence of pH on SDR A5 reduction activity; **D** - Influence of pH on SDR A5 oxidation activity. Legend: ♦ – citrate buffer; ● - sodium phosphate buffer; ▲ – Tris-HCl buffer; ■ – carbonate-bicarbonate buffer.

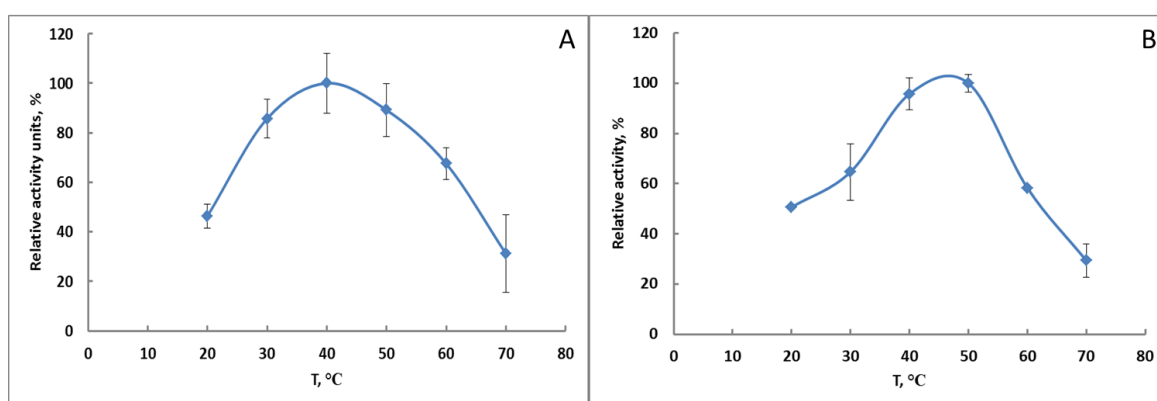


Fig. 4. Temperature optimum for the activity of SDR A5 and SDR B3. 50 mM carbonate-bicarbonate buffer pH 10.5, 1 mM (S)-(+)-2-octanol, 0.5 mM NADP⁺. **A** - Influence of temperature on SDR B3 activity; **B** - Influence of temperature on SDR A5 activity.

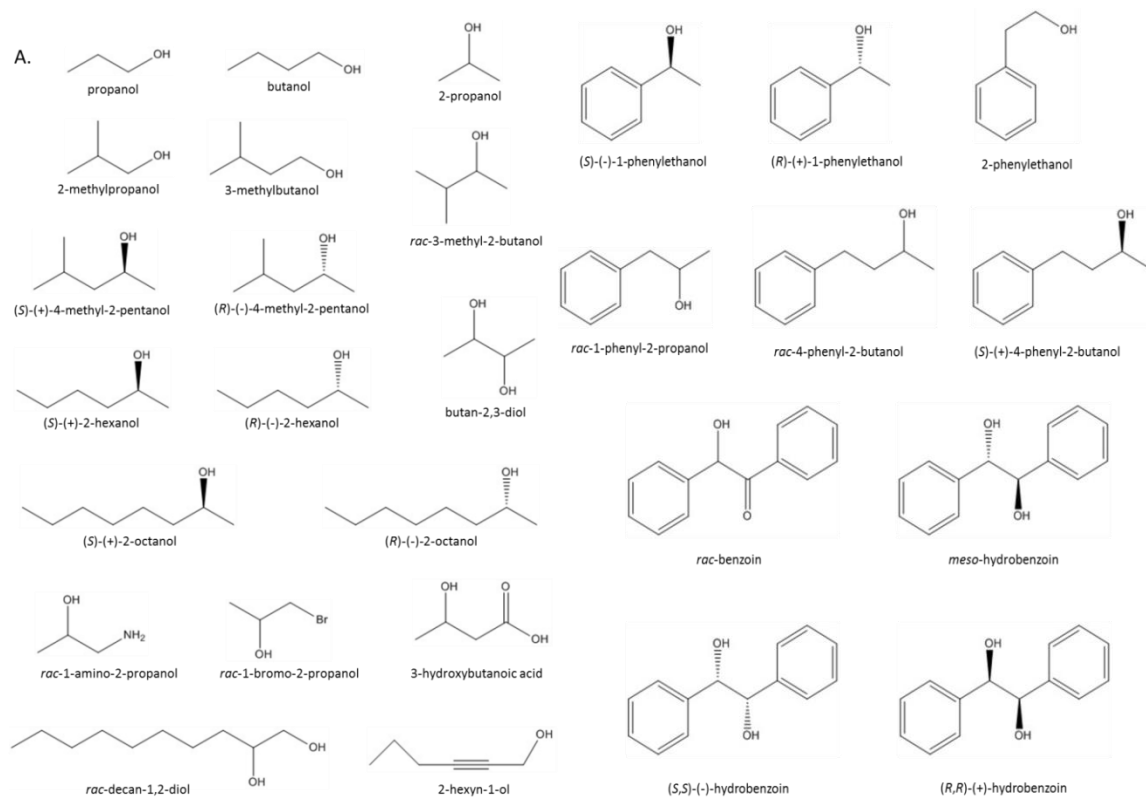


Fig. 5. List of substrates used for spectrophotometric enzyme activity assay. A – substrates used for oxidation reactions; B – substrates used for reduction reactions.

B.

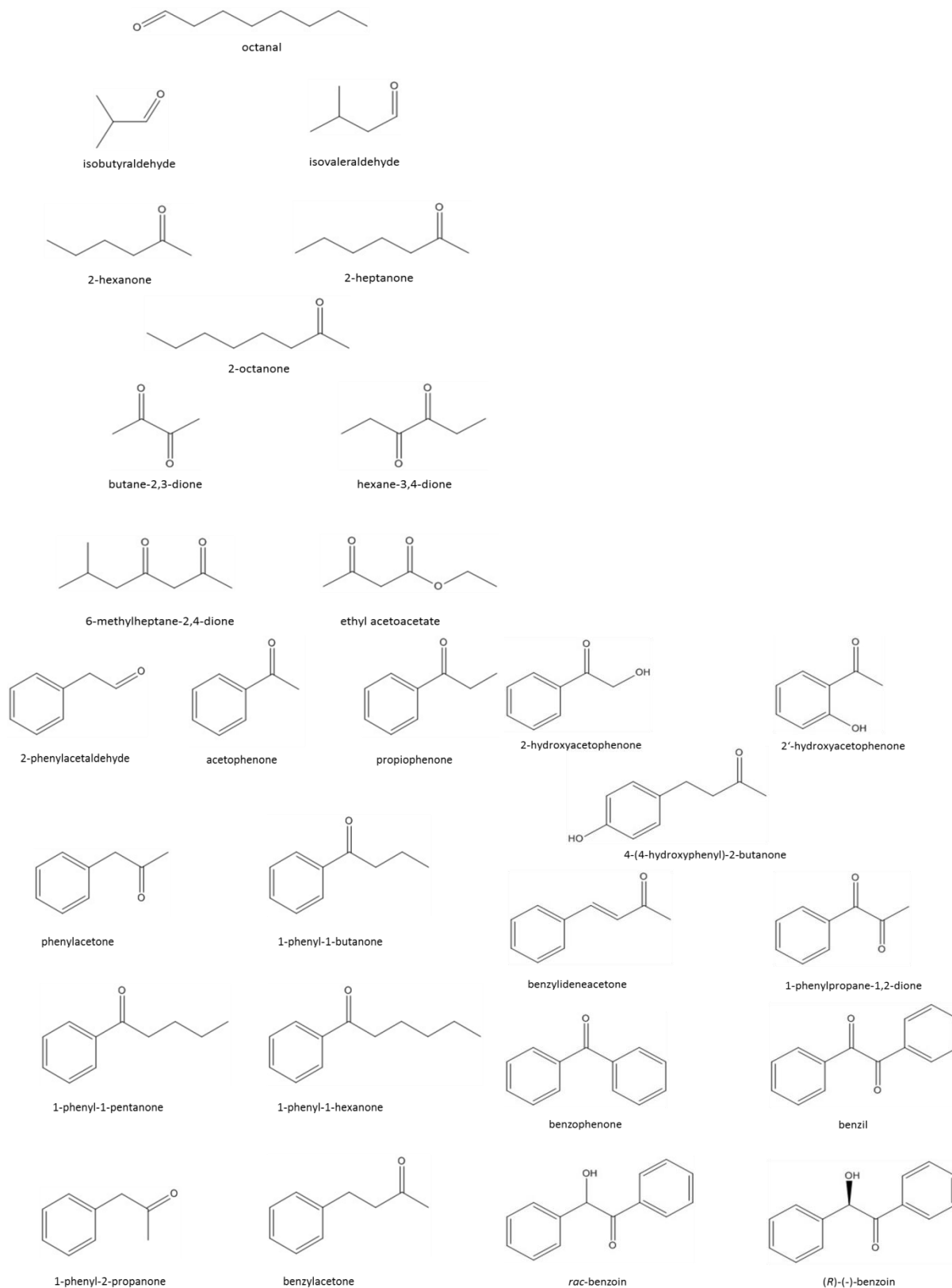


Fig. 5. List of substrates used for spectrophotometric enzyme activity assay. A – substrates used for oxidation reactions; B – substrates used for reduction reactions.

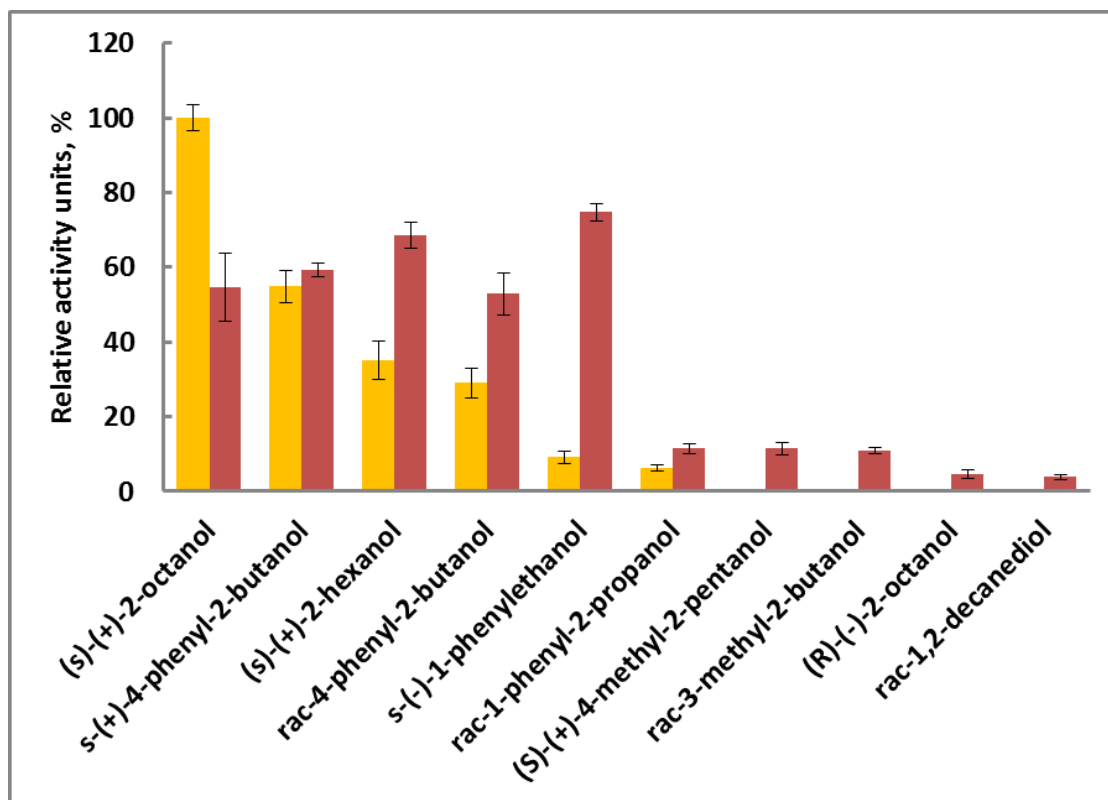


Fig. 6. Substrate preference for oxidation activity of SDR B3 and SDR A5. Reaction conditions for oxidation: T= 40°C, 50 mM carbonate-bicarbonate buffer pH 10.5, 1 mM (S)-(+)-2-octanol, 0.5 mM NADP⁺. Yellow color represents the activity of SDR A5; red color represents the activity of SDR B3. No activity was detected for SDR A5 with propanol, butanol, *rac*-2-propanol, 2-methylpropanol, 3-methylbutanol, *rac*-3-methyl-2-butanol, (S)-(+)-4-methyl-2-pentanol, (R)-(-)-4-methyl-2-pentanol, (R)-(-)-2-hexanol, (R)-(-)-2-octanol, *rac*-1-amino-2-propanol, *rac*-1-bromo-2-propanol, butan-2,3-diol, *rac*-decan-1,2-diol, 3-hydroxybutanoic acid, 2-hexyn-1-ol, (R)-(+)-1-phenylethanol, 2-phenylethanol, *rac*-benzoin, *meso*-hydrobenzoin, (S,S)-(-)-hydrobenzoin, (R,R)-(-)-hydrobenzoin. No activity was detected for SDR B3 with propanol, butanol, *rac*-2-propanol, 2-methylpropanol, 3-methylbutanol, (R)-(-)-4-methyl-2-pentanol, (R)-(-)-2-hexanol, *rac*-1-amino-2-propanol, *rac*-1-bromo-2-propanol, butan-2,3-diol, 3-hydroxybutanoic acid, 2-hexyn-1-ol, (R)-(+)-1-phenylethanol, 2-phenylethanol, *rac*-benzoin, *meso*-hydrobenzoin, (S,S)-(-)-hydrobenzoin, (R,R)-(-)-hydrobenzoin.

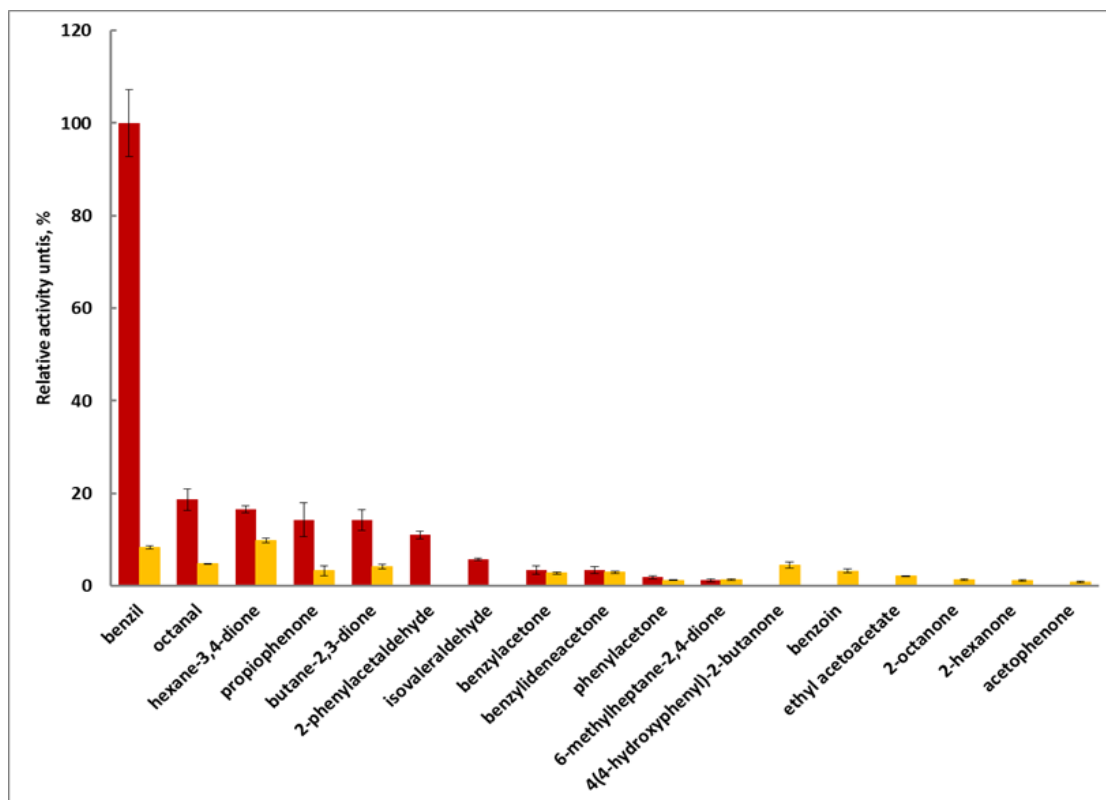


Fig. 7. Substrate preference for reduction activity of SDR B3 and SDR A5. Reaction conditions for reduction: T= 40°C, 50 mM sodium phosphate buffer pH 6.5, 1 mM hexane-3,4-dione, 0.5 mM NADPH. Yellow color represents the activity of SDR A5; red color represents the activity of SDR B3. No activity was detected for SDR A5 with isobutyraldehyde, isovaleraldehyde, 2-heptanone, 2-phenylacetaldehyde, 1-phenyl-1-butanone, 1-phenyl-1-pentanone, 1-phenyl-1-hexanone, 1-phenyl-2-propanone, 2-hydroxyacetophenone, 2'-hydroxyacetophenone, 1-phenylpropane-1,2-dione, benzophenone, (*R*)-(-)-benzoin. No activity was detected for SDR B3 with isobutyraldehyde, 2-hexanone, 2-heptanone, 2-octanone, ethyl acetoacetate, acetophenone, 1-phenyl-1-butanone, 1-phenyl-1-pentanone, 1-phenyl-1-hexanone, 1-phenyl-2-propanone, 2-hydroxyacetophenone, 2'-hydroxyacetophenone, 4-(4-hydroxyphenyl)-2-butanone, 1-phenylpropane-1,2-dione, benzophenone, *rac*-benzoin, (*R*)-(-)-benzoin.

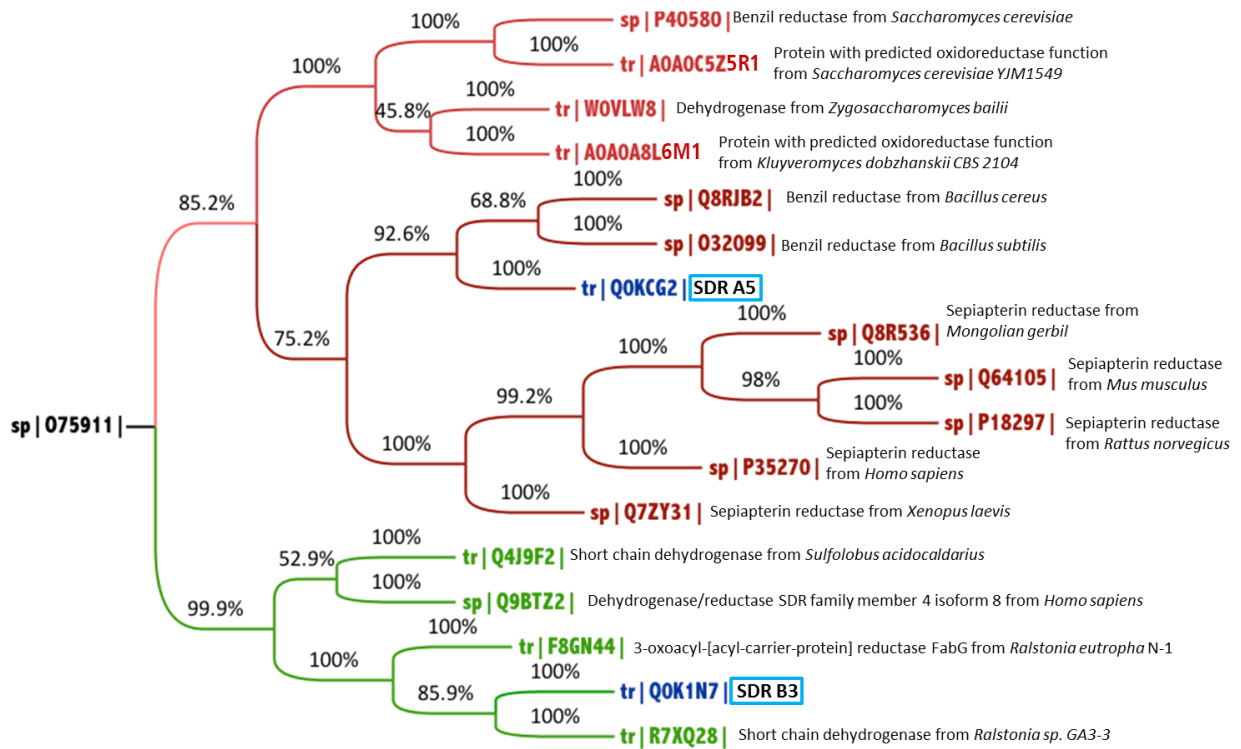


Fig. 8. Bootstrapped Neighbor Joining tree for enzymes with benzil reduction activity. Protein sequences were extracted from UniprotKB. The NCBI PSI-BLAST tool was used to screen for proteins that shared sequence identities. Multiple sequence alignments were made with the Espresso mode of the T-coffee tool set. The phylogenetic tree was inferred using a bootstrap analysis and the PHYLIP suite. The result was visualized and manipulated with the graphical viewer FigTree. Human short chain dehydrogenase/reductase (Uniprot [O75911](#)) was used as an outgroup for the phylogenetic analysis. SDR A5 and SDR B3 are marked with blue boxes.

Table 1. Bacterial strains and plasmids used in this study.

Strain	Genotype	Reference
<i>Ralstonia eutropha</i>		
H16	Wild-type <i>R. eutropha</i> , gentamicin resistant (Gen ^r)	DSMZ 428 ¹
<i>Escherichia coli</i>		
TOP10	F' mcrA Δ(mr(R)-hsdRM(S)-mcrBC) φ80lacZΔM15 ΔlacX74 nupG recA1 araD139 Δ(ara-leu)7697 galE15 galK16 rpsL(Str ^R) endA1 λ ⁻	Invitrogen
BL21	F' Δcm ompT hsdS(r _B ⁻ m _B ⁻) gal [malB ⁺] _{K-12} (λ ^S)	Invitrogen
HB101	Helper strain; F- λ- hsdS20(r _B ⁻ m _B ⁻)recA13 leuB6(Am) araC14 Δ(gpt-proA)62 lacY1 galK2(Oc) xyl-5 mtl-1 thiE1 rpsL20(SmR) glnX44(AS)	(Boyer <i>et al.</i> , 1969)
Plasmid	Description	Reference
pRK2013	Km ^r , <i>coIE1</i>	(Figurski and Helinski, 1979)
pK470	Km ^r , <i>P_{tac}</i> , <i>lacI</i>	this study
pK470-SDR A5	Km ^r , <i>P_{tac}</i> , <i>lacI</i> , H16_A1168	this study
pK470-SDR B3	Km ^r , <i>P_{tac}</i> , <i>lacI</i> , H16_B1297	this study
pK470-His ₆ -SDR A5	Km ^r , <i>P_{tac}</i> , <i>lacI</i> , H16_A1168 N-terminal His ₆ -tag coding sequence	this study
pK470-His ₆ SDR B3	Km ^r , <i>P_{tac}</i> , <i>lacI</i> , H16_B1297, N-terminal His ₆ -tag coding sequence	this study
pKRSF1010-P _{J5} -cymR	Km ^r , P _{J5} , cymR, pBBR1 <i>par</i> region, RSF1010 origin of replication and mobilization region	(Gruber <i>et al.</i> , 2015) (Gruber <i>et al.</i> , manuscript in preparation)
pKRSF1010-P _{J5} -His ₆ -SDR A5-cymR	Km ^r , P _{J5} , cymR, pBBR1 <i>par</i> region, RSF1010 origin of replication and mobilization region H16_A1168, N-terminal His ₆ -tag coding sequence	this study
pKRSF1010-P _{J5} -His ₆ -SDR B3-cymR	Km ^r , P _{J5} , cymR, pBBR1 <i>par</i> region, RSF1010 origin of replication and mobilization region H16_B1297, N-terminal His ₆ -tag coding sequence	this study

¹DSMZ, Deutsche Sammlung für Mikroorganismen und Zellkulturen

Table 2. Oligonucleotides used for PCR amplification in this study

Primer	Sequence (5'-3')
H16_A1168-fwd	ccga <u>agctt</u> tttagtagttgcggagatcg
H16_A1168-rev	cgccat <u>atg</u> agcgaagccaatcacc
H16_B1297-fwd	<u>catatg</u> ggacgtttgtctggaaa
H16_B1297-rev	<u>aagctt</u> caggtgcgcgtgatc

The underlined sequences (*Hind*III; *Nde*I) represent the additional restriction sites at the 5' ends of forward and reverse primers.

Table 3. Summary of the results from the colony assay with different *E. coli* BL21 strains carrying indicated plasmids. The intensity of the observed fluorescence is marked with ‘+’: +++ – relative strong fluorescence; ++ – relative moderate fluorescence; + – relative weak fluorescence; - – no fluorescence

	(S)-(+)-2-octanol	(R)-(-)-2-octanol	rac-butan-2,3-diol	2-methyl-propanol	rac-4-methyl-2-pentanol	butanol	3-methyl-butanol	
<i>E. coli</i> BL21 [pK470-ADH A4]	+++	+++	++	++	++	++	+++	NAD ⁺
	++	++	++	++	+++	++	++	NADP ⁺
<i>E. coli</i> BL21 [pK470-SDR A5]	+++	++	++	++	++	++	++	NAD ⁺
	++	++	++	++	+++	++	++	NADP ⁺
<i>E. coli</i> BL21 [pK470-ADH B1]	++	+	+	+	+	-	++	NAD ⁺
	++	++	++	++	+	+	+	NADP ⁺
<i>E. coli</i> BL21 [pK470-ADH B2]	+	+	+	+	+	+	++	NAD ⁺
	+	+	+	+	+	-	+	NADP ⁺
<i>E. coli</i> BL21 [pK470-ADH B6]	+	+	+	+	+	+	+	NAD ⁺
	+	+	+	-	+	+	-	NADP ⁺
<i>E. coli</i> BL21 [pK470-ADH B8]	-	-	-	-	-	-	-	NAD ⁺
	+	-	-	+	+	-	-	NADP ⁺
<i>E. coli</i> BL21 [pK470-SDR A1]	+	+	++	++	++	++	+++	NAD ⁺
	++	++	++	++	+++	++	++	NADP ⁺
<i>E. coli</i> BL21 [pK470-SDR B3]	+++	+++	+++	+++	+++	+++	+++	NAD ⁺
	+++	+++	+++	+++	+++	+++	+++	NADP ⁺
<i>E. coli</i> BL21 [pK470-SDR B6]	+	+	+	+	+	+	+	NAD ⁺
	+	+	+	+	+	+	+	NADP ⁺
<i>E. coli</i> BL21 [pK470-SDR B7]	+	-	+	-	+	-	+	NAD ⁺
	+	-	+	+	+	-	+	NADP ⁺
<i>E. coli</i> BL21 [pK470-SDR B9]	+	+	+	+	+	+	+	NAD ⁺
	++	+	+	++	++	+	+	NADP ⁺

There were no activities detected for the strains *E. coli* BL21 [pK470-ADH A1], *E. coli* BL21 [pK470-SDR A2], *E. coli* BL21 [pK470-ADH A3], *E. coli* BL21 [pK470-ADH B5], *E. coli* BL21 [pK470-ADH P1], *E. coli* BL21 [pK470-ADH P2], *E. coli* BL21 [pK470-SDR A3], *E. coli* BL21 [pK470-SDR A4], *E. coli* BL21 [pK470-SDR B1], *E. coli* BL21 [pK470-SDR B2], *E. coli* BL21 [pK470-SDR B4].

Table S1. Oligonucleotides used for PCR amplification in this study

Primer	Name	Sequence (5'-3')
H16_A0757-fwd	ADH A1	ttat <u>gc</u> atgctcagtgccgcttgatgg
H16_A0757-rev		tcg <u>cat</u> atgaccgcaatgatgaaagcc
H16_A0861-fwd	ADH A3	actaagcttttacatcgctgcagcg
H16_A0861-rev		<u>aag</u> ctttcaggtgcgctgatc
H16_A0602-fwd	ADH A4	cgaaagcttttacttgggctgcatcc
H16_A0602-rev		gcc <u>cat</u> atgcaaatccaaggcaacg
H16_B0663-fwd	ADH B1	gat <u>cat</u> atgggaatctgcgacgc
H16_B0663-rev		aattg <u>cat</u> gctcagctgccgtagacc
H16_B1834-fwd	ADH B2	tatcg <u>cat</u> gctcagatggcccgg
H16_B1834-rev		cc <u>cat</u> atgtcggagctatcagaccag
H16_B0517-fwd	ADH B5	aat <u>cat</u> atggcgctggcagggaatcag
H16_B0517-rev		cttaagctttcagcgagccgcac
H16_B1699-fwd	ADH B6	atccg <u>cat</u> gctcagaacccttcagcacc
H16_B1699-rev		ccg <u>cat</u> atgaaagccatcggcctgacct
H16_B2470-fwd	ADH B8	tacgg <u>cat</u> gcttaatcgaacaggatcacc
H16_B2470-rev		tgcc <u>cat</u> atgaaggccgctgtcctg
PHG229-fwd	ADH P1	ata <u>cat</u> atggcccagaccatgcg
PHG229-rev		actaagctttcatggggatatctgcc
PHG230-fwd	ADH P2	act <u>cat</u> atggcttcactcgcgcg
PHG230-rev		atcaagcttttagtgacggattctcaggac
H16_A3164-fwd	SDR A1	<u>cat</u> atgaaactgcagggctcggg
H16_A3164-rev		<u>aag</u> ctttcagagcgacatgccgc
H16_A1888-fwd	SDR A2	aa <u>cat</u> atgaaactgaccaatattgtccg
H16_A1888-rev		tcaaagctttcagcgcggtgcc
H16_A1490-fwd	SDR A3	atcc <u>cat</u> atgacgacccaacaccc
H16_A1490-rev		atcaagctttcagcgctgcgaag

H16_A0874-fwd	SDR A4	<u>cgccat</u> atgcaagtcaatctcgatt
H16_A0874-rev		ctaa <u>agctt</u> tcaggccgcttt
H16_B1732-fwd	SDR B1	<u>catatg</u> agtaattcccttgaaggaaa
H16_B1732-rev		<u>aagctt</u> tcaaactgtctcaatccgc
H16_B1767-fwd	SDR B2	<u>catatg</u> aatcgcttcgaaggc
H16_B1767-rev		<u>aagctt</u> ttacagttggctcatgccg
H16_B2339-fwd	SDR B4	<u>catatg</u> tccacaccgaccagc
H16_B2339-rev		<u>aagctt</u> tcagccgttgacgacctc
H16_B0101-fwd	SDR B6	ca <u>acat</u> atgacctccaccccag
H16_B0101-rev		taca <u>agctt</u> tcaggcaaagcccc
H16_B0634-fwd	SDR B7	ct <u>acat</u> atgacatggcgcaaac
H16_B0634-rev		atta <u>agctt</u> tcagagcggaacgcc
H16_B0630-fwd	SDR B9	cag <u>cat</u> atgctgttgaaagacaag
H16_B0630-rev		ctca <u>agctt</u> tcaggcatgaaat

The underlined sequences (*Hind*III; *Nde*I; *Sph*I) represent the additional restriction sites at the 5' ends of forward and reverse primers.

Table S2. Plasmids used in this study.

Plasmid Reference	Description	
pK470-ADH A1	Kan ^r , P _{tac} , <i>lacI</i> , H16_A0757	this study
pK470-ADH A3	Kan ^r , P _{tac} , <i>lacI</i> , H16_A0861	this study
pK470-ADH A4	Kan ^r , P _{tac} , <i>lacI</i> , H16_A0602	this study
pK470-ADH B1	Kan ^r , P _{tac} , <i>lacI</i> , H16_B0663	this study
pK470-ADH B2	Kan ^r , P _{tac} , <i>lacI</i> , H16_B1834	this study
pK470-ADH B5	Kan ^r , P _{tac} , <i>lacI</i> , H16_B0517	this study
pK470-ADH B6	Kan ^r , P _{tac} , <i>lacI</i> , H16_B1699	this study
pK470-ADH B8	Kan ^r , P _{tac} , <i>lacI</i> , H16_B2470	this study
pK470-ADH P1	Kan ^r , P _{tac} , <i>lacI</i> , PHG229	this study

pK470-ADH P2	Kan ^r , P _{tac} , <i>lacI</i> , PHG230	this study
pK470-SDR A1	Kan ^r , P _{tac} , <i>lacI</i> , H16_A3164	this study
pK470-SDR A2	Kan ^r , P _{tac} , <i>lacI</i> , H16_A1888	this study
pK470-SDR A3	Kan ^r , P _{tac} , <i>lacI</i> , H16_A1490	this study
pK470-SDR A4	Kan ^r , P _{tac} , <i>lacI</i> , H16_A0874	this study
pK470-SDR B1	Kan ^r , P _{tac} , <i>lacI</i> , H16_B1732	this study
pK470-SDR B2	Kan ^r , P _{tac} , <i>lacI</i> , H16_B1767	this study
pK470-SDR B4	Kan ^r , P _{tac} , <i>lacI</i> , H16_B2339	this study
pK470-SDR B6	Kan ^r , P _{tac} , <i>lacI</i> , H16_B0101	this study
pK470-SDR B7	Kan ^r , P _{tac} , <i>lacI</i> , H16_B0634	this study
pK470-SDR B9	Kan ^r , P _{tac} , <i>lacI</i> , H16_B0630	this study

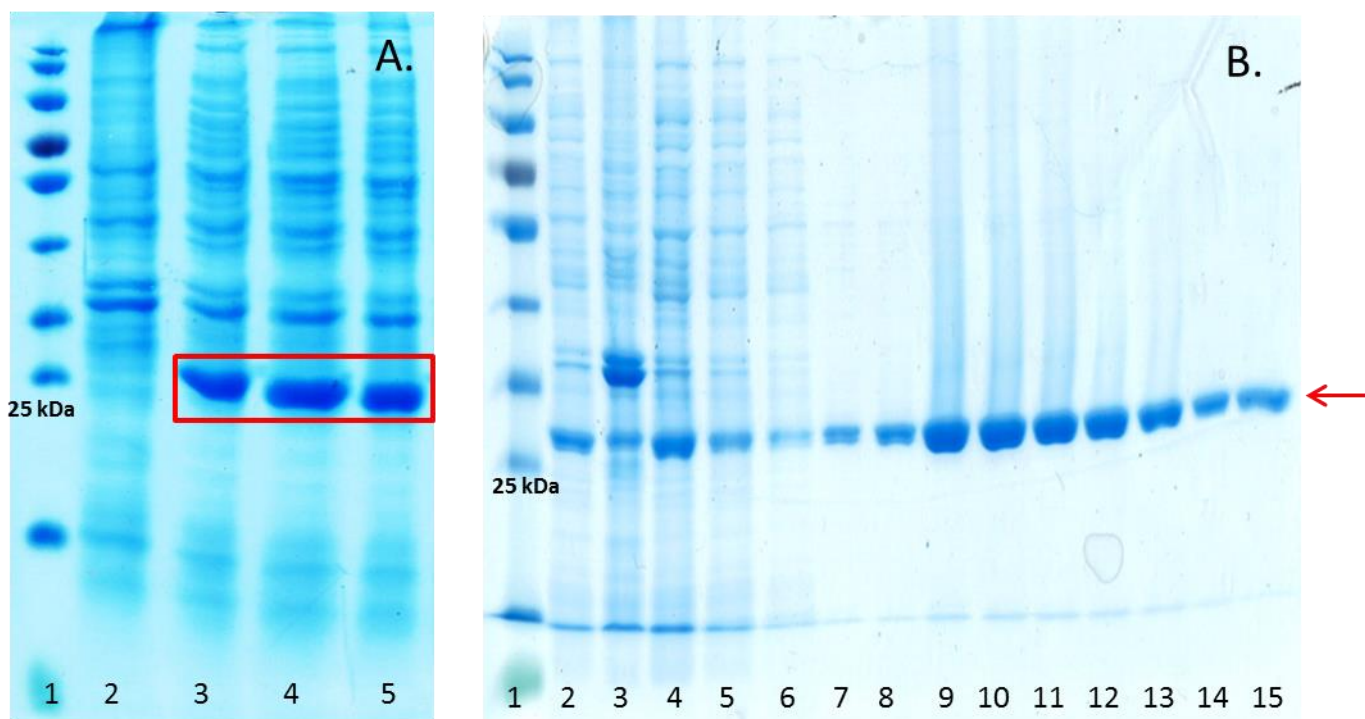


Figure S1. SDS-PAGE for SDR B3 expressed in *R. eutropha* H16.

A - SDS-PAGE of whole cell lysates; expressed SDR B3 with expected size 26 kDa is shown in red box: lane 1 - PageRuler™ Prestained protein ladder; lane 2 – *R. eutropha* H16; lanes 3-5 – *R. eutropha* H16 [pKRSF1010-P_{j5}-SDR B3-cymR] clones 1-3.

B – SDS-PAGE for His₆-SDR B3, purified on PD10 desalting columns, prepacked with Ni Sepharose™ Fast Flow, His₆-SDR B3 with expected size 27 kDa is shown with red arrow: lane 1 - PageRuler™

Prestained protein ladder; lane 2 – *R. eutropha* H16 [pKRSF1010-P_{j5}-His₆-SDR B3-cymR] cell lysate soluble fraction; lane 3 – *R. eutropha* H16 [pKRSF1010-P_{j5}- His₆-SDR B3-cymR] cell lysate insoluble fraction; 4 – flow through; 5 – washing fraction (binding buffer); lane 6 – washing fraction #1 (wash buffer); lane 7 – washing fraction #6 (wash buffer); lanes 8-13 – elution fractions #1-6; lane 14 - elution fractions #10; lane 15 – purified enzyme in storage buffer.

3.1.3.10. Preliminary data on whole cell bioconversion of benzil performed by lithoautotrophically grown cells of *R. eutropha* H16 expressing SDR B3.

The strain *R. eutropha* H16 [pKRSF1010-P_{j5}-SDR B3-cymR] was used for whole-cell bioconversion of benzil under H₂ atmosphere in the absence of any additional regeneration system. Cultivation conditions used for this study are given in chapter 3.1.2.16. *R. eutropha* H16 [pKRSF1010-Tac-Δinsert] was used as a negative control. An SDS gel of crude cell lysate for lithoautotrophically grown cells can be seen in Fig. 55.

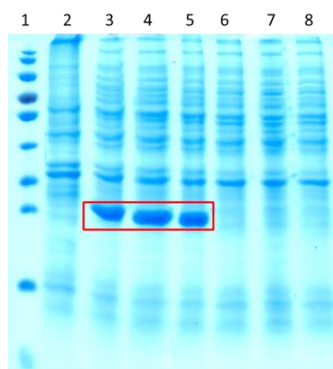


Figure 55. SDS-PAGE of whole cell lysates from *R. eutropha* H16 fermentation of SDR B3 under lithoautotrophic growth conditions. Expected size for SDR B3 is 26 kDa. Expressed SDR B3 is indicated in red box. Lane 1: PageRuler™ Prestained protein ladder; lanes 2: control, *R. eutropha* H16; lanes 3-5: *R. eutropha* H16 [pKRSF1010-P_{j5}-SDR B3-cymR], clones 1-3, induced; lanes 6-8: control, *R. eutropha* H16 [pKRSF1010-P_{taC}-Δinsert], clones 1-3

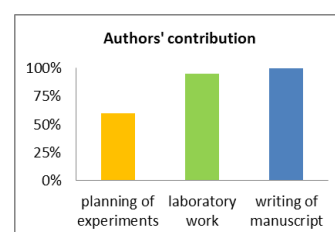
Benzil was added as a substrate to the lithoautotrophically grown cultures, induced by cumate, at OD₆₀₀ = 5.0. After 3 hours of incubation with the substrate samples were analysed by HPLC. A detailed description of the method is given in chapter 3.1.2.16. In the first attempt, data showed that *R. eutropha* H16 [pKRSF1010-P_{j5}-SDR B3-cymR] performed conversion of benzil to (*S*)-benzoin and (*R*)-benzoin at stereoselectivity of 97 % ± 1 % (*S*). Interestingly, the control strain *R. eutropha* H16 [pKRSF1010-Tac-Δinsert] was also able to convert benzil but preferably to (*R*)-benzoin with a stereoselectivity of 52 % ± 4 % (*R*). The whole-cell bioconversion experiments have to be repeated since the analysed samples included only the supernatant of the culture, which does not contain products captured inside the cells, and thus conversion rates could not be calculated properly. An additional experiment was performed in order to determine if substrate and/or product is also present in the cells. Two samples of *R. eutropha* H16 [pKRSF1010-Tac-Δinsert] were analysed by HPLC after 1 hour incubation with benzil as substrate. In first case, 1 ml of the culture supernatant was used as a sample for analysis, in second case, 1 ml of the whole culture was used for HPLC sample preparation as described in Materials and methods in chapter 3.1.2. These preliminary data showed that significant amount of bulky substrate, benzil, was trapped in the cells. Interestingly, the

similarly bulky molecules of the product, benzoin, was found to be present mostly outside of the cell but not inside since there was no significant difference in the amount of benzoin between the two analysed samples. However, these data need also to be confirmed.

These preliminary results confirm that the reduction potential of *R. eutrophas* H16 cells in lithoautotrophic environment is high enough to provide sufficient cofactor for NADPH-dependent reactions (Li et al., 2012; Oda et al., 2013). Moreover, the results indicate that the reduction reactions can be performed in *R. eutropha* H16 by oxidoreductases normally expressed in the wild type of *R. eutropha* H16. It is likely that these oxidoreductases are upregulated under lithoautotrophic growth conditions (Friedrich et al., 1981; Vollbrecht et al., 1979).

3.2. Cloning, expression, purification and functional analysis of aldehyde dehydrogenase originating from *Ralstonia eutropha* H16

This part of work was performed in collaboration with the group of Dipl.-Ing. Dr.techn. Margit Winkler.



Editing and additional suggestions for writing of manuscript were provided by Dr. P. Heidinger and Prof. H. Schwab

3.2.1. Introduction

α,β -dicarbonyls, for example, diacetyl and methylglyoxal, are highly reactive compounds interacting with arginine, lysine, and cysteine residues of the proteins (Degenhardt et al., 1998; Tokikawa et al., 2014). They can damage or cause cross linking of the proteins and were shown to correlate with diseases like diabetic vascular complications, neurodegenerative diseases, atherosclerosis, and general cellular deterioration and aging (Brownlee, 1995; Kovacic and Cooksy, 2005; Roberts et al., 2003; Wondrak et al., 2002). Removal of these dicarbonyl compounds is therefore essential for the maintenance of the cellular health. Therefore, novel enzymes acting on dicarbonyl groups of the organic compounds represent particular interest for biotechnology. The well-studied α,β -dicarbonyl reductase from *Saccharomyces cerevisiae* (Ara1, EC 1.1.1.117, encoded by YBR149W), also called D-arabinose dehydrogenase 1 (Amako et al., 2006a, 2006b; van Bergen et al., 2006) has 82% query covery and 28% sequence identity with the aldehyde dehydrogenases from *R. eutropha* H16 (*RasAIDH*, locus *H16_B2162*).

The aim of presented work was cloning, expression and purification of a His-tagged version of *RasAIDH* and preliminary analysis of reduction enzyme activity with few sugars and diketones. Further detailed analysis of enzyme activity was presented in the doctoral thesis of Kamila Napora (Napora, 2013).

3.2.2. Materials and methods

3.2.2.1. General

E. coli strains used in this study are listed in Table 5.

DNA isolation, preparation and cultivation conditions for expression in *E. coli* BL21 are described in chapter 3.1.2.

3.2.2.2. His₆-tag cloning

pMS470-*RasAIDH*, an *E. coli* expression vector with cloned aldehyde dehydrogenase from *R. eutropha* H16 (constructed by Kamila Napora) was modified for purification via His₆-tag and hence better functional analyses. Since the protein models, generated using Swiss-Prot, showed that the amino termini of these dehydrogenases are exposed (Fig. 56), it was decided to use an amino terminal His₆-tag.

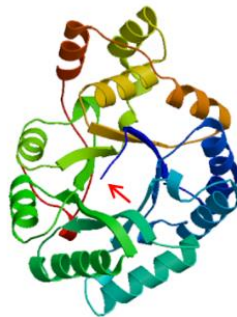


Figure 56. Swiss-Prot protein model of aldehyde dehydrogenase *ReAIDH*. The amino terminus of the protein is marked by red arrow. Reference: Biasini et al., 2014

For insertion of a His₆-tag into the pMS470-*RasAIDH* expression vector two oligonucleotides were designed:

6xhis_sense (#198) 5'-**ctaga**aaggagatataccatgtcgtactaccatcaccatcaccatcaccgattacgacca-3'
6xhis_antisense (#199) 5'-**tatggt**cgtaatcgtgatggtgatggtgatggttagtagcagatggtatatctccttt-3'

Bold letters indicate restriction sites of endonucleases, whereas underlined sequences represent His₆-tag.

These oligonucleotides contain a *Xba*I restriction site on the 5' end and a *Nde*I restriction site on the 3' end, for insertion to the amino terminus of the dehydrogenase respectively. To anneal the oligonucleotides and generate the linker, 2 nmol of each of them were mixed and incubated at 95 °C for 10 min. The mixture was then slowly cooled down to the room temperature (Fig. 57).

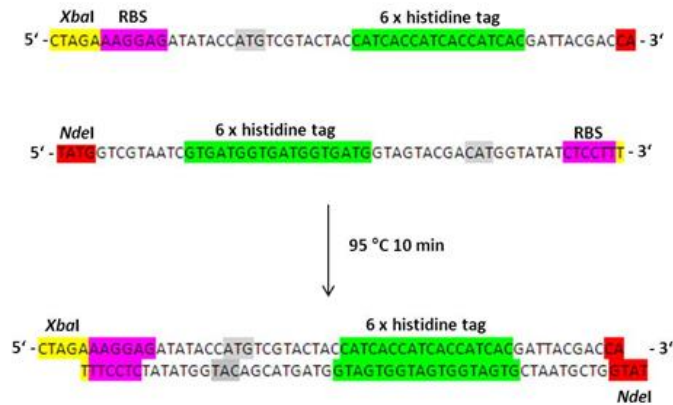


Figure 57. Schematic overview of oligonucleotide structure and their annealing to form the 6 x histidine linker that was inserted into the pMS470-ReAIDH vector. Picture taken from Zach, 2013

The expression vector with cloned aldehyde dehydrogenase from *R. eutropha* H16 pMS470-*RasAIDH* was cut with *XbaI* and *NdeI* restriction enzymes and ligated with the annealed linker using a molar vector to linker ratio of 1 to 100. Afterwards the construct was transformed into competent *E. coli* TOP10 cells. The plasmid was again isolated from the received clones, cut with *XbaI* and *NdeI* restriction enzymes and analysed on a 3 % agarose gel. Constructs containing the 59 bp linker was verified by DNA sequencing (LGC Genomics GmbH; Berlin, Germany) with the following primers:

pM(S)-prom-fwd	(#39)	5'-gcataattcgtgtcgtcaagg-3'
Tac-pM(S)-Stop-neu-rev	(#40)	5'-gcaaattctgtttatcagacc-3'

3.2.2.3. Protein expression

Cultivation conditions for *E. coli* BL21 are described in chapter 3.1.2. Fermentation of the aldehyde dehydrogenase was done in 300 mL culture after IPTG induction overnight at 22°C, 25°C or 28 °C. After expression the cells were harvested with an Avanti centrifuge J-20 (Beckman Coulter). Cell pellets were washed twice with 50 mM sodium phosphate buffer pH 7.4, dissolved in 20 mL of the same buffer and then disrupted with a Branson 102C converter. Power was supplied with a Branson Sonifier 250 (Duty Cycle % 80; Output Control 8) and the cell free extract was obtained by centrifugation for 60 min at 20 000 rpm and 4 °C (Avanti TM J-20 XP centrifuge, JA-25,50 rotor, Beckman Coulter Inc.; Vienna, Austria). When cell free extract was used for further enzyme purification, cell pellets were dissolved in 20mM sodium phosphate buffer supplemented with 0.5 M sodium chloride and 20 mM imidazole. After the centrifugation step the soluble fraction was filtered with a 0.2 µm filtropur (Sarstedt; Nürnberg, Germany) and used for protein purification or enzyme activity assay.

3.2.2.4. Protein purification

The protein was purified using a HisTrap™ FF 5 mL column on an ÄKTA Purifier 100 with Frac-950, software Unicorn 4.11, and desalted using a HiPrep™ 26/10 Desalting column on an ÄKTA Prime, software PrimeView 5.0 (GE Healthcare Life Sciences). Protein samples were analysed with 12 % Tris-glycine SDS-polyacrylamide gels.

3.2.2.5. Enzyme activity assay

The specific enzyme activity was determined by a NAD(P)⁺/NAD(P)H dependent spectrophotometric assay as described in chapter 3.1.2 using both cell free extract and purified enzyme. The oxidation activity of the cell free extracts was tested with the corresponding sugar alcohols D-arabitol, D-ribitol, D-xylitol and D-mannitol. The reduction activity of the purified enzyme was tested with four sugars, namely D-arabinose, D-ribose, D-xylose and D-mannose, and two diketones, 2,3-butanedione and 3,4-hexanedione. For pH range studies following 50 mM buffers were used: citrate buffer pH 5.5, 6.0; sodium phosphate buffer pH 6.0, 6.5; Tris-HCl buffer pH 7.0. Measurements in reduction way of reaction were performed at 30°C; 1mM 2,3-butanedione was used as a substrate; 0.5 mM NADPH was used as a cofactor.

3.2.3. Results and discussion

His₆-tag coding sequence was cloned into pMS470 expression vector at the N-terminus of aldehyde dehydrogenase from *R. eutropha* H16, *RasAIDH* (locus *H16_B2162*) via *Xba*I and *Nde*I (Fig. 58), creating pMS470-His₆-*RasAIDH* (plasmid #31 in internal plasmid list). Strain generated in this study was handed over to the IMBT strain collection under the number #7667 (Supplementary Table 1).

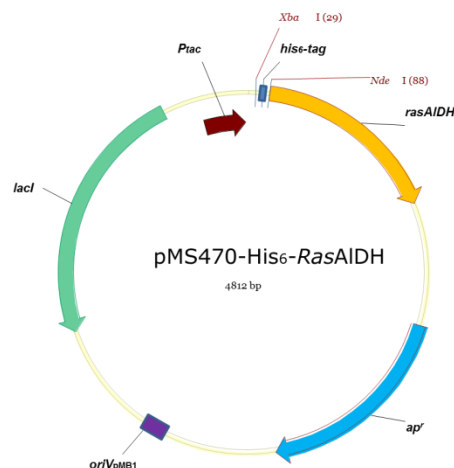


Figure 58. Illustration of the expression vector pMS470-His₆-*RasAIDH*. The plasmid backbone encodes promoter *tac*, replication origin replication origin from pMB1, ampicillin resistance gene *ap^r*, gene encoding LacI repressor protein, N-terminal his₆-tag coding sequence and gene encoding aldehyde dehydrogenase from *R. eutropha* H16

Afterwards, expression of *RasAIDH* with and without histidine tag was done in 300 mL cultures at 28 °C overnight after 0.1 mM IPTG induction at OD₆₀₀ 0.7. The whole cell lysate, cell free extract and pellet were analysed on a 12 % SDS polyacrylamide gel. The size of *RasAIDH* containing the His₆-tag differs in 1 kDa to the size of the same enzyme without the tag. An example of the successful heterologous expression in *E. coli* BL21 is shown in Fig. 59.

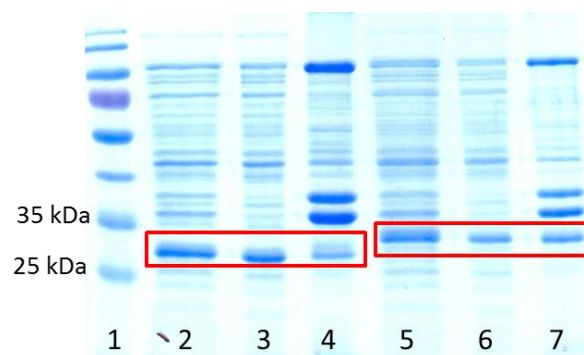


Figure 59. SDS-PAGE of *E. coli* BL21 fermentation of *RasAIDH* and His₆-*RasAIDH* at 22°C. Expected size for aldehyde dehydrogenase is 29 kDa, for His₆-tagged aldehyde dehydrogenase – 31 kDa. Expressed *RasAIDH* is shown in red box. Lane 1: PageRuler™ Prestained protein ladder; lane 2: *E. coli* BL21 [pMS470-*RasAIDH*], whole cell lysate; lane 3: *E. coli* BL21 [pMS470-*RasAIDH*], soluble fraction;

lane 4: *E. coli* BL21 [pMS470-*RasAIDH*], pellet; lane 5: *E. coli* BL21 [pMS470-*His₆-RasAIDH*], whole cell lysate; lane 6: *E. coli* BL21 [pMS470-*His₆-RasAIDH*], soluble fraction; lane 7: *E. coli* BL21 [pMS470-*His₆-RasAIDH*], pellet

As can be seen in Fig. 59, significant amount of overexpressed protein was found in the insoluble fraction. Under high level expression conditions of the recombinant protein can aggregate and form inclusion bodies (Palmer and Wingfield, 2012). Aggregated protein is mostly present in its inactive and denatured form. This problem may be solved by deceleration of the cell growth, for example by use of lower fermentation temperature. Therefore, the expression of *E. coli* BL21 [pMS470-*His₆-RasAIDH*] was additionally performed at 25°C and 22°C. Nevertheless, no significant difference in the amount of formed inclusion bodies was observed comparing to the culture fermented at 28°C. However, the amount of overexpressed protein obtained from the soluble cell free extract was sufficient to proceed with the protein purification and the enzyme activity analysis.

As it was observed on the SDS-PAGE, the adding of the *His₆*-tag slightly increases the presence of overexpressed protein in the insoluble fraction in comparison to the amount of non-aggregated protein in the soluble fraction (for example, Fig. 59). Probably, the presence of the additional amino acids on N-terminus of *RasAIDH* negatively influences the protein folding and increases amount of inappropriately folded enzyme.

In order to determine influence of *His₆*-tag on the functionality of the enzyme, photometric assay for the soluble cell free lysate was performed (Fig. 60).

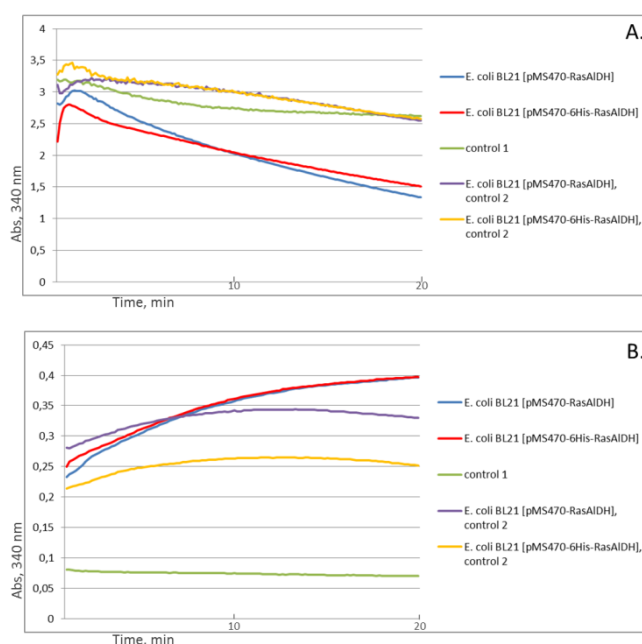


Figure 60. Enzyme activity of the whole cell lysate of *E. coli* BL21 with overexpressed *His₆*-tagged and non-*His₆*-tagged *RasAIDH*. A. Reduction way of reaction with arabinose as a substrate. B. Oxidation way of reaction with arabitol as a substrate. Whereas the substrate is reduced

or oxidized, the cofactor NADP(H) is oxidized or reduce, respectively. The increasing or decreasing amount of NADP(H) due to enzyme activity was monitored over 20 min. Control #1: NADP(H), buffer, substrate. Control #2: NADP(H), buffer, whole cell lysate of *E. coli* BL21 [pMS470-*RasAlaDH*] or *E. coli* BL21 [pMS470-*His₆-RasAlaDH*] as indicated.

When compared to the controls, it was noticed that the photometric reactions with the cell free extract show high level of a background reaction, especially in the reduction way of reaction. An example can be seen in Fig. 60 (control 2). The observed background reaction arises from the soluble proteins of the empty *E. coli* BL21 strain, which are also present in the lysate. Nevertheless, these preliminary data indicated that there is no significant difference in the activity of *His₆*-tagged and non-*His₆*-tagged version of *RasAlaDH* and, additionally, it was observed that aldehyde dehydrogenase has a preference of NADP(H) over NAD(H) as cofactor. For further detailed enzyme activity analysis the overexpressed protein was purified.

To purify *His₆-RasAlaDH* 20mM sodium phosphate buffer supplemented with 0.5 M sodium chloride and 20 mM imidazole, pH 7.4 was used. The protein was eluted using a 20mM sodium phosphate buffer supplemented with 0.5 M sodium chloride and 500 mM imidazole, pH 7.4. Fractions were analysed via SDS-PAGE (Fig. 61) and those, which contain significant amount of purified protein were pooled together. Elution buffer in the final sample was replaced by storage buffer of 20mM Tris-Cl supplemented with 200 mM NaCl, pH 7.5. *His₆-RasAlaDH* could be purified to the final concentration up to 2 mg/ml.

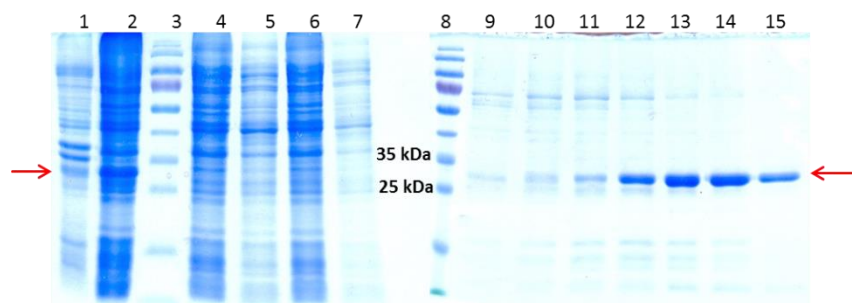


Figure 61. SDS-PAGE of *His₆-RasAlaDH* fermentation samples and purification fractions. Expected size for *His₆*-tagged aldehyde dehydrogenase – 31 kDa. Position of the *His₆-RasAlaDH* is shown with red arrows. Lanes 3, 8: PageRuler™ Prestained protein ladder; lane 1: *E. coli* BL21 [pMS470-*His₆-RasAlaDH*], soluble fraction; lane 2: *E. coli* BL21 [pMS470-*His₆-RasAlaDH*], pellet; lanes 4-7: washing fractions of the protein purification; 9-15: elution fractions of the protein purification

The reduction activity of *His₆-RasAlaDH* was tested via a photometric assay with four sugars, D-arabinose, D-ribose, D-xylose and D-mannose, and two diketones, 2,3-butanedione and 3,4-hexanedione as substrate. The purified *His₆-RasAlaDH* showed only weak reduction activity with such sugars as D-xylose with a maximum detected specific activity of 37 mU/mg and D-ribose with a maximum detected specific activity of 48 mU/mg. Weak but clear activity was also detected with

diketone 2,3-butanedione with specific activity of 34 mU/mg. The pH range for reduction activity of His₆-*RasAIDH* was characterized with 2,3-butanedione as a substrate (Fig. 62). Preliminary results indicate that the enzyme has the highest activity at the lowest tested pH 5.5.

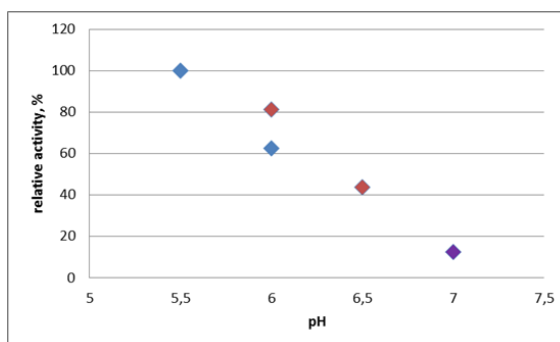


Figure 62. pH optimum for reduction activity of His₆-*RasAIDH* (preliminary data). Reaction conditions for reduction: T= 30°C, 50 mM buffer, 1mM 2,3-butanedione, 0.5 mM NADPH. Reaction conditions for oxidation: T= 40°C, 50 mM buffer, 1 mM (S)-(+)-2-octanol, 0.5 mM NADPH. Legend: blue mark – citrate buffer; red mark - sodium phosphate buffer; violet mark – Tris-HCl buffer

Purified enzyme samples were forwarded to K. Napora for further detailed analysis. Results, presented by K. Napora (Napora, 2013) indicate that the purified His₆-*RasAIDH* can convert 5'-modified ribose sugar such as 5-*O*-trityl- α,β -D-ribose (Fig. 63) to the respective alcohol in almost 60%. Usage of 0.13 mg of the enzyme increased the conversion up to 80%, and the application of a GDH/glucose cofactor recycling system resulted in almost 70% of product after overnight reaction.

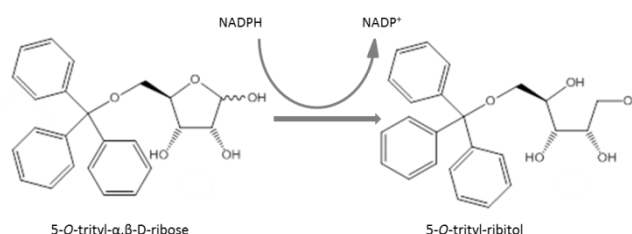
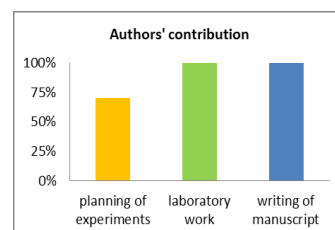


Figure 63. Scheme of the chemical reaction performed by *RasAIDH*. *RasAIDH* reduces 5-*O*-trityl- α,β -D-ribose to 5-*O*-trityl- ribitol. Reference: modified from (Napora, 2013)

3.3. Cloning and expression of bacterial transaminase, alanine dehydrogenases and imine reductases in *Ralstonia eutropha* H16

This experimental section was performed as a side project in collaboration with the group of Univ.-Prof. Dipl.-Ing. Dr.techn. Wolfgang Kroutil, Institute of Chemistry, University of Graz.

A transaminase originating from *Arthrobacter* sp. (improved variant, W. Kroutil), alanine dehydrogenase originating from *Bacillus subtilis* including a His-tagged version, alanine dehydrogenase originating from *R. eutropha* H16 and 4 imine reductases, 2 originating from *Streptomyces* sp., one originating from *Mesorhizobium* sp. and one originating from *Kribbella flavida*, were cloned and expressed in *E. coli* TOP10 and in *R. eutropha* H16 under heterotrophic growth conditions for further functional analysis by the members of Prof. Kroutil's group. Additionally, these enzymes were expressed in *R. eutropha* H16 under lithoautotrophic growth conditions to carry out the reactions of interest in a cell-based cofactor regeneration system .



Editing and additional suggestions for writing of manuscript were provided by Dr. P. Heidinger and Prof. H. Schwab

3.3.1. Introduction.

The potential of using *R. eutropha* H16 as a cell factory for performing oxidoreductase reactions without additional cofactor recycling system was shown by heterologous expression of alcohol dehydrogenase from *Kluyveromyces lactis* for production of (*R*)-1,2-propanediol (Oda et al., 2013). Other chiral molecules, enantiopure amines, which are widely spread in nature, are also among those highly desirable building blocks for pharmaceuticals (Davies and Teng, 2003). One of the methods to generate enantiopure amines is the use of ω -transaminases (ω -TAMs) (EC 2.6.1.18) (Mathew and Yun, 2012; Zhu and Hua, 2009). This type of transaminases is able to accept not only keto acids and amino acids as their substrates but also aliphatic ketones and amines. Despite all advantages of the ω -TAMs approach, as for example, the improved sustainability, a problem arises with keeping the reaction equilibrium towards the desired direction. However, this problem can be solved by removing the co-product or by using an excess of amine donor (Savile et al., 2010). The perfect solution would be to combine both of these approaches in an enzyme-coupled reaction with an alanine dehydrogenase (Fig. 64).

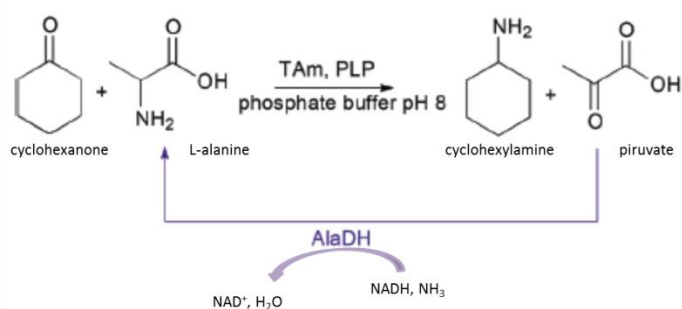


Figure 64. Enzyme-coupled methods to shift the transaminase reaction equilibrium toward the desired amine product. Cyclohexanone is used as a ketone acceptor. TAm – transaminase, PLP - pyridoxal phosphate cofactor. Reference: modified from Richter et al., 2015

In the reaction of transamination, L-alanine is used as an amine donor. For continuous production of L-alanine, NAD(H)-dependent alanine dehydrogenase needs a permanent access of the cofactor. Glucose dehydrogenase and formate dehydrogenase have commonly been applied for cofactor recycling in previous works (Koszelewski et al., 2010; Richter et al., 2015; Tauber et al., 2013). The enormous reduction potential present in the cells of *R. eutropha* H16 under lithoautotrophic growth conditions, provides a highly efficient alternative for the cofactor recycling in the process of chiral amine production (Holzer et al., 2015).

Primary amines production can be catalysed by various enzymes such as lipases, monoamine oxidases and transaminases. In contrast, catalysis of secondary amines is performed by only few enzymatic approaches, for example, with the help of imine reductases (Gand et al., 2014). IREDs attract permanently growing attention since they show high stereoselectivity and, therefore, result in

optically pure secondary amines as a product. Up to now only a few IREDs were described as recombinant proteins capable of performing asymmetric synthesis of secondary amines from the corresponding prochiral imines (Gand et al., 2014; Huber et al., 2014; Mitsukura et al., 2013, 2011). These enzymes belong to the class of NAD(P)(H)-dependent oxidoreductases and, therefore, require cofactors to perform imine reduction as shown in Fig. 65.

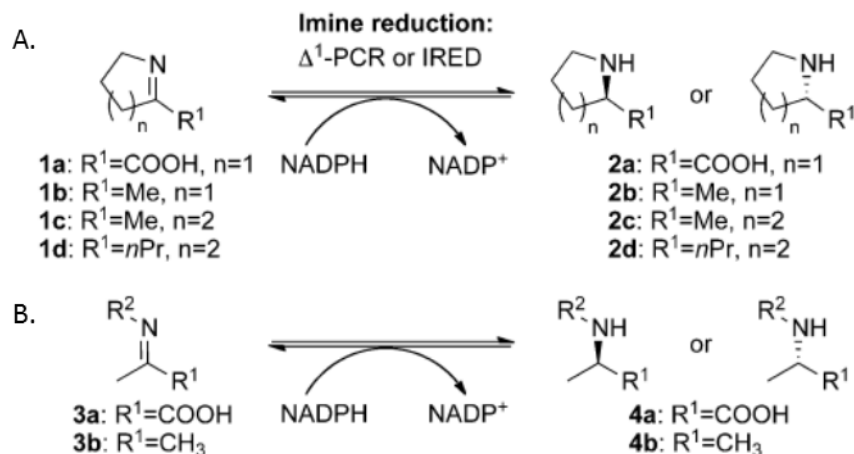


Figure 65. Enzymatic imine reduction. Δ^1 -Pyrroline-carboxylate reductase (Δ^1 -PCR) catalyses the reduction of cyclic imines (reaction A) or acyclic imines (reaction B), $R^1=COOH$, $n=1-2$. Imine reductase (IRED) reduce the analogous cyclic substrates where R^1 is an alkyl substituent, e.g. a methyl group, and $n=1-3$. IREDs can also act on acyclic substrates (reaction B), $R^1=CH_3$. (Gand et al., 2014)

Consequently, there is a great interest in expressing imine reductases in *R. eutropha* H16 as the reaction of imine reduction could be coupled with the activity of hydrogenases, which are highly active under lithoautotrophic growth conditions.

3.3.2. Material and methods

3.3.2.1. Bacterial strains and cultivation conditions

Bacterial strains and plasmids used in this study are listed in Table 5 and Table 15, respectively. Strains derived in this study were handed over to the IMBT strain collection under the numbers ##7668-7675 (Supplementary Table 1).

Table 15. Plasmids, used in this study

Plasmid	Description	Reference
pRK2013	Km ^r , <i>colE1</i>	(Figurski and Helinski, 1979)
pKRSF1010-P _{taC} -Δinsert	Km ^r , P _{taC} , <i>par</i> , RSF1010 mob and origin of replication	this study
pCRSF1010-P _{j5} -cymR	Cm ^r , P _{j5} , <i>par</i> , RSF1010 mob and origin of replication	Gruber et al., unpublished data
pKRSF1010-P _{j5} -OO-cymR	Cm ^r , P _{j5} , <i>par</i> , cumate operators downstream the promoter region RSF1010 mob and origin of replication	Gruber et al., unpublished data
pKRSF1010-P _{j5} -TA-cymR	Km ^r , P _{j5} , <i>par</i> , <i>ta AS</i> , <i>cymR</i> RSF1010 mob and origin of replication	this study
pKRSF1010-P _{j5} -cyOO-AlaDH-cymR	Km ^r , P _{j5} , <i>par</i> , <i>alaDH</i> , <i>cymR</i> RSF1010 mob and origin of replication	this study
pKRSF1010-P _{j5} -His ₆ -AlaDH-cymR	Km ^r , P _{j5} , <i>par</i> , <i>alaDH</i> , <i>cymR</i> N-terminal his-tag coding sequence RSF1010 mob and origin of replication	this study
pKRSF1010-P _{j5} -ReAlaDH-cymR	Km ^r , P _{j5} , <i>par</i> , <i>H16_A2009</i> , <i>cymR</i> RSF1010 mob and origin of replication	this study
pKRSF1010-P _{j5} -PotRIRED-cymR	Km ^r , P _{j5} , <i>par</i> , <i>potrired</i> , <i>cymR</i> RSF1010 mob and origin of replication	this study
pKRSF1010-P _{j5} -PotSIREd-cymR	Km ^r , P _{j5} , <i>par</i> , <i>potsired</i> , <i>cymR</i> RSF1010 mob and origin of replication	this study

pKRSF1010-P _{J5} -cyOO-R-IRED-cymR	Km ^r , P _{J5} , par, r-ired, cymR	this study
	RSF1010 mob and origin of replication,	
	two cumate operators downstream the promoter region	
pKRSF1010-P _{J5} -cyOO-S-IRED-cymR	Kan ^r , P _{J5} , par, s-ired, cymR	this study
	RSF1010 mob and origin of replication,	
	two cumate operators downstream the promoter region	

All chemicals, reagents and basic media components were obtained from Becton, Dickinson and Company (Franklin Lakes, NJ, USA), Sigma-Aldrich (St. Luis, MO, USA) and Carl Roth (Arlesheim, Germany), respectively, unless mentioned otherwise.

3.3.2.2. Cultivation conditions

E. coli strains were propagated at 37°C at 120 rpm in lysogeny broth (LB). *R. eutropha* H16 strains were grown at 28°C at 100 rpm in tryptic soy broth (TSB) under heterotrophic growth conditions or in minimal salt medium (MSM) under lithoautotrophic growth conditions supplemented with 20 µg/ml gentamicin. The description of the media content is given in Table 5. Gas atmosphere for lithoautotrophic growth included 10% CO₂, 10% O₂ and 80% H₂. Pre-cultures for the lithoautotrophic growth were inoculated with the pellet of 5 mL ONC cultures heterotrophically grown in MSM medium supplemented with 0.6 % fructose. For antibiotic selection kanamycin was added when necessary in a concentration of 40 µg/ml for *E. coli* strains and 200 µg/ml for *R. eutropha* H16 strains. For protein expression experiments 1 % glucose was added into LB media for *E. coli* strains and 0.6 % fructose into TSB or MSM media for *R. eutropha* H16 strains (Table 6). Medium was solidified with 20g/l agar-agar (Carl Roth, Arlesheim, Germany) when needed.

3.3.2.3. DNA preparation

DNA preparation and manipulations were performed as described in Materials and methods section in chapter 3.1.2.

3.3.2.4. Plasmid construction

All genes of interest, except for the gene for alanine dehydrogenase from *R. eutropha* H16 (*realaDH*, locus tag *H16_A2009*), were amplified via PCR from the corresponding constructs given by members of Prof. Kroutil's group. PCR for *realaDH* was performed with genomic DNA of *R. eutropha* H16 as a template. Primers used for the amplification are given in Table 16 (PCR-1). Separately, the gene for kanamycin resistance was amplified from pKRSF1010-P_{J5}-SDR B3-cymR with a corresponding set of primers (PCR-2) (See Table 16). Afterwards, each gene of interest and corresponding PCR product for kanamycin resistance gene were combined in one DNA fragment via overlap extension

PCR reaction. Primers used for overlap PCR are given in Table 16. Purified products of the overlap extension PCRs were cloned into the proper expression vector. Alanine dehydrogenase from *Bacillus subtilis* and its His-tagged version were cut with *Xba*I and *Avr*II restriction sites and cloned into the vector cut with the same endonucleases. PCR products for other genes of interest were cut with *Nde*I and *Avr*II restriction sites and cloned into the vector cut with the same endonucleases. The genes for transaminase (*ta AS*), two versions of alanine dehydrogenases (*his₆-alaDH*, *realaDH*) and two imine reductases (*potrired* and *potsired*) were cloned into pCRSF1010-P_{J5}-cymR expression vector. Two other genes coding for imine reductases R-IRED and S-IRED, and the gene coding for AlaDH were cloned into pKRSF1010-P_{J5}-cyOO-cymR expression vector via *Nde*I and *Avr*II restriction sites. Success of the cloning experiments was proven by restriction analysis and subsequent DNA sequencing (LGC Genomics GmbH; Berlin, Germany). Oligonucleotides used for sequencing are given in Table 16. The completed constructs were transformed into *E. coli* TOP10 expression strain via standard electroporation procedure. Plasmid transfer into *R. eutropha* H16 was performed via conjugation.

Table 16. Primers used in this study

Name	Number	Sequence 5'-3'	Cloning step
Trns-Fwd (NdeI)	615	attcatatgggtctgaccgtgca	PCR-1, overlap PCR sequencing
Rev-Trns-Km	616	agccaagcttttagctctgctgccatt	PCR-1
Fwd-Trns-Km	617	gcagagctaaaagcttgctgttttgg	PCR-2
His-AlaDH-Fwd(XbaI)	618	attctagaaaggagatataccatggctagcagaggatcgcatca	PCR-1, overlap PCR sequencing
AlaDH-Fwd(XbaI)	619	attctagaaaggagatataccatgatcataggggttcctaaaga	PCR-1
Rev-AlaDH-Km	620	gccaaagctttaagcaccgccac	PCR-1
Fwd-AlaDH-Km	621	ggtgcttaaaagcttgctgttttgg	PCR-2
ReAlaDH-Fwd(NdeI)	622	attcatatgtggatcggcgtgcctaaag	PCR-1, overlap PCR sequencing
Rev-ReAlaDH-Km	623	agccaagctttcaggtcagcacctgct	PCR-1
Fwd-ReAlaDH-Km	624	gctgacctgaaagcttgctgttttgg	PCR-2
Fwd-PotRIRED-Nde	629	attcatatgagcgatattaccgttattg	PCR-1, overlap PCR sequencing
Rev-PotRIRED-Km	630	agccaagcttttatgaccctgtttgc	PCR-1

Fwd-PotRIRED-Km	631	gggtgcataaaagcttgctgttttg	PCR-2
Fwd-PotSIREN-Nde	632	attcatatgctccgaccgatcgta	PCR-1, overlap PCR sequencing
Rev-PotSIREN-Km	633	agccaagcttttaacgggactacgaa	PCR-1
Fwd-PotSIREN-Km	634	tcccggttaaaagcttgctgttttg	PCR-2
Fwd-R-IRED-Nde	635	attcatatgggtgataatcgtacacc	PCR-1, overlap PCR sequencing
Rev-R-IRED-Km	636	agccaagcttttattcgctcggtttac	PCR-1
Fwd-R-IRED-Km	637	gagcgaataaaagcttgctgttttg	PCR-2
Fwd-S-IRED-Nde	638	attcatatgagcaaacagagcgttac	PCR-1, overlap PCR sequencing
Rev-S-IRED-Km	639	agccaagcttttaactccggttttttc	PCR-1
Fwd-S-IRED-Km	640	ggcagtttaaaagcttgctgttttg	PCR-2
Mid-rev-1	644	atccacacaaaaccgtaac	sequencing
midAlaDH-rev	625	cattttcggcggtttgtcc	sequencing
Mid-rev-2	645	gcctgagcagcggcagttc	sequencing
Pot-RIRED-mid-rev	641	agctgaccgctacacgcatc	sequencing
Pot-SIREN-mid-rev	642	aacttctgccggaccgctat	sequencing
R-IRED-mid-rev	643	agtggcggttcatattttc	sequencing
S-IRED-mid-rev	646	tcagggtatcttcatgggca	sequencing
ter_KanR_rev_Stul/AvrII/Spel		actagtctaggaggcctgtctgacgctcagtggaac	PCR-2, overlap PCR, sequencing; used for all genes of interest

The colored sequences represent the additional restriction sites at the 5' ends of forward and reverse primers: **NdeI**; **XbaI**; **AvrII**

3.3.2.5. Protein expression

Cultivation conditions for *E. coli* and *R. eutropha* H16 strains are given in chapter 3.1.2. The induction of the enzyme expression in plasmid harbouring strains was started at an OD₆₀₀ 1.0 by adding 60 µg/ml cumate and cultures were grown over night at 28°C at 100 rpm. The expression of the proteins in corresponding *E. coli* TOP10 and *R. eutropha* H16 strains was visualizes by SDS-PAGE.

The purification of His₆-tagged recombinant enzymes was performed as described in chapter 3.1.2. When the successful expression of the enzymes was proven, *R. eutropha* H16 strains were grown lithoautotrophically in 30 mL MSM culture, induced at OD₆₀₀ 0.8 and collected at OD₆₀₀ about 1.5-2.0 (detail description for lithoautotrophic growth see in chapter 3.1.2). The cell pellets were frozen in liquid nitrogen and handed over to the members of Prof. W. Kroutil's group for further enzyme activity analysis.

3.3.3. Results and discussion

For cloning the genes of our interest the fine-tuneable expression vector for *R. eutropha* H16 which has been recently developed by Gruber *et al.* (manuscript in preparation, see chapter 4) was used. Native alanine dehydrogenase (locus *H16_A2009*), named *ReAlaDH*, a transaminase from *Arthrobacter sp.*, named TA AS, (improved variant, W. Kroutil), alanine dehydrogenase from *Bacillus subtilis*, named *AlaDH*, including a His-tagged version, named His₆-*AlaDH*, 2 imine reductases originating from *Streptomyces sp.*, named R-IRED and S-IRED, (locuses *AB747176* and *AB74717*, respectively), one imine reductase originating from *Mesorhizobium sp.*, named PotRiRED, (locus *X736_28605*) and one imine reductase originating from *Kribbella flavida*, named PotSIREd, (locus *Kfla_3935*) were successfully cloned under the control of strong *j5* promoter derived from bacteriophage T5 (Fig. 66). This promoter was shown to be the strongest promoter yet to be applied in *R. eutropha* H16 (Gruber *et al.*, 2014).

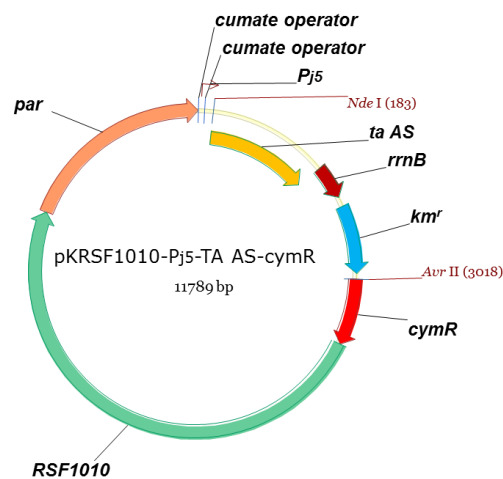


Figure 66. Illustration of the expression plasmid with the cloned transaminase gene (*ta AS*). The plasmid backbone encodes the terminator *rrnB*, pBBR1 partition region *par*, mobilization sequence and origin of replication from RSF1010, kanamycin resistance gene *kmr*, promoter *j5*, cumate operators, *cymR* gene coding for cumate repressor and gene coding for TA

Expression of the constructs in *E. coli* TOP10 showed significant expression of transaminase and of three of imine reductases, PotRiRED, R-IRED and S-IRES (Fig. 67 and 68). However, no protein was found for imine reductase PotSIREd and for alanine dehydrogenases (Fig. 67 and 68).

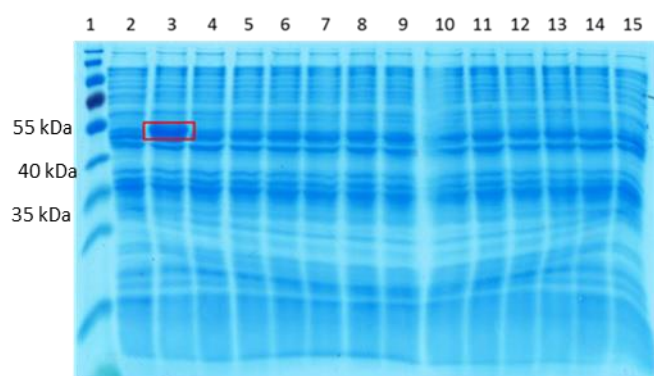


Figure 67. SDS-PAGE of whole cell lysates from *E. coli* TOP10 fermentation of the respective enzymes. Expected size for transaminase (TA) is 53 kDa, for alanine dehydrogenase (AlaDH) – 40 kDa, for his-tagged alanine dehydrogenase (HisAlaDH) – 41 kDa. Expressed transaminase is indicated in red box. Lane 1: PageRuler™ Prestained protein ladder; lane 2: *E. coli* TOP10 [pKRSF1010-P_{j5}-TA-cymR], non-induced; lane 3: *E. coli* TOP10 [pKRSF1010-P_{j5}-TA-cymR], induced; lane 4: *E. coli* TOP10 [pKRSF1010-P_{j5}-cyOO-AlaDH-cymR], clone 1, non-induced; lane 5: *E. coli* TOP10 [pKRSF1010-P_{j5}-cyOO-AlaDH-cymR], clone 1, induced; lane 6: *E. coli* TOP10 [pKRSF1010-P_{j5}-cyOO-AlaDH-cymR], clone 2, non-induced; lane 7: *E. coli* TOP10 [pKRSF1010-P_{j5}-cyOO-AlaDH-cymR], clone 2, induced; lane 8: *E. coli* TOP10 [pKRSF1010-P_{j5}-cyOO-AlaDH-cymR], clone 3, non-induced; lane 9: *E. coli* TOP10 [pKRSF1010-P_{j5}-cyOO-AlaDH-cymR], clone 3, induced; lane 10: *E. coli* TOP10 [pKRSF1010-P_{j5}-HisAlaDH-cymR], clone 1, non-induced; lane 11: *E. coli* TOP10 [pKRSF1010-P_{j5}-HisAlaDH-cymR], clone 1, induced; lane 12: *E. coli* TOP10 [pKRSF1010-P_{j5}-HisAlaDH-cymR], clone 2, non-induced; lane 13: *E. coli* TOP10 [pKRSF1010-P_{j5}-HisAlaDH-cymR], clone 2, induced; lane 14: *E. coli* TOP10 [pKRSF1010-P_{j5}-HisAlaDH-cymR], clone 3, non-induced; lane 15: *E. coli* TOP10 [pKRSF1010-P_{j5}-HisAlaDH-cymR], clone 3, induced

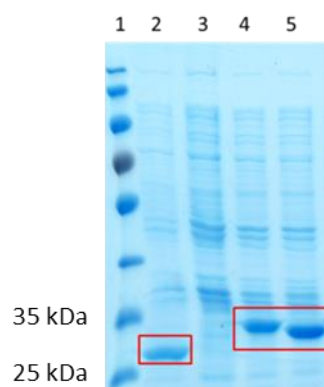


Figure 68. SDS-PAGE of whole cell lysates from *E. coli* TOP10 fermentation of imine reductases. Expected size for imine reductases PotRIRED, PotSIREd, R-IREd and S-IREd are 29.9 kDa, 30.8 kDa, 31.1 kDa and 30.9 kDa, respectively. Expressed imine reductases are indicated in red boxes. Lane 1: PageRuler™ Prestained protein ladder; lane 2: *E. coli* TOP10 [pKRSF1010-P_{j5}-PotRIRED-cymR], induced; lanes 3: *E. coli* TOP10 [pKRSF1010-P_{j5}-PotSIREd-cymR], induced; lane 4: *E. coli* TOP10 [pKRSF1010-P_{j5}-cyOO-R-IREd-cymR], induced; lane 5: *E. coli* TOP10 [pKRSF1010-P_{j5}-cyOO-S-IREd-cymR], induced

All the constructs were further transferred into *R. eutropha* H16 and expression experiments were performed. However, neither putative alanine dehydrogenase from *R. eutropha* H16 nor other

two enzymes, alanine dehydrogenase from *B. subtilis* and Pot-SIRED imine reductase, could be detected in crude cell lysate (for example, Fig. 69). Since the level of protein expression could be too low to be clearly seen on the SDS gel, his-tagged version of AlaDH originating from *B. subtilis* was expressed in *R. eutropha* H16 and purified on Ni-sepharose column. As a result, no protein could be found in the elution fraction. Consequently, it could be concluded that these 3 enzymes are not expressed under the tested conditions. In contrast, expression of transaminase (Fig. 69) and three imine reductases was clearly seen on the SDS-PAGE.

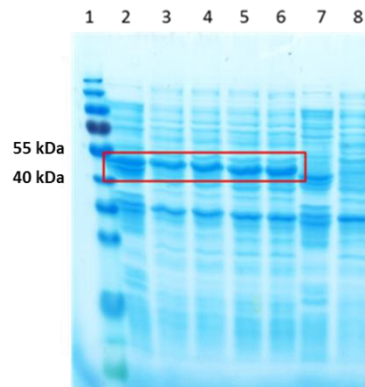


Figure 69. SDS-PAGE of whole cell lysates from *R. eutropha* H16 fermentation of the respective enzymes. Expected size for transaminase (TA) is 53 kDa, for his-tagged alanine dehydrogenase (HisAlaDH) – 41 kDa. Expressed transaminase is indicated in red box. Lane 1: PageRuler™ Prestained protein ladder; lane 2: *E. coli* TOP10 [pKRSF1010-P_{J5}-TA-cymR], induced; lanes 3-6: *R. eutropha* H16 [pKRSF1010-P_{J5}-TA-cymR], clones 1-4, induced; lane 7: *E. coli* TOP10 [pKRSF1010-P_{J5}-HisAlaDH-cymR], induced; lane 8: *R. eutropha* H16 [pKRSF1010-P_{J5}-HisAlaDH-cymR], induced

The enzymes of interest which were shown to be expressed in *R. eutropha* H16 were further expressed under lithoautotrophic conditions and the expression was visualized with SDS-PAGE (Fig. 70 and 71). The lithoautotrophically and heterotrophically grown cell cultures, including negative control, strain *R. eutropha* H16 [pKRSF1010-P_{tac}-Δinsert], were collected and handed over to the members of Prof. Kroutil's group for further analysis.

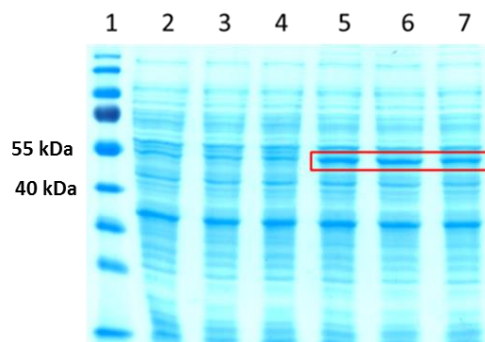


Figure 70. SDS-PAGE of whole cell lysates from *R. eutropha* H16 fermentation of transaminase under lithoautotrophic growth conditions. Expected size for transaminase is 53 kDa. Expressed

3.3. Cloning and expression of bacterial transaminase, alanine dehydrogenases and imine reductases in *R. eutropha* H16

transaminase is indicated in red box. Lane 1: PageRuler™ Prestained protein ladder; lanes 2-4: control, *R. eutropha* H16 [pKRSF1010-P_{tac}-Δinsert], clones 1-3; lanes 5-7: *R. eutropha* H16 [pKRSF1010-P_{j5}-TA-cymR], clones 1-3, induced

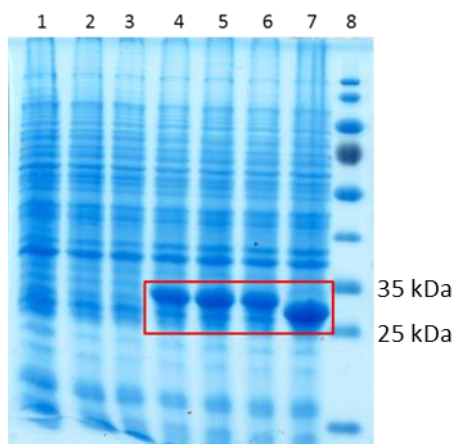


Figure 71. SDS-PAGE of whole cell lysates from *R. eutropha* H16 fermentation of transaminase under lithoautotrophic growth conditions. Expected size for imine reductase R-IRED is 31.1 kDa and for imine reductase S-IRED is 30.9 kDa. Expressed imine reductases are indicated in red box. Lane 1-3: control, *R. eutropha* H16 [pKRSF1010-P_{tac}-Δinsert], clones 1-3; lanes 4-6: *R. eutropha* H16 [pKRSF1010-P_{j5}-cyOO-R-IRED-cymR], clones 1-3, induced; lane 7: *R. eutropha* H16 [pKRSF1010-P_{j5}-cyOO-S-IRED-cymR], clones 1, induced; lane 8: PageRuler™ Prestained protein ladder;

The preliminary results of the enzyme activity tests, performed by the members of Prof. Kroutil's group with lyophilized cells, revealed activity of overexpressed transaminase from *Arthrobacter sp.* (improved variant, W. Kroutil), both in heterotrophically and lithoautotrophically grown cells. Additionally, alanine dehydrogenase activity was detected in the cells with overexpressed transaminase, indicating the presence of functional alanine dehydrogenase in *R. eutropha* H16. Interestingly, the cells of heterotrophically grown culture, although not grown under lithoautotrophic conditions, showed to some extent NAD(P)H recovering activity.

It was also shown by the members of W. Kroutil's group that the imine reductases were also expressed in their active form as the reduction reactions with the glucose/GDH cofactor regeneration system, as well as under H₂ atmosphere in the absence of any additional regeneration system, were successfully carried out. The H₂-driven reactions were shown to be not as fast as the GDH-driven ones but still proceed at a reasonable rate.

4. Contribution to the manuscript on the design of inducible expression systems for protein expression in *Ralstonia eutropha* H16

Design of inducible expression systems for improved protein production in *Ralstonia eutropha* H16

Steffen Gruber, Daniel Schwendenwein, Zalina Magomedova, Eva Thaler, Jeremias Hagen, Helmut Schwab, Petra Heidinger

Institute of Molecular Biotechnology, Graz University of Technology, NAWI Graz, Petersgasse 14, 8010 Graz

Corresponding author:

Dr. Petra Heidinger

Institute of Molecular Biotechnology, Graz University of Technology, NAWI Graz

Petersgasse 14 / 1

A-8010 Graz

Austria

Tel.: +43 316 873 4086

Fax: +43 316 873 4071

E-Mail: petra.heidinger@tugraz.at

4. Contribution to the manuscript on the design of inducible expression systems for protein expression in *R. eutropha* H16

Abstract

Ralstonia eutropha H16 (*Cupriavidus necator* H16) is a Gram-negative, facultative chemolithoautotrophic bacterium which can use H₂ and CO₂ as sole sources of energy and carbon in the absence of organic substrates. The biotechnological use of *R. eutropha* H16 on a large industrial scale has already been established. However, one major problem encountered so far was the lack of inducible expression systems that allow for tunable expression under large scale conditions and do not require an adaptation of/specific growth conditions for induction. Within this study two inducible expression systems were designed on the basis of the strong j5 promoter derived from bacteriophage T5, in combination with the *E.coli lacI* and the *Pseudomonas putida* cumate regulatory elements. Both described systems display the desired regulatory features and further increase the number of suitable inducible expression systems for the production of metabolites and proteins in *R. eutropha* H16.

Keywords: *Ralstonia eutropha* H16; Inducible expression system; Cumate, IPTG, Recombinase

4. Contribution to the manuscript on the design of inducible expression systems for protein expression in *R. eutropha* H16

1. Introduction

Ralstonia eutropha H16 (now named *Cupriavidus necator* H16) is a facultative chemolithoautotrophic, soil-dwelling Gram-negative bacterium. The multi-replicon genome of *R. eutropha* H16 has a total size of 7,416,678 bp and consists of two chromosomes as well as a megaplasmid (pHG1) (Pohlmann et al., 2006). A versatile set of genes for energy and carbon metabolism is encoded within the genome of *R. eutropha* H16, which enables growth under heterotrophic, lithoautotrophic or organoautotrophic conditions (Cramm, 2009). Accordingly, a diversity of growth substrates are accepted by this bacterium including a number of organic acids such as acetic acid and sugars like fructose under heterotrophic growth conditions; which are metabolized via the Entner–Doudoroff (ED) pathway and the tricarboxylic acid (TCA) cycle (Cramm, 2009)(Pohlmann et al., 2006). Moreover, CO₂ and H₂ can serve as the sole carbon and energy sources under lithoautotrophic growth conditions, respectively. In this case CO₂ is fixed via the Calvin-Benson-Bassham (CBB) cycle and H₂ oxidized by [NiFe]-hydrogenases (Bowien and Kusian, 2002). In a similar way *R. eutropha* H16 is also capable of growing organoautotrophically by splitting formic acid into CO₂ and NADH with the help of a membrane-bound formate dehydrogenase, which allows the bacterium to directly utilize NADH and fix the released CO₂ via the CBB cycle (Cramm, 2009)(Grunwald et al., 2015). Based on this great diversity of accepted energy and carbon sources as well as the ability of *R. eutropha* H16 to synthesize large amounts of the biodegradable polymer polyhydroxybutyrate (PHB), widespread biotechnological interest in this bacterium has been developed (Atlić et al., 2011)(Ewering et al., 2006).

Especially the application of *R. eutropha* H16 as a production host for PHB is well-established with fermentation processes on a large industrial scale (Kessler et al., 2001). However, the utilization of *R. eutropha* H16 as a production host is not limited to the synthesis of PHB or derivatives thereof. The ability of the organism to grow to high-cell-densities under lithoautotrophic or heterotrophic conditions further promotes the biotechnological application of *R. eutropha* H16 for the production of metabolites and proteins (Barnard et al., 2004)(Lütte et al., 2012). Unlike *Escherichia coli*, *R. eutropha* H16 can be cultivated in high-cell-density fermentations without accumulating growth inhibiting organic acids. This offers great advantages with respect to the fermentation process including higher product concentrations, increased productivity and improved operating costs (Chen et al., 1992)(Andersson et al., 1994). Large scale high-cell-density fermentation processes employing *R. eutropha* H16 yielded cell densities up to 230 g/l dry weight and high amounts of the target protein (Ryu et al., 1997) (Barnard et al., 2004). In addition to these features, the protein folding capacities of *R. eutropha* H16 enable the production of properly folded proteins under stress conditions with no significant inclusion body formation (Srinivasan et al., 2002)(Gruber et al., 2014). In order to fully take advantage of the natural capabilities of *R. eutropha* H16 in biotechnological processes, natural features need to be refined or others newly established in the organism. One simple and efficient way to introduce such functions is provided by the use of expression plasmids.

The design of stable expression plasmids anticipated for the use in *R. eutropha* H16 requires adapted features related to gene expression, plasmid replication, plasmid stability and segregation (Gruber et al., 2015). The use of replication elements derived from broad-host-range plasmids such as RSF1010, RP4, pBBR1, pSa and the megaplasmid pMOL28 from *Ralstonia metallidurans* CH43 for instance promote successful replication of expression plasmids at different copy numbers in *R. eutropha* H16 (Ditta et al., 1985)(Gruber et al., 2014)(Kovach et al., 1995)(Sato et al., 2013). However, in order to prevent significant plasmid loss during the cultivation of *R. eutropha* H16, which occurs at a significant rate despite the use of antibiotic selection, systems promoting plasmid stability and maintenance need to be implemented. The use of plasmid multimer resolution, plasmid partitioning and toxin/antidote addiction systems or the complementation of essential metabolic functions in auxotrophic strains resulted in significant improvement of plasmid retention rates (Sato et al., 2013)(Gruber et al., 2014)(Voss and Steinbüchel, 2006)(Budde et al., 2011).

A number of functionally active promoters and inducible expression systems were identified to efficiently control the expression of the particular gene of interest in *R. eutropha* H16. This includes heterologous promoters such as P_{lac} , P_{lacUV5} , P_{tac} , P_{BAD} , P_{T5} and P_{T7} as well as numerous native promoters derived from operons involved in pyruvate metabolism, PHB biosynthesis, acetoin metabolism and the *cbb* operon. In addition, a set of promoters derived from the genome of the bacteriophage T5 was shown to be highly active in *R. eutropha* H16 (Bi et al., 2013)(Fukui et al., 2011)(Barnard et al., 2005)(Gruber et al., 2014)(Delamarre and Batt, 2006). Several of these promoters were also used in combination with regulatory elements as inducible expression systems in *R. eutropha* H16. Among these are heterologous expression systems based on the particular operator sites and repressor proteins including the TetR repressor responding to the inducer anhydrotetracycline (ATc) (Li and Liao, 2015), the AraC repressor and the inducer L-arabinose, the LacI repressor and inducer IPTG dependent on an integrated lactose permease (LacY) function and the inducible expression system based on the XylS repressor and the inducer m-toluic acid (Bi et al., 2013). Furthermore, a number of homologous inducible expression systems were characterized for the use in *R. eutropha* H16 on the basis of the *cbbL* promoter, which is induced under lithoautotrophic growth conditions (Lütte et al., 2012) and the *phaP* promoter, which is induced by phosphate depletion (Srinivasan et al., 2002). However, only a small number of inducible expression systems did function in a satisfactory manner or are applicable for large scale fermentation processes with *R. eutropha* H16 under a broad range of growth conditions. The inducible expression systems based on the *cbbL* and *phaP* promoters for example require specific adaptations of the fermentation process in order to create inducing conditions, which constraints their use to fermentation processes that account for phosphate depletion or are performed under lithoautotrophic conditions (Srinivasan et al., 2002)(Lütte et al., 2012). The use of TetR-based expression systems proved to show valuable induction features. Nonetheless, the use of tetracycline inducers in large scale fermentation processes is not feasible due to the antibiotic nature of the inducers (Li and Liao, 2015). The widely used LacI-based expression system was shown to work in *R. eutropha* H16 on the basis of an incorporated lactose permease (LacY) function. However, even though IPTG could be transported across the cellular membranes full

4. Contribution to the manuscript on the design of inducible expression systems for protein expression in *R. eutropha* H16

induction of the applied promoter could not be obtained with this system so far (Bi et al., 2013). In comparison, tightly regulated and highly tunable expression could be achieved by inducible expression systems based on the regulatory elements of the p-cumate (4-isopropylbenzoic acid) degrading operon derived from *Pseudomonas putida* F1. Moreover, the cumate inducible expression systems were found to function efficiently and reliably in a number of microorganism and human cell lines relying on passive transport of the non-toxic and comparatively cheap inducer p-cumate (Mullick et al., 2006)(Kaczmarczyk et al., 2013)(Choi et al., 2010). Accordingly, a cumate-induced expression system was designed for the use in *R. eutropha* H16 in this study.

The aim of this study was to extend and improve the range of inducible expression systems for the biotechnological application in *R. eutropha* H16. A total of two inducible expression systems were designed on the basis of the j5 promoter in combination with the lac and cumate regulatory elements. Both systems exhibit desired regulatory features and increase the number of suitable inducible expression systems for the production of metabolites and proteins in *R. eutropha* H16.

2. Materials and Methods

2.1 Strains, plasmids and primers

All strains and plasmids used in this study are listed in tables 1 and 2. Primers used for PCR amplifications are summarized in table S1 (supplementary data).

2.2 Cultivation of *E. coli* and *R. eutropha* H16 strains

E. coli S17-1 cells were cultivated at 37°C on lysogeny broth (LB) media with kanamycin [40 µg/ml]. *R. eutropha* H16 cells were cultivated at 28°C using nutrient broth (NB) or tryptic soy broth (TSB) media supplemented with gentamicin [20 µg/ml], chloramphenicol [100 µg/ml] or kanamycin [200 µg/ml] and 0.6% or 2% fructose according to application. All basic media components were purchased from Sigma-Aldrich (St. Louis, MO, USA), Carl Roth (Arlésheim, Germany) and Becton Dickinson and Company (Franklin Lakes, NJ, USA).

2.3 DNA preparation

Standard procedures were used for PCR, DNA preparation and manipulation as well as genomic DNA isolation (Sambrook and Russel, 2001). Restriction enzymes, Fast DNA End Repair Kit, Phusion[®] Polymerase and GeneJET Plasmid Miniprep Kits by Thermo Scientific (Waltham, MA, USA), T4 DNA Ligation reaction mixtures and Wizard[®] SV **Gel** and PCR **Clean-Up** System by Promega (**Madison, WI, USA**) and Easy-DNA[™] Kit by Invitrogen (Carlsbad, California, USA) were used according to the manufacturer's protocols.

2.4 Plasmid construction

The plasmids pKRL-P_{J5}-egfp and pKRC-P_{J5}-egfp were constructed on the basis of the pKRSF1010-P_{tac}-egfp backbone (Gruber et al., 2014). Primers Pj5-laco-fwd1, Pj5-cyO-fwd-1 and KanR-Spel-rev were used to amplify *egfp*, *rrnB* and Km^r from pKRSF1010-P_{tac}-egfp. Two subsequent PCR runs were performed with forward primers Pj5-lacO-fwd-2, Pj5-lacO-NotI-fwd-3 or Pj5-cyO-fwd-2, Pj5-cyO-NotI-fwd-3 and the reverse primer KanR-Spel-rev to add the particular *lacO* or cumate operator sequences along with P_{J5} to the previously amplified PCR product. The completed PCR product and pKRSF1010-P_{tac}-egfp were restricted with *NotI/Spel* and combined by ligation. Co-expression cassettes containing *cymR* and *lacI* were constructed by overlap extension PCR of DNA fragments coding for the constitutive promoter of the chloramphenicol resistance marker *P_{Cmr}*, *cymR* or *lacI* and a T7 terminator sequence. *P_{Cmr}* was amplified with primer CymR-P-fwd-Spel and CymR-P-oe from the pSa plasmid, 4. Contribution to the manuscript on the design of inducible expression systems for protein expression in *R. eutropha* H16

cymR was amplified from the genomic DNA of *Pseudomonas Putida* F1 with primers CymR-gen-fwd-oe, CymR-gen-T7tt-rev-1 and CymR-gen-T7tt-rev-2-SpeI, *lacI* was amplified with primers LacI-SpeI-fwd and LacI-SpeI-rev from pMS470Δ8 and the T7 promoter sequence was encoded on the primers. Depending on application the overexpression cassettes were cloned into the particular plasmids via SpeI restriction sites to yield pKRL-P_{j5}-egfp and pKRC-P_{j5}-egfp. The plasmid pKRC-P_{j5}-estA was created by combining the backbone of pKRC-P_{j5}-egfp restricted with XbaI/ClaI and *estA* cut XbaI/ClaI. *EstA* was derived from pKRSF1010-P_{tac}-Ru1 (Gruber et al., 2014). A description of plasmid design used for the construction of *R. eutropha* RS1 is attached in the supplementary data.

2.5 Plasmid transfer

Plasmids were transformed into *E. coli* cells using standard electroporation protocols (Sambrook and Russel, 2001). *E. coli* S17-1 transformants were used as a donor strain to transfer plasmids to *R. eutropha* H16 by conjugation (Srivastava et al., 1982). Conjugation was performed according to the protocol of Simon et al. (1983). The cell suspensions were plated out on TSB gentamicin [20 µg/ml] and kanamycin [200 µg/ml] or gentamicin [20 µg/ml] and chloramphenicol [100 µg/ml] agar plates for selection of *R. eutropha* H16 transconjugants.

2.6 Strain construction

R. eutropha RS1 was constructed by integration of the expression cassette $P_{H16_B1772}lacY_{Cm}^r$ at the *phaC* locus followed by recycling the Cm^r marker. Therefore the plasmid plnt_{lacY_phaC_loxP} was transferred to *R. eutropha* H16 by conjugation. After integration at the *phaC* locus the excision of the resistance marker by the Cre-loxP system was induced with p-cumate in the integration strain *R. eutropha* H16 Δ*phaC*Ω*P*_{H16_B1772}*lacY**Cm*^r. This was accomplished by selection on TSB gentamicin [20 µg/ml] and p-cumate [20 µg/ml] agar plates following transfer by conjugation from *E. coli* S-17 carrying the plasmid containing the Cre recombinase (pCm-Cre).

2.7 Fluorescence unit measurement

ONCs of *R. eutropha* H16 transconjugants were grown in liquid TSB kanamycin [200 µg/ml] media and used to inoculate TSB media to an OD₆₀₀ of 0.2. The cultures were grown to an OD₆₀₀ of approximately 0.8 when they were induced with 30 µM, 60 µM or 120 µM p-cumate and 0.01 mM, 0.1 mM or 1 mM IPTG. Afterwards samples were taken every 2 hours and eGFP expression levels were determined based on fluorescence unit measurements with FLUOstar Omega (BMG Labtech, Ortenberg, Germany) at excitation wavelength of 480 nm and emission wavelength of 510 nm. Fluorescence units (FU) were determined for *R. eutropha* H16 transconjugants and related to the

OD₆₀₀ values of the culture to obtain the relative fluorescence units (RFU). In either case the RFU values of all samples were related to *R. eutropha* H16 (pKRSF1010Δegfp), which served as negative control.

2.8 SDS-PAGE and Western Blot analysis

Sodium dodecyl sulfate polyacrylamide gel electrophoresis (SDS-PAGE) was performed with 4–12% NuPAGE[®] Bis-Tris Gel (Invitrogen) to separate proteins of the whole cell extract. In each case 10 µg of total protein or 0.2 OD₆₀₀ units were added per lane. Transfer of proteins to a Roti-NC HP40.1, 0.2 µm nitrocellulose membrane (Carl Roth) was accomplished with the TE22 Mini Transfer Tank Unit (Hoefer Inc., Holliston, MA, USA) according to manufacturer's recommendations. A primary mouse antibody (Monoclonal anti GFP, G6795; Sigma-Aldrich) and a horseradish peroxidase linked secondary goat-anti-mouse antibody (Sigma-Aldrich) were used for eGFP detection on a nitrocellulose membrane. A primary rabbit antibody (Monoclonal anti HIS; D3I10; NEB) and a horseradish peroxidase linked secondary anti-rabbit antibody (NEB) were used for HIS detection on a nitrocellulose membrane. Proteins were visualized using SuperSignal (Pierce, Rockford, USA).

3. Results and Discussion

3.1 Setup of *lacI* and *cymR* based inducible expression systems

Several promoter sequences derived from the bacteriophage T5 were previously shown to be highly active in *R. eutropha* H16 (Gruber et al., 2014). Out of these, the j5 promoter was selected for the characterization of the IPTG and cumate-induced expression systems in *R. eutropha* H16. An experimental set-up was chosen on the basis of a pKRSF1010 backbone in which the j5 promoter was used to drive the expression of the reporter genes *egfp* or *estA*. The pKRSF1010 vector backbone encodes next to the RSF1010 *oriV* and *mob* sequences, a RP4 partitioning system, which includes a site specific recombination system and a toxin/antitoxin system in order to significantly increase plasmid stability and propagation in *R. eutropha* H16. All regulatory and functional elements of the IPTG or cumate-induced expression cassettes were organized identically: P_{j5} , followed by the particular operator sites, a Shine-Dalgarno sequence and the genes to be expressed (*egfp* or *estA* in this study) (Figure 1). The expression cassettes containing the repressor genes *lacI* and *cymR* were included in the particular pKRSF1010 backbone. Both repressor genes were expressed from a weak constitutive promoter, P_{cmr} derived from the chloramphenicol resistance gene of the pSa plasmid.

4. Contribution to the manuscript on the design of inducible expression systems for protein expression in *R. eutropha* H16

3.2 Construction of the *lacY* containing *R. eutropha* strain RS1

In order to enable the use of the IPTG-induced expression system in *R. eutropha* H16 an IPTG transport function had to be integrated additionally, since this kind of transport cannot be accomplished naturally. Therefore, the *E. coli* derived lactose permease gene (*lacY*; JF300162.1) was engineered to be under the control of the constitutive H16_B1772 promoter derived from *R. eutropha* H16. The expression cassette containing *lacY* was integrated into the *phaC* (*H16_A1437*) locus on chromosome 1 of *R. eutropha* H16 and the chloramphenicol resistance marker was subsequently removed by the Cre-loxP system to obtain *R. eutropha* RS1. Unlike previously reported for a similar IPTG-induced expression system that was designed for an application in *R. eutropha* H16 (Bi et al., 2013), the integrated lactose permease function in the current study did enable sufficient IPTG transport across the cells' membranes and triggered the induction of the *j5* promoter completely.

3.3 Characterization of the *lacI* based inducible expression system

Characterization of the IPTG-induced expression system was performed on the basis of *R. eutropha* RS1 (pKRL-P_{j5}-egfp) and RFU were determined to monitor the expression of *egfp* over a time period of nine hours and at 24 hours after induction. Furthermore, protein expression data were obtained on basis of SDS-PAGE and Western Blot analysis. *R. eutropha* RS1 (pKRL-P_{j5}-egfp) cultures were induced 3 hours after inoculation at an OD₆₀₀ of approximately 0.8 with 0.01 mM, 0.1 mM or 1 mM of IPTG. *R. eutropha* RS1 (pKRL-P_{j5}-egfp) cultures induced with a concentration of 0.01 mM IPTG exhibited increasing fluorescence values from 2500 RFU to 5500 RFU at 2 hours and 6 hours after induction, respectively. After 24 hours the measured fluorescence had increased to 20000 RFU. A tenfold increased induction concentration of 0.1 mM IPTG resulted in 4500 RFU after 2 hours, 11000 RFU after 6 hours and 33000 RFU after 24 hours. Accordingly, an IPTG induction concentration of 1 mM triggered strong eGFP expression, corresponding to 5200 RFU, 13000 RFU and 36000 RFU after 2, 6 and 24 hours after induction, respectively. Moreover, the RFU values obtained for the uninduced cultures of *R. eutropha* RS1 (pKRL-P_{j5}-egfp) did also increase steadily over time, from 600 RFU after 3 hours to 1500 RFU after 9 hours and 5500 RFU at 24 hours after inoculation. The obtained RFU values and eGFP expression data (see Figures 2A and S2) for the uninduced *R. eutropha* RS1 (pKRL-P_{j5}-egfp) cultures, revealing significant eGFP expression, do most likely result from remaining activity of the comparatively strong *j5* promoter. This does presumably result from the weak interactions of the LacI repressor protein and the lac operator DNA sequence (Penumetcha et al., 2010), which allows for leaky eGFP expression in significant amounts in uninduced *R. eutropha* RS1 (pKRL-P_{j5}-egfp) cultures, despite the use of two consecutive lac operator sequences. In induced cultures of *R. eutropha* RS1 (pKRL-P_{j5}-egfp) the rapid and strong induction of eGFP expression in response to IPTG did significantly decrease the growth of the culture (see Figure 2). Generally, higher concentrations of the

inducer IPTG resulted in enhanced eGFP formation and strongly decreased culture growth; however, the level of eGFP production did not directly correlate with the amount of IPTG applied. A stepwise increase in inducer concentration by a factor of ten from 0.01 mM IPTG to 0.1 mM IPTG to 1 mM IPTG did yield RFU values of 5500 RFU, 11000 RFU and 12600 RFU after 6 hours of induction, respectively. The minor increase observed in RFU values for the cultures induced with 0.1 mM IPTG and 1 mM IPTG could result either from a limitation in the IPTG transport capacity of the lactose permease or fully induced *j5* promoter activity that is already reached at an inducer concentration of approximately 0.1 mM IPTG. Consequently, a tenfold increase in IPTG inducer concentration does not cause any significant increase in eGFP expression levels.

Nevertheless, a large amount of eGFP was produced in *R. eutropha* RS1 (pKRL-P_{j5}-egfp) in a short amount of time despite the significant decline of growth in the induced cultures. Moreover, the high level of eGFP expression was maintained for at least 24 hours in all induced cultures at a low growth rate (see Figure 2 and S2). Results of previous studies examining the induction pattern of IPTG-induced expression systems on the basis of *E. coli* cultures in flow-cytometry experiments revealed great differences in the strength of induced expression levels of individual cells across the entire culture (Choi et al., 2010). An unequal distribution of the inducer IPTG due to the active transport across the cells' membranes resulted in very heterologously occurring IPTG-based expression across the population. Moreover, in a significant number of cells expression was highly induced and caused cell lysis (Choi et al., 2010).

3.4 Characterization of the *cymR* based inducible expression system

In comparison to the IPTG-induced expression system, the cumate-induced expression system does not require active transport of the inducer p-cumate. The inducer diffuses through the membrane and triggers a smooth and steady expression of the gene of interest across the entire culture (Choi et al., 2010). The characterization of the cumate-induced expression system was performed on the basis of *R. eutropha* H16 (pKRC-P_{j5}-egfp). In accordance with the measurements performed for the IPTG-induced expression system, cumate-induced *egfp* expression was observed over a time period of nine hours and 24 hours after induction (see Figure 3A and S1). EGFP expression was induced in *R. eutropha* H16 (pKRC-P_{j5}-egfp) cultures with 30 μ M, 60 μ M or 120 μ M p-cumate 3 hours after inoculation at an OD₆₀₀ of approximately 0.8. A concentration of 120 μ M p-cumate was found to be sufficient to induce maximum expression. The induction of eGFP expression in *R. eutropha* H16 (pKRC-P_{j5}-egfp) cultures with a concentration of 20 μ M p-cumate did increase fluorescence values from 500 RFU at 2 hours to 1600 RFU at 6 hours and 19000 RFU at 24 hours after induction. Induction with a concentration of 60 μ M p-cumate resulted in fluorescence units of 800 RFU after 2 hours, 2200 RFU after 6 hours and 21000 RFU after 24 hours. An induction concentration of 120 μ M triggered steady eGFP expression from 1100 RFU, 2700 RFU and 21000 RFU after 2, 6 and 24 hours, respectively. The RFU values obtained for the uninduced *R. eutropha* H16 (pKRC-P_{j5}-egfp) cultures

on the other hand did increase slightly from 230 RFU after 2 hours to 650 RFU after 24 hours. The induction of *egfp* expression with different concentrations of p-cumate did strongly depend on the amount of inducer applied and enabled highly tunable expression characteristics. Moreover, the induction of expression did not occur as quick and intense as seen for the IPTG-induced expression system, but increased slowly and steadily over time. This is most likely a result of the diffusion process of the inducer through the membranes of *R. eutropha* H16 and appears to be significantly slower in comparison to other bacteria such as *E. coli* (Choi et al., 2010). However, the slow uptake of p-cumate by *R. eutropha* H16 enabled continuous cell growth at a higher rate that yielded OD₆₀₀ values of approximately 19 after 24 hours for all cumate-induced cultures (see Figure 3B). In comparison, the IPTG-induced cultures grew slowly to approximately a third of the cell density, however, yielding eGFP expression in a comparable range after 24 hours (see Figure S3). Furthermore, the cumate-induced expression system was strongly repressed and remaining promoter activity was determined to be 650 RFU after 24 hours in comparison to 5500 RFU that were obtained for the IPTG-induced expression system after the same time (see Figure 2, 3 and S3). The tight regulation of eGFP expression is most likely based on the strong interaction of the cumate repressor and operator sequences, which do not allow for significant promoter activity in an uninduced state (Choi et al., 2010)(Kaczmarczyk et al., 2013). Furthermore, p-cumate is a significantly cheaper inducer compared to IPTG which is an essential factor in large scale fermentations.

3.5. Production of esterase EstA in *R. eutropha* H16

Esterase EstA derived from *R. ruber* was used as a model protein for analyzing the capacity of the inducible expression systems in *R. eutropha* H16. Since expression plasmids containing constitutive expression cassettes based on the j5 promoter and *estA* could not be assembled, most likely due to significant stress of constitutive expression, the *estA* gene was cloned into the IPTG- and cumate-based inducible expression systems to obtain plasmids pKRC-P_{j5}-*estA* and pKRL-P_{j5}-*estA*. However, after induction with different concentrations of IPTG, EstA activity or protein could not be detected anymore in *R. eutropha* RS1 (pKRL-P_{j5}-*estA*) cultures. Sequencing of pKRL-P_{j5}-*estA* plasmids obtained after induction from the cultures did reveal deletion or insertion events in the promoter region, Shine-Dalgarno sequence or the N-terminal region of *estA* (data not shown). These events did most likely cause an arrest of *estA* expression in response to significant stress due to the rapid and strong induction by the IPTG-induced expression system. Unlike the extensively engineered *E. coli* strains, with respect to knocked-out recombinase A or deleted transposon functions, the wild-type strain *R. eutropha* H16 used in this experimental setup does most likely still contain a number of such functions. On the contrary, the induction of expression in *R. eutropha* H16 (pKRC-P_{j5}-*estA*) with 120 μM p-cumate resulted in the formation of significant amounts of active EstA over a time period of 24 hours indicating that an induction occurring slowly and steadily over time maybe beneficial for the expression of more complex proteins (see Figure 4). Accordingly, the tightly regulated cumate expression system

represents a valuable alternative regarding the expression of complex or even toxic proteins in *R. eutropha* H16.

4. Authors' Contributions

SG, PH, HS planned and started the project. Wet laboratory work was carried out by SG, JH, ZM, ET and PH. SG and PH wrote the manuscript. All authors read, corrected and approved the final version

Acknowledgment

The authors gratefully acknowledge support from NAWI Graz.

5. References

- Andersson, L., Strandberg, L., Haggstrom, L., Enfors, S.-O., 1994. Modeling of high cell density fed batch cultivation. *FEMS Microbiol. Rev.* 14, 39–44. doi:10.1111/j.1574-6976.1994.tb00070.x
- Atlić, A., Koller, M., Scherzer, D., Kutschera, C., Grillo-Fernandes, E., Horvat, P., Chiellini, E., Braunegg, G., 2011. Continuous production of poly([R]-3-hydroxybutyrate) by *Cupriavidus necator* in a multistage bioreactor cascade. *Appl. Microbiol. Biotechnol.* 91, 295–304. doi:10.1007/s00253-011-3260-0
- Balzer, D., Ziegelin, G., Pansegrau, W., Kruff, V., Lanka, E., 1992. KorB protein of promiscuous plasmid RP4 recognizes inverted sequence repetitions in regions essential for conjugative plasmid transfer 20, 1851–1858.
- Barnard, G.C., Henderson, G.E., Srinivasan, S., Gerngross, T.U., 2004. High level recombinant protein expression in *Ralstonia eutropha* using T7 RNA polymerase based amplification. *Protein Expr. Purif.* 38, 264–71. doi:10.1016/j.pep.2004.09.001
- Barnard, G.C., Mccool, J.D., Wood, D.W., Gerngross, T.U., 2005. Integrated Recombinant Protein Expression and Purification Platform Based on *Ralstonia eutropha* 71, 5735–5742. doi:10.1128/AEM.71.10.5735
- Bi, C., Su, P., Müller, J., Yeh, Y.-C., Chhabra, S.R., Beller, H.R., Singer, S.W., Hillson, N.J., 2013. Development of a broad-host synthetic biology toolbox for *Ralstonia eutropha* and its application to engineering hydrocarbon biofuel production. *Microb. Cell Fact.* 12, 107. doi:10.1186/1475-2859-12-107
- Bowien, B., Kusian, B., 2002. Genetics and control of CO₂ assimilation in the chemoautotroph *Ralstonia eutropha*. *Arch. Microbiol.* 178, 85–93. doi:10.1007/s00203-002-0441-3
- Budde, C.F., Riedel, S.L., Willis, L.B., Rha, C., Sinskey, A.J., 2011. Production of poly(3-hydroxybutyrate-co-3-hydroxyhexanoate) from plant oil by engineered *Ralstonia eutropha* strains. *Appl. Environ. Microbiol.* 77, 2847–54. doi:10.1128/AEM.02429-10
- Chen, H.C., Hwang, C.F., Mou, D.G., 1992. High-density *Escherichia coli* cultivation process for hyperexpression of recombinant porcine growth hormone. *Enzyme Microb. Technol.* 14, 321–6.
- Choi, Y.J., Morel, L., Le François, T., Bourque, D., Bourget, L., Groleau, D., Massie, B., Míguez, C.B., 2010. Novel, versatile, and tightly regulated expression system for *Escherichia coli* strains. *Appl. Environ. Microbiol.* 76, 5058–66. doi:10.1128/AEM.00413-10
- Cramm, R., 2009. Genomic view of energy metabolism in *Ralstonia eutropha* H16. *J. Mol. Microbiol. Biotechnol.* 16, 38–52. doi:10.1159/000142893
- Delamarre, S.C., Batt, C.A., 2006. Comparative study of promoters for the production of polyhydroxyalkanoates in recombinant strains of *Wautersia eutropha*. *Appl. Microbiol. Biotechnol.* 71, 668–79. doi:10.1007/s00253-005-0217-1
- Ditta, G., Schmidhauser, T., Yakobson, E., Lu, P., Liang, X.W., Finlay, D.R., Guiney, D., Helinski, D.R., 1985. Plasmids related to the broad host range vector, pRK290, useful for gene cloning and for monitoring gene expression. *Plasmid* 13, 149–153.
- Ewering, C., Heuser, F., Benölken, J.K., Brämer, C.O., Steinbüchel, A., 2006. Metabolic engineering of strains of *Ralstonia eutropha* and *Pseudomonas putida* for biotechnological production of 2-methylcitric acid. *Metab. Eng.* 8, 587–602. doi:10.1016/j.ymben.2006.05.007
4. Contribution to the manuscript on the design of inducible expression systems for protein expression in *R. eutropha* H16

- Fukui, T., Ohsawa, K., Mifune, J., Orita, I., Nakamura, S., 2011. Evaluation of promoters for gene expression in polyhydroxyalkanoate-producing *Cupriavidus necator* H16. *Appl. Microbiol. Biotechnol.* 89, 1527–36. doi:10.1007/s00253-011-3100-2
- Gruber, S., Hagen, J., Schwab, H., Koefinger, P., 2014. Versatile and stable vectors for efficient gene expression in *Ralstonia eutropha* H16. *J. Biotechnol.* 186, 74–82. doi:10.1016/j.jbiotec.2014.06.030
- Gruber, S., Schwab, H., Koefinger, P., 2015. Versatile plasmid-based expression systems for Gram-negative bacteria-General essentials exemplified with the bacterium *Ralstonia eutropha* H16. *N. Biotechnol.* 32, 552–8. doi:10.1016/j.nbt.2015.03.015
- Grunwald, S., Mottet, A., Grousseau, E., Plassmeier, J.K., Popović, M.K., Uribelarrea, J.-L., Gorret, N., Guillouet, S.E., Sinskey, A., 2015. Kinetic and stoichiometric characterization of organoautotrophic growth of *Ralstonia eutropha* on formic acid in fed-batch and continuous cultures. *Microb. Biotechnol.* 8, 155–63. doi:10.1111/1751-7915.12149
- Kaczmarczyk, A., Vorholt, J.A., Francez-Charlot, A., 2013. Cumate-inducible gene expression system for sphingomonads and other Alphaproteobacteria. *Appl. Environ. Microbiol.* 79, 6795–802. doi:10.1128/AEM.02296-13
- Kessler, B., Weusthuis, R., Witholt, B., Eggink, G., 2001. Production of microbial polyesters: fermentation and downstream processes. *Adv. Biochem. Eng. Biotechnol.* 71, 159–82.
- Kovach, M.E., Elzer, P.H., Hill, D.S., Robertson, G.T., Farris, M. a, Roop, R.M., Peterson, K.M., 1995. Four new derivatives of the broad-host-range cloning vector pBBR1MCS, carrying different antibiotic-resistance cassettes. *Gene* 166, 175–6.
- Li, H., Liao, J.C., 2015. A synthetic anhydrotetracycline-controllable gene expression system in *Ralstonia eutropha* H16. *ACS Synth. Biol.* 4, 101–6. doi:10.1021/sb4001189
- Lütte, S., Pohlmann, A., Zaychikov, E., Schwartz, E., Becher, J.R., Heumann, H., Friedrich, B., 2012. Autotrophic production of stable-isotope-labeled arginine in *Ralstonia eutropha* strain H16. *Appl. Environ. Microbiol.* 78, 7884–90. doi:10.1128/AEM.01972-12
- Mullick, A., Xu, Y., Warren, R., Koutroumanis, M., Guilbault, C., Broussau, S., Malenfant, F., Bourget, L., Lamoureux, L., Lo, R., Caron, A.W., Pilotte, A., Massie, B., 2006. The cumate gene-switch: a system for regulated expression in mammalian cells. *BMC Biotechnol.* 6, 43. doi:10.1186/1472-6750-6-43
- Pansegrau, W., Lanka, E., Barth, P.T., Figurski, D.H., Guiney, D.G., Haas, D., Helinski, D.R., Schwab, H., Stanisich, V.A., Thomas, C.M., 1994. Complete Nucleotide Sequence of Birmingham IncPa Plasmids: Compilation and Comparative Analysis. *J. Mol. Biol.* 239, 623–663. doi:http://dx.doi.org/10.1006/jmbi.1994.1404
- Penumetcha, P., Lau, K., Zhu, X., Davis, K., Eckdahl, T.T., Campbell, A.M., 2010. Improving the Lac System for Synthetic Biology. *Bios* 81, 7–15. doi:10.1893/011.081.0104
- Pohlmann, A., Fricke, W.F., Reinecke, F., Kusian, B., Liesegang, H., Cramm, R., Eitinger, T., Ewering, C., Pötter, M., Schwartz, E., Strittmatter, A., Voss, I., Gottschalk, G., Steinbüchel, A., Friedrich, B., Bowien, B., 2006. Genome sequence of the bioplastic-producing “Knallgas” bacterium *Ralstonia eutropha* H16. *Nat. Biotechnol.* 24, 1257–62. doi:10.1038/nbt1244
- Ryu, H.W., Hahn, S.K., Chang, Y.K., Chang, H.N., 1997. Production of poly(3-hydroxybutyrate) by high cell density fed-batch culture of *Alcaligenes eutrophus* with phosphate limitation. *Biotechnol. Bioeng.* 55, 28–32. doi:10.1002/(SICI)1097-0290(19970705)55:1<28::AID-BIT4>3.0.CO;2-Z

- Sambrook, J., Russel, D., 2001. Molecular cloning: A laboratory manual, 3rd ed. ed. Cold Spring, NY: Cold Spring Harbor Laboratory Press.
- Sato, S., Fujiki, T., Matsumoto, K., 2013. Construction of a stable plasmid vector for industrial production of poly(3-hydroxybutyrate-co-3-hydroxyhexanoate) by a recombinant *Cupriavidus necator* H16 strain. *J. Biosci. Bioeng.* 116, 677–681. doi:10.1016/j.jbiosc.2013.05.026
- Schwab, H., Lidauer, A., Gudelj-Wyletal, M., Pressing, M., Faber, K., Pogorevc, M., Trauthwein, H., 2003. Esterase EstA aus *Rhodococcus ruber*. DE 101 49 715 B4.
- Simon, R., Priefer, U., Pühler, A., 1983. A broad host range mobilization system for in vivo genetic engineering: transposon mutagenesis in gram-negative bacteria. *Bio/Technology* 1:784–791.
- Srinivasan, S., Barnard, G.C., Tillman, U., Gerngross, T.U., 2002. A Novel High-Cell-Density Protein Expression System Based on *Ralstonia eutropha* A Novel High-Cell-Density Protein Expression System Based on *Ralstonia eutropha*. doi:10.1128/AEM.68.12.5925
- Srivastava, S., Urban, M., Friedrich, B., 1982. Mutagenesis of *Alcaligenes eutrophus* by insertion of the drug-resistance transposon Tn5. *Arch. Micro- biol.* 131, 203–207.
- Tait, R., Lundquist, R., Kado, C., 1982. Genetic map of the crown gall suppressive IncW plasmid pSa. *Mol Gen Genet* 186: 10–15.
- Voss, I., Steinbüchel, A., 2006. Application of a KDPG-aldolase gene-dependent addiction system for enhanced production of cyanophycin in *Ralstonia eutropha* strain H16. *Metab. Eng.* 8, 66–78. doi:10.1016/j.ymben.2005.09.003

6. Figures

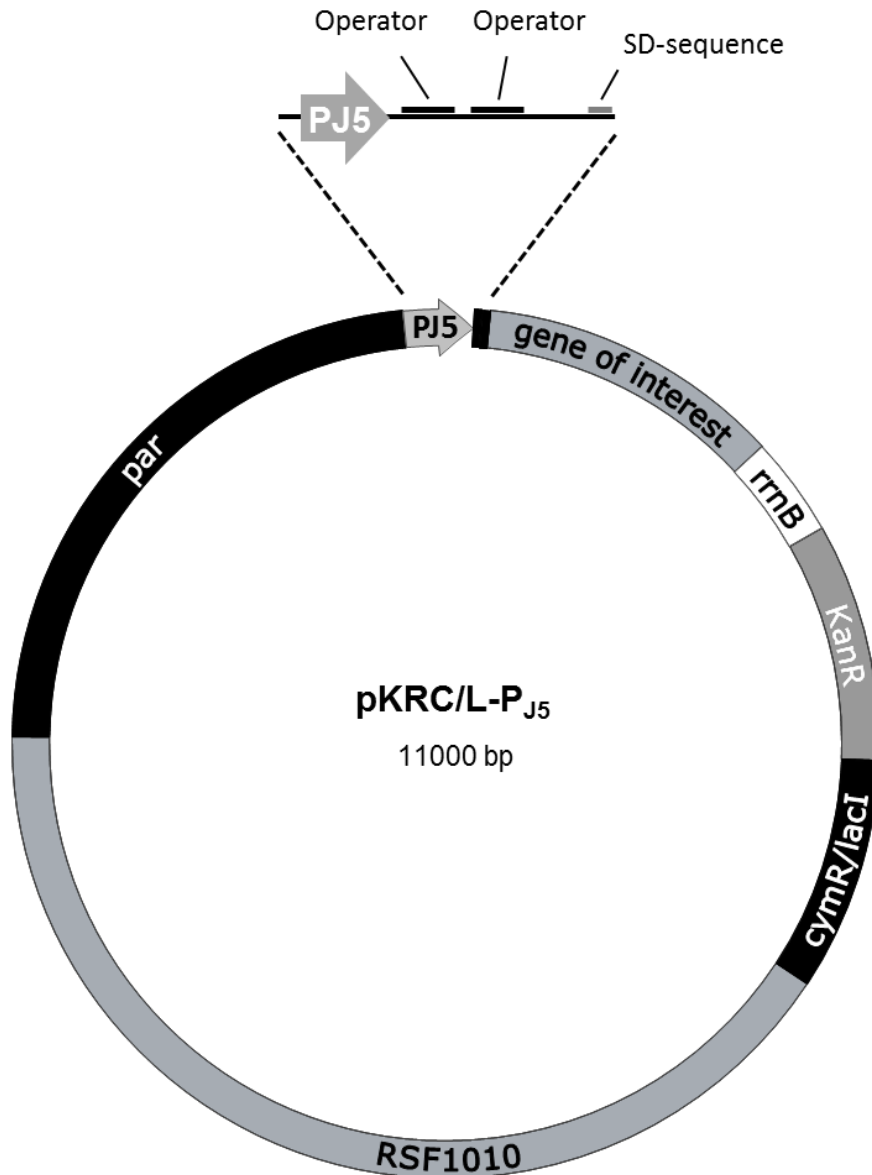


Figure 1: Illustration of the basic plasmid design. The plasmid backbone of pKRL-P_{J5} or pKRC-P_{J5} encode the terminator *rrnB*, the RP4 partition region *par*, a gene of interest (*estA* or *egfp*), the kanamycin resistance *Km^r*, the j5 promoter, the RSF1010 *mob* and *oriV* sequences and the genes coding for the Lacl or CymR repressor proteins as well as the particular operator sequences according to the inducible expression system in use.

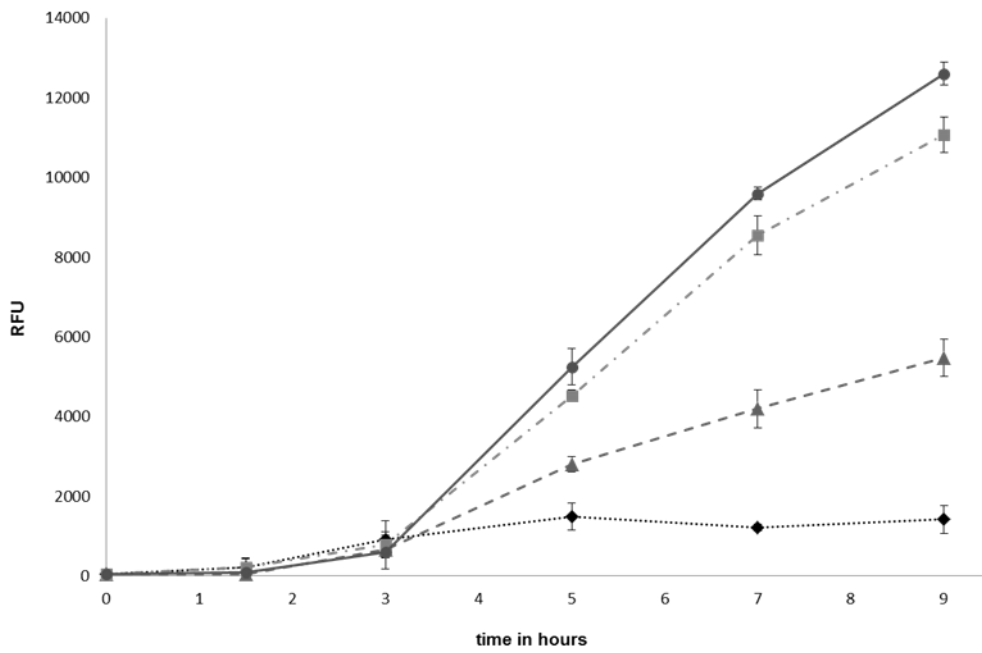


Figure 2A

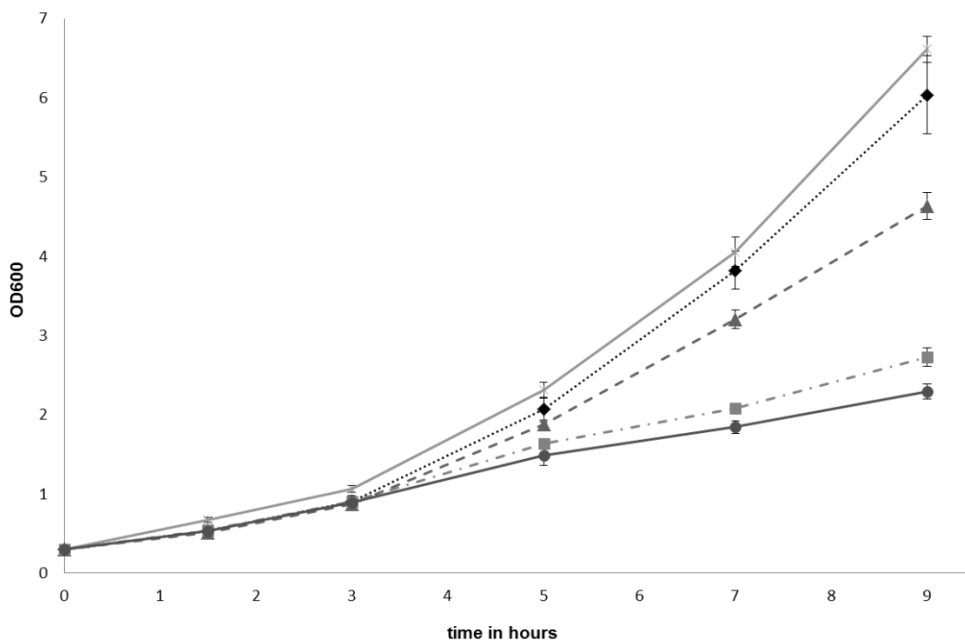


Figure 2B

Figure 2: Time course of IPTG-induced eGFP expression (A) and growth (B) based on *R. eutropha* RS1 (pKRL-P_{j5}-eGFP). (A) *R. eutropha* RS1 transconjugants harboring plasmids pKRL-P_{j5}-eGFP. The cultures remained uninduced (black diamonds) or were induced with 0.01 mM IPTG (grey triangles), 0.1 mM IPTG (grey squares) and 1 mM IPTG (black circles). (B) The sample labels are identical to (A). Moreover, the solid grey line refers to the empty vector control *R. eutropha* H16 (pKRSF1010Δegfp)

4. Contribution to the manuscript on the design of inducible expression systems for protein expression in *R. eutropha* H16

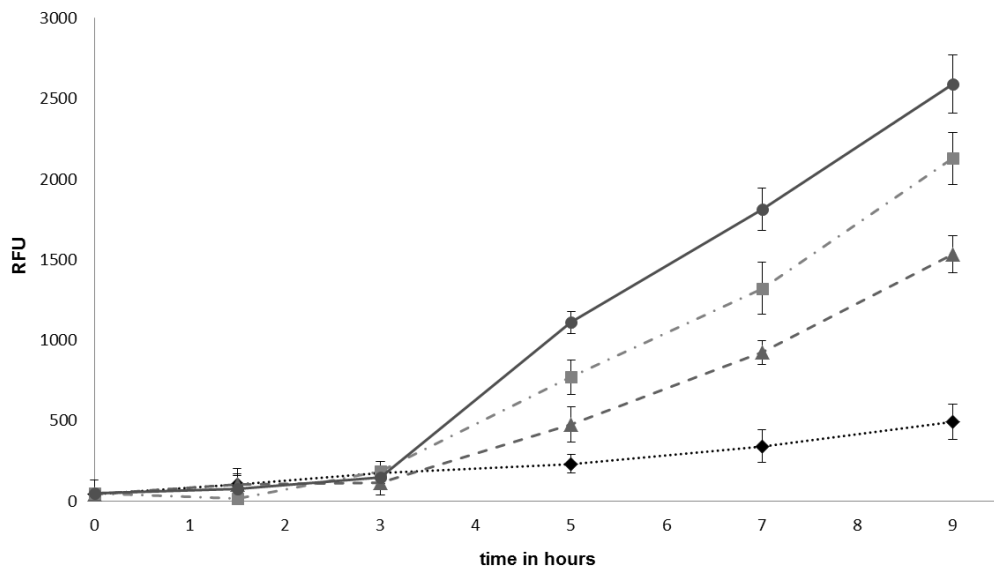


Figure 3A

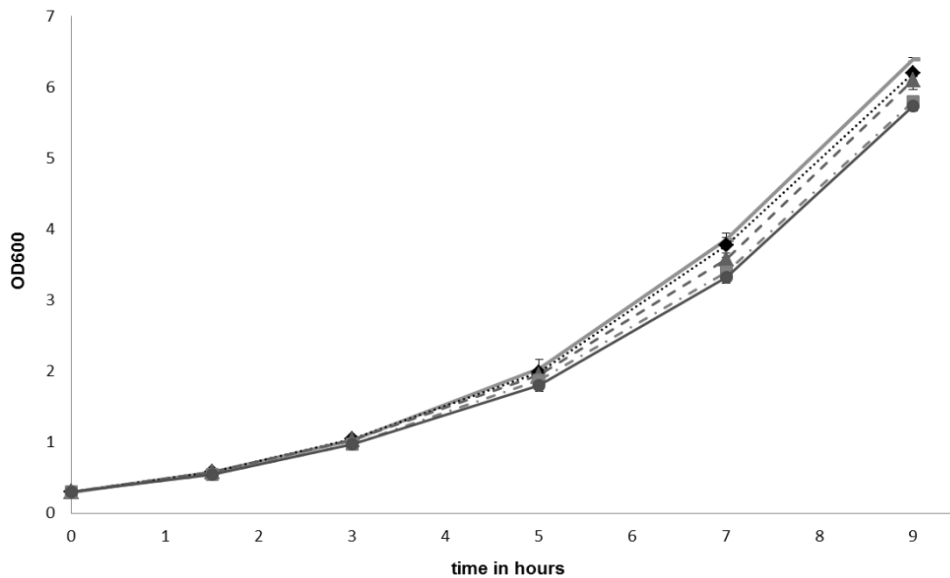


Figure 3A

Figure 3: Time course of cumate-induced eGFP expression (A) and growth (B) based on *R. eutropha* H16 (pKRC-P_{j5}-eGFP). (A) *R. eutropha* H16 transconjugants harboring plasmids pKRC-P_{j5}-eGFP. The cultures remained uninduced (black diamonds) or were induced with 30 μM p-cumate (grey triangles), 60 μM p-cumate (grey squares) and 120 μM p-cumate (black circles). (B) The sample

labels are identical to **(A)**. Moreover, the solid grey line refers to the empty vector control *R. eutropha* H16 (pKRSF1010 Δ egfp)

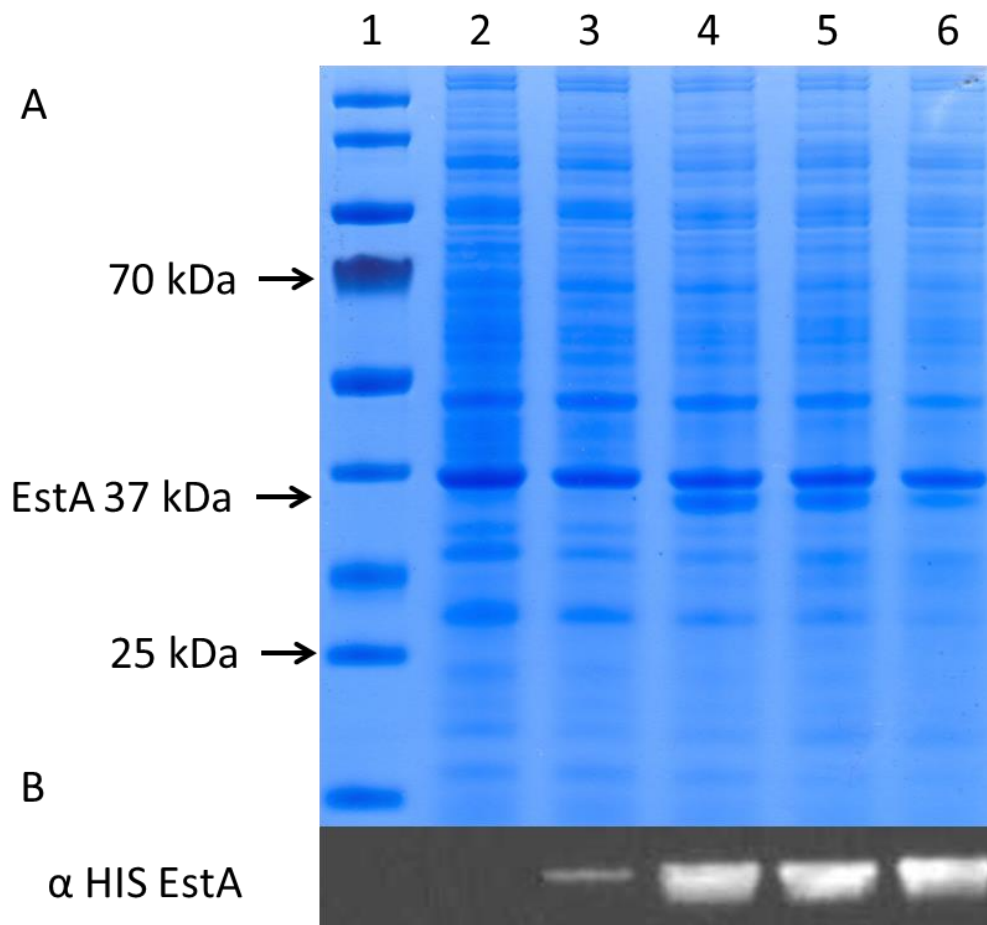


Figure 4: SDS-PAGE (A) and Western Blot (B) illustrating Cumate-induced EstA expression in *R. eutropha* H16 (A) SDS-PAGE of whole cell lysates of *R. eutropha* H16 (pKRC-P_{j5}-estA): Lane 1: PageRuler Prestained Protein Standard (Fermentas), Lane 2: *R. eutropha* H16 (pKRSF1010 Δ egfp), Lane 3: *R. eutropha* H16 pKRC-P_{j5}-estA at induction, Lane 4: *R. eutropha* H16 pKRC-P_{j5}-estA 8 hours after induction, Lane 5: *R. eutropha* H16 pKRC-P_{j5}-estA 24 hours after induction, Lane 6: *R. eutropha* H16 pKRC-P_{j5}-estA 32 hours after induction. (B) Western Blot of whole cell lysates of *R. eutropha* H16 (pKRC-P_{j5}-estA). Polyhistidine-tagged EstA was detected with a monoclonal anti-his antibody (α -HIS). The samples were applied in the same order as in (A).

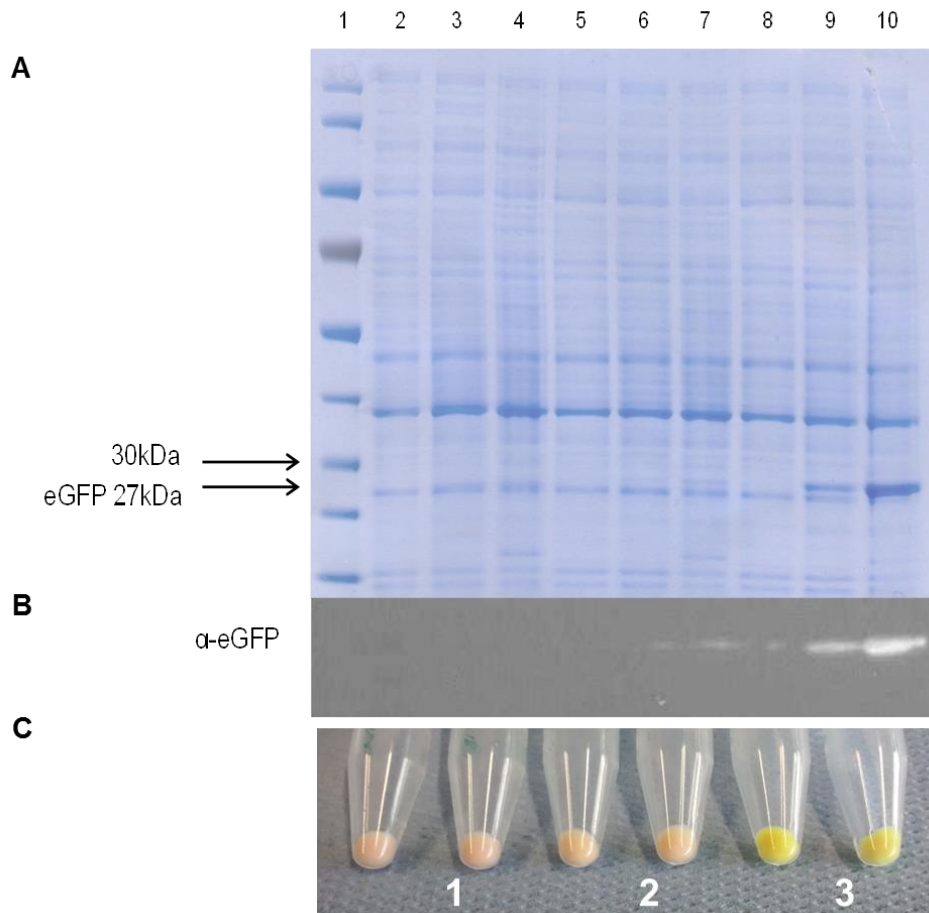


Figure S1: Cumate-induced eGFP expression in *R. eutropha* H16 (pKRC-P_{j5}-egfp) illustrated on the basis of a SDS-PAGE (A), Western Blot (B) and pelleted cells (C). EGFP expression was induced with 120 μM p-cumate at an OD₆₀₀ of 0.8 (A) SDS-PAGE of whole cell lysates of *R. eutropha* H16 (pKRSF1010Δegfp) and *R. eutropha* H16 (pKRC-P_{j5}-egfp): Lane 1: PageRuler Prestained Protein Standard (Fermentas), Lane 2: *R. eutropha* H16 (pKRSF1010Δegfp) at the point of induction, Lane 3: *R. eutropha* H16 (pKRSF1010Δegfp) 8 hours after the induction, Lane 4: *R. eutropha* H16 (pKRSF1010Δegfp) 24 hours after induction, Lane 5: Uninduced culture of *R. eutropha* H16 (pKRC-P_{j5}-egfp) at the point of induction, Lane 6: Uninduced culture of *R. eutropha* H16 (pKRC-P_{j5}-egfp) 8 hours after induction, Lane 7: Uninduced culture of *R. eutropha* H16 (pKRC-P_{j5}-egfp) 24 hours after induction, Lane 8: Induced culture of *R. eutropha* H16 (pKRC-P_{j5}-egfp) at the point of induction, Lane 9: Induced culture of *R. eutropha* H16 (pKRC-P_{j5}-egfp) 8 hours after the point of induction, Lane 10: Induced culture of *R. eutropha* H16 (pKRC-P_{j5}-egfp) 24 hours after the point of induction. (B) Western Blot of whole cell lysates of *R. eutropha* H16 (pKRSF1010Δegfp) and *R. eutropha* H16 (pKRC-P_{j5}-egfp). EGFP was detected with a monoclonal GFP antibody (α-eGFP). The samples were applied in the same order as in (A). (C) Cell pellets 24 hours after induction of the culture 1: *R. eutropha* H16 (pKRSF1010Δegfp), 2: *R. eutropha* H16 (pKRC-P_{j5}-eGFP) uninduced and 3: *R. eutropha* H16 (pKRC-P_{j5}-eGFP) induced with 120 μM p-cumate.

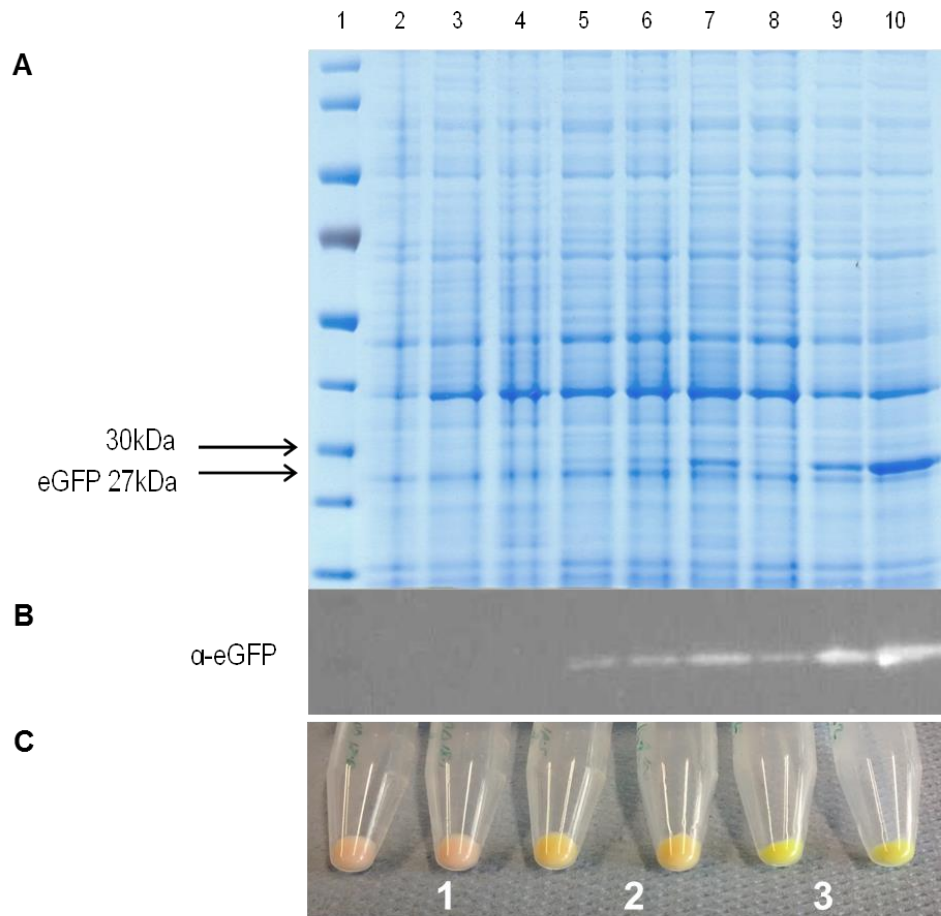


Figure S2: IPTG-induced eGFP expression in *R. eutropha* RS1 (pKRL-P_{j5}-egfp) illustrated on the basis of a SDS-PAGE (A), Western Blot (B) and pelleted cells (C). EGFP expression was induced with 0.1 mM IPTG at an OD₆₀₀ of 0.8 (A) SDS-PAGE of whole cell lysates of *R. eutropha* H16 (pKRSF1010Δegfp) and *R. eutropha* RS1 (pKRL-P_{j5}-egfp): Lane 1: PageRuler Prestained Protein Standard (Fermentas), Lane 2: *R. eutropha* H16 (pKRSF1010Δegfp) at the point of induction, Lane 3: *R. eutropha* H16 (pKRSF1010Δegfp) 8 hours after induction, Lane 4: *R. eutropha* H16 (pKRSF1010Δegfp) 24 hours after induction, Lane 5: Uninduced culture of *R. eutropha* RS1 (pKRL-P_{j5}-egfp) at the point of induction, Lane 6: Uninduced culture of *R. eutropha* RS1 (pKRL-P_{j5}-egfp) 8 hours after induction, Lane 7: Uninduced culture of *R. eutropha* RS1 (pKRL-P_{j5}-egfp) 24 hours after induction, Lane 8: Induced culture of *R. eutropha* RS1 (pKRL-P_{j5}-egfp) at the point of induction, Lane 9: Induced culture of *R. eutropha* RS1 (pKRL-P_{j5}-egfp) 8 hours after induction, Lane 10: Induced culture of *R. eutropha* RS1 (pKRL-P_{j5}-egfp) 24 hours after induction. (B) Western Blot of whole cell lysates of *R. eutropha* H16 (pKRSF1010Δegfp) and *R. eutropha* RS1 (pKRL-P_{j5}-egfp). EGFP was detected with a monoclonal GFP antibody (α-eGFP). The samples were applied in the same order as in (A). (C) Cell pellets 24 hours after induction of the culture 1: *R. eutropha* H16 (pKRSF1010Δegfp), 2: *R. eutropha* RS1 (pKRL-P_{j5}-eGFP) undinduced and 3: *R. eutropha* RS1 (pKRL-P_{j5}-eGFP) induced with 0.1 mM IPTG.

Table(s)**Table1: Strains used in this study**

Strain	Description	References or Source
<i>E. coli</i> MG1655	F ⁻ λ ⁻ <i>ilvG-rfb-50 rph-1</i>	Invitrogen
<i>E. coli</i> S17-1	<i>recA pro hsdR</i> RP4-2-Tc::Mu-Km::Tn7 integrated into the chromosome	Invitrogen
<i>E. coli</i> TOP10	F ['] (<i>proAB, lacIq, lacZ</i> ΔM15, Tn10(tet-r)), <i>mcrA</i> , Δ(<i>mrr-hsdRMS-mcrBC</i>), Φ80Δ <i>lacZ</i> ΔM15, Δ <i>lacX74, deoR, recA1, araD139(ara, leu), 7697, galU, galK, λ-, rpsL</i> (streptomycin-r), <i>endA1, nupG</i>	Invitrogen
<i>Pseudomonas Putida</i> F1	wildtype	DSMZ6899 ^a
<i>R. eutropha</i> H16	wildtype	DSMZ428 ^a
<i>R. eutropha</i> RS1	H16 Δ <i>phaC</i> ΩPH16_B1772 <i>lacY</i>	this work

Table 2: Plasmids used in this work

Plasmids		
RP4	broad-host-range plasmid, IncP	(Pansegrau et al., 1994)
pSa	broad-host-range plasmid, IncW	(Tait et al., 1982)
pMS470Δ8	Ap ^r , P _{tac}	(Balzer et al., 1992)
pMS470Ru1	Ap ^r , P _{tac} , estA	(Schwab et al., 2003)
pK470MobRk2	Km ^r , P _{tac} , mob, colE1	This work
pInt_lacY_phaC	pK470MobRK2, lacY gene, P _{H16_B1772} , two phaC homologous regions	This work
pInt_lacY_phaC_loxP	pK470MobRK2, lacY gene, P _{H16_B1772} , two phaC homologous regions, loxP sites	This work
pCM_Cre	Cm ^r , P _{tac} , mob, colE1, cre, cymR	This work
pKRSF1010-P _{j5} -egfp	Km ^r , P _{j5} , egfp, par, RSF1010 mob and origin of replication	(Gruber et al., 2014)
pKRSF1010Δegfp	Km ^r , P _{tac} , par, RSF1010 mob and origin of replication, deleted egfp	(Gruber et al., 2014)
pKRL-P _{j5} -egfp	Km ^r , P _{j5} , egfp, par, lacI, RSF1010 mob and origin of replication	This work
pKRC-P _{j5} -egfp	Km ^r , P _{j5} , egfp, par, cymR, RSF1010 mob and origin of replication	This work
pKRC-P _{j5} -estA	Km ^r , P _{j5} , estA, par, cymR, RSF1010 mob and origin of replication	This work

^a DSMZ, Deutsche Sammlung für Mikroorganismen und Zellkulturen.

^b Km^r, kanamycin resistance; Ap^r, ampicillin resistance; Cm^r, chloramphenicol resistance, par, site specific partitioning (recombination) system from the RP4 plasmid

Table S3

RFU of *R. eutropha* H16 [pKRC-P_{j5}-eGFP9 induced with 122 μM, 60 μM and 30 μM *p*-cumate (*p*-isopropylbenzoate)

RFU values after 24 hours:

<u>Strain</u>	<u>RFU</u>
<i>R. eutropha</i> H16 [pKRC-P _{j5} -eGFP] uninduced	640
<i>R. eutropha</i> H16 [pKRC-P _{j5} -eGFP] induced with 30 μM <i>p</i> -cumate	19400
<i>R. eutropha</i> H16 [pKRC-P _{j5} -eGFP] induced with 60 μM <i>p</i> -cumate	20700
<i>R. eutropha</i> H16 [pKRC-P _{j5} -eGFP] induced with 122 μM <i>p</i> -cumate	21200

Growth of *R. eutropha* H16 [pKRRSF1010Δegfp] and *R. eutropha* H16 [pKRC-P_{j5}-eGFP] induced with 122 μM, 60 μM and 30 μM *p*-cumate over time

OD₆₀₀ values after 24 hours:

<u>Strain</u>	<u>OD₆₀₀</u>
<i>R. eutropha</i> H16 [pKRSF1010Δegfp]	19,5
<i>R. eutropha</i> H16 [pKRC-P _{j5} -eGFP] uninduced	19,7
<i>R. eutropha</i> H16 [pKRC-P _{j5} -eGFP] induced with 30 μM <i>p</i> -cumate	19,7
<i>R. eutropha</i> H16 [pKRC-P _{j5} -eGFP] induced with 60 μM <i>p</i> -cumate	19,5
<i>R. eutropha</i> H16 [pKRC-P _{j5} -eGFP] induced with 122 μM <i>p</i> -cumate	19,7

RFU of *R. eutropha* RS1 [pKRL-P_{j5}-eGFP] induced with 1 mM, 0,1 mM and 0,01 mM IPTG

RFU values after 24 hours:

<u>Strain</u>	<u>RFU</u>
<i>R. eutropha</i> S1 [pKRL-P _{j5} -eGFP] uninduced	5400
<i>R. eutropha</i> S1 [pKRL-P _{j5} -eGFP] induced with 0,01 mM IPTG	20400
<i>R. eutropha</i> S1 [pKRL-P _{j5} -eGFP] induced with 0,1 mM IPTG	33100
<i>R. eutropha</i> S1 [pKRL-P _{j5} -eGFP] induced with 1 mM IPTG	36100

Growth of *R. eutropha* H16 pKRSF1010-Δegfp and *R. eutropha* RS1 pKRL-P_{j5}-eGFP induced with 1 mM, 0,1 mM and 0,01 mM IPTG

OD₆₀₀ values after 24 hours:

<u>Strain</u>	<u>OD₆₀₀</u>
<i>R. eutropha</i> H16 [pKRSF1010-Δegfp]	20,8
<i>R. eutropha</i> H16 [pKRL-P _{j5} -eGFP] uninduced	17,1
<i>R. eutropha</i> H16 [pKRL-P _{j5} -eGFP] induced with 0,01 mM IPTG	9,7
<i>R. eutropha</i> H16 [pKRL-P _{j5} -eGFP] induced with 0,1 mM IPTG	7,4
<i>R. eutropha</i> H16 [pKRL-P _{j5} -eGFP] induced with 1 mM IPTG	7,0

4. Contribution to the manuscript on the design of inducible expression systems for protein expression in *R. eutropha* H16

5. Conclusions

- Genes for 11 putative alcohol dehydrogenases, 12 putative short chain dehydrogenases/reductases and 10 putative reductases originating from *R. eutropha* H16 were cloned and the corresponding proteins were heterologously expressed in *E. coli* BL21
 - 5 alcohol dehydrogenases, 9 short-chain dehydrogenases/reductases and 5 reductases were successfully heterologously expressed in *E. coli* BL21 and analysed for their enzyme activity.
 - N-terminal His-tag cloning was performed for genes for 2 dehydrogenases ADH A5 and SDR B6. Four dehydrogenases ADH A5, SDR A1, SDR B3 and SDR B6 were heterologously expressed in *E. coli* BL21, purified and analysed for the reduction and oxidation activity
 - ADH A5 and SDR B3 were successfully homologously expressed in *R. eutropha* H16 from the novel cumate-inducible expression vector system
 - ADH A5 and SDR B3 were characterized in more detail as (S)-enantioselective NADP⁺/NADPH-dependent short-chain dehydrogenases
 - ADH A5 and SDR B3 showed preference bulky substrates such as (S)-octanol and benzil
 - ADH A5 and SDR B3 were found to belong to the different phylogenetic groups of known benzil reductases
-
- His₆-*Ras*ALDH was purified out of *E. coli* BL21 up to 2 mg/ml
 - Enzyme has preference towards phosphorylated form of cofactor NADP(H)
 - Purified enzyme is active with sugars like D-ribose and D-xylose and the diketone 2,3-butanedione
-
- Modified transaminase originating from *Arthrobacter sp.*, alanine dehydrogenase of *Bacillus subtilis* including its His-tagged version, alanine dehydrogenase from *R. eutropha* H16 and 4 bacterial imine reductases (origin not specified) were successfully cloned into novel cumate inducible expression vector for *R. eutropha* H16.
 - Bacterial transaminase and 3 imine reductases were heterologously expressed in *R. eutropha* H16 in their active form (shown by the members of Prof. W. Kroutil's group).
 - Bacterial transaminase and 3 imine reductases were successfully expressed in *R. eutropha* H16 under lithoautotrophic growth conditions and forwarded for further enzyme activity analysis.

Biocatalysis has significant advantages over organic synthesis in the field of “white biotechnology” (Drepper et al., 2006). Enzymes usually exhibit high substrate specificity and enantioselectivity, and, at the same time, work in aqueous environment and under mild reaction conditions. Cofactor-dependent enzymes, for example NAD(P)(H)-dependent oxidoreductases, are widely distributed in biotechnological processes, and require proper cofactor regeneration system (Chenault, H. Keith Simon, Ethan S. Whitesides, 1988; Zhao and Van Der Donk, 2003). A simple alternative for cofactor regeneration is provided by hydrogenase enzymes, which oxidize H_2 , as a cheap reducing agent, and transfer a hydride onto $NAD(P)^+$ (Lauterbach et al., 2013).

Under lithoautotrophic conditions, NAD(P)-reducing hydrogenases of *R. eutropha* H16 provide reducing equivalents for the oxidoreduction reactions. An *in vivo* coupled reaction for production of (*R*)-1,2-propanediol has recently been performed by an alcohol dehydrogenase from *Kluyveromyces lactis* and an indigenous hydrogenase of *R. eutropha* H16. In this experiment, *R. eutropha* H16 served as a whole cell biocatalyst under lithoautotrophic environment conditions (Oda et al., 2013). However, as an organism with diverse metabolic behaviour, *R. eutropha* has a genome, which can also be used as a very promising source of biotechnologically interesting enzymes. For example, stereoselective alcohol dehydrogenase from *R. eutropha* sp. has been recently characterized for its ability to perform rare reaction of bulky-bulky ketone conversion (Kulig et al., 2013; Ivan Lavandera et al., 2008). Additionally, it is known, that under conditions of restricted oxygen supply, the facultative lithoautotrophic organism *R. eutropha* H16 also produces a variety of NAD(P)⁺/NAD(P)H-dependent dehydrogenases (Steinbüchel et al., 1983).

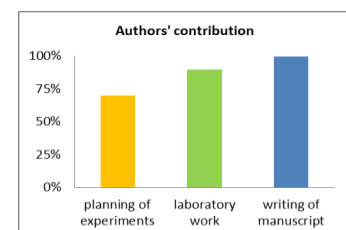
In our project we were interested in constructing *R. eutropha* H16 as a whole cell system by expressing dehydrogenases and reductases that catalyse biotechnologically interesting reduction reactions. In this system no cofactor recycling is needed due to an excess of NAD(P)H generated under lithoautotrophic growth conditions. As a result of this PhD thesis, a number of dehydrogenases and reductases of *R. eutropha* H16 were cloned, heterologously expressed in *E. coli* BL21 and analysed for their oxidation and reduction activities. The most promising two dehydrogenases were additionally homologously expressed in *R. eutropha* H16, purified and characterized in more detail. They were found to be highly stereoselective in the reduction of bulky substrates. The computational analysis showed that these two enzymes, ADH A5 and SDR B3, belong to different phylogenetic clusters of the enzymes with known benzil reduction activity. Fermentation under lithoautotrophic growth conditions was performed for *R. eutropha* H16 [pKRSF1010-j5-SDR B3-cymR] strain. Preliminary data of this experiment indicate that whole cell biocatalysis with the industrially important substrate benzil could be performed in *R. eutropha* H16 without external cofactor source, though additional experiments are needed.

As a perspective for the research presented in this PhD thesis further detailed biochemical studies on the activities of SDR A5 and SDR B3 need to be carried out in order to determine the kinetic parameters of the reactions. Additionally, the whole cell bioconversion studies need to be performed with the lithoautotrophically grown cells of *R. eutropha* H16 expressing enzyme of interest.

On the base of the experiments performed in this PhD thesis, it may be concluded that the Gram negative β -proteobacterium *R. eutropha* H16 has a big potential as source for biotechnologically interesting enzymes and can successfully be used for the whole cell biocatalysis.

6. Appendix

6.1. Cloning, heterologous expression and functional characterisation of esterase-like protein originating from *Ralstonia eutropha* H16



Editing and additional suggestions for writing of manuscript were provided by Dr. P. Heidinger and Prof. H. Schwab

6.1.1. Introduction

Since the complete sequencing of the *R. eutrophas* H16 genome is available (Pohlmann et al., 2006; Schwartz et al., 2003), several novel enzymes of this bacteria have been characterized due to a biotechnological interest (Brigham et al., 2010; Gai et al., 2014; Lu et al., 2014, 2013). A novel lipase and its chaperone were characterized in connection to the studies devoted to extend of substrate utilization range of *R. eutropha* H16 (Brigham et al., 2010; Lu et al., 2013).

Lipases belong to the carboxylic ester hydrolases (EC 3.1.1). This family, also called carboxylesterases, include two groups of enzymes: non-specific esterases (EC 3.1.1.1) and lipases (EC 3.1.1.3) which have been differentiated on the basis of their substrate specificity. The lipases show high activity towards the aggregated state of its substrate, whereas the esterases are usually active towards the soluble state of its substrate (Fojan et al., 2000). The ability of lipases to hydrolyse water-insoluble long chain triacylglycerols in contrast to esters, could be explained by the difference in the distribution of hydrophobic amino acid residues at the vicinity of their active site (Chahiniana and Sarda, 2009). Members of esterase/lipase family share a common alpha/beta hydrolase fold in their structure (Nardini and Dijkstra, 1999). This fold can be found in hydrolytic enzymes of widely differing phylogenetic origin and catalytic function. The core is presented by eight beta-sheets connected by alpha-helices (Ollis et al., 1992) (Fig. 72).

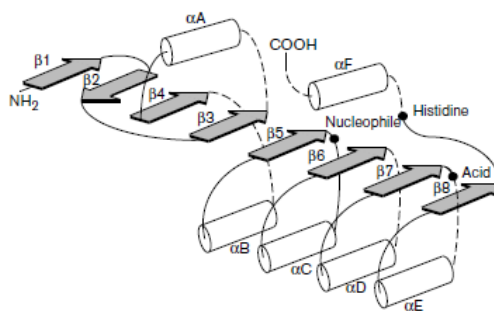


Figure 72. Secondary structure diagram of the 'canonical' α/β hydrolase fold. α -helices and β -strands are represented by white cylinders and grey arrows, respectively. The location of the catalytic triad is indicated by black dots. Dashed lines indicate the location of possible variable insertions, which might be present within the enzymes with α/β hydrolase fold. Reference: Ollis et al., 1992

The catalytic triad in alpha/beta hydrolase fold is represented by a nucleophile–acid–histidine combination and may be variable in two positions (Nardini and Dijkstra, 1999) (Fig. 72). In many cases the nucleophile in the catalytic site is represented by a serine. For the members of the esterase/lipase group this serine residue is also a part of highly conserved classical consensus Gly-X-Ser-X-Gly motif (Ollis et al., 1992).

Microbial lipases and esterases are popular biocatalysts capable of hydrolysis, esterification, and acidolysis of the substrates. They can efficiently work in aqueous and non-aqueous environment. Lipases are chemo-, regio- and enantio-specific, and therefore are highly desirable in pharmaceutical industry (Tan et al., 2015). A number of bacterial lipases has been applied for the production of chiral compounds (Drepper et al., 2006). Lipases also play an important role in the area of detergents and the production of food ingredients (Jaeger et al., 1999).

Analysis of the protein databases of *R. eutropha* H16 revealed a putative esterase-like protein with an unusual constitution of the catalytic triad. This putative enzyme was cloned, expressed and characterized for various functional activities.

6.1.2. Materials and methods

6.1.2.1. Bacterial strains, plasmids and cultivation condition

Bacterial strains and plasmids used in this study are listed in Table 17 and Table 18. Cultivation of *E. coli* strains was performed as described in Materials and methods in chapter 3.1.2. Strains generated in this study were handed over to the IMBT strain collection under the numbers ##7633 – 7635 (Supplementary Table 1).

Table 17. Bacterial strains used in this study.

Strain	Genotype	Reference
<i>Escherichia coli</i>		
TOP10	F' mcrA Δ(mr(R)-hsdRM(S)-mcrBC) φ80lacZΔM15 ΔlacX74 nupG recA1 araD139 Δ(ara-leu)7697 galE15 galK16 rpsL(Str ^R) endA1 λ ⁻	Invitrogen
BL21	F' Δcm ompT hsdS(r _B ⁻ m _B ⁻) gal [malB ⁺] _{K-12} (λ ^S)	Invitrogen
BL21(DE3)	fhuA2 [lon] ompT gal (λ DE3) [dcm] ΔhsdS λ DE3 = λ sBamHlo ΔEcoRI-B int:::(lacI::PlacUV5::T7 gene1) i21 Δnin5	Stratagene

Table 18. Plasmids used in this study

Plasmid	Description	Reference
pK470Δ	Km ^r , P _{tao} lacI	this study
pK470-Est	Km ^r , P _{tao} lacI, H16_B1112	this study
pK470-EstX	Km ^r , P _{tao} lacI, H16_B1112, codon optimized for expression in <i>E. coli</i>	this study
pET28a(+)_Ru1	Km ^r , P _{tao} lacI, Ru1 esterase gene	(Rathbone et al., 1997)
pET26b(+)-AChNL	Km ^r , P _{tao} lacI, gene encoding AChNL	(Wiedner et al., 2014)

All chemicals, reagents and basic media components were obtained from Becton, Dickinson and Company (Franklin Lakes, NJ, USA), Sigma-Aldrich (St. Luis, MO, USA) and Carl Roth (Arlenheim, Germany), respectively, unless mentioned otherwise.

6.1.2.2. Cloning of esterase/lipase into pK470

DNA preparation and manipulations were performed as described in the section Materials and methods in chapter 3.1.2.

Putative esterase-like protein originating from *R. eutropha* H16 (locus *H16_B1112*) was amplified out of genomic DNA with primers #262 and #212 (Table 19). The purified PCR product was cloned into the pK470 expression vector via *Nde*I and *Hind*III restriction sites. The success of the plasmid construction was proven by the restriction analysis and DNA sequencing (LGC Genomics GmbH; Berlin, Germany) with the primers #39 and #40 (Table 19).

Table 19. Primers used in this study

Name	Number	Sequence 5'-3'
pM(S)-prom-fwd	39	5' – gcataattcgtgtcgcctcaagg – 3'
Tac-pM(S)-Stop-neu-rev	40	5' – gcaaattctgtttatcagacc – 3'
Est-Nde-fwd-new	262	5' - <u>cagcatatgtccgagaagccaggc</u> - 3'
Est-Hind-rev	212	5' - <u>attaagcttcagccggcggg</u> - 3'
EstX-Nde-fwd	471	5' – <u>atacatatgagcga</u> aaaaccggg – 3'
EstX-HindIII-rev	472	5' – <u>ccaagcttgc</u> atgcttattaacc – 3'

The underlined sequences (*Hind*III; *Nde*I) represent the additional restriction sites at the 5' ends of forward and reverse primers

For the optimization of the protein expression in *E. coli* codon-optimized synthetic esterase/lipase gene (*estX*) was ordered (GeneArt Gene Synthesis, Thermo Scientific, Waltham, MA, USA) with the following DNA sequence (5'-3'):

```
Atgagcgaaaaaccgggtcagcgtccggatgcagcaagcgcagcaagtgcaccgaccgcagcaggtcagggtcaggttcgtgttg
cagaacacaccgttaccagtgatggctgtgaaattctggttcgtgtgttatccggcaggctatccggcaccgggtgcagaaggtgcagcactgc
tgccgtggctggtttatctgcacgcaggtggtttgtgaaggtggctggaacatgcctgtcatctggttcaggatctggcaaccaccgttccggca
gttgtgttacaccggcatatagcctggcaccggatcatccgtttccggcagcaccggaagatgcatatagcaccgttcagtggttctgcgtaat
gcacgtcgtctgaaactggataaaaattcgttttcactggttggaagaagcaggcggtaaatctggcaattgactggcacagatgctgcgtgat
ctggcaccgcacagcctcgtggctcagtggtgattcgtccggttaccgatccgtgtctgcagcacgcaagctgtgcaggtttgatgggtggtcag
gtgccgatggataccctgcgtcgtctggcagataactatcgtgattatctgccgacaccggcagataccgttcatccgtatgcggcaccggcactg
gcaagtcgctggcaggtctgcctccgacctggcaggtgcagaatatgatgcactgcgtgccgaaggtgaagcatttgcaggccgtctggc
aaaagccggtgttccggcacaggcaatgattatgcctggctgatgtggtgatgggttgaagaagcccacgatagctgtaggcatgggtgatg
aaggtgcacgttttctgcgtcgttctggcagcagcagatgataaccagcagcctgaccgaacgtcgtgcagatgcaaatgcaagccgtccgggt
gcaaaaccggcaggttaataa
```

Primers #471 and #472 were used to amplify gene of interest (Table 19). The purified PCR product was cloned into pK470 expression vector via *Nde*I and *Hind*III restriction sites. Success of the

cloning experiments was proven by restriction analysis and subsequent DNA sequencing (LGC Genomics GmbH; Berlin, Germany) with the primers #39 and #40.

6.1.2.3. Expression of esterase-like protein in *E. coli* BL21

Fermentation conditions for *E. coli* BL21, visualization of protein expression via SDS-PAGE, colony-based enzyme activity assay and photometric enzyme activity assay with the lysates were performed as described in the section Materials and methods given in chapter 3.1.2.

6.1.2.4. Esterase activity assay

To test for the esterase activity of the putative esterase-like protein, plasmid with the gene of interest pK470-EstX was transformed into *E. coli* BL21. *E. coli* BL21 [pK470Δ] was used as a negative control. *E. coli* BL21 [pET28a_Ru1] was used as a positive control. pET28a_Ru1 encodes active esterase from *Rhodococcus ruber* pET28a_Ru1. Clones, grown after transformation on the selective plate supplemented with 0.1 mM IPTG, were lifted on the filter paper disks (Whatman International Ltd; Maidstone, United Kingdom). After 5 min at 37°C, 1 ml of the reaction solution was added on the surface of each filter. 5 mL reaction solution contained 125 μl FastBlue B Dye (20 mg/ml in ddH₂O), 375 μl α-naphthylacetate (12 mg/ml in acetone) and 4.5 ml 0.1 M TrisCl buffer. After 2-3 minutes development of colour was monitored.

6.1.2.5. Hydroxynitrile lyase activity

To examine whether EstX has a hydroxynitrile lyase activity, a colony-based filter assay was performed. ONCs in 2 ml LB media supplemented with 40 μg/ml kanamycin were prepared, containing following strain: *E. coli* BL21 [pK470-EstX], *E. coli* BL21 [pK470Δ] used as a negative control and *E. coli* BL21(DE3) [pET26b(+)-AChNL] used as a positive control (this strain was kindly provided by Dipl.-Ing. Dr. Romana Wiedner). AChNL encodes hydroxynitrile lyase from *Acidobacterium capsulatum*. On the next day nylon membranes (Biodyne A, 0.2 μm, PALL Life Sciences, Port Washington, NY) were placed on the LB agar plates supplemented with 40 μg/ml kanamycin. 0.1 ml of each ONC, diluted 10⁷ times, were plated out on the membranes, and the cells were grown overnight at 37°C. The membranes with the colonies were then transferred onto LB agar plates containing 40 μg/ml kanamycin and 0.1 mM IPTG, which induces protein expression. The cells were grown overnight at 20°C. The colonies were pre-incubated with 100 mM citrate buffer, pH 3.5, after which buffer with 12 mM (R)-mandelonitrile (97%) was added. A piece of plastic mosquito net was placed on top of the membranes to prevent wetting, and overlaid by a filter paper (Whatman No. 1, GE Healthcare, Uppsala, Sweden) soaked with the mix of copper-(II) ethylacetoacetate and 4,4'-methylenebis(N,N-dimethyl-aniline) solutions, each 1% in chloroform. Development of a blue colour displays the release of hydrogen cyanide (HCN) and thereby indicates enzyme activity.

6.1.3. Results and discussion

6.1.3.1. Cloning and heterologous expression of esterase/lipase

The members of esterase/lipase group of enzymes have a highly conserved classical consensus Gly-X-Ser-X-Gly motif (Ollis et al., 1992). For the putative esterase-like protein from *R. eutropha* H16 (locus *H16_B1112*) this central serine of Gly-X-Ser-X-Gly sequence was found to be replaced by an acidic glutamic acid. The gene, coding for the enzyme carrying unusual amino acid in the highly conserved motif, was amplified from the genomic DNA and cloned into pK470 expression vector. However, no expression of this protein was observed on the SDS-PAGE with the crude cell lysates of *E. coli* BL21 [pK470-Est]. As *R. eutropha* H16 is known for its high GC content of the genomic DNA, a codon optimized synthetic gene for the expression in *E. coli*, named EstX, was ordered, amplified via PCR and cloned into the pK470 expression vector. The construct was transformed into *E. coli* BL21 cells, and the enzyme was successfully expressed (Fig. 73).

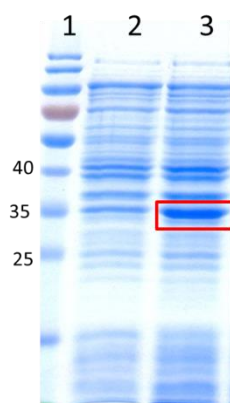


Figure 73. SDS-PAGE of the whole cell lysate of *E. coli* BL21 [pK470-EstX]. Expected size for EstX is 36 kDa, the expressed esterase is indicated in the red box. Lane 1: PageRuler™ Prestained protein ladder; lane 2: *E. coli* BL21 [pK470Δ], negative control; lane 3: *E. coli* BL21 [pK470-EstX]

6.1.3.2. Enzyme activity assays

In order to determine a possible esterase activity of the enzyme, a filter assay was performed. In this assay the substrate alpha-naphthyl acetic acid ester is hydrolysed by esterase to alpha-naphthol which couples to *Fast Blue* B dye and lead to the development of the violet colour. However, no activity was detected, indicating that the catalytic serine replacement in the Gly-X-Ser-X-Gly motif might be crucial for esterase functionality.

Since esterases are closely related to the group of hydroxynitrile lyases with the alpha/beta hydrolase fold, a hydroxynitrile lyase activity colony-based filter assay was performed. An active enzyme will cleave the (R)-mandelonitrile to benzaldehyde and HCN. The hydrogen cyanide produced by the organisms reacts with copper(II) ethylacetoacetate and 4,4'-methylenebis-(N,N-dimethylaniline) in a paper disk placed above the membrane with the cells, resulting in the

development of a blue colour (Castric and Castric, 1983). However, no hydroxynitrile activity was detected for the EstX (Fig. 74).

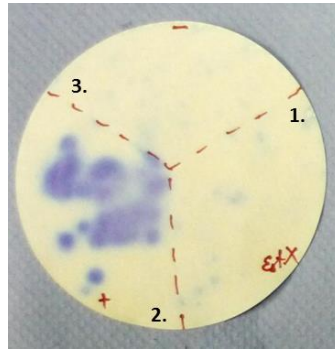


Figure 74. Filter paper with the results of HNL colony-based activity assay for *E. coli* BL21 [pK470-EstX]. Blue colour indicates the release of HCN. The incubation time is 10 min. 1 - *E. coli* BL21 [pK470-EstX]; 2 – positive control *E. coli* BL21(DE3) [pET-CH_2]; 3 – negative control *E. coli* BL21 [pK470Δ]

On the basis of the performed experiments, it was shown that the enzyme doesn't show any esterase nor hydroxynitrile lyase activity. Therefore, one may conclude, that the serine in highly conserved Gly-X-Ser-X-Gly motif might be essential for the esterase and hydroxynitrile lyase activity. Another explanation could be that the actual function of this enzyme is not discovered till now.

6.1.4. Conclusions

- Putative esterase-like protein originating from *R. eutropha* H16 codon-optimized for expression in *E. coli* was cloned and expressed in *E. coli* BL21
- The enzyme did not show any esterase nor hydroxynitril lyase activity

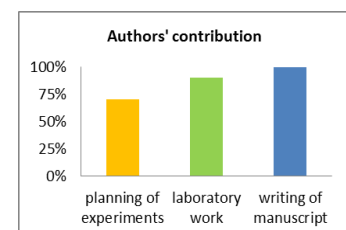
6.2. Report about research stay

Department of Bioengineering, University of Massachusetts Dartmouth, USA

Group of Dr. Christopher J. Brigham, Assistant Professor at UMassD, USA

10th July 2013 – 20th December 2013

This research was supported by a personal scholarship for short time academic research (KUWI), TU Graz



Editing and additional suggestions for writing of manuscript were provided by Dr. P. Heidinger and Prof. H. Schwab

6.2.1. Introduction

Dr. Christopher J. Brigham is a researcher with great experience in the field of *R. eutropha* H16 studies. He is an author of many publications devoted to manufacturing of bioproducts, including production of biofuels (e.g., Brigham et al., 2012a; Lu et al., 2012) and bioplastic from different types of carbon sources (e.g., Brigham et al., 2012c; Jeon et al., 2014; Riedel et al., 2012). Additionally, he is an expert in bacterial carbon dioxide utilization metabolism (e.g., Brigham et al., 2011; Gai et al., 2014). The topic of the joint planned research at the department of Bioengineering, University of Massachusetts, Dartmouth in Dr. C.J. Brigham's group involved studying methods for producing gene knock out strains. Four selected dehydrogenases (locus *H16_A3164*, *H16_A1168*, *H16_B1297*, *H16_B0101*), acetoacetyl-CoA reductase (locus *H16_A1439*) and one esterase/lipase (locus *H16_B1112*) were chosen for construction of *R. eutrophas* knockout strains in order to obtain more in-depth knowledge of metabolic behaviour under lithoautotrophic cultivation conditions. Production of an acetoacetyl-CoA knockout strain was of a particular interest since this enzyme is known to be upregulated under lithoautotrophic growth conditions and may possibly interfere with the overexpressed oxidoreductases of interest (Schwartz et al., 2009).

A gene knockout organism is a genetically modified organism, which carries inactive gene due to introduced mutations or deletion of the gene sequence. In 2007 the Nobel Prize in Physiology and Medicine was given to M. Capecchi, M. Evans and O. Smithies for "principles for introducing specific gene modifications in mice by the use of embryonic stem cells" (*The Nobel Prize in Physiology or Medicine 2007 - Press Release*, 2007). Nowadays, techniques for generating gene knockouts are widely used in different fields of molecular biology, medicine and biotechnology. For example, deletion of two putative fatty acid β -oxidation pathway operons of *R. eutropha* H16 were used to increase methyl ketones production (Lu et al., 2012). Brigham et al. produced knockout strain for lipase genes and potential β -oxidation genes in order to obtain more information about triacylglycerol and fatty acid degradation pathways (Brigham et al., 2010). Genetically modified strains of *R. eutropha* H16 with β -ketothiolase gene deletions were used for production of polyhydroxyalkanoates (Insomphun et al., 2015). The main technique which is used in these studies, including the one performed by Dr. Brigham and his colleagues, involves homologous recombination and subsequent screening of the knockout strains on the selective media.

6.2.2. Materials and methods

Bacterial strains used in this study are listed in Table 20. Plasmids and oligonucleotide primers used in this work are listed in Table 21 and Table 22, respectively. *E. coli* strains derived in this study were handed over to the IMBT strain collection under the numbers ##7676-7680 (Supplementary Table 1).

Table 20. Bacterial strains used in this study.

Strain	Genotype	Reference or source
<i>Ralstonia eutropha</i>		
H16	Wild-type <i>R. eutropha</i> , gentamicin resistant (Gen ^r)	ATCC 17699
H16 Δ sdr_A1	<i>H16_A3164</i> deleted strain, derived from <i>R. eutropha</i> H16	this study #7048 in IMBT strain collection
H16 Δ sdr_B6	<i>H16_B0101</i> deleted strain, derived from <i>R. eutropha</i> H16	this study #7046 in IMBT strain collection
H16 Δ est	<i>H16_B1112</i> deleted strain, derived from <i>R. eutropha</i> H16	this study #7049 in IMBT strain collection
H16_ Δ A1439	<i>H16_A1439</i> deleted strain, derived from <i>R. eutropha</i> H16	this study #7047 in IMBT strain collection
<i>Escherichia coli</i>		
S17-1	TpR SmR recA, thi, pro, hsdR-M+RP4: 2-Tc:Mu: Km Tn7 λ pir	(Simon et al., 1983)

Table 21. Plasmids, used in this study

Plasmid	Description	Reference
pRK2013	Km ^r , <i>colE1</i>	(Figurski and Helinski, 1979)
pJV7	Km ^r , <i>sucB</i> , pGY46 with additional <i>SwaI</i> site	(Budde et al., 2011)
pJV7 Δ sdr_A1	Km ^r , <i>sucB</i> , <i>H16_ΔA3164</i>	this study
pJV7 Δ sdr_B6	Km ^r , <i>sucB</i> , <i>H16_ΔB0101</i>	this study

pJV7 Δ est	Km ^r , <i>sucB</i> , H16_ Δ B1112	this study
pJV7H16_ Δ A1439	Km ^r , <i>sucB</i> , H16_ Δ A1439	this study

Table 22. Primers used in this study

Name	Number	Sequence 5'-3'	Cloning step
H16_A1168-del1	476	T <u>AGGATCCC</u> GGGCGGCCAGCACATCAAC	PCR-1, overlap extension PCR
H16_A1168-del2	477	TTATCTGTTAATTAAGCACATGGTGCCCCGGTTCGGAAAGG	PCR-1
H16_A1168-del3	478	TGCTTAATTAACAGATAAGCCGCACCCATCAAGCCATC	PCR-2
H16_A1168-del4	479	G <u>CGGATCC</u> CAGACCTCTTCGCCGACCTTG	PCR-2, overlap extension PCR
H16_A3164-del1	480	G <u>CCGGATCCC</u> CATATTTGCCATACTGTGGTGC	PCR-1, overlap extension PCR
H16_A3164-del2	481	TTCGCTCAGTCACGCATCTCGTGGTCTCTTTCTTGG	PCR-1
H16_A3164-del3	482	CGTGACTGAGCGAATGAACTGCGTGGGTGCAC	PCR-2
H16_A3164-del4	483	G <u>CGGATCCT</u> GGCAGCTCCACCTGGTAAG	PCR-2, overlap extension PCR
H16_B1297-del1	484	CG <u>CGGATCC</u> CATCCGGCCAAATGTGACCG	PCR-1, overlap extension PCR
H16_B1297-del2	485	TCTGTGAATTAGGCACATGATCGATCTCCGGTCTG	PCR-1
H16_B1297-del3	486	TGCCTAATTCACAGAACCTGACCCACCGGCGC	PCR-2
H16_B1297-del4	487	G <u>CGGATCC</u> GCACGTTGGTGATGACCGGA	PCR-2, overlap extension PCR
H16_B0101-del1	488	CG <u>CGGATCCC</u> CAGCGTTTCCTCATAGTTGGC	PCR-1, overlap extension PCR
H16_B0101-del2	489	TCTGTGAATTAGGCAGGTCATGGCAGTTTCCTTGGG	PCR-1
H16_B0101-del3	490	TGCCTAATTCACAGATGAGCCGTTGCCCGCCGG	PCR-2
H16_B0101-del4	491	AC <u>GATCCTT</u> GCACTGTGCGCGGGGATG	PCR-2, overlap extension PCR

H16_B1112-del1	492	<u>GCCGGATCCC</u> GGGTGAATGCCTGCATTG	PCR-1, overlap extension PCR
H16_B1112-del2	493	TCTGTGAATTAGGCACATGGCGTTGGCGCACGGC	PCR-1
H16_B1112-del3	494	TGCCTAATTCACAGATGAGCCGCTCCAGACAACCG	PCR-2
H16_B1112-del4	495	<u>GCCGGATCCC</u> GGGTCAATCGTGAAGAGCGG	PCR-2, overlap extension PCR
H16_A1439-del1	496	TTAG <u>GATCCC</u> ACGCTGGACAGCATGTCC	PCR-1, overlap extension PCR
H16_A1439-del2	497	TCTGTGAATTAGGCACATGTCCACTCCTTGATTGGC	PCR-1
H16_A1439-del3	498	TGCCTAATTCACAGATGACCTGCCGGCCTGGTT	PCR-2
H16_A1439-del4	499	<u>GCCGGATCCTT</u> CGTCACCAGACTTGGCGT	PCR-2, overlap extension PCR

Primers used to screen for re-integration event check:

SCDH A1-Nde fwd	78	CATATGAAACTGCAGGGTCGGG
SCDH A1-Nde rev	79	AAGCTTTCAGAGCGACATGCCGC
SCDH B6-Nde fwd	221	CAACATATGACCTCCACCCCAG
SCDH B6-Hind-rev	222	TACAAGCTTTCAGGCAAAGCCCC
H16_A1439-fwd	474	ATGACTCAGCGCATTGCGTATG
H16_A1439-rev	475	TCAGCCCATATGCAGGCCG
H16_B1112-fwd	262	CAGCATATGTCCGAGAAGCCAGGC
H16_B1112-rev	212	ATTAAGCTTTCAGCCGGCGGG

The underlined sequence represent additional *Bam*HI restriction site at the 5' ends of forward and reverse primers.

DNA preparation and manipulations and HPLC analysis were performed as described in Materials and methods section in chapter 3.1.2.

The first step of the gene deletion technique includes construction of the deletion vector for each gene of interest. An insert, which includes DNA sequence fragments upstream and downstream of the gene to be deleted, is cloned into pJV7 vector (Fig. 75). This vector carries *sacB*, a *Bacillus subtilis* gene encoding a levansucrase. In the presence of active levansucrase, the cells are not able to grow on sucrose-containing media. A kanamycin resistance gene is the second selective marker, present on the vector pJV7. After the transfer of deletion vector into the cells of *R. eutropha* H16, first recombination event happens via homologous DNA regions introduced into vector and the

whole sequence of the deletion vector is inserted next to the gene of interest. As Kan^r genes are also inserted into the genome, *R. eutropha* H16 acquires an ability to grow on kanamycin supplemented media and the conjugants can be selected for further analysis.

On the next step, the cells are grown in the media without kanamycin. The absence of the selective pressure lets the second recombination happen. After this event vector's backbone is cut out of the genomic DNA sequence, including *sacB* and Kan^r genes. As a result, the cells lose the ability to grow on the sucrose and kanamycin supplemented media and, therefore can be distinguished from the cells, where second recombination did not take place (Fig. 76).

The second recombination event can happen in two different ways. As one of the possible versions, the vector backbone is cut out together with the gene of interest, generating the desired knockout strain. Another situation includes excision of the vector backbone without the gene of interest, restoring the original situation in the genomic DNA sequence (Fig. 76). These two situations can be distinguished by the size of the colony PCR products (details are described below).

The initial step of vector construction includes amplification of the flanking 400-600 bp sequences, one directly upstream of the gene of interest and another directly downstream of the gene. Primers were designed in a way that the two fragments had identical 15-18 bp sequences at the ends for connection of the template DNA fragments in overlap extension PCR (Fig. 75). A single DNA fragment containing the upstream and downstream DNA fragments was created by overlap extension PCR. Primers used in the overlap PCR were designed in a way that the resulting fragment had *Bam*HI restriction sites at each end. The product of the overlap PCR was isolated and purified using the QIAquick gel extraction kit (Qiagen, Valencia, CA), digested with *Bam*HI, purified and then ligated into the backbone of integration vector pJV7, which was also digested with *Bam*HI (Table 21).

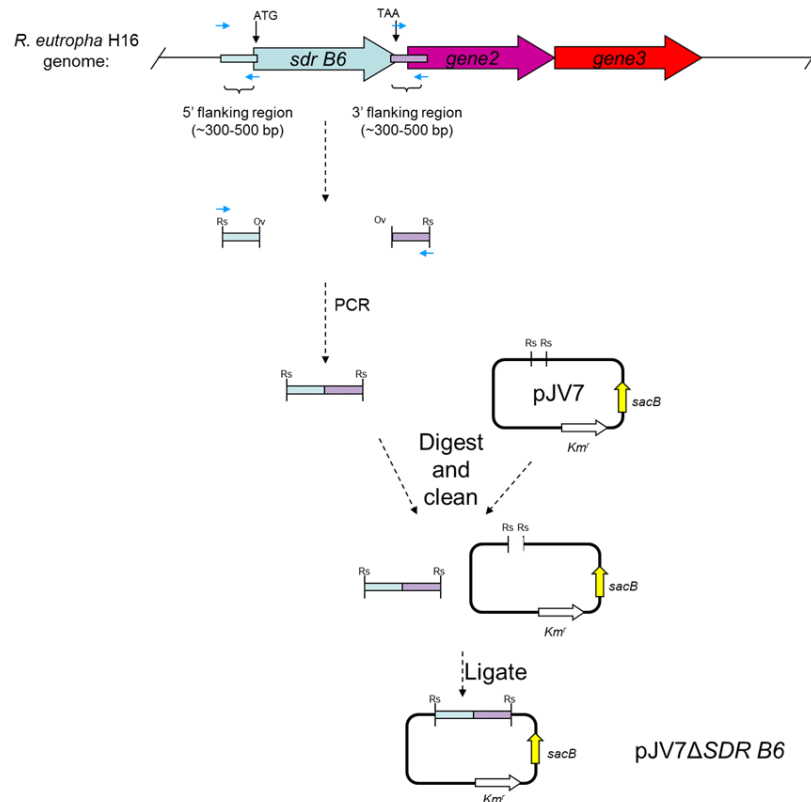


Figure 75. Schematic overview of the pJV7ΔSDR B6 construction. Rs - restriction site; ov - overlap region, *sacB* – levansucrase gene, *kmr* – kanamycin resistance gene. Construct of deletion vector includes four steps: PCRs of the homologous regions upstream and downstream gene to be deleted, overlap extension PCR to generate gene deletion insert, digestion of the overlap extension PCR product and the vector backbone with *Bam*HI and ligation of the deletion vector. Picture modified from lecture of Dr. C.J. Brigham.

Newly constructed gene deletion plasmids were transformed into *E. coli* S17-1 and introduced into *R. eutropha* by a standard mating procedure (Simon et al., 1983). Grown colonies of *R. eutropha* H16 were picked from the selection LB plates supplemented with 10 µg/ml gentamicin and 300 µg/ml kanamycin and grown overnight at 28°C and 100 rpm in TSB with 10 µg/mL gentamicin. On the next day they were plated out on an LB plate supplemented with 10 µg/ml gentamicin and 0.2 % fructose. The absence of kanamycin pressure allows to a certain extent for the second recombination event to occur, excising the kanamycin resistance gene and *sacB* gene from the genome (Fig. 76).

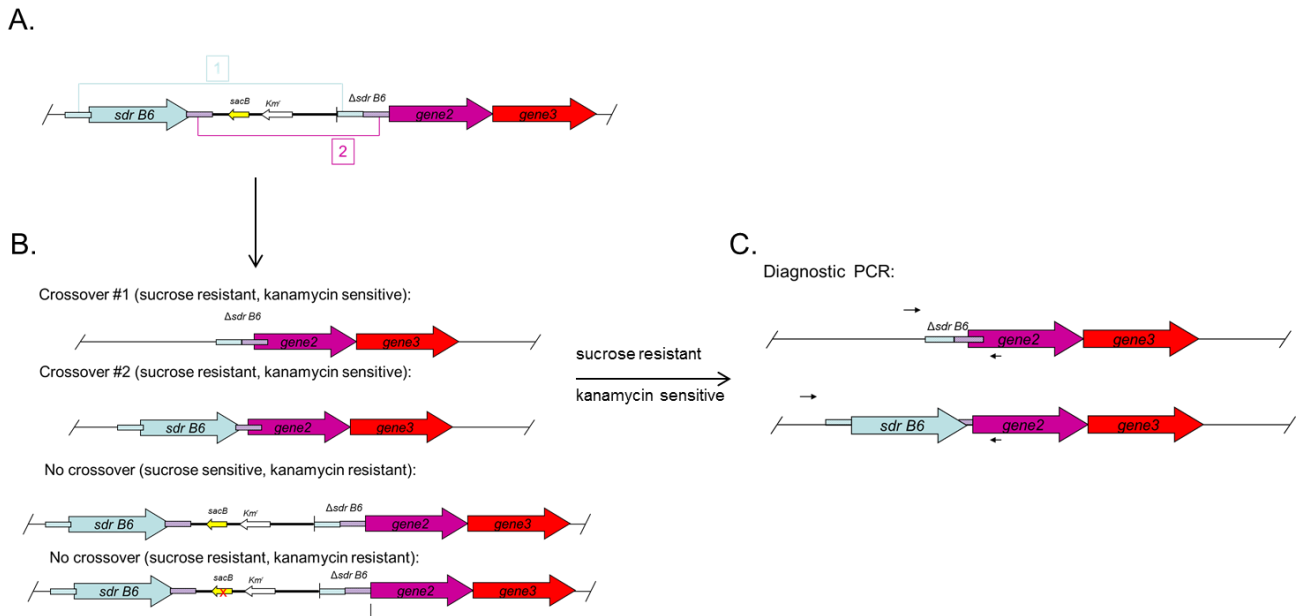


Figure 76. Illustration of the experiments for knockouts selection. *sacB* – levansucrase gene, *km^r* – kanamycin resistance gene. A – Second recombination event can happen in two ways, resulting in appearance of either crossover #1 or crossover #2. B – After growing the cells on the non-selective media 4 different strains can be distinguished: crossover #1 and crossover #2 don't grow on kanamycin-containing media but can grow on sucrose-containing media; non-crossover, in contrast, cannot grow on sucrose-containing media but can grow on kanamycin-containing media; the fourth possible type of strain is a non-crossover with defective *sacB* gene, which can grow both on sucrose and kanamycin-containing media; C – Crossover #1 and crossover #2 can be distinguished by the size of the colony PCR with the set primers, which binds outside the gene of interest, PCR product for deletion strain is smaller in size than the product of crossover #2 strain; Picture modified from lecture of Dr. C.J. Brigham.

sacB is a *B. subtilis* gene encoding a levansucrase (Kunst et al., 1997; Steinmetz et al., 1985). In the presence of 5% sucrose, the growth of Gram negative cells encoding *sacB* is inhibited. The precise mode of action is not yet completely understood. However, it was suggested that high amounts of produced levans (fructose polymers) which is built up and accumulated in periplasm could be toxic for the cells. As a result, by selecting for sucrose resistant cells we selected for the cells that have lost *sacB* gene or for the cells that have somehow inactivated it (Fig. 76). For this step of selection clones grown on LB_{Gm} plate were streaked out on two types of plates: LB supplemented with 0.2 % fructose, 10 µg/ml gentamicin and 300 µg/ml kanamycin; and LB supplemented with 0.2 % fructose, 10 µg/ml gentamicin and 5 % sucrose. The knockout colonies, which can grow on the plate with sucrose but not on the one with kanamycin, were selected and the deletions were confirmed using diagnostic colony PCR with the same set of the primers, which was used for overlap extension PCR and binds outside of the gene of interest (Table 22). As a last step, ready knockouts were also checked for a reintegration event with the corresponding forward and reverse primers to the gene (Table 22).

6.2.3. Results and discussion

pJV7 Δ SDR_A1, pJV7 Δ SDR_B6, pJV7 Δ Est and pJV7H16_ Δ A1439 deletion vectors were successfully designed (Fig. 77). However, for two other enzymes, SDR A5 and SDR B3 (locus H16_A1168 and H16_B1297), construction of deletion vectors failed due to unknown reasons. Despite the various conditions used for ligation experiments, such as use of polyethyleneglycol (PEG), use of ligase and reagents from different manufacturers, different time and temperature settings, various vector and insert concentrations and screening of significant amount of clones grown on the selective media, no positive colonies were detected after transformation of ligation mixtures.

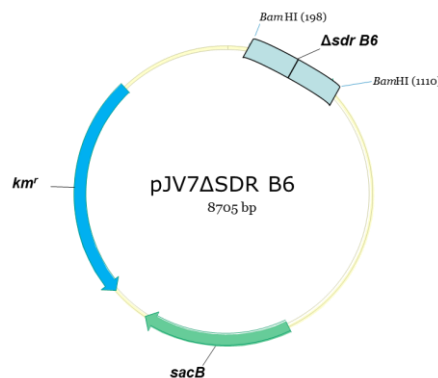


Figure 77. Illustration of pJV7 Δ SDR_B6. The integration vector with *sdr B6* gene deletion encodes kanamycin resistance gene *kmr* and levansucrase gene *sacB*; light blue squares indicate homologous regions for integration of the vector into the genome

In the next step, deletion vectors for other enzymes of interest were transferred into *R. eutropha* H16 via conjugation from the strain *E. coli* S17-1 carrying the corresponding deletion vector. After picking the positive transconjugants, antibiotic selective pressure was released by growing the cells in TSB_{Gm} medium only. Newly grown colonies were streaked out each on two different types of the selective plates, LB_{Gm+Km} and LB_{Gm+sucrose}, in order to reveal colonies where second recombination event has happened (Fig. 76). These clones are sucrose resistant and kanamycin sensitive at the same time. There are two types of the colonies: one is a desirable knockout strain and another one is a wild type strain, restored after the sequence of deletion vector was excised from the genomic DNA by second recombination event. They can be distinguished by colony PCR with the set primers which bind outside of the gene region. PCR product for the deletion strain will be smaller than the PCR product for the wild type strain. An example of colony PCR results for *R. eutropha* H16 Δ SDR_B6 could be seen in Figure 78.

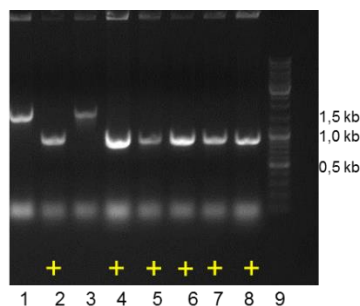


Figure 78. Agarose gel for colony PCR of *R. eutropha* H16 Δ SDR B6. 1, 3 – *R. eutropha* H16, product of the colony PCR for this strain is bigger in size (see Fig. 76), expected size 1.6 kb; 2, 4-8 – *R. eutropha* H16 Δ SDR B6 clones; product of the colony PCR for this strain is smaller in size (marked with plus) (see Fig. 76), expected size 0.9 kb; 9 - GeneRuler DNA Ladder Mix (0.5 μ g)

At a certain level there is a probability for reintegration of the excised gene sequence via the homologous regions. In order to reveal the clones where this has happened, colony PCR with the internal set of the primers to the corresponding gene sequence was performed. In case, when there was a clear band representing the amplified gene sequence on the agarose gel of colony PCR products, corresponding clones were discarded (Fig. 79). In contrast, positive knockout clones, which did not show the gene product obtained by colony PCR on the agarose gel, were preserved and forwarded to IMBT culture collection under numbers ## 7046-7049 (Supplementary Table 1).

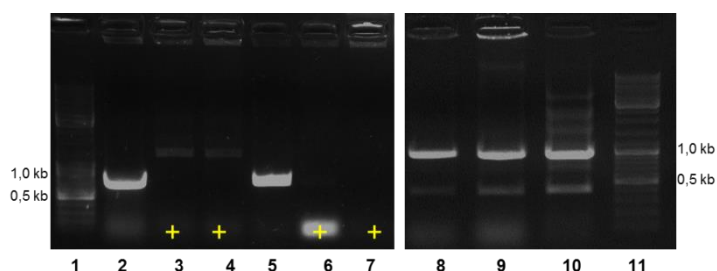


Figure 79. Agarose gels for colony PCR of *R. eutropha* H16 knockout strains with the corresponding internal set of the primers, reintegration event check. Controls were performed with the original genomic DNA of *R. eutropha* H16 as a template. Positive knockouts are marked with plus. 1, 11 – GeneRuler DNA Ladder Mix (0.5 μ g), 2 – *R. eutropha* H16, control for reintegration of *sdr A1* gene, expected size about 750 bp; 3-4 – *R. eutropha* H16/ Δ *sdr A1*; 5 – *R. eutropha* H16, control for reintegration check of *sdr B6* gene, expected size about 760 bp; 6-7 – *R. eutropha* H16/ Δ *sdr B6*; 8 – *R. eutropha* H16, control for reintegration check of *est* gene, expected size about 975 bp; 9-10 – *R. eutropha* H16/ Δ *est*

Four dehydrogenases (SDR A1, SDR A5, SDR B3 and SDR B6) characterized in chapter 3.1 (locus *H16_A3164*, *H16_A1168*, *H16_B1297* and *H16_B0101*, respectively), one esterase/lipase (Est) characterized in Section 4.1 (locus *H16_B1112*) were chosen for the construction of *R. eutrophas* knockout strains in order to learn gene knockout technique. Additionally, acetoacetyl-CoA reductase (locus *H16_A1439*), was selected for deletion. This enzyme does not participate in the maintenance of basic cellular function and was shown to be 3.4 times upregulated under lithoautotrophic growth conditions (Schwartz et al., 2009). As a member of oxidoreductase class of

enzymes, it requires NADPH as cofactor. By using this knockout strain growing in lithoautotrophic environment, additional reducing equivalents could be available for the oxidoreduction reactions of biotechnological interests.

R. eutropha H16/H16_ΔA1439 deletion strain and *R. eutropha* H16, both carrying pKRSF1010-P_{J5}-SDR B3-cymR plasmid, were used to compare activity of the overexpressed short chain dehydrogenase B3, which requires NADPH as cofactor. 2-phenylacetaldehyde was added as a substrate to the lithoautotrophically grown cultures, induced by cumate, at OD₆₀₀ = 5.0. After 3 hours of incubation with the substrate samples were analysed by HPLC. In more detail the method is described in chapter 3.1.2.16. In the first attempt, preliminary data showed that there is no significant difference in the rate of conversion for *R. eutropha* H16 [pKRSF1010-P_{J5}-SDR B3-cymR] and *R. eutropha* H16/H16_ΔA1439 [pKRSF1010-P_{J5}-SDR B3-cymR]. On the base of these results it can be speculated that acetoacetyl-CoA reductase, which is upregulated under lithoautotrophic growth conditions, does not interfere with the activity of overexpressed short-chain dehydrogenase.

6.2.4. Conclusions

- Four knockout strains, *R. eutropha* H16/ Δ *sdr A1*, *R. eutropha* H16/ Δ *sdr B6*, *R. eutropha* H16/ Δ *est* and *R. eutropha* H16/*H16_* Δ *A1439* were created
- Preliminary data indicate that reduction potential of *R. eutropha* H16 under lithoautotrophic growth conditions is high enough to meet the demands of overexpressed NADPH-dependent oxidoreductase
- The method was established in the group of Mag.rer.nat. Dr.rer.nat. Petra Heidinger and Univ.-Prof.i.R. Dipl.-Ing. Dr.techn. Helmut Schwab

7. Supplementary information

Table S.1. List of the strains handed over to the IMBT collection.

Name	Number
<i>R. eutropha</i> H16/ Δ sdr B6	7046
<i>R. eutropha</i> H16/H16_ Δ A1439	7047
<i>R. eutropha</i> H16/ Δ sdr A1	7048
<i>R. eutropha</i> H16/ Δ est	7049
<i>E. coli</i> TOP10 [pK470]	7597
<i>E. coli</i> XL1 [pK470-ADH A1]	7598
<i>E. coli</i> XL1 [pK470-ADH A1]	7599
<i>E. coli</i> XL1 [pK470-ADH A4]	7600
<i>E. coli</i> TOP10 [pK470-ADH A5]	7601
<i>E. coli</i> TOP10 [pK470-ADH B1]	7602
<i>E. coli</i> TOP10 [pK470-ADH B2]	7603
<i>E. coli</i> XL1 [pK470-ADH B5]	7604
<i>E. coli</i> XL1 [pK470-ADH B6]	7605
<i>E. coli</i> XL1 [pK470-ADH B8]	7606
<i>E. coli</i> XL1 [pK470-ADH P1]	7607
<i>E. coli</i> TOP10 [pK470-ADH P2]	7608
<i>E. coli</i> XL1 [pK470-SDR A1]	7609
<i>E. coli</i> TOP10 [pK470-SDR A2]	7610
<i>E. coli</i> TOP10 [pK470-SDR A3]	7611
<i>E. coli</i> TOP10 [pK470-SDR A4]	7612
<i>E. coli</i> TOP10 [pK470-SDR B1]	7613
<i>E. coli</i> TOP10 [pK470-SDR B2]	7614
<i>E. coli</i> XL1 [pK470-SDR B3]	7615
<i>E. coli</i> TOP10 [pK470-SDR B4]	7616
<i>E. coli</i> TOP10 [pK470-SDR B6]	7617
<i>E. coli</i> TOP10 [pK470-SDR B7]	7618
<i>E. coli</i> TOP10 [pK470-SDR B9]	7619
<i>E. coli</i> TOP10 [pK470-SDR B11]	7620

<i>E. coli</i> TOP10 [pK470-RED A1]	7621
<i>E. coli</i> XL1 [pK470-RED A2]	7622
<i>E. coli</i> TOP10 [pK470-RED A4]	7623
<i>E. coli</i> TOP10 [pK470-RED A5]	7624
<i>E. coli</i> TOP10 [pK470-RED A6]	7625
<i>E. coli</i> TOP10 [pK470-RED A9]	7626
<i>E. coli</i> TOP10 [pK470-RED A10]	7627
<i>E. coli</i> TOP10 [pK470-RED A11]	7628
<i>E. coli</i> TOP10 [pK470-RED B1]	7629
<i>E. coli</i> TOP10 [pK470-RED B4]	7630
<i>E. coli</i> TOP10 [pK470-His ₆ -ADH A5]	7631
<i>E. coli</i> TOP10 [pK470-His ₆ -SDR A5]	7632
<i>E. coli</i> TOP10 [pK470-Est]	7633
<i>E. coli</i> TOP10 [pMT-A_EstX]	7634
<i>E. coli</i> TOP10 [pK470-EstX]	7635
<i>E. coli</i> XL1 [pKR-P _{tac} - Δ lacI-par-ADH A5]	7636
<i>E. coli</i> XL1 [pKR-P _{tac} - Δ lacI-par-ADH A4]	7637
<i>E. coli</i> TOP10 [pKR-P _{tac} - Δ lacI-par-His ₆ -SDR B3]	7638
<i>E. coli</i> TOP10 [pKR-P _{lac} - Δ lacI-Par- His ₆ -SDR B3]	7639
<i>E. coli</i> TOP10 [pKR-P _{tac} -par-T7MCS-lacI-His ₆ -SDR B3]	7640
<i>E. coli</i> TOP10 [pKR-P _{tac} -par-T7Pol/T7MCS-lacI-His ₆ -SDR B3]	7641
<i>E. coli</i> TOP10 [pKR-P _{tac} -par-T7Pol/T7MCS-lacI-His ₆ -SDR B3-mob]	7642
<i>E. coli</i> TOP10 [pKR-P _{tac} -par-mob-SDR A1]	7643
<i>E. coli</i> TOP10 [pKR-P _{tac} - par-mob-SDR B3]	7644
<i>E. coli</i> TOP10 [pKR-P _{tac} -par-mob-SDR B6]	7645
<i>E. coli</i> TOP10 [pKR-P _{tac} -par-mob-His ₆ -ADH A5]	7646
<i>E. coli</i> TOP10 [pKR-P _{tac} -par-mob-His ₆ -SDR A1]	7647
<i>E. coli</i> TOP10 [pKR-P _{tac} -par-mob-His ₆ -SDR B3]	7648
<i>E. coli</i> TOP10 [pKR-P _{tac} -par-mob-His ₆ -SDR B6]	7649

<i>E. coli</i> TOP10 [pKREP-P _{T5} -Δinsert]	7650
<i>E. coli</i> TOP10 [pKREP-P _{T5} -ADH A5]	7651
<i>E. coli</i> TOP10 [pKREP-P _{T5} -SDR A1]	7652
<i>E. coli</i> TOP10 [pKREP-P _{T5} -SDR B3]	7653
<i>E. coli</i> TOP10 [pKREP-P _{T5} -SDR B6]	7654
<i>E. coli</i> TOP10 [pKREP-P _{T5} -His ₆ -ADH A5]	7655
<i>E. coli</i> TOP10 [pKREP-P _{T5} -His ₆ -SDR B3]	7656
<i>E. coli</i> TOP10 [pKRSF1010-P _{T5} -ADH A5]	7657
<i>E. coli</i> TOP10 [pKRSF1010-P _{T5} -SDR A1]	7658
<i>E. coli</i> TOP10 [pKRSF1010-P _{T5} -SDR B3]	7659
<i>E. coli</i> TOP10 [pKRSF1010-P _{T5} -SDR B6]	7660
<i>E. coli</i> TOP10 [pKRSF1010-P _{T5} - His ₆ -ADH A5]	7661
<i>E. coli</i> TOP10 [pKRSF1010-P _{T5} - His ₆ -SDR B3]	7662
<i>E. coli</i> TOP10 [pKRSF1010-P _{Tac} -Δinsert]	7663
<i>E. coli</i> TOP10 [pKRSF1010-P _{j5} -SDR B3-cymR]	7664
<i>E. coli</i> TOP10 [pKRSF1010-P _{j5} -cyOO-His ₆ -ADH A5-cymR]	7665
<i>E. coli</i> TOP10 [pKRSF1010-P _{j5} -cyOO- His ₆ -SDR B3-cymR]	7666
<i>E. coli</i> TOP10 [pMS470-His ₆ -RasAIDH]	7667
<i>E. coli</i> TOP10 [pKRSF1010-P _{j5} -TA-cymR]	7668
<i>E. coli</i> TOP10 [pKRSF1010-P _{j5} -cyOO-AlaDH-cymR]	7669
<i>E. coli</i> TOP10 [pKRSF1010-P _{j5} -His ₆ -AlaDH-cymR]	7670
<i>E. coli</i> TOP10 [pKRSF1010-P _{j5} -ReAlaDH-cymR]	7671
<i>E. coli</i> TOP10 [pKRSF1010-P _{j5} -PotRIRED-cymR]	7672
<i>E. coli</i> TOP10 [pKRSF1010-P _{j5} -PotSIREDC-cymR]	7673
<i>E. coli</i> TOP10 [pKRSF1010-P _{j5} -cyOO-RIRED-cymR]	7674
<i>E. coli</i> TOP10 [pKRSF1010-P _{j5} -cyOO-SIREDC-cymR]	7675
<i>E. coli</i> S17-1 [pJV7Δsdr A1]	7676
<i>E. coli</i> S17-1 [pJV7Δsdr B6]	7677
<i>E. coli</i> S17-1 [pJV7Δest]	7678

E. coli S17-1 [pJV7H16_ΔA1439]

7679

E. coli TOP10 [pJV7]

7680

8. References

- Aehle, W., 2006. *Enzymes in Industry: Products and Applications*. John Wiley & Sons.
- Amako, K., Fujita, K., Iwamoto, C., Sengee, M., Fuchigami, K., Fukumoto, J., Ogishi, Y., Kishimoto, R., Goda, K., 2006a. NADP⁺-Dependent *D*-Arabinose Dehydrogenase Shows a Limited Contribution to Erythroascorbic Acid Biosynthesis and Oxidative Stress Resistance in *Saccharomyces cerevisiae*. *Biosci. Biotechnol. Biochem.* 70, 3004–3012. doi:10.1271/bbb.60399
- Amako, K., Fujita, K., Shimohata, T., Hasegawa, E., Kishimoto, R., Goda, K., 2006b. NAD⁺-specific d-arabinose dehydrogenase and its contribution to erythroascorbic acid production in *Saccharomyces cerevisiae*. *FEBS Lett.* 580, 6428–6434. doi:10.1016/j.febslet.2006.10.058
- Andersson, M., Holmberg, H., Adlercreutz, P., 1998. Evaluation of *Alcaligenes eutrophus* cells as an NADH regenerating catalyst in organic-aqueous two-phase system. *Biotechnol. Bioeng.* 57, 79–86. doi:10.1002/(SICI)1097-0290(19980105)57:1<79::AID-BIT10>3.0.CO;2-3
- Aragno, M., Schlegel, H.G., 1992. The mesophilic hydrogen-oxidizing (knallgas) bacteria., in: Balows, A., Trüper, H.G., Dworkin, M., Hader, W., Schleifer, K.-H. (Eds.), *The Prokaryotes*. Springer-Verlag Inc., pp. 344–384.
- Armstrong, F.A., Vincent, K.A., Friedrich, B., Lenz, O., 2006. Biochemical fuel cell.
- Atlić, A., Koller, M., Scherzer, D., Kutschera, C., Grillo-Fernandes, E., Horvat, P., Chiellini, E., Braunegg, G., 2011. Continuous production of poly([R]-3-hydroxybutyrate) by *Cupriavidus necator* in a multistage bioreactor cascade. *Appl. Microbiol. Biotechnol.* 91, 295–304. doi:10.1007/s00253-011-3260-0
- Atsumi, S., Hanai, T., Liao, J.C., 2008. Non-fermentative pathways for synthesis of branched-chain higher alcohols as biofuels. *Nature* 451, 86–89. doi:10.1038/nature06450
- Baker, P.J., Britton, K.L., Fisher, M., Esclapez, J., Pire, C., Bonete, M.J., Ferrer, J., Rice, D.W., 2009. Active site dynamics in the zinc-dependent medium chain alcohol dehydrogenase superfamily. *Proc. Natl. Acad. Sci. U. S. A.* 106, 779–784. doi:10.1073/pnas.0807529106
- Barnard, G.C., Henderson, G.E., Srinivasan, S., Gerngross, T.U., 2004. High level recombinant protein expression in *Ralstonia eutropha* using T7 RNA polymerase based amplification. *Protein Expr. Purif.* 38, 264–271. doi:10.1016/j.pep.2004.09.001
- Barski, O. a, Tipparaju, S.M., Bhatnagar, A., 2008. The aldo-keto reductase superfamily and its role in drug metabolism and detoxification., *Drug metabolism reviews.* doi:10.1080/03602530802431439.
- Bi, C., Su, P., Müller, J., Yeh, Y.-C., Chhabra, S.R., Beller, H.R., Singer, S.W., Hillson, N.J., 2013. Development of a broad-host synthetic biology toolbox for *ralstonia eutropha* and its application to engineering hydrocarbon biofuel production. *Microb. Cell Fact.* 12, 107. doi:10.1186/1475-2859-12-107
- Biasini, M., Bienert, S., Waterhouse, a., Arnold, K., Studer, G., Schmidt, T., Kiefer, F., Cassarino, T.G., Bertoni, M., Bordoli, L., Schwede, T., 2014. SWISS-MODEL: modelling protein tertiary and

- quaternary structure using evolutionary information. *Nucleic Acids Res.* 42, W252–W258. doi:10.1093/nar/gku340
- Bömmer, D., Schäferjohann, J., Bowien, B., 1996. Identification of *cbbBc* as an additional distal gene of the chromosomal *cbb* CO₂ fixation operon from *Ralstonia eutropha*. *Arch. Microbiol.* 166, 245–51.
- Bongers, L., 1967. Phosphorylation in hydrogen bacteria. *J. Bacteriol.* 93, 1615–23.
- Bowien, B., Kusian, B., 2002. Genetics and control of CO₂ assimilation in the chemoautotroph *Ralstonia eutropha*. *Arch. Microbiol.* 178, 85–93. doi:10.1007/s00203-002-0441-3
- Boyer, H.W., Roulland-Dussoix, D., Francisco, S., Francisco, B., 1969. A Complementation Analysis of the Restriction and Modification of DNA in *Escherichia coli*. *J. Mol. Biol.* 41, 459–472.
- Brigham, C.J., Budde, C.F., Holder, J.W., Zeng, Q., Mahan, A.E., Rha, C., Sinskey, A.J., 2010. Elucidation of beta-oxidation pathways in *Ralstonia eutropha* H16 by examination of global gene expression. *J. Bacteriol.* 192, 5454–5464. doi:10.1128/JB.00493-10
- Brigham, C.J., Gai, C.S., Lu, J., Speth, D.R., Worden, R.M., Sinskey, A.J., 2012a. *Advanced Biofuels and Bioproducts*. Springer New York, New York, NY. doi:10.1007/978-1-4614-3348-4
- Brigham, C.J., Kurosawa, K., Rha, C., Sinskey, A.J., 2011. Bacterial Carbon Storage to Value Added Products. *Microb. Biochem. Technol.* doi:10.4172/1948-5948.S3-002
- Brigham, C.J., Speth, D.R., Rha, C., Sinskey, A.J., 2012b. Whole-genome microarray and gene deletion studies reveal regulation of the polyhydroxyalkanoate production cycle by the stringent response in *Ralstonia eutropha* H16. *Appl. Environ. Microbiol.* 78, 8033–8044. doi:10.1128/AEM.01693-12
- Brigham, C.J., Zhila, N., Shisgatskaya, E., Volova, T.G., Sinskey, A.J., 2012c. Manipulation of *Ralstonia eutropha* carbon storage pathways to produce useful bio-based products, in: *Reprogramming Microbial Metabolic Pathways*. pp. 343–366. doi:10.1007/978-94-007-5055-5
- Brownlee, M., 1995. Advanced protein glycosylation in diabetes and aging. *Annu. Rev. Med.* 46, 223–234. doi:10.1146/annurev.med.46.1.223
- Budde, C.F., Riedel, S.L., Willis, L.B., Rha, C., Sinskey, A.J., 2011. Production of poly(3-hydroxybutyrate-co-3-hydroxyhexanoate) from plant oil by engineered *Ralstonia eutropha* strains. *Appl. Environ. Microbiol.* 77, 2847–2854. doi:10.1128/AEM.02429-10
- Buhrke, T., Lenz, O., Krauss, N., Friedrich, B., 2005. Oxygen tolerance of the H₂-sensing [NiFe] hydrogenase from *Ralstonia eutropha* H16 is based on limited access of oxygen to the active site. *J. Biol. Chem.* 280, 23791–23796. doi:10.1074/jbc.M503260200
- Burgdorf, T., Bömmer, D., Bowien, B., 2001. Involvement of an unusual *mol* operon in molybdopterin cofactor biosynthesis in *Ralstonia eutropha*. *J. Mol. Microbiol. Biotechnol.* 3, 619–29.
- Burgdorf, T., Lenz, O., Buhrke, T., Van Der Linden, E., Jones, A.K., Albracht, S.P.J., Friedrich, B., 2006. [NiFe]-hydrogenases of *Ralstonia eutropha* H16: Modular enzymes for oxygen-tolerant biological hydrogen oxidation. *J. Mol. Microbiol. Biotechnol.* 10, 181–196. doi:10.1159/000091564

- Cantet, J., Bergel, A., Comtat, M., 1996. Coupling of the electroenzymatic reduction of NAD⁺ with a synthesis reaction. *Enzyme Microb. Technol.* 18, 72–79. doi:10.1016/0141-0229(96)00059-2
- Castric, K.F., Castric, P. a, 1983. Method for rapid detection of cyanogenic bacteria. *Appl. Environ. Microbiol.* 45, 701–2.
- Chahiniana, H., Sarda, L., 2009. Distinction Between Esterases and Lipases: Comparative Biochemical Properties of Sequence-Related Carboxylesterases | BenthamScience. *Protein Pept. Lett.* 16, 1149–1161. doi:10.2174/092986609789071333#sthash.7TMMZo10.dpuf
- Chenault, H. Keith Simon, Ethan S. Whitesides, G.M., 1988. Cofactor regeneration for enzyme catalysed synthesis. *Biotechnol. Genet. Eng. Rev.* doi:10.1080/02648725.1988.10647849
- Citron, B. a, Milstien, S., Gutierrez, J.C., Levine, R. a, Yanak, B.L., Kaufman, S., 1990. Isolation and expression of rat liver sepiapterin reductase cDNA. *Proc. Natl. Acad. Sci. U. S. A.* 87, 6436–6440. doi:10.1073/pnas.87.16.6436
- Cramm, R., 2008. Genomic view of energy metabolism in *Ralstonia eutropha* H16. *J. Mol. Microbiol. Biotechnol.* 16, 38–52. doi:10.1159/000142893
- Davies, N.M., Teng, X.W., 2003. Importance of Chirality in Drug Therapy and Pharmacy Practice : Implications for Psychiatry I, 242–252.
- Davis, D.H., Doudoroff, M., Stanier, R.Y., Mandel, M., 1969. Proposal to reject the genus *Hydrogenomonas*: taxonomic implications. *Int. J. Syst. Bacteriol.* 19, 375–390.
- Degenhardt, T.P., Thorpe, S.R., Baynes, J.W., 1998. Chemical modification of proteins by methylglyoxal. *Cell. Mol. Biol. (Noisy-le-grand)*. 44, 1139–45.
- Delamarre, S.C., Batt, C. a., 2006. Comparative study of promoters for the production of polyhydroxyalkanoates in recombinant strains of *Wautersia eutropha*. *Appl. Microbiol. Biotechnol.* 71, 668–679. doi:10.1007/s00253-005-0217-1
- Di Tommaso, P., Moretti, S., Xenarios, I., Orobittg, M., Montanyola, A., Chang, J.M., Taly, J.F., Notredame, C., 2011. T-Coffee: A web server for the multiple sequence alignment of protein and RNA sequences using structural information and homology extension. *Nucleic Acids Res.* 39, 13–17. doi:10.1093/nar/gkr245
- Drepper, T., Eggert, T., Hummel, W., Leggewie, C., Pohl, M., Rosenau, F., Wilhelm, S., Jaeger, K.E., 2006. Novel biocatalysts for white biotechnology. *Biotechnol. J.* 1, 777–786. doi:10.1002/biot.200600059
- Dudzik, A., Snoch, W., Borowiecki, P., Opalinska-Piskorz, J., Witko, M., Heider, J., Szaleniec, M., 2015. Asymmetric reduction of ketones and β -keto esters by (S)-1-phenylethanol dehydrogenase from denitrifying bacterium *Aromatoleum aromaticum*. *Appl. Microbiol. Biotechnol.* 99, 5055–5069. doi:10.1007/s00253-014-6309-z
- Dumon-Seignovert, L., Cariot, G., Vuillard, L., 2004. The toxicity of recombinant proteins in *Escherichia coli*: a comparison of overexpression in BL21(DE3), C41(DE3), and C43(DE3). *Protein Expr. Purif.* 37, 203–206. doi:10.1016/j.pep.2004.04.025

- Ewering, C., Heuser, F., Benölken, J.K., Brämer, C.O., Steinbüchel, A., 2006. Metabolic engineering of strains of *Ralstonia eutropha* and *Pseudomonas putida* for biotechnological production of 2-methylcitric acid. *Metab. Eng.* 8, 587–602. doi:10.1016/j.ymben.2006.05.007
- Felsenstein, J., 2005. PHYLIP (Phylogeny Inference Package) version 3.6.
- Figurski, D.H., Helinski, D.R., 1979. Replication of an origin-containing derivative of plasmid RK2 dependent on a plasmid function provided in trans. *Proc. Natl. Acad. Sci. U. S. A.* 76, 1648–1652. doi:10.1073/pnas.76.4.1648
- Fojan, P., Jonson, P.H., Petersen, M.T.N., Petersen, S.B., 2000. What distinguishes an esterase from a lipase: A novel structural approach. *Biochimie* 82, 1033–1041. doi:10.1016/S0300-9084(00)01188-3
- Franz, A., Rehner, R., Kienle, A., Grammel, H., 2012. Rapid selection of glucose-utilizing variants of the polyhydroxyalkanoate producer *Ralstonia eutropha* H16 by incubation with high substrate levels. *Lett. Appl. Microbiol.* 54, 45–51. doi:10.1111/j.1472-765X.2011.03171.x
- Friedrich, B., Hogrefe, C., Schlegel, H.G., 1981. Naturally occurring genetic transfer of hydrogen-oxidizing ability between strains of *Alcaligenes eutrophus*. *J. Bacteriol.* 147, 198–205.
- Friedrich, B., Schwartz, E., 1993. Molecular biology of hydrogen utilization in aerobic chemolithotrophs. *Annu. Rev. Microbiol.* 47, 351–83.
- Fritsch, J., Lenz, O., Friedrich, B., 2013. Structure, function and biosynthesis of O₂-tolerant hydrogenases. *Nat. Rev. Microbiol.* 11, 106–14. doi:10.1038/nrmicro2940
- Fritsch, J., Lenz, O., Friedrich, B., 2011. The maturation factors HoxR and HoxT contribute to oxygen tolerance of membrane-bound [NiFe] hydrogenase in *Ralstonia eutropha* H16. *J. Bacteriol.* 193, 2487–2497. doi:10.1128/JB.01427-10
- Fukui, T., Abe, H., Doi, Y., 2002. Engineering of *Ralstonia eutropha* for production of poly(3-hydroxy-co-3-hydroxyhexanoate) from fructose and solid-state properties of the copolymer. *Biomacromolecules* 3, 618–624.
- Fukui, T., Mukoyama, M., Orita, I., Nakamura, S., 2014. Enhancement of glycerol utilization ability of *Ralstonia eutropha* H16 for production of polyhydroxyalkanoates. *Appl. Microbiol. Biotechnol.* 98, 7559–68. doi:10.1007/s00253-014-5831-3
- Fukui, T., Ohsawa, K., Mifune, J., Orita, I., Nakamura, S., 2011. Evaluation of promoters for gene expression in polyhydroxyalkanoate-producing *Cupriavidus necator* H16. *Appl. Microbiol. Biotechnol.* 89, 1527–36. doi:10.1007/s00253-011-3100-2
- Gai, C.S., Lu, J., Brigham, C.J., Bernardi, A.C., Sinskey, A.J., 2014. Insights into bacterial CO₂ metabolism revealed by the characterization of four carbonic anhydrases in *Ralstonia eutropha* H16. *AMB Express* 4, 2. doi:10.1186/2191-0855-4-2
- Gand, M., Müller, H., Wardenga, R., Höhne, M., 2014. Characterization of three novel enzymes with imine reductase activity. *J. Mol. Catal. B Enzym.* 110, 126–132. doi:10.1016/j.molcatb.2014.09.017

- Goldberg, J.B., Ohman, D.E., 1984. Cloning and expression in *Pseudomonas aeruginosa* of a gene involved in the production of alginate. *J. Bacteriol.* 158, 1115–1121.
- Goldberg, K., Schroer, K., Lütz, S., Liese, A., 2007. Biocatalytic ketone reduction - A powerful tool for the production of chiral alcohols - Part II: Whole-cell reductions. *Appl. Microbiol. Biotechnol.* 76, 249–255. doi:10.1007/s00253-007-1005-x
- Gottschalk, G., Eberhardt, U., 1964. Utilization of fructose by *Hydrogenomonas H16*. *Arch. Mikrobiol.* 48, 95–108.
- Green, M.R., Sambrook, J., 2012. *Molecular cloning: a laboratory manual*, Cold Sprin. ed.
- Grousseau, E., Lu, J., Gorret, N., Guillouet, S.E., Sinskey, A.J., 2014. Isopropanol production with engineered *Cupriavidus necator* as bioproduction platform. *Appl. Microbiol. Biotechnol.* 98, 4277–90. doi:10.1007/s00253-014-5591-0
- Gruber, S., Hagen, J., Schwab, H., Koefinger, P., 2014. Versatile and stable vectors for efficient gene expression in *Ralstonia eutropha H16*. *J. Biotechnol.* 186, 74–82. doi:10.1016/j.jbiotec.2014.06.030
- Gruber, S., Schwab, H., Koefinger, P., 2015. Versatile plasmid-based expression systems for Gram-negative bacteria—General essentials exemplified with the bacterium *Ralstonia eutropha H16*. *N. Biotechnol.* 00. doi:10.1016/j.nbt.2015.03.015
- Hanukoglu, I., 2015. Proteopedia: Rossmann fold: A beta-alpha-beta fold at dinucleotide binding sites. *Biochem. Mol. Biol. Educ.* 43, 206–9. doi:10.1002/bmb.20849
- Hartley, D.L., Kane, J.F., 1988. Properties of inclusion bodies from recombinant *Escherichia coli*. *Biochem. Soc. Trans.* 16, 101–102.
- Heumann, H., 2000. Method for labeling biopolymers using isotopes.
- Höffken, H.W., Duong, M., Friedrich, T., Breuer, M., Hauer, B., Reinhardt, R., Rabus, R., Heider, J., Ho, H.W., 2006. Crystal Structure and Enzyme Kinetics of the (S)-Specific 1-Phenylethanol Dehydrogenase of the Denitrifying Bacterium Strain EbN1. *Filtration* 45, 82–93. doi:10.1021/bi051596b
- Hollmann, F., Hofstetter, K., Schmid, a., 2006. Non-enzymatic regeneration of nicotinamide and flavin cofactors for monooxygenase catalysis. *Trends Biotechnol.* 24, 163–171. doi:10.1016/j.tibtech.2006.02.003
- Holzer, A.K., Hiebler, K., Mutti, F.G., Simon, R.C., Lauterbach, L., Lenz, O., Kroutil, W., 2015. Asymmetric Biocatalytic Amination of Ketones at the Expense of NH₃ and Molecular Hydrogen. *Org. Lett.* 17, 2431–2433. doi:10.1021/acs.orglett.5b01154
- Hoyos, P., Sinisterra, J.-V., Molinari, F., Alcántara, A.R., Domínguez de María, P., 2010. Biocatalytic strategies for the asymmetric synthesis of alpha-hydroxy ketones. *Acc. Chem. Res.* 43, 288–299. doi:10.1021/ar900196n
- Huber, T., Schneider, L., Präg, A., Gerhardt, S., Einsle, O., Müller, M., 2014. Direct Reductive Amination of Ketones: Structure and Activity of S-Selective Imine Reductases from *Streptomyces*. *ChemCatChem* 6, 2248–2252. doi:10.1002/cctc.201402218

- Huisman, G.W., Liang, J., Krebber, A., 2010. Practical chiral alcohol manufacture using ketoreductases. *Curr. Opin. Chem. Biol.* 14, 122–129. doi:10.1016/j.cbpa.2009.12.003
- Hummel, W., 1999. Large-scale applications of NAD(P)-dependent oxidoreductases: recent developments. *Trends Biotechnol.* 17, 487–492. doi:10.1016/S0167-7799(98)01207-4
- Hummel, W., 1997. New alcohol dehydrogenases for the synthesis of chiral compounds, *Advances in Biochemical Engineering/Biotechnology*. Springer Berlin Heidelberg, Berlin, Heidelberg. doi:10.1007/BFb0103299
- Hummel, W., Kula, M.-R., 1989. Dehydrogenases for the synthesis of chiral compounds. *Eur. J. Biochem.* 184, 1–13. doi:10.1111/j.1432-1033.1989.tb14983.x
- Hyeon, J.E., Kim, S.W., Park, C., Han, S.O., 2015. Efficient biological conversion of carbon monoxide (CO) to carbon dioxide (CO₂) and for utilization in bioplastic production by *Ralstonia eutropha* through the display of an enzyme complex on the cell surface. *Chem. Commun.* 51, 10202–10205. doi:10.1039/C5CC00832H
- Hyndman, D., Bauman, D.R., Heredia, V. V., Penning, T.M., 2003. The aldo-keto reductase superfamily homepage. *Chem. Biol. Interact.* 143-144, 621–631. doi:10.1016/S0009-2797(02)00193-X
- Ihara, M., Nishihara, H., Yoon, K.-S., Lenz, O., Friedrich, B., Nakamoto, H., Kojima, K., Honma, D., Kamachi, T., Okura, I., 2006. Light-driven hydrogen production by a hybrid complex of a [NiFe]-hydrogenase and the cyanobacterial photosystem I. *Photochem. Photobiol.* 82, 676–682. doi:10.1562/2006-01-16-RA-778
- Insomphun, C., Mifune, J., Orita, I., Numata, K., Nakamura, S., Fukui, T., 2014. Modification of β -oxidation pathway in *Ralstonia eutropha* for production of poly(3-hydroxybutyrate-co-3-hydroxyhexanoate) from soybean oil. *J. Biosci. Bioeng.* 117, 184–190. doi:10.1016/j.jbiosc.2013.07.016
- Insomphun, C., Xie, H., Mifune, J., Kawashima, Y., Orita, I., Nakamura, S., Fukui, T., 2015. Improved artificial pathway for biosynthesis of poly(3-hydroxybutyrate-co-3-hydroxyhexanoate) with high C₆-monomer composition from fructose in *Ralstonia eutropha*. *Metab. Eng.* 27, 38–45. doi:10.1016/j.ymben.2014.10.006
- Itoh, N., Morihama, R., Wang, J., Okada, K., Mizuguchi, N., 1997. Purification and characterization of phenylacetaldehyde reductase from a styrene-assimilating *Corynebacterium* strain, ST-10. *Appl. Environ. Microbiol.* 63, 3783–3788.
- Jaeger, K.E., Dijkstra, B.W., Reetz, M.T., 1999. Bacterial biocatalysts: molecular biology, three-dimensional structures, and biotechnological applications of lipases. *Annu. Rev. Microbiol.* 53, 315–351. doi:10.1146/annurev.micro.53.1.315
- Jajesniak, P., Eldin, H., Omar, M., Wong, T.S., 2014. Carbon Dioxide Capture and Utilization using Biological Systems: Opportunities and Challenges. *Bioprocess. Biotech.* 4, 15. doi:10.4172/2155-9821.1000155
- Jeon, J.M., Brigham, C.J., Kim, Y.H., Kim, H.J., Yi, D.H., Kim, H., Rha, C., Sinskey, A.J., Yang, Y.H., 2014. Biosynthesis of poly(3-hydroxybutyrate-co-3-hydroxyhexanoate) (P(HB-co-HHx)) from butyrate using engineered *Ralstonia eutropha*. *Appl. Microbiol. Biotechnol.* 98, 5461–5469. doi:10.1007/s00253-014-5617-7

- Johnson, B.F., Stanier, R.Y., 1971. Dissimilation of aromatic compounds by *Alcaligenes eutrophus*. *J. Bacteriol.* 107, 468–475.
- Jörnvall, H., Hedlund, J., Bergman, T., Oppermann, U., Persson, B., 2010. Superfamilies SDR and MDR: From early ancestry to present forms. Emergence of three lines, a Zn-metalloenzyme, and distinct variabilities. *Biochem. Biophys. Res. Commun.* 396, 125–130. doi:10.1016/j.bbrc.2010.03.094
- Jörnvall, H., Höög, J.O., Persson, B., 1999. SDR and MDR: Completed genome sequences show these protein families to be large, of old origin, and of complex nature. *FEBS Lett.* 445, 261–264. doi:10.1016/S0014-5793(99)00130-1
- Jörnvall, H., Landreh, M., Östberg, L.J., 2015. Alcohol dehydrogenase, SDR and MDR structural stages, present update and altered era. *Chem. Biol. Interact.* 234, 75–79. doi:10.1016/j.cbi.2014.10.017
- Jörnvall, H., Persson, B., 1995. Short-Chain Dehydrogenases/Reductases(SDR) 34.
- Jörnvall, H., Persson, M., Jeffery, J., 1981. Alcohol and polyol dehydrogenases are both divided into two protein types, and structural properties cross-relate the different enzyme activities within each type. *Proc. Natl. Acad. Sci. U. S. A.* 78, 4226–4230. doi:10.1073/pnas.78.7.4226
- Kallberg, Y., Oppermann, U., Jörnvall, H., Persson, B., 2002. Short-chain dehydrogenase/reductase (SDR) relationships: A large family with eight clusters common to human, animal, and plant genomes. *Protein Sci.* 11, 636–641. doi:10.1110/ps.26902.spite
- Kavanagh, K.L., Jörnvall, H., Persson, B., Oppermann, U., 2008. Medium- and short-chain dehydrogenase/reductase gene and protein families: the SDR superfamily: functional and structural diversity within a family of metabolic and regulatory enzymes. *Cell. Mol. Life Sci.* 65, 3895–906. doi:10.1007/s00018-008-8588-y
- Kawai, S., Mori, S., Mukai, T., Hashimoto, W., Murata, K., 2001. Molecular characterization of *Escherichia coli* NAD kinase. *Eur. J. Biochem.* 268(15), 4359–65. doi:10.1046/j.1432-1327.2001.02358.x
- Kemena, C., Notredame, C., 2009. Upcoming challenges for multiple sequence alignment methods in the high-throughput era. *Bioinformatics* 25, 2455–2465. doi:10.1093/bioinformatics/btp452
- Kleiger, G., Eisenberg, D., 2002. GXXXG and GXXXA motifs stabilize FAD and NAD(P)-binding rossmann folds through C-alpha-H...O hydrogen bonds and van der Waals interactions. *J. Mol. Biol.* 323, 69–76. doi:10.1016/S0022-2836(02)00885-9
- Kniemeyer, O., Heider, J., 2001. (S)-1-phenylethanol dehydrogenase of *Azoarcus* sp. strain EbN1, an enzyme of anaerobic ethylbenzene catabolism. *Arch. Microbiol.* 176, 129–135. doi:10.1007/s002030100303
- Koszelewski, D., Tauber, K., Faber, K., Kroutil, W., 2010. ω -Transaminases for the synthesis of non-racemic α -chiral primary amines. *Trends Biotechnol.* 28, 324–332. doi:10.1016/j.tibtech.2010.03.003
- Kovach, M.E., Elzer, P.H., Hill, D.S., Robertson, G.T., Farris, M. a, Roop, R.M., Peterson, K.M., 1995. Four new derivatives of the broad-host-range cloning vector pBBR1MCS, carrying different antibiotic-resistance cassettes. *Gene*.

- Kovacic, P., Cooksy, A.L., 2005. Role of diacetyl metabolite in alcohol toxicity and addiction via electron transfer and oxidative stress. *Arch. Toxicol.* 79, 123–128. doi:10.1007/s00204-004-0602-z
- Kroutil, W., Mang, H., Edegger, K., Faber, K., 2004. Recent advances in the biocatalytic reduction of ketones and oxidation of sec-alcohols. *Curr. Opin. Chem. Biol.* 8, 120–126. doi:10.1016/j.cbpa.2004.02.005
- Kruger, K., Grabowski, P.J., Zaug, A.J., Sands, J., Gottschling, D.E., Cech, T.R., 1982. Self-splicing RNA: Autoexcision and autocyclization of the ribosomal RNA intervening sequence of tetrahymena. *Cell* 31, 147–157. doi:10.1016/0092-8674(82)90414-7
- Kuhn, M., Steinbuchel, a., Schlegel, H.G., 1984. Hydrogen evolution by strictly aerobic hydrogen bacteria under anaerobic conditions. *J. Bacteriol.* 159, 633–639.
- Kulig, J., Frese, A., Kroutil, W., Pohl, M., Rother, D., 2013. Biochemical characterization of an alcohol dehydrogenase from *Ralstonia* sp. *Biotechnol. Bioeng.* 110, 1838–48. doi:10.1002/bit.24857
- Kulig, J., Simon, R.C., Rose, C.A., Husain, S.M., Häckh, M., Lüdeke, S., Zeitler, K., Kroutil, W., Pohl, M., Rother, D., 2012. Stereoselective synthesis of bulky 1,2-diols with alcohol dehydrogenases. *Catal. Sci. Technol.* 2, 1580. doi:10.1039/c2cy20120h
- Kunasundari, B., Murugaiyah, V., Kaur, G., Maurer, F.H.J., Sudesh, K., 2013. Revisiting the Single Cell Protein Application of *Cupriavidus necator* H16 and Recovering Bioplastic Granules Simultaneously. *PLoS One* 8, 1–15. doi:10.1371/journal.pone.0078528
- Kunst, F., Ogasawara, N., Moszer, I., Albertini, a M., Alloni, G., Azevedo, V., Bertero, M.G., Bessières, P., Bolotin, a, Borchert, S., Borriss, R., Boursier, L., Brans, a, Braun, M., Brignell, S.C., Bron, S., Brouillet, S., Bruschi, C. V, Caldwell, B., Capuano, V., Carter, N.M., Choi, S.K., Codani, J.J., Connerton, I.F., Danchin, a, 1997. The complete genome sequence of the gram-positive bacterium *Bacillus subtilis*. *Nature* 390, 249–256. doi:10.1038/36786
- Kusian, B., Bednarski, R., Husemann, M., Bowien, B., Kusian, B., Bednarski, R., Husemann, M., 1995. Characterization of the duplicate ribulose-1,5-bisphosphate carboxylase genes and *cbp* promoters of *Alcaligenes eutrophus*. *Am. Soc. Microbiol.* 177, 4442–4450.
- Kusian, B., Bowien, B., 1997. Organization and regulation of *cbp* CO₂ assimilation genes in autotrophic bacteria. *FEMS Microbiol. Rev.* 21, 135–155. doi:10.1016/S0168-6445(97)00054-5
- Kusian, B., Bowien, B., 1995. Operator binding of the *CbbR* protein, which activates the duplicate *cbp* CO₂ assimilation operons of *Alcaligenes eutrophus*. *J. Bacteriol.* 177, 6568–6574.
- Kusian, B., Sültemeyer, D., Bowien, B., 2002. Carbonic anhydrase is essential for growth of *Ralstonia eutropha* at ambient CO₂ concentrations. *J. Bacteriol.* 184, 5018–26. doi:10.1128/JB.184.18.5018
- Lancaster, C.R.D., 2002. Succinate : quinone oxidoreductases : an overview. *Biochim. Biophys. Acta* 1553, 1–6.
- Lauterbach, L., Lenz, O., Vincent, K. a, 2013. H₂-driven cofactor regeneration with NAD(P)⁺-reducing hydrogenases. *FEBS J.* 280, 3058–68. doi:10.1111/febs.12245

- Lavandera, I., Kern, A., Ferreira-Silva, B., Glieder, A., De Wildeman, S., Kroutil, W., 2008a. Stereoselective bioreduction of bulky-bulky ketones by a novel ADH from *Ralstonia* sp. *J. Org. Chem.* 73, 6003–6005. doi:10.1021/jo800849d
- Lavandera, I., Kern, A., Ferreira-silva, B., Glieder, A., Wildeman, S. De, Kroutil, W., 2008. Stereoselective Bioreduction of Bulky-Bulky Ketones by a Novel ADH from *Ralstonia* sp . *J. Org. Chem.* 73, 6003–6005. doi:10.1021/jo800849d
- Lavandera, I., Kern, A., Schaffenberger, M., Gross, J., Glieder, A., de Wildeman, S., Kroutil, W., 2008b. An exceptionally DMSO-tolerant alcohol dehydrogenase for the stereoselective reduction of ketones. *ChemSusChem* 1, 431–436. doi:10.1002/cssc.200800032
- Lee, J.-N., Shin, H.-D., Lee, Y.-H., 2003. Metabolic engineering of pentose phosphate pathway in *Ralstonia eutropha* for enhanced biosynthesis of poly-beta-hydroxybutyrate. *Biotechnol. Prog.* 19, 1444–1449. doi:10.1021/bp034060v
- Lee, S.Y., 2006a. Deciphering bioplastic production. *Nat. Biotechnol.* 24, 1227–9. doi:10.1038/nbt1006-1227
- Lee, S.Y., 2006b. Deciphering bioplastic production. *Nat. Biotechnol.* 24, 1227–1229. doi:10.1038/nbt1006-1227
- Lenz, O., Bernhard, M., Buhrke, T., Schwartz, E., Friedrich, B., 2002. The hydrogen-sensing apparatus in *Ralstonia eutropha*. *J. Mol. Microbiol. Biotechnol.* 4, 255–262.
- Li, H., Opgenorth, P.H., Wernick, D.G., Rogers, S., Wu, T.-Y., Higashide, W., Malati, P., Huo, Y.-X., Cho, K.M., Liao, J.C., 2012. Integrated Electromicrobial Conversion of CO₂ to Higher Alcohols. *Science* (80-.). 335, 1596–1596. doi:10.1126/science.1217643
- Li, Z., Cai, L., Wu, Q., Chen, G., 2009. Overexpression of NAD kinase in recombinant *Escherichia coli* harboring the *phbCAB* operon improves poly (3-hydroxybutyrate) production. *Appl. Microbiol. Biotechnol.* 83, 939–947. doi:10.1007/s00253-009-1943-6
- Löwenstein, J., Lauterbach, L., Teutloff, C., Lenz, O., Bittl, R., Löwenstein, J., Lauterbach, L., Teutloff, C., Lenz, O., 2015. The Active Site of the NAD⁺-Reducing Hydrogenase from *Ralstonia eutropha* Studied by EPR Spectroscopy. doi:10.1021/acs.jpcc.5b04144
- Lu, J., Brigham, C.J., Gai, C.S., Sinskey, A.J., 2012. Studies on the production of branched-chain alcohols in engineered *Ralstonia eutropha*. *Appl. Microbiol. Biotechnol.* 96, 283–297. doi:10.1007/s00253-012-4320-9
- Lu, J., Brigham, C.J., Plassmeier, J.K., Sinskey, A.J., 2014. Characterization and modification of enzymes in the 2-ketoisovalerate biosynthesis pathway of *Ralstonia eutropha* H16. *Appl. Microbiol. Biotechnol.* 99, 761–774. doi:10.1007/s00253-014-5965-3
- Lu, J., Brigham, C.J., Rha, C., Sinskey, A.J., 2013. Characterization of an extracellular lipase and its chaperone from *Ralstonia eutropha* H16. *Appl. Microbiol. Biotechnol.* 97, 2443–2454. doi:10.1007/s00253-012-4115-z
- Ludwig, B., Akundi, A., Kendall, K., 1995. A Long-Chain Secondary Alcohol Dehydrogenase from *Rhodococcus erythropolis* ATCC 4277. *J. Biol. Chem.* 270, 3729–3733.

- Lütke-Eversloh, T., Fischer, A., Remminghorst, U., Kawada, J., Marchessault, R.H., Bögershausen, A., Kalwei, M., Eckert, H., Reichelt, R., Liu, S.-J., Steinbüchel, A., 2002. Biosynthesis of novel thermoplastic polythioesters by engineered *Escherichia coli*. *Nat. Mater.* 1, 236–240. doi:10.1038/nmat773
- Lütte, S., Pohlmann, A., Zaychikov, E., Schwartz, E., Becher, J.R., Heumann, H., Friedrich, B., 2012. Autotrophic production of stable-isotope-labeled arginine in *Ralstonia eutropha* strain H16. *Appl. Environ. Microbiol.* 78, 7884–7890. doi:10.1128/AEM.01972-12
- Lutz, B.J., Fan, Z.H., Burgdorf, T., Friedrich, B., 2005. Hydrogen sensing by enzyme-catalyzed electrochemical detection. *Anal. Chem.* 77, 4969–4975. doi:10.1021/ac050313i
- Makino, Y., Inoue, K., Dairi, T., Itoh, N., 2005. Engineering of Phenylacetaldehyde Reductase for Efficient Substrate Conversion in Concentrated 2-Propanol. *Appl. Environ. Microbiol.* 71, 4713–4720. doi:10.1128/AEM.71.8.4713
- Maruyama, R., Nishizawa, M., Itoi, Y., Ito, S., Inoue, M., 2002. The enzymes with benzil reductase activity conserved from bacteria to mammals. *J. Biotechnol.* 94, 157–169. doi:10.1016/S0168-1656(01)00426-6
- Maruyama, R., Nishizawa, M., Itoi, Y., Ito, S., Inoue, M., 2001. Isolation and expression of a *Bacillus cereus* gene encoding benzil reductase. *Biotechnol. Bioeng.* 75, 630–633. doi:10.1002/bit.1191
- Mathew, S., Yun, H., 2012. omega-Transaminases for the Production of Optically Pure Amines and Unnatural Amino Acids. *Acs Catal.* 2, 993–1001. doi:10.1021/cs300116n
- Matsuda, T., Yamanaka, R., Nakamura, K., 2009. Recent progress in biocatalysis for asymmetric oxidation and reduction. *Tetrahedron Asymmetry* 20, 513–557. doi:10.1016/j.tetasy.2008.12.035
- May, S.R., Padgett, S.R., 1983. Oxidoreductase enzymes in biotechnology: current status and future potential. *Nature* 677–686. doi:10.1038/nmat1434
- Merlin, C., Masters, M., Mcateer, S., Coulson, A., 2003. Why Is Carbonic Anhydrase Essential to *Escherichia coli*? Why Is Carbonic Anhydrase Essential to *Escherichia coli*? *J. Bacteriol.* 185, 6415–6424. doi:10.1128/JB.185.21.6415
- Meyer, R., 2000. Identification of the mob genes of plasmid pSC101 and characterization of a hybrid pSC101-R1162 system for conjugal mobilization. *J. Bacteriol.* 182, 4875–4881. doi:10.1128/JB.182.17.4875-4881.2000
- Mindnich, R.D., Penning, T.M., 2009. Aldo-keto reductase (AKR) superfamily: genomics and annotation. *Hum. Genomics* 3, 362–370.
- Mitsukura, K., Kuramoto, T., Yoshida, T., Kimoto, N., Yamamoto, H., Nagasawa, T., 2013. A NADPH-dependent (S)-imine reductase (SIR) from *Streptomyces* sp. GF3546 for asymmetric synthesis of optically active amines: purification, characterization, gene cloning, and expression. *Appl. Microbiol. Biotechnol.* 97, 8079–8086. doi:10.1007/s00253-012-4629-4
- Mitsukura, K., Suzuki, M., Shinoda, S., Kuramoto, T., Yoshida, T., Nagasawa, T., 2011. Purification and Characterization of a Novel (R)-Imine Reductase from *Streptomyces* sp. GF3587. *Biosci. Biotechnol. Biochem.* 75, 1778–1782. doi:10.1271/bbb.110303

- Moore, J.C., Pollard, D.J., Kosjek, B., Devine, P.N., 2007. Advances in the Enzymatic Reduction of Ketones Background: Whole Cell Bioreductions. *Acc. Chem. Res.* 40, 1412–1419. doi:10.1021/ar700167a
- Müller, J., MacEachran, D., Burd, H., Sathitsuksanoh, N., Bi, C., Yeh, Y.C., Lee, T.S., Hillson, N.J., Chhabra, S.R., Singer, S.W., Beller, H.R., 2013. Engineering of *Ralstonia eutropha* H16 for autotrophic and heterotrophic production of methyl ketones. *Appl. Environ. Microbiol.* 79, 4433–4439. doi:10.1128/AEM.00973-13
- Musa, M.M., Ziegelmann-Fjeld, K.I., Vieille, C., Zeikus, J.G., Phillips, R.S., 2007. Asymmetric reduction and enantioselective oxidation using W110A secondary alcohol dehydrogenase from *Thermoanaerobacter ethanolicus*. *J. Org. Chem.* 72, 30–34.
- Nakamura, K., Yamanaka, R., Matsuda, T., Harada, T., 2003. Recent developments in asymmetric reduction of ketones with biocatalysts. *Tetrahedron-Asymmetry* 14, 2659–2681. doi:10.1016/S0957-4166(03)00526-3
- Napora, K., 2013. Aldehyde dehydrogenase from *Ralstonia eutropha* H16.
- Nardini, M., Dijkstra, B.W., 1999. Alpha/beta hydrolase fold enzymes: the family keeps growing. *Curr. Opin. Struct. Biol.* 9, 732–7. doi:10.1016/S0959-440X(99)00037-8
- NC-IUBMB, 2015. Enzyme nomenclature [WWW Document]. URL <http://www.chem.qmul.ac.uk/iubmb/enzyme/EC1/0101a.html> (accessed 9.25.15).
- Nei, M., 1987. The Neighbor-joining Method: A New Method for Reconstructing Phylogenetic Trees'. *Mol. Biol. Evol.* 4, 406–425.
- Ni, Y., Xu, J.H., 2012. Biocatalytic ketone reduction: A green and efficient access to enantiopure alcohols. *Biotechnol. Adv.* 30, 1279–1288. doi:10.1016/j.biotechadv.2011.10.007
- Oda, T., Oda, K., Yamamoto, H., Matsuyama, A., Ishii, M., Igarashi, Y., 2013. Hydrogen-driven asymmetric reduction of hydroxyacetone to (R)-1,2-propanediol by *Ralstonia eutropha* transformant expressing alcohol dehydrogenase from *Kluyveromyces lactis*. *Microb. Cell Fact.* 12, 1–9.
- Ollis, D., Cheah, E., Cyqler, M., Dijkstra, B., Frolow, F., Franken, S., Harel, M., Remington, S., Silman, I., Schraq, J., Al, E., 1992. The α/β hydrolase fold. *Protein Eng.* 5, 197–211.
- Oppermann, U., Filling, C., Hult, M., Shafqat, N., Wu, X., Lindh, M., Shafqat, J., Nordling, E., Kallberg, Y., Persson, B., Jörnvall, H., 2003. Short-chain dehydrogenases/reductases (SDR): The 2002 update. *Chem. Biol. Interact.* 143-144, 247–253. doi:10.1016/S0009-2797(02)00164-3
- Overhage, J., Steinbüchel, A., Priefert, H., 2002. Biotransformation of eugenol to ferulic acid by a recombinant strain of *Ralstonia eutropha* H16. *Appl. Environ. Microbiol.* 68, 4315–4321. doi:10.1128/AEM.68.9.4315-4321.2002
- Pal, M., Srivastava, G., Sharma, A.N., Kaur, S., Jolly, R.S., 2015. Biocatalyzed asymmetric reduction of benzils to either benzoin or hydrobenzoin: pH dependent switch. *Catal. Sci. Technol.* 5, 4017–4028. doi:10.1039/C5CY00158G

- Palmer, I., Wingfield, P.T., 2012. Preparation and Extraction of Insoluble (Inclusion-Body) Proteins from *Escherichia coli* 1–25. doi:10.1002/0471140864.ps0603s38.Preparation
- Park, J.M., Kim, T.Y., Lee, S.Y., 2011. Genome-scale reconstruction and in silico analysis of the *Ralstonia eutropha* H16 for polyhydroxyalkanoate synthesis, lithoautotrophic growth, and 2-methyl citric acid production. *BMC Syst. Biol.* 5, 101. doi:10.1186/1752-0509-5-101
- Patel, R.N., 2008. Synthesis of chiral pharmaceutical intermediates by biocatalysis. *Coord. Chem. Rev.* 252, 659–701. doi:10.1016/j.ccr.2007.10.031
- Pennacchio, A., Sannino, V., Sorrentino, G., Rossi, M., Raia, C. a., Esposito, L., 2013. Biochemical and structural characterization of recombinant short-chain NAD(H)-dependent dehydrogenase/reductase from *Sulfolobus acidocaldarius* highly enantioselective on diaryl diketone benzil. *Appl. Microbiol. Biotechnol.* 97, 3949–3964. doi:10.1007/s00253-012-4273-z
- Penning, T.M., 2014. The aldo-keto reductases (AKRs): Overview. *Chem. Biol. Interact.* 234, 236–246. doi:10.1016/j.cbi.2014.09.024
- Persson, B., 2002. Coenzyme-based functional assignments in completed genomes 4417, 4409–4417. doi:10.1046/j.1432-1033.2002.03130.x
- Persson, B., Kallberg, Y., Bray, J.E., Bruford, E., Dellaporta, S.L., Favia, A.D., Duarte, R.G., Jörnvall, H., Kavanagh, K.L., Kedishvili, N., Kisiela, M., Maser, E., Mindnich, R., Orchard, S., Penning, T.M., Thornton, J.M., Adamski, J., Oppermann, U., 2009. The SDR (short-chain dehydrogenase/reductase and related enzymes) nomenclature initiative. *Chem. Biol. Interact.* 178, 94–98. doi:10.1016/j.cbi.2008.10.040
- Persson, B., Oppermann, U., Jo, H., 2003. Coenzyme-based functional assignments of short-chain dehydrogenases/reductases (SDRs). *Chem. Biol. Interact.* 143-144, 271–278.
- Peters, J., Minuth, T., Kula, M.R., 1993. A novel NADH-dependent carbonyl reductase with an extremely broad substrate range from *Candida parapsilosis*: Purification and characterization. *Enzyme Microb. Technol.* 15, 950–958. doi:10.1016/0141-0229(93)90171-W
- Pfützner, J., Schlegel, H.G., 1973. Denitrifikation bei *Hydrogenomonas eutropha* Stamm H16. *Arch. für Mikrobiol. Mikrobiol.* 90, 199–211. doi:10.1007/BF00424972
- Pohlmann, A., Fricke, W.F., Reinecke, F., Kusian, B., Liesegang, H., Cramm, R., Eitinger, T., Ewering, C., Pötter, M., Schwartz, E., Strittmatter, A., Voss, I., Gottschalk, G., Steinbüchel, A., Friedrich, B., Bowien, B., 2006. Genome sequence of the bioplastic-producing “Knallgas” bacterium *Ralstonia eutropha* H16. *Nat. Biotechnol.* 24, 1257–1262. doi:10.1038/nbt1244
- Pötter, M., Müller, H., Reinecke, F., Wiczorek, R., Fricke, F., Bowien, B., Friedrich, B., Steinbüchel, A., 2004. The complex structure of polyhydroxybutyrate (PHB) granules: Four orthologous and paralogous phasins occur in *Ralstonia eutropha*. *Microbiology* 150, 2301–2311. doi:10.1099/mic.0.26970-0
- Raberg, M., Bechmann, J., Brandt, U., Schlüter, J., Uischner, B., Voigt, B., Hecker, M., Steinbüchel, A., 2011. Versatile metabolic adaptations of *Ralstonia eutropha* H16 to a loss of PdhL, the E3 component of the pyruvate dehydrogenase complex. *Appl. Environ. Microbiol.* 77, 2254–2263. doi:10.1128/AEM.02360-10

- Rathbone, D. a, Holt, P.J., Lowe, C.R., Bruce, N.C., 1997. Molecular analysis of the *Rhodococcus* sp. strain H1 her gene and characterization of its product, a heroin esterase, expressed in *Escherichia coli*. *Appl. Environ. Microbiol.* 63, 2062–2066.
- Reinecke, F., Steinbüchel, A., 2009. *Ralstonia eutropha* strain H16 as model organism for PHA metabolism and for biotechnological production of technically interesting biopolymers. *J. Mol. Microbiol. Biotechnol.* 16, 91–108. doi:10.1159/000142897
- Reisinger, C., van Assema, F., Schürmann, M., Hussain, Z., Remler, P., Schwab, H., 2006. A versatile colony assay based on NADH fluorescence. *J. Mol. Catal. B Enzym.* 39, 149–155. doi:10.1016/j.molcatb.2006.01.014
- Repaske, R., 1962. Nutritional requirements for *Hydrogenomonas eutropha*. *J. Bacteriol.* 83, 418–22.
- Richter, N., Simon, R.C., Lechner, H., Kroutil, W., Ward, J.M., Hailes, H.C., 2015. ω -Transaminases for the amination of functionalised cyclic ketones. *Org. Biomol. Chem.* 13, 8843–8851. doi:10.1039/C5OB01204J
- Riedel, S.L., Bader, J., Brigham, C.J., Budde, C.F., Yusof, Z.A.M., Rha, C., Sinskey, A.J., 2012. Production of poly(3-hydroxybutyrate-co-3-hydroxyhexanoate) by *Ralstonia eutropha* in high cell density palm oil fermentations. *Biotechnol. Bioeng.* 109, 74–83. doi:10.1002/bit.23283
- Riedel, S.L., Lu, J., Stahl, U., Brigham, C.J., 2014. Lipid and fatty acid metabolism in *Ralstonia eutropha*: Relevance for the biotechnological production of value-added products. *Appl. Microbiol. Biotechnol.* 98, 1469–1483. doi:10.1007/s00253-013-5430-8
- Roberts, M.J., Wondrak, G.T., Laurean, D.C., Jacobson, M.K., Jacobson, E.L., 2003. DNA damage by carbonyl stress in human skin cells. *Mutat. Res.* 522, 45–56. doi:10.1016/S0027-5107(02)00232-4
- Romermann, D., Friedrich, B., 1985. Denitrification by *Alcaligenes eutrophus* is plasmid dependent. *J. Bacteriol.* 162, 852–854.
- Rosano, G.L., Ceccarelli, E. a., 2014. Recombinant protein expression in *Escherichia coli*: Advances and challenges. *Front. Microbiol.* 5, 1–17. doi:10.3389/fmicb.2014.00172
- Rulli, G., Heidlindemann, M., Berkessel, A., Hummel, W., Gröger, H., 2013. Towards catalyst compartmentation in combined chemo- and biocatalytic processes: Immobilization of alcohol dehydrogenases for the diastereoselective reduction of a β -hydroxy ketone obtained from an organocatalytic aldol reaction. *J. Biotechnol.* 168, 271–276. doi:10.1016/j.jbiotec.2013.08.031
- Rundbäck, F., Fidanoska, M., Adlercreutz, P., 2012. Coupling of permeabilized cells of *Gluconobacter oxydans* and *Ralstonia eutropha* for asymmetric ketone reduction using H₂ as reductant. *J. Biotechnol.* 157, 154–158. doi:10.1016/j.jbiotec.2011.09.029
- Sallantin, M., Huet, J.C., Demartean, C., Pernollet, J.C., 1990. Reassessment of commercially available molecular weight standards for peptide sodium dodecyl sulfate-polyacrylamide gel electrophoresis using electroblotting and microsequencing. *Electrophoresis* 11, 34–36. doi:10.1002/elps.1150110108

- Saratale, G.D., Oh, M.-K., 2015. Characterization of poly-3-hydroxybutyrate (PHB) produced from *Ralstonia eutropha* using an alkali-pretreated biomass feedstock. *Int. J. Biol. Macromol.* 80, 627–635. doi:10.1016/j.ijbiomac.2015.07.034
- Saurugger, P.N., Hrabak, O., Schwab, H., Lafferty, R.M., 1986. Mapping and cloning of the par-region of broad-host-range plasmid RP4. *J. Biotechnol.* 4, 333–343. doi:10.1016/0168-1656(86)90047-7
- Savile, C.K., Janey, J.M., Mundorff, E.C., Moore, J.C., Tam, S., Jarvis, W.R., Colbeck, J.C., Krebber, a., Fleitz, F.J., Brands, J., Devine, P.N., Huisman, G.W., Hughes, G.J., 2010. Biocatalytic Asymmetric Synthesis of Chiral Amines from Ketones Applied to Sitagliptin Manufacture. *Science* (80-). 329, 305–309. doi:10.1126/science.1188934
- Scheper, T., Wittman, C., Krull, R., 2010. Biosystems engineering, *Advances in biochemical engineering/biotechnology*. Springer. doi:10.1007/10_2009_57
- Schlegel, H.G., Gottschalk, G., Von Bartha, R., 1961. Formation and utilization of poly-beta-hydroxybutyric acid by Knallgas bacteria (*Hydrogenomonas*). *Nature* 191, 463–465. doi:10.1038/191463a0
- Schlegel, H.G., Steinbüchel, A., 1981. Fermentation. Chapter: Die relative Respirationsrate (RRR), ein neuer Belüftungsparameter. Springer Vienna, Vienna. doi:10.1007/978-3-7091-8634-3
- Schwartz, E., Friedrich, B., 2001. A physical map of the megaplasmid pHG1, one of three genomic replicons in *Ralstonia eutropha* H16. *FEMS Microbiol. Lett.* 201, 213–219. doi:10.1016/S0378-1097(01)00265-8
- Schwartz, E., Gerischer, U., Friedrich, B., 1998. Transcriptional regulation of *Alcaligenes eutrophus* hydrogenase genes. *J. Bacteriol.* 180, 3197–3204.
- Schwartz, E., Henne, A., Cramm, R., Eitinger, T., Friedrich, B., Gottschalk, G., 2003. Complete nucleotide sequence of pHG1: A *Ralstonia eutropha* H16 megaplasmid encoding key enzymes of H₂-based lithoautotrophy and anaerobiosis. *J. Mol. Biol.* 332, 369–383. doi:10.1016/S0022-2836(03)00894-5
- Schwartz, E., Voigt, B., Zühlke, D., Pohlmann, A., Lenz, O., Albrecht, D., Schwarze, A., Kohlmann, Y., Krause, C., Hecker, M., Friedrich, B., 2009. A proteomic view of the facultatively chemolithoautotrophic lifestyle of *Ralstonia eutropha* H16. *Proteomics* 9, 5132–5142. doi:10.1002/pmic.200900333
- Senkovich, O., Speed, H., Grigorian, A., Bradley, K., Ramarao, C.S., Lane, B., Zhu, G., Chattopadhyay, D., 2005. Crystallization of three key glycolytic enzymes of the opportunistic pathogen *Cryptosporidium parvum*. *Biochim. Biophys. Acta - Proteins Proteomics* 1750, 166–172. doi:10.1016/j.bbapap.2005.04.009
- Sezena, M.L., 2011. *Proteobacteria: Phylogeny, Metabolic Diversity and Ecological Effects*.
- Shaked, Z., Whitesides, G.M., 1980. Enzyme-Catalyzed Organic Synthesis: NADH Regeneration by Using Formate Dehydrogenase. *Am. Chem. Soc.* 102, 7104–7105.
- Shimizu, R., Dempo, Y., Nakayama, Y., Nakamura, S., Bamba, T., Fukusaki, E., Fukui, T., 2015. New Insight into the Role of the Calvin Cycle: Reutilization of CO₂ Emitted through Sugar Degradation. *Sci. Rep.* 5, 11617. doi:10.1038/srep11617

- Shimizu, S., Ogawa, J., Kataoka, M., Kobayashi, M., 1997. Screening of novel microbial enzymes for the production of biologically and chemically useful compounds. *Adv. Biochem. Eng. Biotechnol.* 58, 45–87.
- Shumilin, I.A., Nikandrov, V.V., Popov, V.O., Krasnovsky, A.A., 1992. Photogeneration of NADH under coupled action of CdS semiconductor and hydrogenase from *Alcaligenes eutrophus* without exogenous mediators. *FEBS Lett.* 306, 125–128. doi:10.1016/0014-5793(92)80982-M
- Sichwart, S., Hetzler, S., Bröker, D., Steinbüchel, A., 2011. Extension of the substrate utilization range of *Ralstonia eutropha* strain H16 by metabolic engineering to include mannose and glucose. *Appl. Environ. Microbiol.* 77, 1325–1334. doi:10.1128/AEM.01977-10
- Siedow, A., Cramm, R., Siddiqui, R. a., Friedrich, B., 1999. A megaplasmid-borne anaerobic ribonucleotide reductase in *Alcaligenes eutrophus* H16. *J. Bacteriol.* 181, 4919–4928.
- Simon, R., Priefer, U., Pühler, a., 1983. A Broad Host Range Mobilization System for *In Vivo* Genetic Engineering: Transposon Mutagenesis in Gram Negative Bacteria. *Bio/Technology* 1, 784–791. doi:10.1038/nbt1183-784
- Soderberg, T., 2010. Organic Chemistry With a Biological Emphasis - Chemwiki [WWW Document]. URL http://chemwiki.ucdavis.edu/Organic_Chemistry/Organic_Chemistry_With_a_Biological_Emphasis (accessed 10.1.15).
- Srinivasan, S., Barnard, G.C., Gerngross, T.U., 2002. A Novel High-Cell-Density Protein Expression System Based on *Ralstonia eutropha* 68, 5925–5932. doi:10.1128/AEM.68.12.5925
- Steinbüchel, a., 2001. Perspectives for Biotechnological Production and Utilization of Biopolymers: Metabolic Engineering of Polyhydroxyalkanoate Biosynthesis Pathways as a Successful Example. *Macromol. Biosci.* 1, 1–24. doi:10.1002/1616-5195(200101)1:1<::AID-MABI1>3.0.CO;2-B
- Steinbüchel, A., Fächtenbusch, B., 1998. Bacterial and other biological systems for polyester production. *Trends Biotechnol.* 16, 419–427.
- Steinbüchel, A., Kuhn, M., Niedrig, M., Schlegel, H.G., 1983. Fermentation Enzymes in Strictly Aerobic Bacteria: Comparative Studies on Strains of the Genus *Alcaligenes* and on *Nocardia opaca* and *Xanthobacter autotrophicus* 2825–2835.
- Steinbüchel, A., Schlegel, H.G., 1984. A multifunctional fermentative alcohol dehydrogenase from the strict aerobic *Alcaligenes eutrophus*: purification and properties. *Eur. J. Biochem.* 130, 555–564.
- Steinbüchel, A., Schlegel, H.G., 1983. NAD-linked L(+)-lactate dehydrogenase from the strict aerobic *Alcaligenes eutrophus*. 2. Kinetic properties and inhibition by oxaloacetate. *Eur. J. Biochem.* 130, 329–34.
- Steinbüchel, A., Schlegel, H.G., 1983. NAD-linked L(+)-lactate dehydrogenase from the strict aerobic *Alcaligenes eutrophus*. 1. Purification and Properties. *Eur. J. Biochem.* 130, 321–328. doi:10.1111/j.1432-1033.1983.tb07155.x
- Steinmetz, M., Le Coq, D., Aymerich, S., Gonzy-Tréboul, G., Gay, P., 1985. The DNA sequence of the gene for the secreted *Bacillus subtilis* enzyme levansucrase and its genetic control sites. *Mol. Gen. Genet.* 200, 220–8.

- Tan, C.H., Show, P.L., Ooi, C.W., Ng, E.-P., Lan, J.C.-W., Ling, T.C., 2015. Novel lipase purification methods - a review of the latest developments. *Biotechnol. J.* 10, 31–44. doi:10.1002/biot.201400301
- Tanaka, N., Nonaka, T., Nakamura, K., Hara, A., 2001. SDR Structure, Mechanism of Action, and Substrate Recognition. *Curr. Org. Chem.* 5, 89–111. doi:10.2174/1385272013375751
- Tanaka, N., Nonaka, T., Nakanishi, M., Deyashiki, Y., Hara, A., Mitsui, Y., 1996. Crystal structure of the ternary complex of mouse lung carbonyl reductase at 1.8 Å resolution: the structural origin of coenzyme specificity in the short-chain dehydrogenase/reductase family. *Structure.* doi:10.1016/S0969-2126(96)00007-X
- Tauber, K., Fuchs, M., Sattler, J.H., Pitzer, J., Pressnitz, D., Koszelewski, D., Faber, K., Pfeffer, J., Haas, T., Kroutil, W., 2013. Artificial Multi-Enzyme Networks for the Asymmetric Amination of *sec*-Alcohols. *Chem. - A Eur. J.* 19, 4030–4035. doi:10.1002/chem.201202666
- The Nobel Prize in Physiology or Medicine 2007 - Press Release, 2007.
- Tian, J., Sinskey, A.J., Stubbe, J., 2005. Kinetic Studies of Polyhydroxybutyrate Granule Formation in *Wautersia eutropha* H16 by Transmission Electron Microscopy Kinetic Studies of Polyhydroxybutyrate Granule Formation in *Wautersia eutropha* H16 by Transmission Electron Microscopy. *Society* 187, 3814–3824. doi:10.1128/JB.187.11.3814
- Tokikawa, R., Loffredo, C., Uemi, M., Machini, M.T., Bechara, E.J.H., 2014. Radical acylation of L-lysine derivatives and L-lysine-containing peptides by peroxynitrite-treated diacetyl and methylglyoxal. *Free Radic. Res.* 48, 357–70. doi:10.3109/10715762.2013.871386
- Torella, J.P., Gagliardi, C.J., Chen, J.S., Bediako, D.K., Colón, B., Way, J.C., Silver, P. a., Nocera, D.G., 2015. Efficient solar-to-fuels production from a hybrid microbial–water-splitting catalyst system. *Proc. Natl. Acad. Sci.* 112, 2337–2342. doi:10.1073/pnas.1424872112
- Ugwu, S.O., Apte, S.P., 2004. The Effect of Buffers on Protein Conformational Stability. *Pharm. Technol.* 28, 86–109. doi:10.1016/j.saa.2011.06.021
- Van Bergen, B., Strasser, R., Cyr, N., Sheppard, J.D., Jardim, A., 2006. α,β -dicarbonyl reduction by *Saccharomyces d-arabinose* dehydrogenase. *Biochim. Biophys. Acta - Gen. Subj.* 1760, 1636–1645. doi:10.1016/j.bbagen.2006.08.025
- Van Der Donk, W. a., Zhao, H., 2003. Recent developments in pyridine nucleotide regeneration. *Curr. Opin. Biotechnol.* 14, 421–426. doi:10.1016/S0958-1669(03)00094-6
- Vandamme, P., Coenye, T., 2004. Taxonomy of the genus *Cupriavidus*: A tale of lost and found. *Int. J. Syst. Evol. Microbiol.* 54, 2285–2289. doi:10.1099/ijs.0.63247-0
- Vanechoutte, M., Kämpfer, P., De Baere, T., Falsen, E., Verschraegen, G., 2004. *Wautersia* gen. nov., a novel genus accomodating the phylogenetic lineage including *Ralstonia eutropha* and related species, and proposal of *Ralstonia* [*Pseudomonas*] *syzygii* (Roberts et al. 1990) comb. nov. *Int. J. Syst. Evol. Microbiol.* 54, 317–327. doi:10.1099/ijs.0.02754-0
- Verstraete, K., Savvides, S.N., Vergauwen, B., 2013. Structural and biochemical characterization of an atypical short-chain dehydrogenase / reductase reveals an unusual cofactor preference 280, 1358–1370. doi:10.1111/febs.12128

- Vollbrecht, D., Schlegel, H.G., Stoschek, G., Janczikowski, A., 1979. Excretion of metabolites by hydrogen bacteria.IV. Respiration rate-dependent formation of primary metabolites and of poly-3-hydroxybutanoate. *Eur. J. Appl. Microbiol. Biotechnol.* 7, 267–276. doi:10.1007/BF00498021
- Voss, I., Steinbüchel, A., 2006. Application of a KDPG-aldolase gene-dependent addiction system for enhanced production of cyanophycin in *Ralstonia eutropha* strain H16. *Metab. Eng.* 8, 66–78. doi:10.1016/j.ymben.2005.09.003
- Wang, Z.-X., Brämer, C.O., Steinbüchel, A., 2003. The glyoxylate bypass of *Ralstonia eutropha*. *FEMS Microbiol. Lett.* 228, 63–71. doi:10.1016/S0378-1097(03)00722-5
- Waterhouse, A.M., Procter, J.B., Martin, D.M. a, Clamp, M., Barton, G.J., 2009. Jalview Version 2-A multiple sequence alignment editor and analysis workbench. *Bioinformatics* 25, 1189–1191. doi:10.1093/bioinformatics/btp033
- Weckbecker, A., Hummel, W., 2005. Glucose Dehydrogenase for the Regeneration of NADPH and NADH. *Microb. Enzym. Biotransformations SE - 14* 17, 225–238. doi:10.1385/1-59259-846-3:225
- Wiedner, R., Gruber-Khadjawi, M., Schwab, H., Steiner, K., 2014. Discovery of a novel (R)-selective bacterial hydroxynitrile lyase from *Acidobacterium capsulatum*. *Comput. Struct. Biotechnol. J.* 10, 58–62. doi:10.1016/j.csbj.2014.07.002
- Wilde, E., 1962. Untersuchungen ueber Wachstum und Speicherstoffsynthese von *Hydrogenomonas*. *Arch. Mikrobiol.* 43, 109–137. doi:10.1007/BF00406429
- Wohlgemuth, R., 2010. Asymmetric biocatalysis with microbial enzymes and cells. *Curr. Opin. Microbiol.* 13, 283–292. doi:10.1016/j.mib.2010.04.001
- Wondrak, G.T., Cervantes-Laurean, D., Roberts, M.J., Qasem, J.G., Kim, M., Jacobson, E.L., Jacobson, M.K., 2002. Identification of alpha-dicarbonyl scavengers for cellular protection against carbonyl stress. *Biochem. Pharmacol.* 63, 361–73. doi:10.1016/S0006-2952(01)00915-7
- Wu, C.F.J., 1986. Jackknife, Bootstrap and other resampling methods in regression analysis. *Ann. Stat.* 14, 1261–1295. doi:10.1214/aos/1176350161
- Wu, X., Zhang, C., Orita, I., Imanaka, T., Fukui, T., Xing, X.H., 2013. Thermostable alcohol dehydrogenase from *Thermococcus kodakarensis* KOD1 for enantioselective bioconversion of aromatic secondary alcohols. *Appl. Environ. Microbiol.* 79, 2209–2217. doi:10.1128/AEM.03873-12
- Yabuuchi, E., Kosako, Y., Yano, I., Hotta, H., Nishiuchi, Y., 1995. Transfer of two Burkholderia and an Alcaligenes species to *Ralstonia* gen. Nov.: Proposal of *Ralstonia pickettii* (Ralston, Palleroni and Doudoroff 1973) comb. Nov., *Ralstonia solanacearum* (Smith 1896) comb. Nov. and *Ralstonia eutropha* (Davis 1969) comb. No. *Microbiol. Immunol.* 39, 897–904.
- Yan, Y., Song, X., Liu, G., Su, Z., Du, Y., Sui, X., Chang, X., Huang, D., 2012. Human NRDRB1, an alternatively spliced isoform of NADP(H)-dependent retinol dehydrogenase/reductase enhanced enzymatic activity of Benzil. *Cell. Physiol. Biochem.* 30, 1371–1382. doi:10.1159/000343326

- Yu, J., Si, Y., 2004. Metabolic carbon fluxes and biosynthesis of polyhydroxyalkanoates in *Ralstonia eutropha* on short chain fatty acids. *Biotechnol. Prog.* 20, 1015–1024. doi:10.1021/bp034380e
- Zach, C., 2013. Heterologous protein expression and functional analyses of dehydrogenases of *Ralstonia eutropha* H16. Graz Technical University.
- Zarnt, G., Schröder, T., Andreesen, J.R., 1997. Degradation of tetrahydrofurfuryl alcohol by *Ralstonia eutropha* is initiated by an inducible pyrroloquinoline quinone-dependent alcohol dehydrogenase. *Appl. Environ. Microbiol.* 63, 4891–4898.
- Zhao, H., Van Der Donk, W. a., 2003. Regeneration of cofactors for use in biocatalysis. *Curr. Opin. Biotechnol.* 14, 583–589. doi:10.1016/j.copbio.2003.09.007
- Zhu, D., Hua, L., 2009. Biocatalytic asymmetric amination of carbonyl functional groups - a synthetic biology approach to organic chemistry. *Biotechnol. J.* 4, 1420–1431. doi:10.1002/biot.200900110